ABSTRACT

Title of Document: ASSESSMENT OF NATURAL VERTICAL VENTILATION FOR SMOKE AND HOT GAS LAYER CONTROL IN A RESIDENTIAL SCALE STRUCTURE

Kelly Marie Opert, Master of Science, 2012

Directed By: Professor and Chair, Dr. James A. Milke

Department of Fire Protection Engineering

In firefighting, ventilation tactics are used to increase visibility for firefighter rescue and fire suppression operations, to increase survivability of the occupants of the structure, and to decrease property damage. Improperly implemented ventilation tactics or unplanned, fire-induced ventilation can lead to rapid changes in fire behavior creating fatal conditions inside a building for occupants and firefighters. In this set of experiments, measurements were made within a single, full scale compartment varying the fire size and the ceiling vent conditions between no vents, one 1.2 m by 1.2m (4' by 4') vent, and two combined 1.2 m by 1.2m (4' by 4') vents. The objective was to assess the vents' ability to relieve smoke and the hot gas layer. Thirty-two experiments were conducted using natural gas. These fires were allowed to burn until conditions within the enclosure reached steady state. With one open vent, the hot gas layer was not fully vented. With two open vents, the hot gas layer was fully vented for all three fires sizes.

Simulations of the natural gas experiments were produced using the National Institute of Standards and Technology's Fire Dynamics Simulator in order to explore how well the experiments were simulated based on the same fire sizes and vent conditions. The simulated steady state hot gas layer depths were significantly less than the experimental depths in the doorway when both vents were open, due to a discrepancy in whether or not a hot gas layer existed. The steady state hot gas layer temperatures were significantly under-predicted near the burner when both vents were open (meaning the simulated temperatures were cooler than the measured temperatures) and over-predicted in the doorway when one vent was open and two vents were open (meaning the simulated temperatures were hotter than the measured temperatures). Two additional experiments were conducted using sleeper sofas as fuel, in order to evaluate the differences between controlled natural gas fires and furniture. Neither one open vent nor two open vents was enough to raise the hot gas layer interface height. In the experiment with two sofas, two open vents did reduce the hot gas layer temperature at the doorway by as much as 300 °C (600 °F), but the temperature was still in excess of 200 °C (400 °F). In conclusion, the minimum vertical vent size of one 1.2 m by 1.2m (4' by 4') that firefighters are instructed to use does not remove all hazards, even in a 0.5 MW fire. More discussion is needed in the fire service to define the goals of vertical ventilation and how to best address each goal. More validation of the Fire Dynamics Simulator is needed before vertical ventilation can be accurately simulated in a multi-room structure fire.

Assessment of Natural Vertical Ventilation for Smoke and Hot Gas Layer Control in a Residential Scale Structure

By

Kelly Marie Opert

Thesis submitted to the Faculty of the Graduate School of the University of Maryland, College Park, in partial fulfillment of the requirements for the degree of Master of Science

2012

Advisory Committee:

Professor and Chair, Dr. James A. Milke

Assistant Professor, Dr. Stanislav Stoliarov

Dr. Anthony Hamins

Acknowledgements

The author would like to thank Daniel Madrzykowski from NIST and Dr. James Milke from the University of Maryland (UMD) for their continuous guidance and support throughout the duration of this project and Stephen Kerber from UL for providing resources and the facility needed to conduct the experiments. The author would also like acknowledge Adam Barowy (NIST) and Roy McLane (NIST) for their technical support during the experiments. Lastly, the author wishes to express gratitude to Dr. Anthony Hamins (NIST) and Dr. Stanislav Stoliarov (UMD) for their valuable review of this work.

Table of Contents

List of Figures

List of Tables

1. Introduction

During firefighting, ventilation tactics are used to increase visibility for firefighter rescue and fire suppression operations, to increase survivability of the occupants of the structure, and decrease property damage. Ventilation, when used correctly, allows hot smoke to exit a structure and cool, fresh air into the structure. Ventilation tactics are described as natural or mechanical and horizontal or vertical. Natural ventilation is any opening in a structure that allows smoke and fresh air to flow between the structure and exterior naturally. Firefighters utilize natural ventilation when they break a window to allow the hot gases to exit the structure and fresh air into the structure. Mechanical ventilation consists of using a mechanical device, such as a fan, to direct the flow of fresh air into a structure or exhaust hot gases and smoke out of the structure. Horizontal ventilation refers to any horizontal opening created by firefighters, such as breaking a window or opening a door. In firefighting, vertical ventilation refers specifically to venting the roof of a structure. This can include using a saw to cut a hole in the roof or breaking a skylight.

Natural horizontal ventilation is most commonly used by firefighters, given that it is the logistically easiest type of ventilation to perform and is typically necessary to gain entry to the building. Mechanical ventilation involves owning and bringing fans to a fire scene. Vertical ventilation requires firefighters to have axes or saws and to climb on the roof. In the last ten years, research has led to significant progress in understanding and maximizing the benefits of horizontal and mechanical ventilation for firefighting purposes [1-7]. However, little research is available for vertical ventilation with respect to firefighting. The purposes of this study are to:

- Examine the effectiveness of natural vertical ventilation in a residential scale compartment with well controlled gas burner fires (representing the different stages of a compartment fire)
- Explore the ability of a computer fire model to simulate the gas burner results for a compartment with a doorway and zero, one, and two ceiling vents
- Explore the effectiveness of natural vertical ventilation in a furniture-fueled compartment fire.

1.1. Hazards of Ventilation

Improperly implemented ventilation tactics and unplanned, fire-induced ventilation can lead to rapid changes in fire behavior, creating fatal conditions for occupants and firefighters. In the early stages of fire development, a fire has all of the components necessary to sustain itself – fuel, oxygen, heat, and an uninhibited chemical chain reaction. Venting the structure containing the fire has minimal impact on fire growth, but releases the hot gases and products of combustion to prevent them from building up inside the structure [8]. In late stages of fire development inside a structure, the fire can become oxygen-deprived as the production of the combustion products occurs faster than oxygen is coming into the structure [8]. In this scenario, venting the structure can provide the fire with the component it was previously lacking to sustain the chemical reaction and to grow.

In Washington D.C., two firefighters died and two firefighters were injured in a townhouse fire in 1999. According to the final National Institute for Occupational Safety and Health (NIOSH) report, the homeowners left the rear 2nd floor windows open and the front door open [9]. Firefighters arrived to find smoke rolling out of the front door. Firefighters entered the front door with an attack line in search of the fire. Firefighters then vented a front window on the 1st floor and two windows in the front of the 2nd floor. Meanwhile, firefighters from a separate company arrived at the rear of the townhouse, which was level with the basement. They vented the basement sliding doors. The fire rapidly intensified in the basement. This caused a rush of fire and hot smoke to flow upwards towards the 1st floor. Two of the firefighters on the 1st floor received fatal injuries and two others escaped with severe but survivable burns. Using information collected by the District of Columbia Fire and Emergency Medical Services Department Reconstruction Committee, the National Institute of Standards and Technology (NIST) simulated the possible conditions created by this deadly fire [10]. The simulation showed that the fire in the basement had likely become under-ventilated and venting the first and second floor windows had little impact on the conditions in the house. But, when the basement sliding doors were vented, ample oxygen was provided directly to the fire resulting in flashover. The fire and hot gases from the basement flowed upstairs and quickly into the room where the firefighters were located.

In 2002, two firefighters died in a live fire training evolution in an acquired, one-story, single family home in Florida. An instructor and trainee were carrying out a search and rescue drill. The firefighters were radioed and did not respond. It was assumed that they were not near the designated burn room. The burn room window was vented. The bodies were discovered within the burn room after the fire was suppressed. NIOSH determined that two of the significant contributing factors were the usage of fuel without "known burning characteristics," a mattress in addition to five wooden pallets and a bale of straw, and not properly coordinating ventilation with interior operations [11]. NIST investigated the fire conditions and determined that the fuel load was sufficient to support flashover within the burn room and that venting the window facilitated rapid fire growth, shortening the time to flashover [12].

More recently in 2007, nine firefighters died in a furniture showroom in South Carolina. NIOSH reported that the fire originated in a loading dock and when firefighters arrived there was no signs of fire or smoke in the main showroom [13]. Firefighters began operations inside the showrooms. A smoke layer quickly developed and spread to the showrooms. The firefighters inside the showrooms became disoriented as the conditions intensified and radioed for aid. Several of the front windows were vented. Fire rapidly spread through the showrooms. NIST developed simulations based on information from the fire ground, recreating the likely development and spread of the fire throughout the store [14]. NIST reported that while the firefighters were fighting the fire, an underventilated fire developed in the interstitial space between the ceiling above them and the roof. The hot underventilated gases transported downwards, below the ceiling. When the windows were vented, the hot gases ignited.

In addition to the dangers of changing the oxygen levels inside a structure, vertical ventilation poses a unique secondary threat to life. It requires firefighters to stand on the roof of a structure while they are

working. As a fire progresses, the structural integrity of the roof may become compromised. When firefighters arrive at a fire scene, the amount of degradation of the structural elements is unknown. The combination of a weakened roof and vertical ventilation can lead to firefighters falling through the roof, causing serious injury or death [15].

In 2002, firefighters in Iowa arrived at a house fire. According to the NIOSH report [15], the interior attack crew was unable to move to the top floor of the structure because of the heat. An order was given to vent the roof. Two firefighters climbed onto the roof from an aerial platform. One of them, wearing his self-contained breathing apparatus (SCBA), took a chain saw and cut a section of the roof. The other firefighter, the victim, was not wearing a SCBA as he instructed the first firefighter on cutting the vent. Before the first firefighter could remove the cut section, the victim indicted that they needed to immediately get off the roof. Both firefighters moved back toward the platform. The victim fell to his knees, presumably from the thick smoke coming from the fire. The first firefighter tried to keep him moving, but then the roof failed and the victim fell ten feet into the smoke and fire. The first firefighter did make it off the roof.

Using current ventilation tactics to control structure fires is not based on a thorough scientific understanding of fire behavior. The transition between when it is beneficial to use ventilation and harmful to use ventilation is not understood. Between the unknown burning time, ventilation conditions before arrival, variations in wind, and amount and types of fuel in the structure, the transition varies vastly from structure to structure. This study is being conducted to contribute to the understanding of the effectiveness of ventilation and quantifying any danger ventilation may pose. The research results are used to educate firefighters about the environments they may encounter and how changing the ventilation will impact the fire.

1.2. Previous Horizontal Ventilation Research

In the last decade, understanding the effects of ventilation on structure fires has been a research priority for the Fire Fighting Technology Group at NIST. Extensive work has been done to determine if positive pressure ventilation can be used to improve conditions in a structure during a fire, the effect of wind on fire development, and how to mitigate wind driven fires. In recent years, Underwriters Laboratories (UL) has also made significant contributions, studying the impact of opening windows and doors on residential structure fires.

In 2005, NIST released *Effect of Positive Pressure Ventilation* [1]. In this report, a 4.3 m × 3.7 m room was built and furnished similar to a bedroom. The room had one window and one door to a corridor that led to the exterior. The window was closed at the start. A mattress was ignited. After 5 minutes and 45 seconds, the window was opened. In one experiment, the room was allowed to vent naturally. In the other, a fan positioned in front of the exterior entrance to the corridor was turned on. The mechanically ventilated fire resulted in a greater heat release rate (HRR), but significantly lesser temperatures in the corridor and improved visibility throughout the structure.

This work was followed with the *Full Scale Evaluation of Positive Pressure Ventilation in a Fire Fighter Training Building* in 2006, in which natural and positive pressure ventilation was studied in a multi-floor, multi-room burn building used for firefighter training [2]. The fuel source was a combination of wood pallets and dry hay. Thirty-one experiments were performed varying the location of the vent and fire room. In each experiment, the fire was allowed to become underventilated and then a door and window were opened. In the experiments with positive pressure ventilation, a fan was turned on in the doorway at the same time. In most of the experiments, temperatures at and below 1.2 m (4 ft) were lowered and visibility increased. But in some of the PPV experiments the temperatures increased.

In 2007, the research was moved into large structures. One hundred and sixty experiments were conducted in a high rise building in Toledo, Ohio [16]. Positive pressure ventilation was used to pressurize a stairwell in an attempt to keep the pressure high enough to prevent smoke from leaking into the stairwell, above the NFPA 92 minimum requirements. NIST determined the size, quantity, angle, location, and alignment of the fans for optimal pressurization in the stairwell to combat high-rise fire smoke.

Also in 2007, six experiments were conducted in Chicago, Illinois analyzing the effectiveness of firefighter fan pressurization in a high-rise building stairwell during a fire [3]. Fans were used successfully to quickly remove smoke from the stairwell and prevent further smoke from entering the stairwell, even when the door to the fire floor was open.

In 2008, pressure and fire experiments were executed in a Toledo, Ohio high school [4]. The objective was to determine the effectiveness of using fans to remove smoke from specific areas, prevent smoke spread into the specific areas of the school, and reduce the room temperature. The study showed that fans can achieve these goals even in buildings with large open areas.

The next priority became wind driven fires. A series of experiments were conducted in NIST's Large Fire Laboratory (LFL) and followed up with large scale experiments in a high rise building on Governor's Island, New York [5;17]. The laboratory experiments were executed in a three room structure separated by a hallway, arranged to simulate an apartment. An air boat fan was used to simulate high winds (9m/s to 11 m/s, 20 mph to 25 mph) and was positioned in front of the open bedroom window. The fires were started in the bedroom. It was determined that when the window was vented several minutes into the fire, the HRR of the fire drastically increased. The greatest increase was on the order of 20 times the fire size prior to the window opening. The results also showed that in a laboratory setting, covering the window with a wind control device (a fire resistant curtain) prevented the wind from entering the structure, reduced the fire size, improved the conditions inside the structure, and made the fire more manageable for firefighters to suppress. On Governor's Island two to three rooms from an apartment were used for each of the experiments. The fires were ignited and either the window in the initial fire room self vented, a window was intentionally vented, or a door was opened providing fresh air to the fire. Combinations of wind control devices, positive pressure ventilation, and hose lines were evaluated to determine the most effective way to control the fires. The study found that the use of wind control devices first, followed by water suppression and/or positive pressure ventilation in the stairwells

significantly reduced the size of the fire and improved tenability in the apartments for building occupants and firefighters.

In the last several years, Stephen Kerber at UL investigated the impact of horizontal ventilation on fires in residential structures constructed with legacy and modern materials [6]. The research demonstrated that modern materials significantly shortened the time to flashover because of the increased popularity of using synthetic materials. He showed that after a structure fire became oxygen deprived and a door or window was vented, conditions became untenable for firefighters within two to three minutes, if water was not immediately applied to the fire. Opening multiple vents without applying water further aggravated the conditions in the structure and did not necessarily prevent the fire from going to flashover. When the doors inside the structure were closed during the experiments, the tenability in the isolated rooms was significantly increased.

The research conducted in previous years has laid the ground work for understanding the effects of horizontal, natural, and mechanical ventilation on fire behavior. The remaining area that has not been addressed on a residential structure scale is vertical ventilation. This priority of this study is to lay the foundation for residential scale vertical ventilation fire experiments.

1.3. Previous Vertical Ventilation Research

Until recently, the majority of vertical ventilation research was conducted for the purpose of investigating the use of vertical ventilation as a built-in fire protection feature in structures. These vents are opened or closed to exhaust smoke from a fire or to prevent smoke from entering a section of the structure. Vertical vents are commonly installed in a building along with other types of fire protection systems, such as sprinklers and smoke curtains. Research over the last 60 years has focused on optimizing the best combination, quantity, and timing of vertical vents, sprinklers, and smoke curtains as applied primarily to commercial buildings.

Using vertical ventilation as a tool to improve conditions early in building fire development first became a focus of fire protection research after a fire destroyed a General Motors factory in 1953 [18]. The extensive amount of smoke and heat prevented fire fighters from reaching the fire in the interior of the building to put water on the fire. As a result, the company funded vertical ventilation research at the Armour Research Foundation at the Illinois Institute of Technology to address the problem [18]. Researchers suggested that vertical vents should be used in combination with sprinklers to best improve conditions in a building fire [18]. Through that and similar research, in 1958 the National Fire Protection Association (NFPA) was able to draft the first version of what is now NFPA 204 Standard for Smoke and Heat Venting, a standard dedicated to ventilation as a built-in fire protection feature of a building [19]. The standard provides the safe design requirements for venting buildings with and without sprinklers and applies to all buildings.

In 1964, Miles Suchomel at Underwriters' Laboratories, Inc. produced a study exploring the advantages and disadvantages of using sprinklers with and without automatic vertical vents [20]. The experiments were conducted in a 18 m × 18 m × 4.8 m (60 ft × 60 ft × 15.75 ft) room. Thirty-four upright sprinklers,

rated for 74 °C (165 °F), were used with a 3 m (10 ft) spacing. The vent was 1.8 m × 1.8 m (6.0 ft × 6.0 ft) and was offset from the fuel by about 6.1 m (20 ft). In the experiments where the fuel was a 2.0 m (6.5 ft) high wooden test crib, when the results of the experiments with a vent and without a vent were compared:

1) "The number of sprinklers which operated decreased.
2) The total flow rate (water demand) was reduced.
3) The pattern of sprinkler operation was uniform in effect causing an increase in the effective sprinkler-discharge density immediately over the crib
4) The percentage crib-weight loss decreased
5) The average ceiling temperature over the crib, for the first 5 min of each of the tests, was increased
6) The time at which the first sprinkler operated decreased [20]"

Suchomel showed that the combination of sprinklers and vertical ventilation could be beneficial. He suggested that ordinary- degree sprinklers used in combination with vents produced benefits similar to higher degree sprinklers and the combination should be further investigated.

In 1963, "the Joint Fire Research Organization in collaboration with Colt Ventilation and Heating Ltd. …carried out an experimental and theoretical investigation of the flow of hot gases in roof venting [21]." Based on the results of that investigation, Thomas and Hinkley wrote a report (Ref. [21]) on how the design of roof vents as a fire protection method should be changed. They stated that it was possible to lift the hot gas layer using vertical vents for any vent size and that the appropriate vent size was a function of the fire size, not of the dimensions of the building. They recommended that the size of the vents providing air and oxygen to the fire (such as open doors and windows) be less than the size of the vent or combined size of the vents exhausting the hot gases. They suggested that buildings with large open areas under the roof subdivide the area with each area including a vent to restrict smoke and fire damage to that area. The most historically significant argument the authors made was when the vertical vents were opened prior to the activation of local sprinklers that the gases near the sprinklers could cool enough to delay or prevent the sprinklers from activating. Requiring sprinklers to active before vertical opening vents was then incorporated into many fire codes. In the years after the Thomas and Hinkley report, a focus the fire research community became proving or disproving their findings about the interaction of sprinklers and vertical vents.

In 1989, Hinkley et al. conducted an extensive series of fire experiments in Ghent, Belgium investigating the interaction between sprinklers and vents [22]. The experiments took place in a 50 m × 20 m × 10 m (164 ft × 66 ft × 33 ft) building. The building had forty 1.64 m^2 (17.7 ft^2) vertical vents and openings in the sides of the building to provide fresh air as the smoke was vented. Upright sprinklers were positioned in a 2.4 m × 3.6 m (8 ft × 12 ft) grid near the ceiling. In the experiments, the fire was fueled by hexane. The fire size was exponentially increased from 1 MW to 14 MW. The number of open vents evaluated was zero, ten, and twenty. They determined that the time the first sprinkler operated was delayed 12 seconds with twenty open vents and 10 s with ten open vents. Hinkley stated that this delay was negligible. They also determined that the number of overall sprinklers and the number of sprinklers

activated in the first 60 s was significantly reduced. After this report was released, it was debated whether the sprinkler delay was indeed negligible or not. N.E. Gustafsson of Industrial Mutual, Helsinki noted that one fire grew an additional 4 MW in one experiment during the delay time [23]. Whether or not it is necessary to open the vents before the sprinklers operate is to this day still debated.

In addition to evaluating the best way to combine and standardize vertical ventilation with sprinklers, in the 1990's, researchers began to focus on combinations of vertical ventilation, sprinklers, and draft curtains. In 1997, McGrattan et al. conducted a comprehensive experimental series consisting of thirty-nine experiments exploring the interaction of all three factors [23]. The experiments were conducted under a 30 m × 30 m (100 ft × 100 ft) flat ceiling. Draft curtains were attached to the ceiling to create a 20.4 m × 21.6 m (67.1 ft × 71.2 ft) perimeter. The curtains were 1.8 m (6.0 ft) long. Upright sprinklers with a rating of 74 °C (165 °F) had a 3 m (10 ft) spacing within the boundaries of the draft curtains. One 1.2 m × 2.4 m (4.0 ft × 8.0 ft) vent was cut in the ceiling. For 34 of the 39 experiments, the fuel was a heptane spray burner. The burner position varied between four locations within the confines of the draft curtain. One location was directly under the vent. For the remaining five experiments, the fuel was the Factory Mutual Research Corporation Standard commodity, Group A Plastic. The researchers concluded that:

1) "The tests … showed that when the fire was not ignited directly under a roof vent, venting had no significant effect on the sprinkler activation times, the number of activated sprinklers, the near-ceiling gas temperatures, or the quantity of combustibles consumed.
2) The tests … showed that when the fire was ignited directly under a roof vent, automatic vent activation usually occurred at about the same time as the first sprinkler activation, but the average activation time of the first ring of sprinklers was delayed. The length of the delay depended on the difference in activation times between the vent and the first sprinkler.
3) The tests … showed that when the fire was ignited directly under a roof vent that activated either before or at about the same time as the first sprinkler, the number of sprinkler activations decreased by as much as 50% compared to tests performed with the vent closed.
4) The tests … showed that when draft curtains were installed, up to twice as many sprinklers activated compared to tests performed without curtains.
5) In one rack storage test where the ignition of the fire took place near a draft curtain and the fuel array extended underneath the curtain, disruption of the sprinkler spray and delay in sprinkler operation caused by the draft curtain led to a fire that consumed more commodity compared to the other tests where the fires were ignited away from the draft curtains. This result was demonstrated by the model simulation, as well.
6) The significant cooling effect of sprinkler sprays on the near-ceiling gas flow often prevented the automatic operation of vents. This conclusion is based on thermocouple measurements within the vent cavity, the presence of drips of solder on the fusible links recovered from unopened vents, and several tests where vents remote from the fire and the sprinkler spray activated. In one cartoned plastic commodity experiment, a vent did not open when the fire was ignited directly beneath it [23]."

The purpose of vertical ventilation in buildings is to exhaust smoke and hot gases in the early stages of fire development while the smoke and hot gas layer is beginning to form. Decades of research has been conducted evaluating and maximizing the effectiveness of vertical ventilation in the early stages of fire development. This research has extended into exploring the interactions of vertical vents with sprinklers and draft curtains. But the challenging fires that fire fighters face exceed the purposes of the vertical ventilation design. Firefighters typically open vents when a room or rooms are already fully engulfed in flames. Firefighters are currently not able to estimate the fire size and therefore do not know how many vents are necessary to exhaust enough smoke for them to operate within areas of a building. They often do not know the location of the fire and therefore do not know where to place the vents most effectively. They do not have the luxury of cutting 20 vents across the roof of a building like fire protection engineers may have done to install vents in a roof as a fire protection system. There is an element of guess work to their choice of vent location. Another factor is whether or not the best location for a vent is even safe to be standing on to open the vent. For vertical ventilation to be used effectively as a fire fighting tactic, it is necessary for research to extend beyond the understanding of vertical vents as a fire protection system.

Currently, there is little information available on vertical ventilation as a fire fighting tactic. UL is studying vertical ventilation in two full scale single-family houses concurrently with this study [7]. The purpose of UL's research is to specifically address the effectiveness of roof vents in a variety of fire scenarios [7]. The final report on UL's study is expected to be completed in 2013.

1.4. Study Objectives & Document Structure

The following document covers three separate objectives. The first was to evaluate the effectiveness of two different sized ceiling vents to reduce the hazards resulting from the hot gas and smoke layer produced by well controlled, steady state natural gas fires. The benefit of using a gaseous fuel like natural gas was that the gas flow to the burner can be controlled, allowing for the fire size to be controlled and set to specific sizes. In setting specific fire sizes, there are fewer variables effecting the experimental measurements, allowing for the effects of the vents to be better understood. The second objective was to compare the results of the experiment to the output of computer fire models to determine whether the models can be reliably used to simulate a residential scale compartment fire when vertical ventilation is introduced. If the experiments are well simulated, the fire models can be used to simulate structure fires with vertical ventilation with a greater degree of confidence in the ability of the model to correctly simulate the fire and the conditions inside the structure. This is helpful in planning future research, planning firefighting tactics in the fire service, and the investigation of fires. The final objective was to explore and evaluate the effectiveness of two different sized ceiling vents to reduce the hazards produced by the hot gas and smoke layer produced by furniture fires. The furniture consisted of multiple materials with unknown thermal properties and provided a sooty fire with an unsteady fire growth. A furniture fire is more consistent with what firefighters typically encounter.

In Section 2, the technical approach of all of the fire experiments is provided, because the approach varied little between the natural gas experiments and the furniture experiments. The conditions and results of the experiments fueled by natural gas are described in Section 3. In Section 4, the computer

simulations of the natural gas experiments are discussed and the results of the natural gas experiments are compared to the results of the simulations. The conditions and results of the furniture fires are presented in Section 5. The changes in the hot gas layer interface height and temperature resulting from the changing ventilation conditions are discussed in Section 6 for each of the study objectives. The findings are summarized in Section 7. In the last section, the implications of the findings are discussed.

2. Technical Approach of Experiments

The NIST and UL collaborated to conduct 33 experiments in Northbrook, IL. Natural gas fire experiments were conducted varying the heat release rate (HRR) and the size of a vertical vent in the ceiling of a full size room structure in order to collect information about the steady state environment within the room under those conditions. The experiments were each repeated at least three times to examine repeatability. In addition, two more experiments were conducted, one with a sleeper sofa and the second with two sleeper sofas as the initial fuel load in place of the natural gas burner.

2.1. Experimental Design

The burn room was designed to replicate a common room typically found in contemporary residential structures. The walls were reinforced in some areas to withstand the repeated and continuous fire load as was necessary. The structure included a single doorway. It also included two ceiling vents to relieve fire conditions within the structure. In most experiments natural gas was used as the fuel to collect data on the conditions in the room exposed to steady state burning. These experiments were followed with two experiments using furniture.

2.2. Room Design

The interior dimensions of the room were 6.1 m × 4.3 m × 2.4 m (20 ft × 14 ft × 8.0 ft). The walls were constructed like walls in typical residential structures as seen in Figure 2-1. They were constructed with nominally 6 cm × 12 cm (2 in. × 4 in.) lumber. The interior was lined with 1.22 m × 3.66 m × 15.9 mm (4 ft × 12 ft × 5/8 in.) sheets of type X gypsum wallboard and in some places 1.22 m × 2.44 m × 12.7 mm (4 ft × 8 ft × 1/2 in.) or 0.91 m × 1.52 m × 12.7 mm (3 ft × 5 ft × 1/2 in.) sheets of cement board. For all of the experiments, the floor inside the room was covered with a layer of cement board. During the first eleven experiments, the walls and ceiling were lined with a single layer of gypsum wallboard. Two 2.4 m × 2.4 m × 2.4 m (8 ft × 8 ft × 8 ft) areas in the corner containing the burner were lined with cement board on top of the gypsum board. At the end of the eleventh experiment, it became apparent that the wall linings were not sufficient to handle the extended fire exposure. The fire began to extend to the wooden structural support beams of the room. For the remainder of the experiments, the walls were lined with two layers of gypsum wallboard. The ceiling was entirely covered with cement board. Most of the left wall and about half of the back was also covered with cement board. The placement and dimensions of the cement board for both cases can be seen in Figure 2-2.

Because firefighters have been taught to cut at least a 1.2 m × 1.2 m (4.0 ft × 4.0 ft) vent into a roof [24], the effectiveness of a 1.2 m × 1.2 m (4.0 ft × 4.0 ft) vent was evaluated as well as a vent double that size,

1.2 m × 2.4 m (4.0 ft × 8.0 ft). A 1.2 m × 2.4 m (4.0 ft × 8.0 ft) vent was installed in the center of the room. The vent extended from the ceiling to 0.6 m (2 ft) above the ceiling. The additional height of the vent was used for the installation of bidirectional probes to measure the velocity in the vent. Two doors slightly larger than 1.2 m × 1.2 m (4 ft × 4 ft) were attached to the top of the vent by hinges. To change the ventilation in the ceiling, the doors were lifted and closed from the ground by a wire pulley system. A photograph of the ceiling vent and the pulley system is presented in Figure 2-3. In addition to the ceiling vent, there was a 2.1 m × 0.90 m (6.9 ft × 3.0 ft) doorway that remained open throughout each experiment.

Figure 2-1: Picture of the room structure

Figure 2-2: Photograph of the cement board placement for the first ten experiments (left) and the following experiments (right)

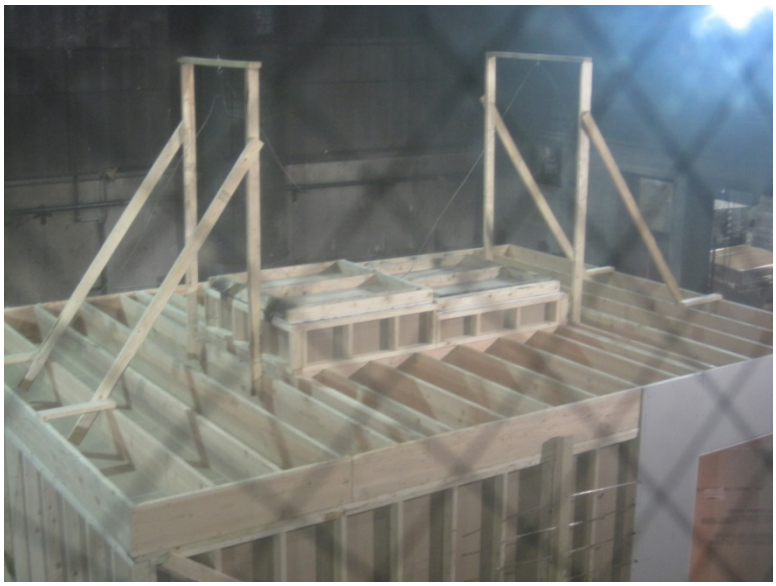

Figure 2-3: Photograph of the ceiling vent from the exterior and the door opening pulley system

2.3. Fuel Characterization

Throughout most of the experiments, the fuel source was a natural gas burner. The composition and properties of the natural gas, as reported by the gas provider, are provided in Appendix A. The burner was located in the corner of the room and had dimensions of 0.76 m × 0.76 m × 0.24 m (30 in. × 30 in. × 9.5 in.). The burner was elevated 0.15 m (6.0 in.) from the floor and constructed of 0.003 m (1/8 in.) thick metal. The upper 0.13 m (5.0 in.) of the burner was nearly filled with ceramic half rings on top of a metal grate for the purpose of diffusing the gas coming into the burner. The area below the grate was empty. The burner contained 32.3 kg (71.1 lbs) of ceramic half rings.

The half rings had an inner diameter of 0.019 m (3/4 in.) and an outer diameter of 0.032 m (1 1/4 in.) and a thickness of 0.003 m (1/8 in.). Photographs of the burner and ceramic half rings are shown in Figure 2-4. The gas entered the burner through two 0.05 m (2 in.) diameter pipes attached to the bottom of the burner.

Figure 2-4: Photograph of the gas burner (left) and the ceramic half rings (right)

In the last two experiments, commercially available sleeper sofas were used as the fuel source. The average mass of a sofa was 80.7 kg (178 lbs). The average cushion weight was 2.53 kg (5.58 lbs) and varied ± 0.03 kg (0.07 lbs). The sofa had a width of (35 in.), length of (68 in.) and height of (35 in.). The sleeper sofas had a wooden frame, metal springs, a fold-out mattress, a metal frame for the mattress, canvas to support the mattress, foam for comfort, and four different fabric materials. Photographs of the sofa and the underside of the sofa are shown in Figure 2-5 and Figure 2-6. The cushions contained foam with a layer of a polymer stuffing on the top and bottom as shown in Figure 2-7.

A similar sleeper sofa to the ones used in the experiments was burned under the calorimeter to determine the stand alone HRR of the sleeper sofa. The HRR of the sofa is presented in Figure 2-8. The maximum HRR was about 2.0 MW (1,900 Btu/s). The total amount of energy in the sofa was 840 MJ (790,000 Btu), which was calculated by summing the HRR every second.

Figure 2-5: Photograph of the sleeper sofa

Figure 2-6: Photograph of the underside of the sleeper sofa

Figure 2-7: Photograph of the cushion of the sleeper sofa

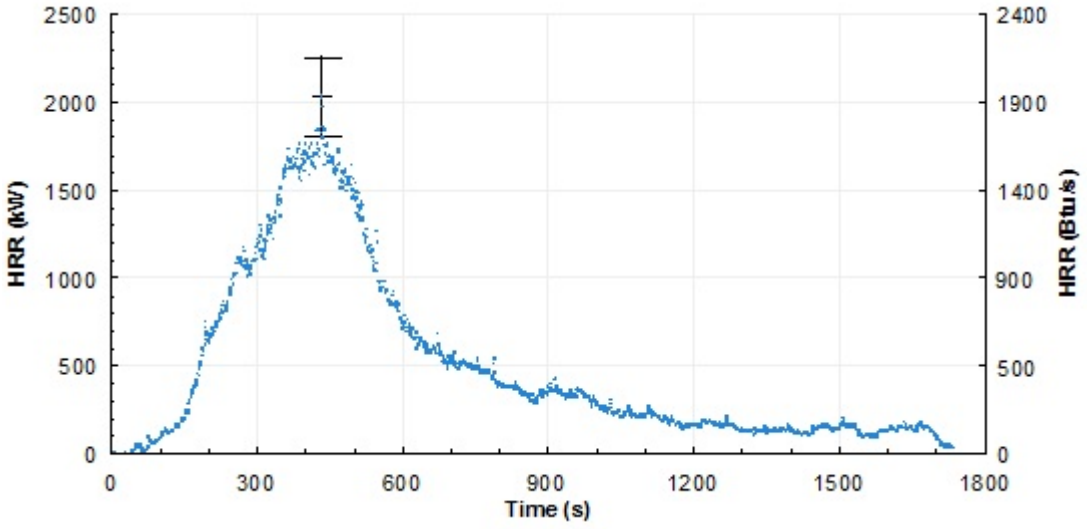

Figure 2-8: Plot of the HRR over time for a sleeper sofa

2.4. Types of Instrumentation

The HRR of the fires was measured using UL's calorimeter. In the natural gas experiments, the gas flow rate was measured by a diaphragm gas flowmeter. Temperatures were record using type K, bare-bead thermocouples. Schmidt-Boelter heat flux gauges cooled with water and containing embedded type K thermocouples were used to collect heat flux data. Bidirectional probes in addition to type K, 1.6 mm (0.063 in.) diameter, inconel shielded thermocouples were used to measure the gas velocities. The dimensions and locations of instrumentation were measured with a measuring tape for distances under 0.6 m (2 ft) and a digital laser measurer for distances over 0.6 m (2 ft). The mass of the sleeper sofas and sofa cushions were determined using a mass load cell.

2.5. Instrumentation Location

The fuel and instrumentation layout and locations for Experiments 1-29, Experiment 30, and Experiment 31 are presented in Figure 2-9, Figure 2-10, and Figure 2-11, respectively.

Two thermocouple arrays were used in the burn room for all of the experiments. Each was located 0.91 m (3.0 ft) away from a side wall and they were centered across the width of the room. Each array had a thermocouple located at 0.03 m, 0.3 m, 0.6 m, 0.9 m, 1.2 m, 1.5 m, 1.8 m, and 2.1 m (1.0 in., 1.0 ft, 2.0 ft, 3.0 ft, 4.0 ft, 5.0 ft, 6.0 ft, and 7.0 ft) from the ceiling.

There were six heat flux gauges in total for Experiments 1-30. Two heat flux gauges on the ground were located 15 cm (6 in.) from each thermocouple array toward the vent and 15 cm (6.0 in.) above the floor. These two heat flux gauges were facing the ceiling. The other four heat flux gauges were at a height of 0.9 m (3 ft). Two heat flux gauges were located 0.3 m (1 ft) away from each thermocouple array in the direction away from the vent. At 0.9 m (3 ft), there was one heat flux gauge facing the fire and another facing the ceiling for each thermocouple array. This height related to the height of a crawling firefighter. The heat flux gauges stayed in this configuration until the final experiment with two sleeper sofas. In this experiment, only three heat flux gauges were used. They were repositioned in the room to the locations shown in Figure 2-11. One was located at the floor facing the ceiling and the other two were at a height of 0.9 m (3 ft), one facing the ceiling and one facing the fire.

Ten bidirectional probes, each with a thermocouple, were centered in the doorway and located at 0.03 m (1.0 in.) from the top of the door and at 0.2 m (8 in.) intervals starting from the top of the door. Ten bidirectional probes with thermocouples were positioned in the vent. One probe was centered in the vent and the others were positioned 15 cm (6 in.) away from the edges of the vent. The 1.2 m (4.0 ft) centerline of the vent was also treated like a vent. The locations of the bidirectional probes relative to the vent are presented in Figure 2-12. In addition, the numbering convention used to refer to the bidirectional probe/thermocouple locations is shown.

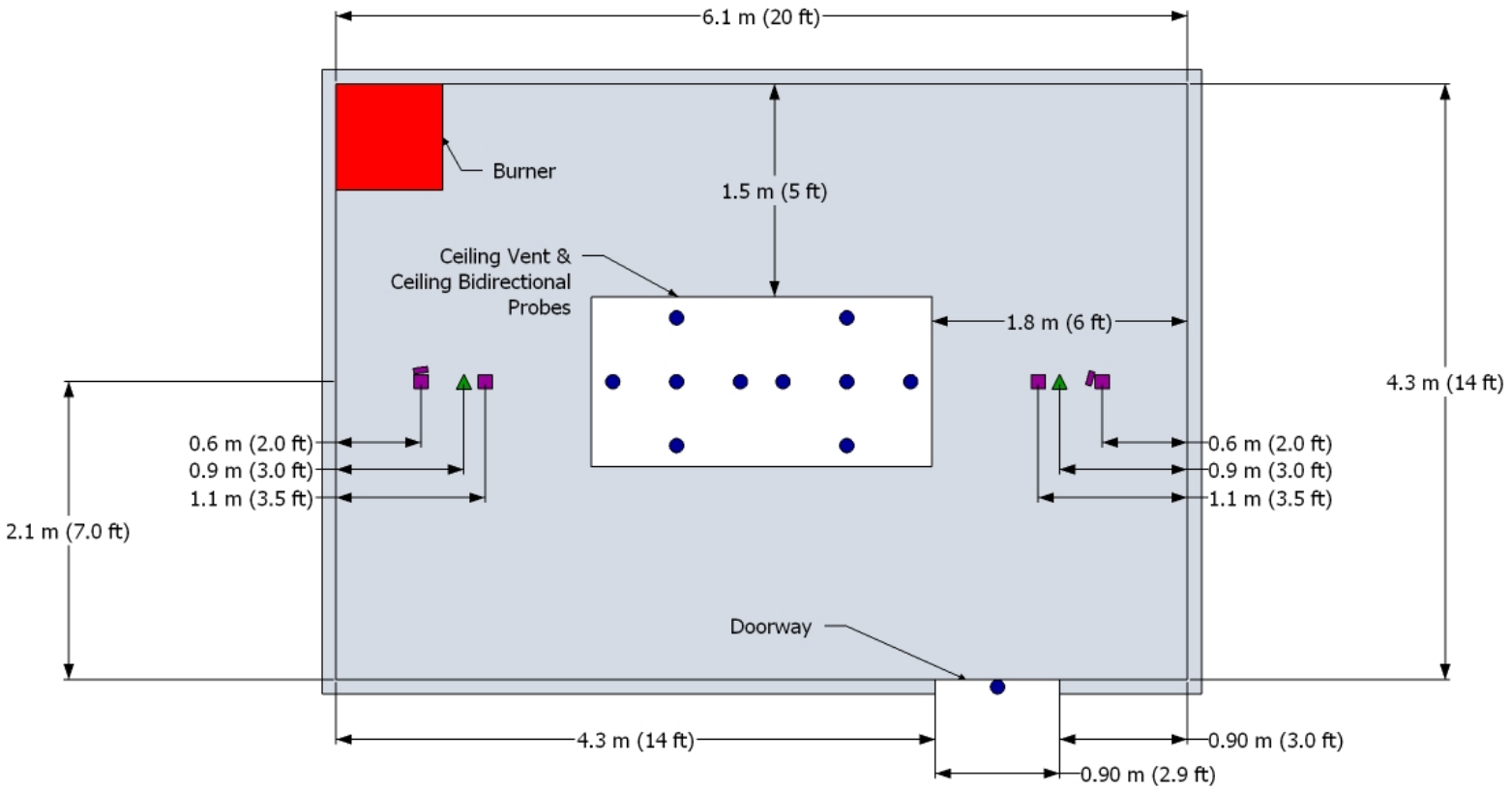

Figure 2-9: Layout of Experiments 1-29 with the ceiling vent and bidirectional probes shown. The thermocouple array (green triangle), heat flux gauge (purple rectangle), and bidirectional probe (blue circle) locations are displayed.

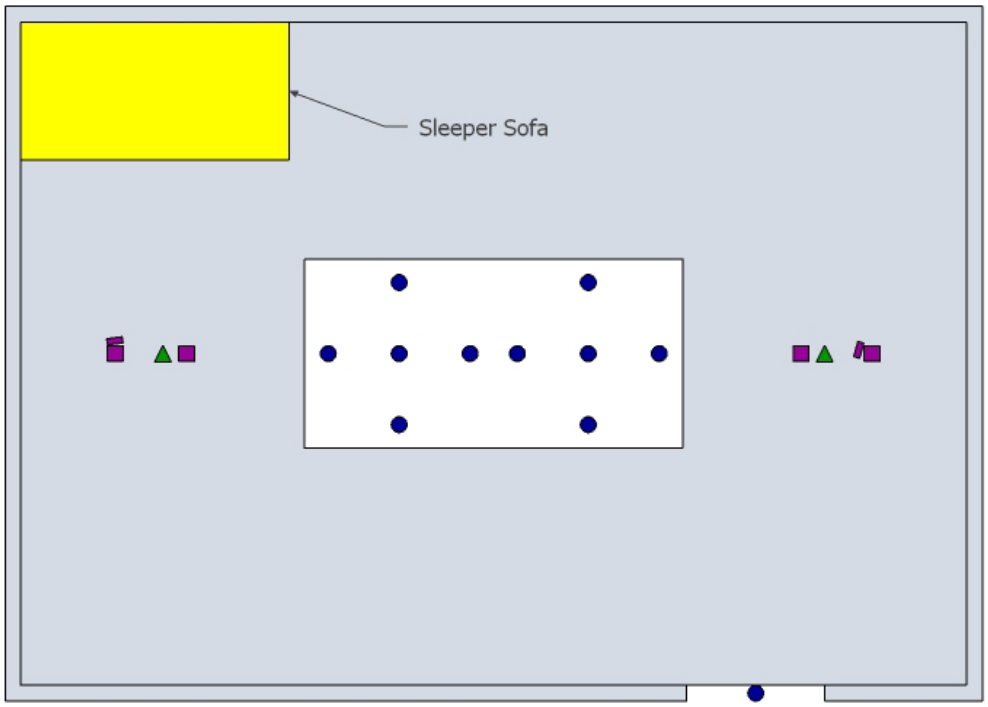

Figure 2-10: Layout of fuel and instrumentation for Experiment 30. The thermocouple array (green triangle), heat flux gauge (purple rectangle), and bidirectional probe (blue circle) locations are displayed.

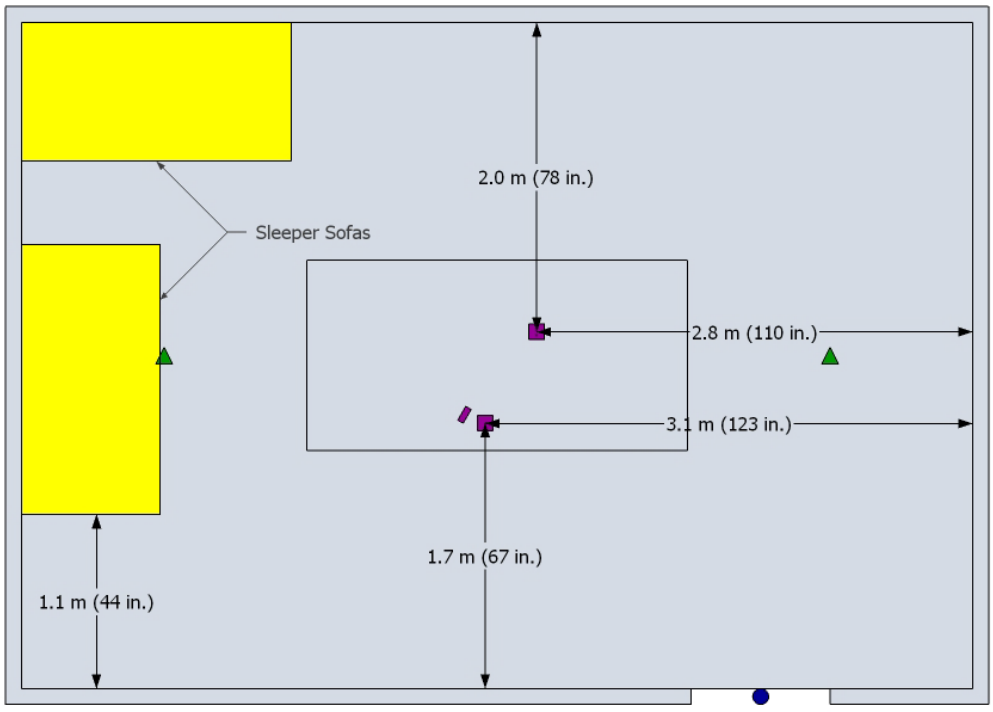

Figure 2-11: Layout of fuel and instrumentation for Experiment 31 with the ceiling vent bidirectional probes not shown. The thermocouple array (green triangle), heat flux gauge (purple rectangle), and bidirectional probe (blue circle) locations are displayed.

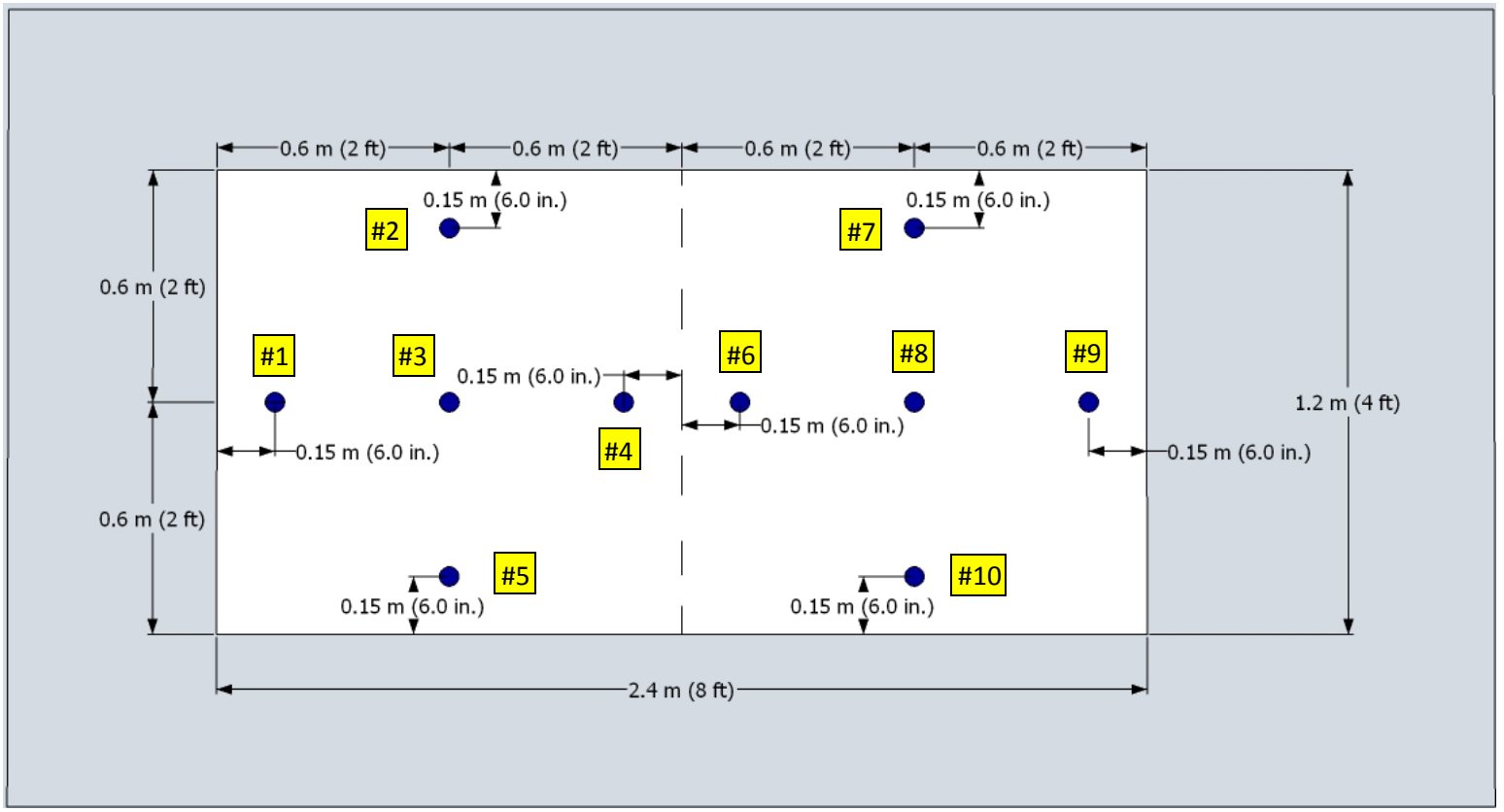

Figure 2-12: Locations of the bidirectional probes (blue circles) relative to the vent and display of the numbering convention for later reference to their locations

2.6. Measurement Uncertainty

The following table provides representative values of the total expanded uncertainties for each type of measurement and references to documents containing detailed discussions of the uncertainties. The total expanded uncertainties represent a 95% confidence interval, except for the HRRs which are a 68% confidence interval.

Table 2-1: Measurement Uncertainties

Measurement	Total Expanded Uncertainty	Reference
Calorimeter HRR	±10%	[25] [26]
Fuel-based HRR	±5%	[26]
Temperature	±15%	[27] [28]
Heat Flux	±8%	[29] [30]
Differential Pressure	±10%	[31] [32]
Velocity	±18%	[8]
Mass	±5%	[33]
HGL Interface Height	±13%	[34]
HGL Temperature	±10%	[34]

3. Gas Burner Experiment Conditions & Results

In the table below, the varying conditions for each experiment are provided. For most of the experiments, natural gas fueled the fire. The benefit of using natural gas is that the amount of fuel supplied to the burner can be controlled and measured. The fuel based HRR was the fire size estimated from the gas mass flow to the burner. According to the gas information provided in Appendix A, the average amount of energy produced by burning 0.28 m^3 (10 ft^3) of natural gas (one revolution of the diaphragm gas flow meter dial) is 10700 kJ. The time for one revolution in each experiment was recorded and used to determine the HRR. The last HRR provided was measured by the calorimeter. In the natural gas experiments, the calorimeter HRR is the average HRR of the last 90 s of each experiment. For the last two experiments in which sleeper sofas were used as fuel, the calorimeter HRR is the peak HRR measured by the calorimeter. This is because the sofas never reach steady state burning. The last column identifies how many of the vent doors were open during the experiment. "None" means that the only vent to the structure was the doorway. "One" and "Two" vents means that one or two of the 1.2 m × 1.2 m (4.0 ft × 4.0 ft) vent doors were opened for the experiment. Due to time constraints, most of the experiments were conducted continuously, one right after the other, without turning the gas off. The black bar separating some of the rows in the table indicate when the fire was fully extinguished before continuing experimentation.

Table 3-1: Experiment Conditions

Experiment #	Fuel Type	Intended HRR (kW)	Fuel Based HRR (kW)	Calorimeter HRR (kW)	Vents Open
1	Natural Gas	500	430	450	None
2	Natural Gas	500	430	494	One
3	Natural Gas	500	430	515	Two
4	Natural Gas	500	430	390	None
5	Natural Gas	1000	1011	1088	None
6	Natural Gas	1000	1011	1340	One
7	Natural Gas	1000	1011	1247	Two
8	Natural Gas	1000	1011	926	None
9	Natural Gas	2000	2188	1863	None
10	Natural Gas	2000	2188	2914	One
11	Natural Gas	2000	2144	1718	None
12	Natural Gas	2000	2144	2401	One
13	Natural Gas	2000	2144	2361	Two
14	Natural Gas	500	476	389	None
15	Natural Gas	500	476	519	One
16	Natural Gas	500	476	494	Two
17	Natural Gas	1000	1002	798	None
18	Natural Gas	1000	1002	1097	One
19	Natural Gas	1000	1002	1077	Two
20	Natural Gas	1000	1011	759	None
21	Natural Gas	1000	1011	1021	One
22	Natural Gas	1000	1011	976	Two
23	Natural Gas	500	470	421	Two
24	Natural Gas	500	470	422	One
25	Natural Gas	500	470	337	None
26	Natural Gas	500	470	464	One
27	Natural Gas	500	470	453	Two
28	Natural Gas	2000	2188	2094	Two
29	Natural Gas	2000	2188	-	None
30	Natural Gas	2000	2188	2419	One
31	Natural Gas	2000	2188	2333	Two
32	1 Sofa	NA	NA	3.1 MW (Peak)	Multiple Vent Conditions
33	2 Sofas	NA	NA	6.0 MW (Peak)	Multiple Vent Conditions

During the gas burner experiments, the natural gas flow was set at specific flow rates to produce fires of certain sizes. The temperatures were monitored in real time to establish that room conditions had reached steady state before starting the next experiment. The temperatures were deemed "steady" when the temperature gradient of a 90 s moving average was less than 0.5 °C/s (0.9 °F/s) at the two highest thermocouples in both thermocouple arrays inside the room. Figure 3-1 shows the unprocessed temperatures near the burner for Experiments 15-20. Just before each event marker, the temperatures were steady. The experiments were allowed to continue for greater than 90 s after reaching steady state. The steady state data was averaged over the 90 s prior to an event to determine the steady state values presented in the sections below. For example, the average of the 90 s before the event "First Vent Opened" for the temperature at a height of 2.05 m (6.73 ft) is the steady state temperature at that height. The raw steady state values of the measurements along with the standard deviations are provided in Appendix B.

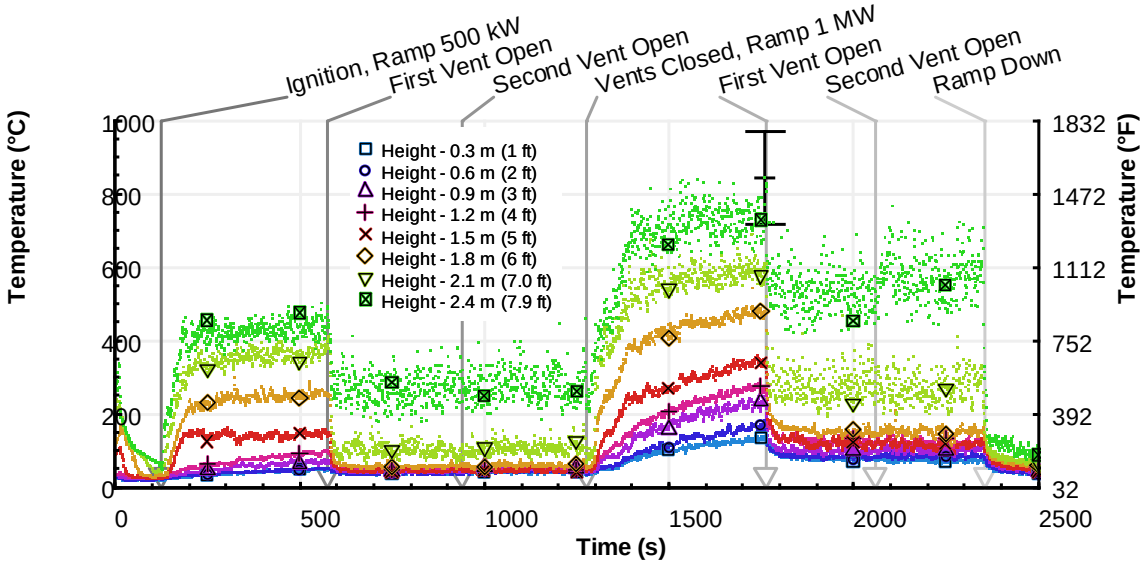

Figure 3-1: Temperature over time from the thermocouples near the burner during Experiments 15-20

3.1. HRR

The HRR of a fire is a measure of how much energy is being released over time, which is related to the size of a fire. A large fire will produce a large amount of energy per second. As a point of reference, the largest size of the natural gas fires was a little larger than the size of the sofa fire discussed in Section 2.3 when it was fully engulfed by the fire. The steady state HRRs measured by the calorimeter are provided in Table 3-2 along with the standard deviation.

Table 3-2: Calorimeter Mean HRRs (kW)

Experiment #	Calorimeter HRR	Standard Deviation
1	450	30
2	494	32
3	515	28
4	390	34
5	1088	48
6	1340	62
7	1247	45
8	926	62
9	1863	154
10	2914	150
11	1718	112
12	2401	95
13	2361	90
14	389	26
15	519	28
16	494	30
17	798	49
18	1097	50
19	1077	43
20	759	46
21	1021	41
22	976	43
23	421	23
24	422	29
25	337	29
26	464	27
27	453	26
28	2094	105
29	-	-
30	2419	99
31	2333	92

3.2. Temperature

Throughout the experiments, the temperatures were recorded inside the room on either side of the ceiling vents and across the ceiling and doorway vents. The value of measuring the temperature at locations on either side of the ceiling vents was being able to determine where the hot gases exist on the fire side and the doorway side. The temperatures in the ceiling vent gave insight into the temperature of the gases exiting the room, specifically whether or not the temperature of the hot gases was cooling. The temperatures in the door provided information about where hot gases were exiting the room and cool air was entering the room.

3.2.1. Interior

Figure 3-2 to Figure 3-4 provide bar graphs of the temperatures from the thermocouple array located close to the burner for the 0.5 MW, 1 MW, and 2 MW fires. Each bar graph shows the results for the experiments without ceiling vents, with one ceiling vent, and with two ceiling vents. In Figure 3-2, there was a decrease in temperatures when one vent was opened, but the addition of the second vent had no effect on the temperatures at this location. The temperatures recorded at the same location for the experiments with one and two vents have overlapping error bars indicating no significant difference in temperature at any location. The largest difference in steady state temperature between the temperatures measured when the vents were closed and one vent was opened was about 250 °C (480 °F) at a height of 2.1 m (7.0 ft). The highest steady state temperature dropped from approximately 425 °C (797 °F) to 275 °C (527 °F) when one vent was opened.

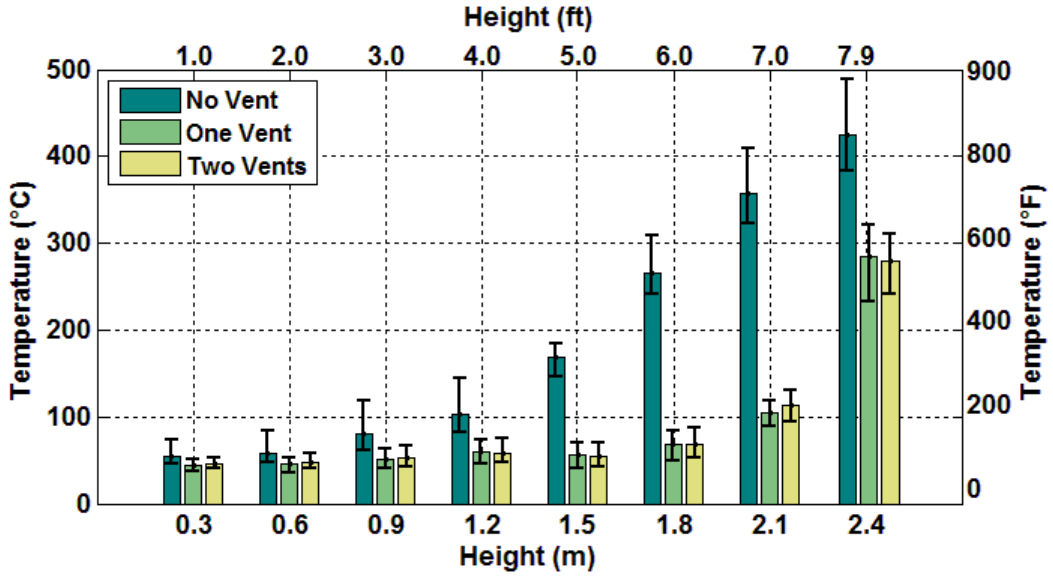

Figure 3-2: Mean steady state temperatures measured by the thermocouple array near the burner versus the heights of the thermocouples in the array for the 0.5 MW fires. The error bars represent the range of the steady state temperatures.

In Figure 3-3, the fire size is 1 MW, twice the HRR of the fires in the previous figure. The largest drop in temperature between the case without vents and with one vent was almost 300 °C (600 °F) at 1.8 m (6.0 ft). At the thermocouple closest to the ceiling, the change average steady state temperature was about 100 °C (200 °F). When the second vent was included in the experiments, the average steady state temperatures at each location did not change or minimally changed.

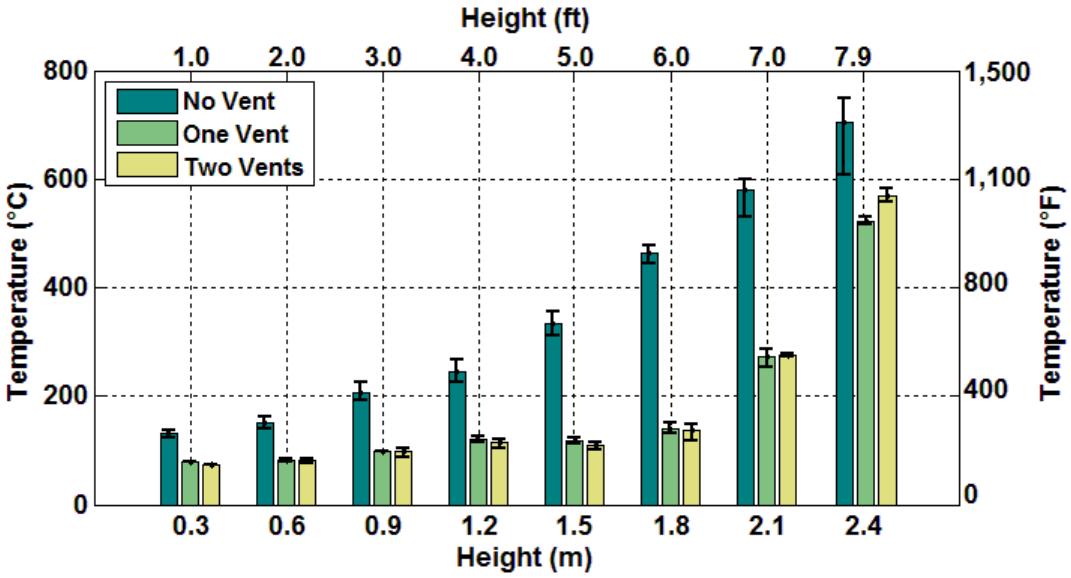

Figure 3-3: Mean steady state temperatures measured by the thermocouple array near the burner versus the heights of the thermocouples in the array for the 1 MW fires. The error bars represent the range of the steady state temperatures.

In the 2 MW fires, the temperature behavior over the height was the same as in the 1 MW for each of the vents scenarios. The addition of the second vent had no impact on the average steady state temperatures at any location. The greatest change in average steady state temperature occurred at 1.8 m (6.0 ft). The difference in temperature was about 400 °C (800 °F). At the thermocouple near the ceiling, there was maybe a 100 °C (200 °F) difference, but given that the error bar for the two vent case overlaps the temperature error bars from the other cases, this difference may be negligible, indicating the conditions near the ceiling were becoming unaffected by the vertical ventilation as the fire size has increased. At 2 MW, the temperatures are reduced with the opening of the vents. At this location in the room, the minimum average steady state temperature was about 200 °C (400 °F). Firefighter turnout gear is tested to withstand 260 °C (500 °F) for five minutes [35]. It is likely that a firefighter could withstand the conditions at this location for only a short amount of time.

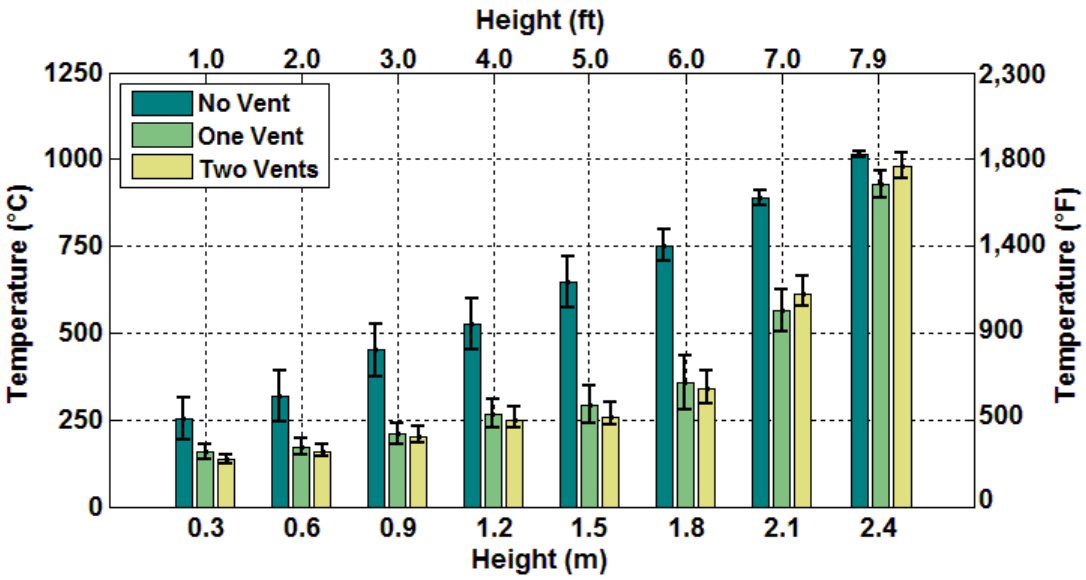

Figure 3-4: Mean steady state temperatures measured by the thermocouple array near the burner versus the heights of the thermocouples in the array for the 2 MW fires. The error bars represent the range of the steady state temperatures.

The next three figures show the mean steady state temperatures collected from the thermocouple array on the opposite side of the vents and near the doorway for 0.5 MW, 1 MW, and 2MW fires. In Figure 3-5 when both vents were opened, the steady state temperatures did not deviate from the temperatures recorded with one vent opened. The greatest difference in steady state temperature between the no vent and one vent cases was about 200 °C (400 °F) at the height of 1.8 m (6.0 ft). The difference between the highest average steady state temperatures recorded by the thermocouple array was 125 °C (257 °F) at 2.1 m (7.0 ft) between the no vent and one vent experiments. In the lower half of the room where the cool temperatures were located, all of the mean steady state temperatures were within the expanded uncertainty. The reduction in temperature was at most 25 °C (77 °F).

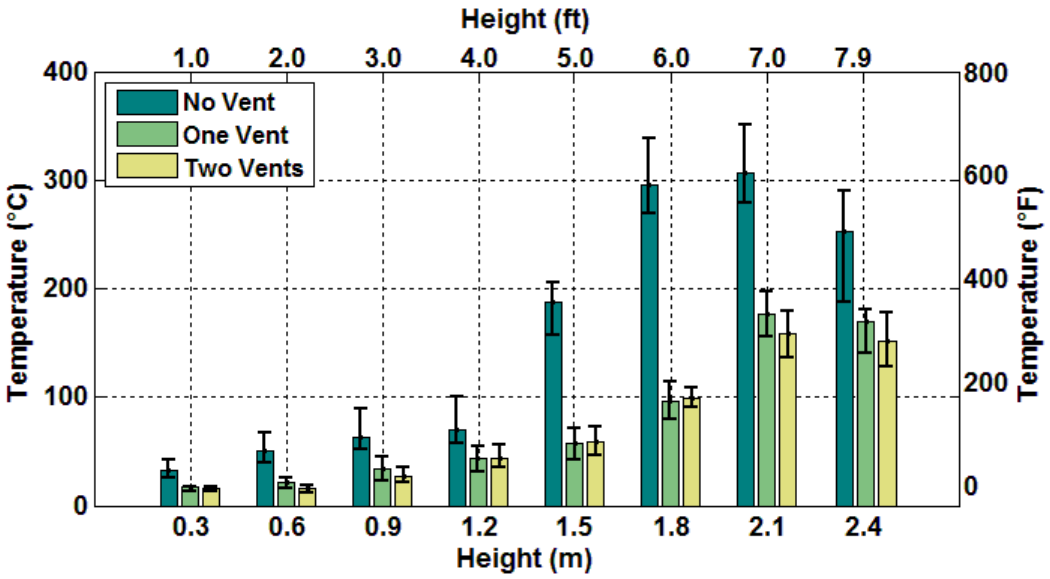

Figure 3-5: Mean steady state temperatures measured by the thermocouple array near the doorway versus the heights of the thermocouples in the array for the 0.5 MW fires. The error bars represent the range of the steady state temperatures.

In Figure 3-5 when the vents were closed, the highest mean steady state temperature was 500 °C (900 °F) at a height of 2.1 m (7.0 ft). With one vent opened, the temperature decreased to about 300 °C (600 °F), and with the second vent it dropped again to 250 °C (480 °F). At this fire size, changing the conditions from one to two vents only reduced the temperature at the two highest locations in the hot gas layer. The greatest drop in temperature occurred at 1.5 m and 1.8 m (5.0 ft and 6.0 ft) from the ceiling between the no vent experiments and the one open vent experiments. The difference in temperature was 250 °C (480 °F). At 1.8 m (6.0 ft) and below, all of the mean steady state temperatures were reduced by at least half, comparing conditions with no vents open to one vent opened.

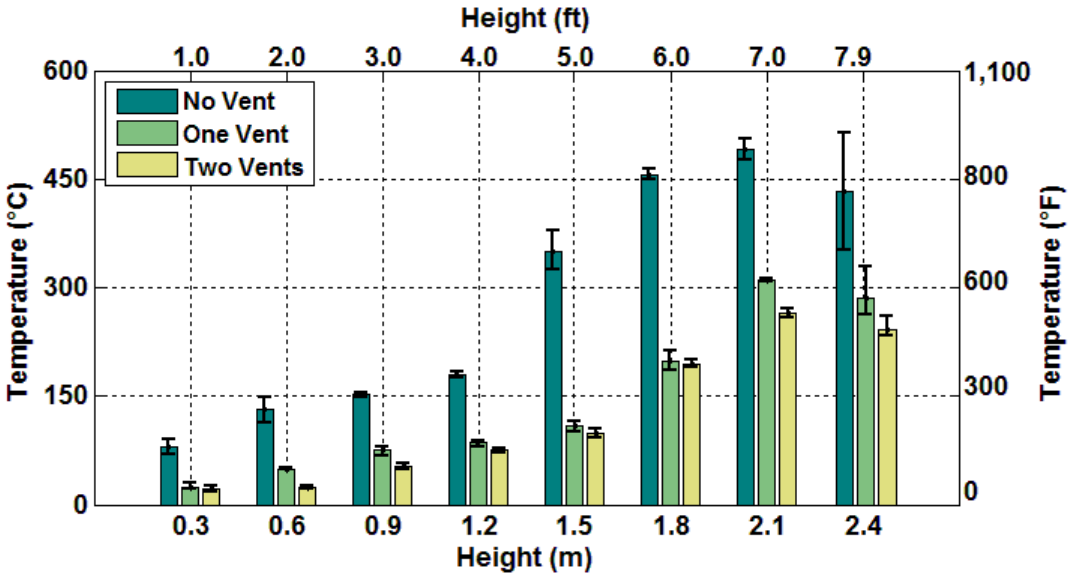

Figure 3-6: Mean steady state temperatures measured by the thermocouple array near the doorway versus the heights of the thermocouples in the array for the 1 MW fires. The error bars represent the range of the steady state temperatures.

When the fire size was increased to 2 MW, the highest mean steady state temperature was achieved at 2.1 m (7.0 ft) by the thermocouple array near the doorway when the vents were closed. The temperature reached about 600 °C (1,100 °F). When the first vent was opened, this temperature dropped more than 50 °C (120 °F) and upon opening the second vent, dropped the temperature dropped an additional 50 °C (120 °F). Below 1.8 m (6.0 ft) all of the mean steady state temperatures were reduced by at least half. This reduction in temperature was almost 300 °C (600 °F) at 1.5 m (5.0 ft), changing conditions in the lower half of the room from unbearable to temperatures fire fighters could survive for a short duration. Changing the conditions from no open vents to one open vent, resulted in a decrease in temperatures at all locations except at 2.1 m (7.0 ft), where the highest temperatures were experienced. When the conditions were changed from one vent to two open vents, the mean steady state temperature was reduced at 0.30 m, 0.60 m, 2.1 m, and 2.4 m (1.0 ft, 2.0 ft, 7.0 ft, and 7.9 ft).

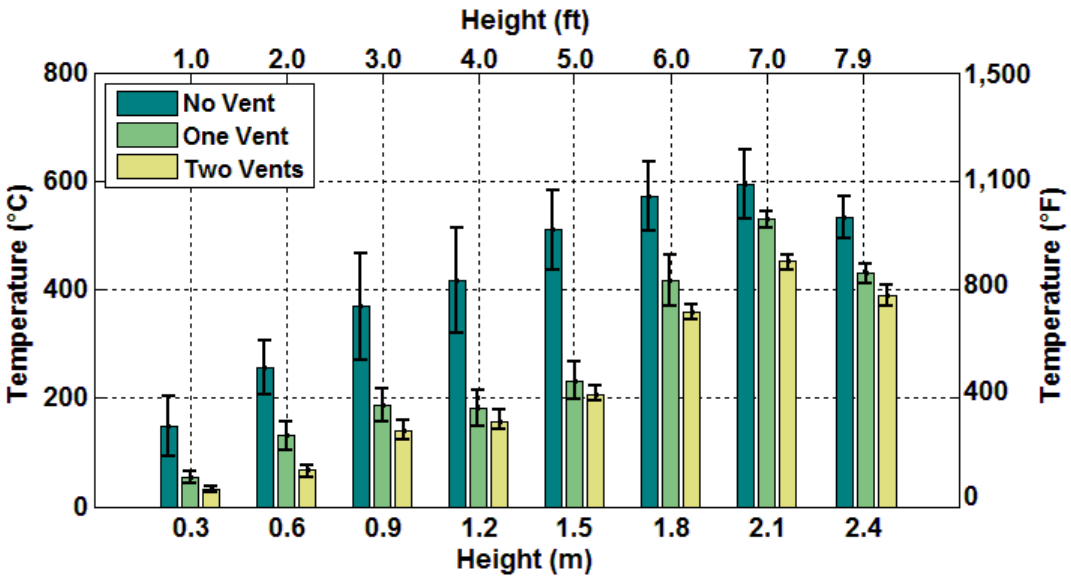

Figure 3-7: Mean steady state temperatures measured by the thermocouple array near the doorway versus the heights of the thermocouples in the array for the 2 MW fires. The error bars represent the range of the steady state temperatures.

3.2.2. Doorway

The mean steady state temperatures collected in the doorway are presented in the next three figures for the 0.5 MW, 1 MW, and 2 MW fires. When the fire size was 0.5 MW, the mean steady state temperatures were unaffected by the change in ventilation below 1.3 m (4.2 ft). The maximum average steady state temperature with the vents closed was 275 °C (527 °F). That temperature was reduced to about 125 °C (257 °F) with a single vent open and to 25 °C (77 °F) with two open vents. With two open vents no heat was exiting through the doorway.

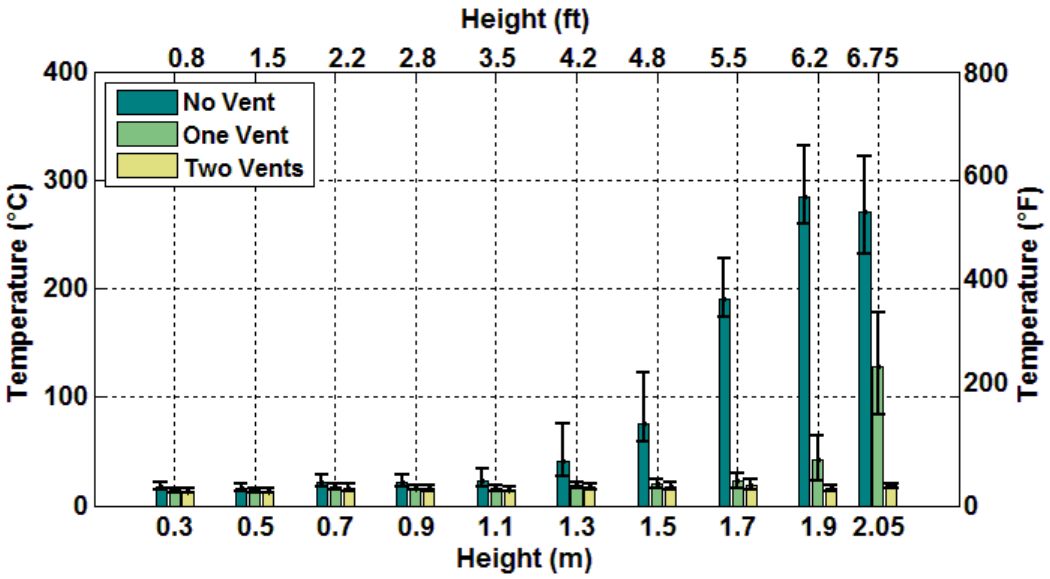

Figure 3-8: Mean steady state temperatures measured by the thermocouple array in the doorway versus the heights of the thermocouples in the array for the 0.5 MW fires. The error bars represent the range of the steady state temperatures.

In Figure 3-8, the highest mean steady state temperature was 450 °C (840 °F) in the doorway with the vents closed. This temperature dropped 150 °C (300 °F) with the one open vent. With both vents opened, all of the temperatures were about 25 °C (77 °F), which is close to the air temperature outside of the compartment. With the single open vent, there were temperatures well above the exterior air temperature at only two locations, 1.9 m and 2.05 m (6.2 ft and 6.75 ft).

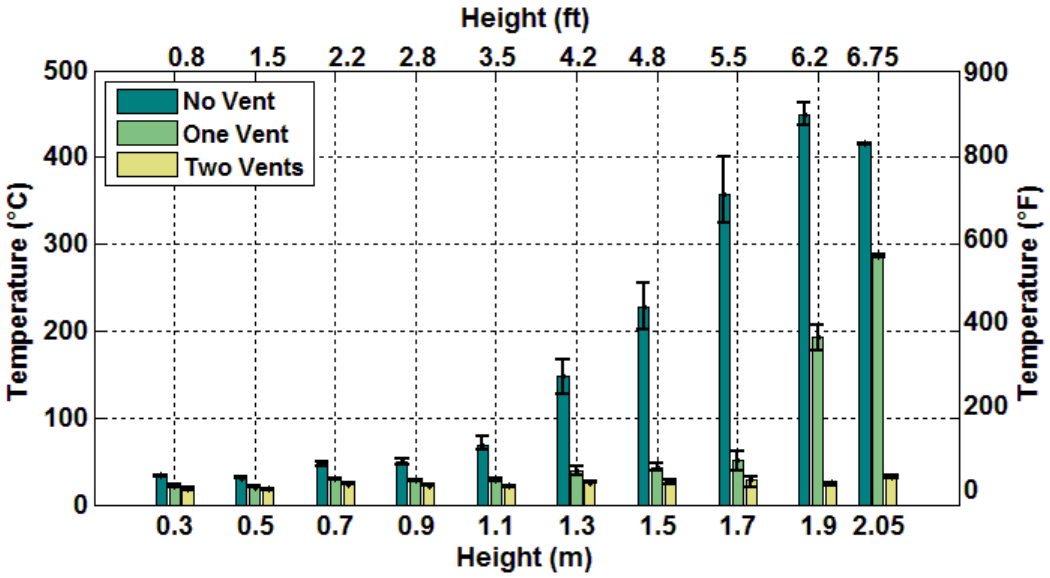

Figure 3-9: Mean steady state temperatures measured by the thermocouple array in the doorway versus the heights of the thermocouples in the array for the 1 MW fires. The error bars represent the range of the steady state temperatures.

When the fire sizes were set to 2 MW, the maximum mean steady state temperature was 600 °C (1,100 °F) with the vents closed, 450 °C (840 °F) with one open vent, and less than 100 °C (200 °F) with two open vents. With two open vents, the heat was fully exhausted out of the vent. Changing the conditions from no vent to one open vent, the temperatures decreased at heights of 1.1 m to 1.9 m (3.5 ft to 6.2 ft). The addition of the second vent reduced the remaining elevated mean steady state temperatures to reasonable temperatures.

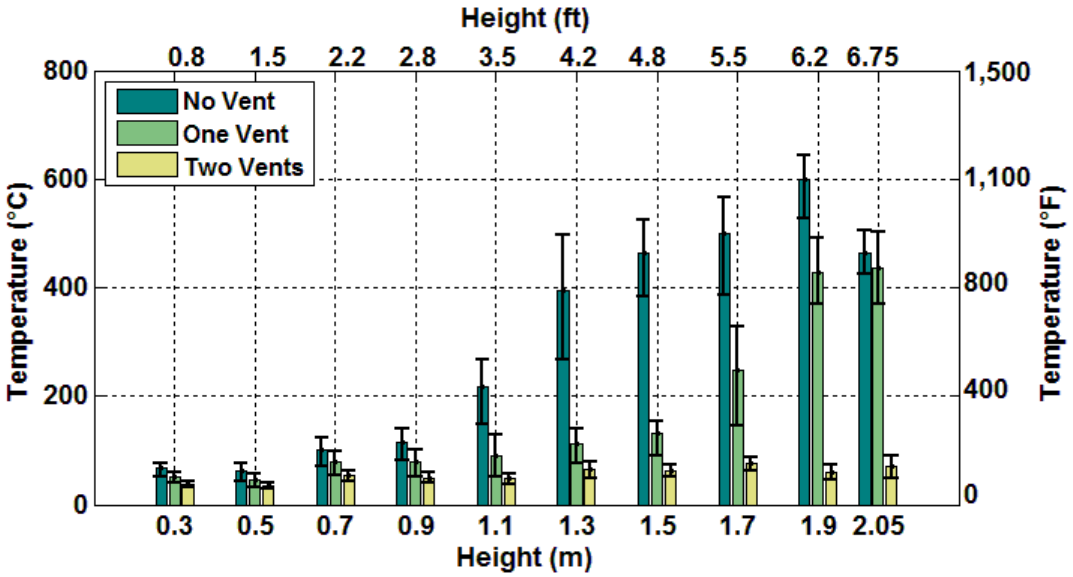

Figure 3-10: Mean steady state temperatures measured by the thermocouple array in the doorway versus the heights of the thermocouples in the array for the 2 MW fires. The error bars represent the range of the steady state temperatures.

3.2.3. Ceiling Vents

In Figure 3-11 through Figure 3-13 the steady state temperatures measured in the ceiling vents are plotted versus their locations for the 0.5 MW, 1 MW, and 2 MW fires. The location naming convention was depicted in Figure 2-12. Locations 1-5 were located in the vent closer to the fire and Locations 6-10 were in the vent closer to the doorway. In the 0.5 MW fires, the mean steady state gas temperature was about 300 °C (600 °F) across the vent shaft. With the burner side vent opened, the temperatures drop to between 100 °C and 200 °C (200 °F and 400 °F). This indicates that the temperature of the hot gas layer has been reduced. With the second vent open (the doorway side vent), the average temperatures then range between 100 °C and 150 °C (200 °F and 300 °F).

When a vent was closed, the average steady state temperatures were more uniform across that area of the vent shaft. When the vent was opened, there was variability in the temperature between the locations. This indicated that the hot gases were not evenly and most efficiently exiting the vent. Given that all of the mean steady state temperatures are well above the cold gases coming in the doorway, this means that hot gases were exiting throughout the entire area of the vent. The variability in the average steady state temperatures in an open vent was not so significant that a portion of the vent did not contribute to the improvement of the conditions in the room.

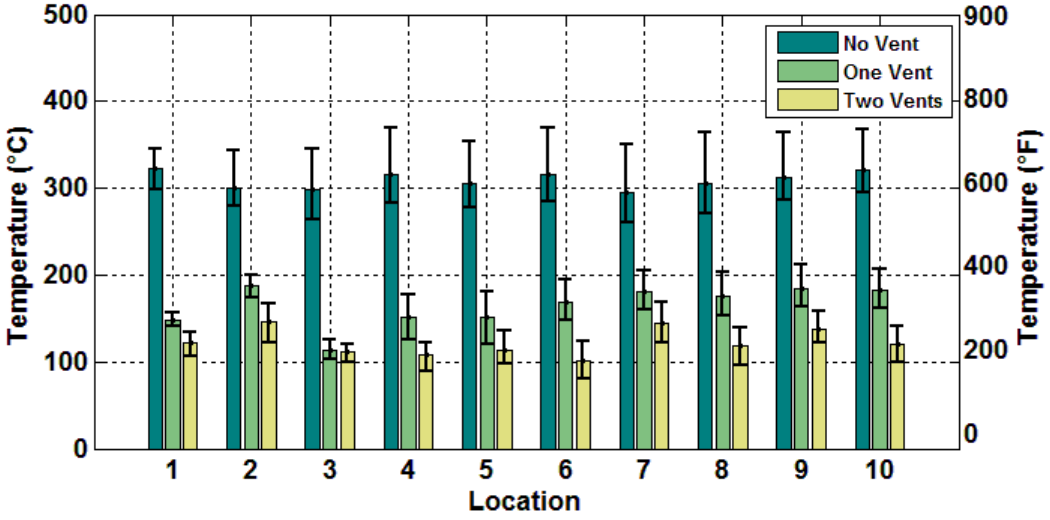

Figure 3-11: Mean steady state temperatures measured by the thermocouple array in the ceiling vents versus the locations of the thermocouples in the array for the 0.5 MW fires. The error bars represent the range of the steady state temperatures.

When the fire size was doubled to 1 MW, the average steady state temperatures increased to 500 °C to 550 °C (900 °F to 1020 °F) when the vents were closed. With one vent opened, the temperatures ranged between 150 °C and 350 °C (300 °F and 660 °F). The temperature range decreases to 150 °C and 250 °C (300 °F and 480 °F) when both vents were open.

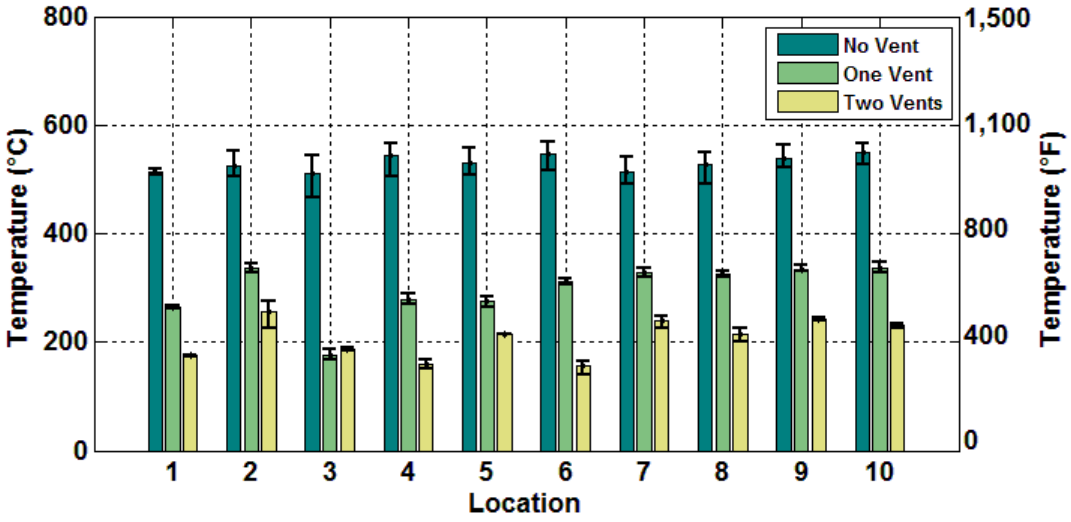

Figure 3-12: Mean steady state temperatures measured by the thermocouple array in the ceiling vents versus the locations of the thermocouples in the array for the 1 MW fires. The error bars represent the range of the steady state temperatures.

In Figure 3-13 the mean steady state temperatures for the 2 MW fires with the vents closed ranged 700 °C to 750 °C (1,300 °F to 1,380 °F). With one vent opened, the temperature range changed to 350 °C to 650 °C (660 °F to 1200 °F). With the addition of the second vent, it dropped to 350 °C to 550 °C (660 °F to 1020 °F).

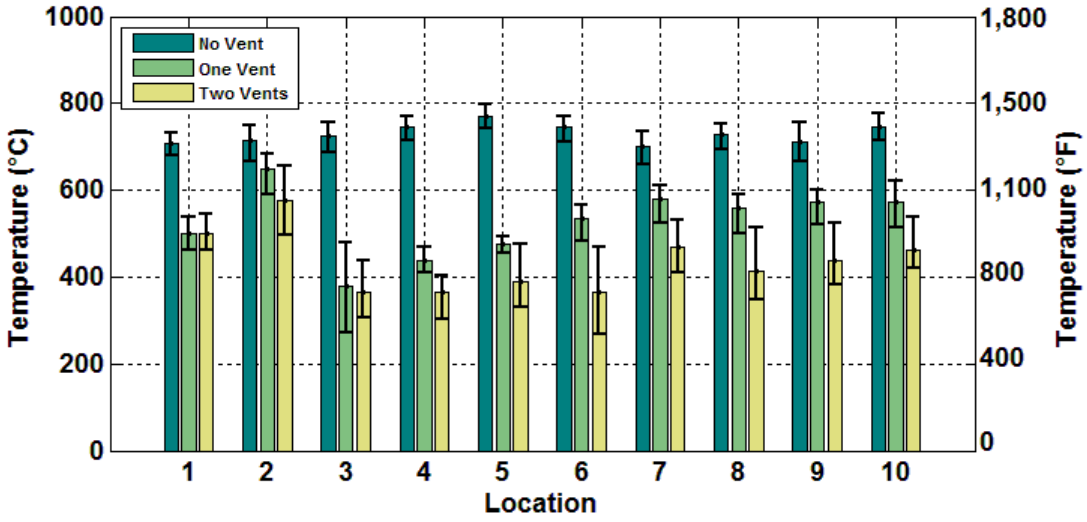

Figure 3-13: Mean steady state temperatures measured by the thermocouple array in the ceiling vents versus the locations of the thermocouples in the array for the 2 MW fires. The error bars represent the range of the steady state temperatures.

3.3. Heat Flux

The heat flux was measured at multiple locations on either side of the ceiling vent, described in Section 2.5. The mean steady state heat fluxes are presented in Figure 3-14, Figure 3-15, and Figure 3-16 for fire sizes of 0.5 MW, 1 MW, and 2 MW. The location names consist of three parameters: the side of the room the heat flux gauge was located (burner side, B, or doorway side, D), the height of the heat flux gauge in meters, and direction the heat flux gauge was facing (towards the ceiling, C, or towards the fire, F). In Figure 3-14, the average steady state heat fluxes are unaffected by the changing ventilation conditions. In these experiments, the measured heat fluxes did not change much (or at all) because natural gas produces very little soot when it burns and there was nothing else in the room to ignite. The heat fluxes spanned 3 kW/m^2 to 12 kW/m^2 (0.3 Btu/ft^2-s to 1.1 Btu/ft^2-s). The heat fluxes measured on the side of the room with the burner were greater than the heat fluxes on the doorway side because they were measured closer to the fire.

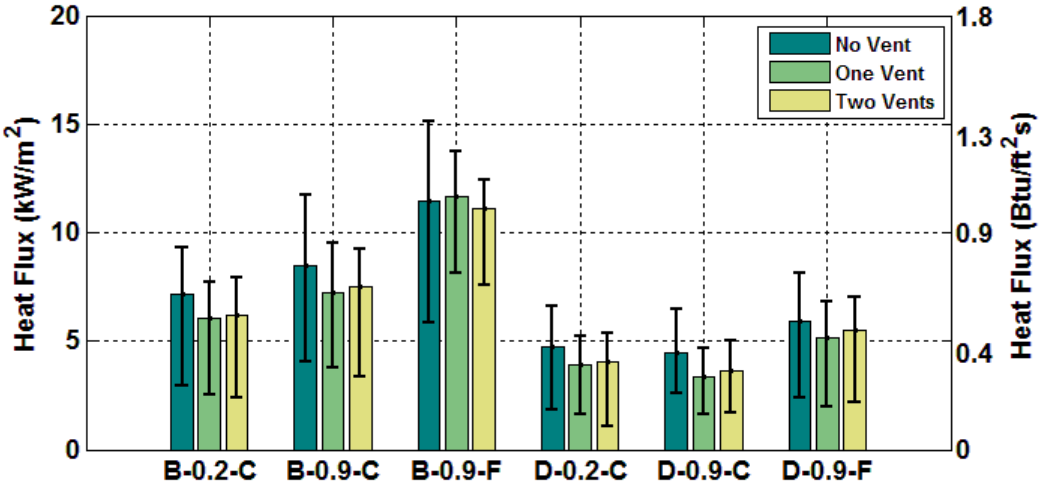

Figure 3-14: Mean steady state heat fluxes versus the locations of the heat flux gauges for the 0.5 MW fires. The error bars represent the range of the steady state heat fluxes.

In Figure 3-15, when the vents were closed the mean steady state heat fluxes were higher than when one vent and two vents were opened at B-0.9-F and at each of the locations on the doorway side of the room. The difference in heat flux at those locations between the no vent and one vent experiments spanned 5 kW/m^2 to 10 kW/m^2 (0.4 Btu/ft^2-s to 0.9 Btu/ft^2-s). There were no significant changes in the heat fluxes from experiments with one vent opened and two vents opened. At the remaining locations, the ventilation changes had no effect on the average steady state heat fluxes. The average steady state heat fluxes ranged from 5 kW/m^2 to 35 kW/m^2 (0.4 Btu/ft^2-s to 3.1 Btu/ft^2-s).

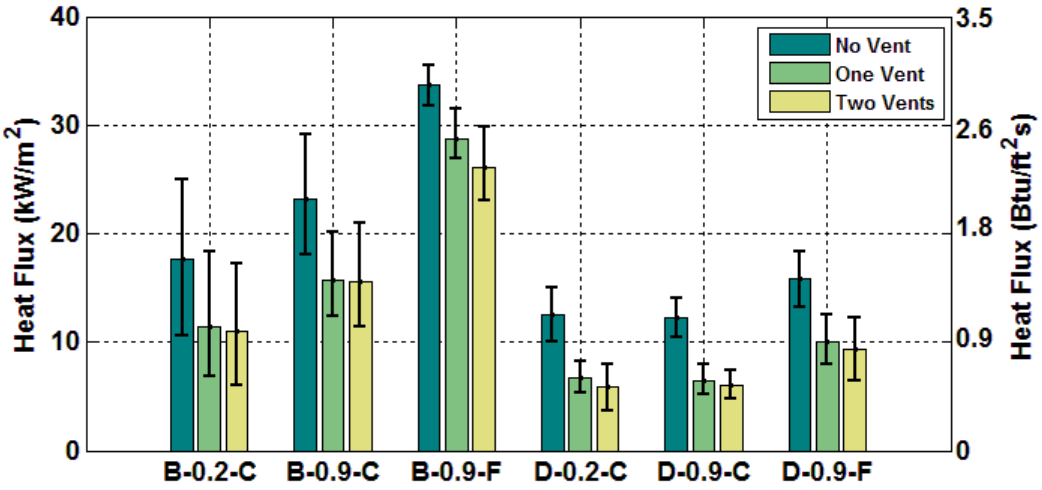

Figure 3-15: Mean steady state heat fluxes versus the locations of the heat flux gauges for the 1 MW fires. The error bars represent the range of the steady state heat fluxes.

While there were some changes in the mean steady state heat fluxes in the 1 MW experiments as the ventilation was changed, there were no changes in the 2 MW experiments as is seen in Figure 3-16. The mean steady state heat fluxes spanned from 15 kW/m^2 to 50 kW/m^2 (1.3 Btu/ft^2-s to 4.8 Btu/ft^2-s).

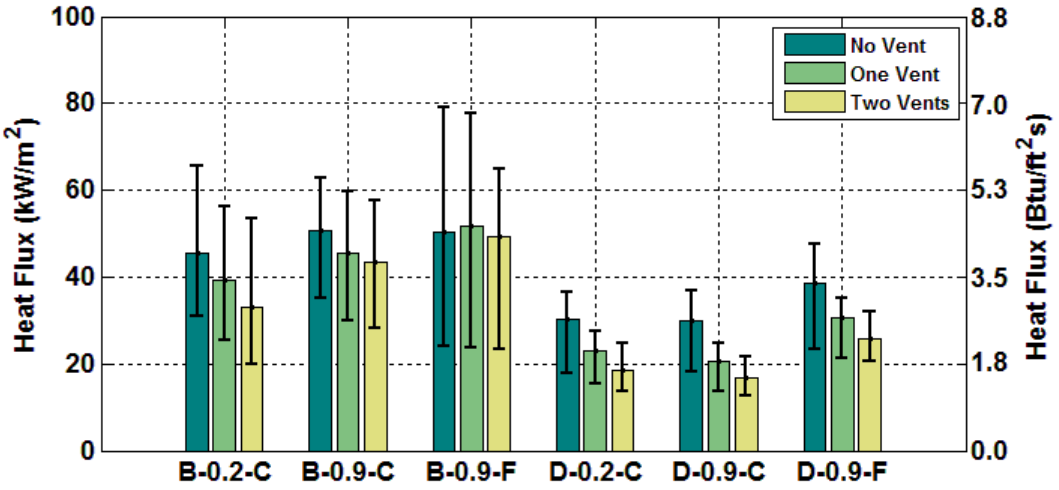

Figure 3-16 Mean steady state heat fluxes versus the locations of the heat flux gauges for the 2 MW fires. The error bars represent the range of the steady state heat fluxes.

3.4. Velocity

As a compartment fire develops, it consumes cool, oxygen rich air and releases a variety of hot gases. The hot gases are less dense than the cool air, which causes the hot gases to rise toward the ceiling and the cool air to stay low to the ground. The temperature difference begins a cycle of gas movement where hot gases rise and cool gases are pulled into the fire to replace them. Also, as the gases are heated, the gases expand. This causes the heated gases to move away from the fire faster than the cool gases come into the fire. In these experiments, the velocity was recorded in the doorway to determine at which heights the hot gases were exiting the room and cool air was entering the room, therefore identifying the location of the hot gas layer in the doorway. Velocities were also measured in the vent shaft to verify that the vents were exhausting the hot gases and to see how evenly distributed the velocities were across the vent. The direction of the gas movement in and out of a room can be determined from whether the velocity is positive or negative. In this report, when the velocity was positive the gases were exiting the room. When the velocity was negative, the gases were entering the room.

3.4.1. Doorway

The mean steady state velocities recorded in the doorway are provided for the 0.5 MW fires, 1 MW fires, and 2 MW fires in the next three figures. In Figure 3-17, when the vents were closed, the velocities below a height of 1.3 m (4.2 ft) were negative and the velocities above that height were positive. As discussed previously, below 1.3 m (4.2 ft) the cool air was being drawn into the room. Above this height, the hot gases exiting the room. In the lower half of the room, the average steady state velocities are less than 0.5 m/s (1 mph). In the hot gas layer, the velocity reached 3 m/s (7 mph). At 1.3 m (4.2 ft), there were both positive and negative velocities. This meant that in at least one of the 0.5 MW experiments, the velocity behaved like the upper layer with gases exiting the room and in at least one experiment the velocity at that location behaved like the lower layer entering the room. The dual behavior indicated that a height of 1.3 m (4.2 ft) was close to the interface between the layers. After the first vent was opened, all mean steady state velocities were negative, which meant that the vent was able to exhaust enough of the hot gases that none of the gases were exiting through the door. This contradicted the temperatures at the same location under the same vent condition (Figure 3-8). The temperatures were elevated near the top of the door indicting gas flow out the door. This difference was due to using bidirectional probes, which results in the velocities under 1 m/s (2 mph) being under-reported [36]. The addition of the second vent does not result in a significant change in any of the average steady state velocities. The average steady state velocity varied between 0.5 m/s (1 mph) to 2 m/s (4 mph) in magnitude in the experiment with one vent and two vents open.

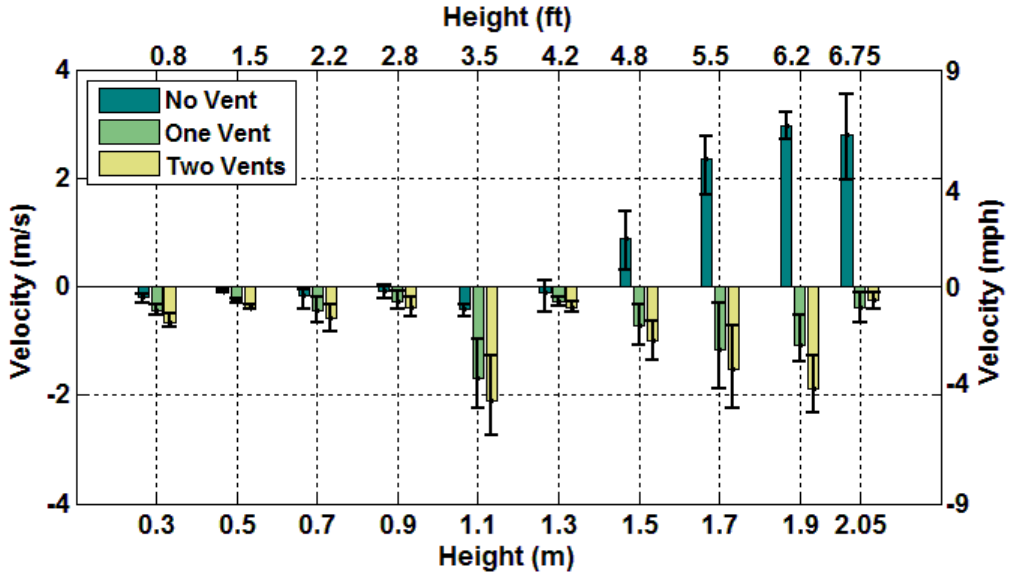

Figure 3-17: Mean steady state velocities measured in the doorway versus the heights of the measurements for the 0.5 MW fires. The error bars represent the range of the steady state velocities.

In Figure 3-18, the mean steady state velocities are shown for the 1 MW fires. When both ceiling vents were closed, the mean steady state velocities above 1.3 m (4.2 ft) were all positive and below 1.1 m (3.5 ft) were all negative. At the two heights in between, there were both negative and positive values indicating the approximate location of the transition point between the gases entering and exiting the room. In the upper layer the average steady state velocity reached 4.5 m/s (10 mph), while in the lower layer the velocity never exceeded 0.5 m/s (1 mph). The opening of the first vent resulted in all negative mean steady state velocities at every location except for 1.9 m (6.2 ft). In at least one experiment, a positive velocity was recorded. This meant that the hot gases were beginning to confirm that the hot gases were not fully exhausting from the vent. With the second vent opened, all of the velocities are negative. The highest magnitude mean steady state velocity was almost 2 m/s (4 mph) with one open vent and 2.5 m/s (6 mph) for two open vents.

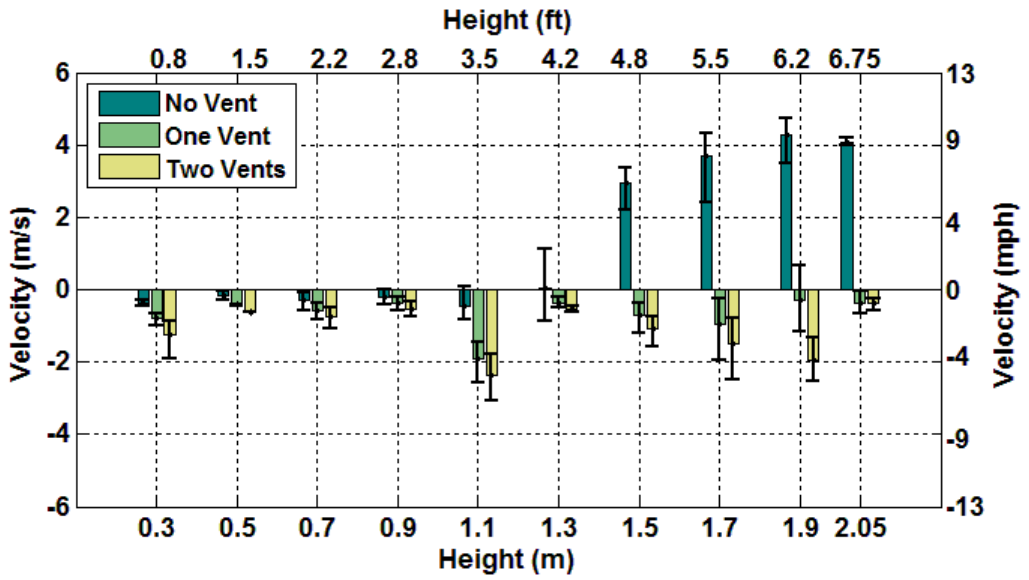

Figure 3-18: Mean steady state velocities measured in the doorway versus the heights of the measurements for the 1 MW fires. The error bars represent the range of the steady state velocities.

When the fire size was doubled again to 2 MW and the vents were closed (Figure 3-19), the behavior was similar to the corresponding velocities with a fire size of 1 MW. The mean steady state velocities below 1.1 m (3.5 ft) were negative and above 1.3 m (4.2 ft) were positive. At 1.1 m and 1.3 m (3.5 ft and 4.2 ft), there were both positive and negative values, indicating the approximate location of the transition between the upper and lower layers. The maximum mean steady state velocity of the gases entering the doorway was less than 1 m/s (2 mph) and reached 5 m/s (11 mph) for the gases exiting the doorway. With one vent open, gases were still exiting the room at 1.9 m and 2.05 m (6.2 ft and 6.75 ft) with a maximum mean steady state velocity of 1.5 m/s (3 mph). The transition height existed at about 1.7 m (5.5 ft). The maximum average steady state velocity of the gases entering the doorway was above 2 m/s (4 mph). With two vents open, only cool air entered the doorway and all of the hot gases were exhausted out of the vents. The highest mean steady state velocity of the gases entering the doorway was 3 m/s (7 mph).

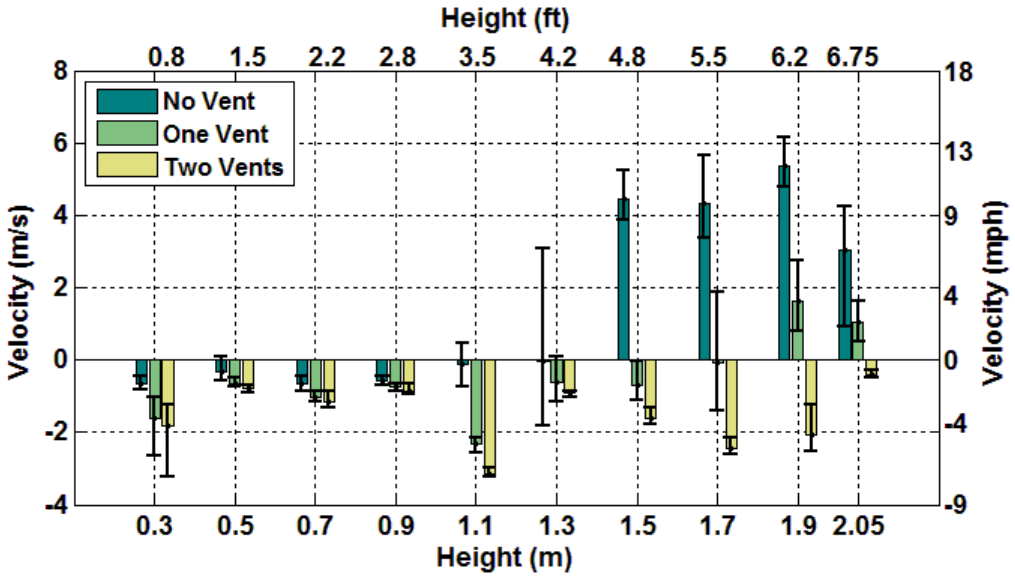

Figure 3-19: Mean steady state velocities measured in the doorway versus the heights of the measurements for the 2 MW fires. The error bars represent the range of the steady state velocities.

3.4.2. Ceiling Vents

The mean steady state velocities measured in the ceiling vents are provided in Figure 3-20 - Figure 3-22 for the 0.5 MW, 1 MW, and 2 MW fire sizes. When the vents were closed, the velocities measured in the vent for all of the fire sizes provided a baseline for comparison to evaluate the changes in gas velocity that resulted from changes in the ventilation. Any negative mean steady state velocities that were recorded were located under a closed vent as a result of the gas moving up the vent shaft encountering the closed vent door and mixing back into the room.

In Figure 3-20, the mean steady state velocities ranged from less than -1 m/s to just less than 1.5 m/s (-2 mph to 3.4 mph). With one vent opened, the range changed to a range from -0.5 m/s to almost 3.5 m/s (-1 mph to 7.8 mph). The velocities in the open vent spanned 1 m/s to 3.5 m/s (2 mph to 7.8 mph). When both vents were opened, the velocities measured were above 0.5 m/s and below 2.5 m/s (1.1 mph and 5.6 mph). In the one vent and two vent opened cases, all of the mean steady state velocities are positive where the vent or vents were opened, confirming both ventilation conditions were contributing to exhausting the hot gas layer. During the one vent and two vents opened experiments, the highest velocity was recorded at Location 2, which was the location closest to the fire. The velocity at Location 2 also varied from the velocities at the other locations much more than any other two locations for both the one open vent and two open vent experiments. As was indicated by the temperatures recorded in the vents in Section 3.2.3, the hot gases were not evenly exhausting across the vent. Excluding Location 2, the variation between the locations was much smaller. The velocities ranged from 1 m/s to 1.5 m/s (2 mph to 3.4 mph) in the open vent for the one vent experiments and 0.5 m/s to 1.5 m/s (1.1 mph to 3.4 mph) in the two open vent experiments.

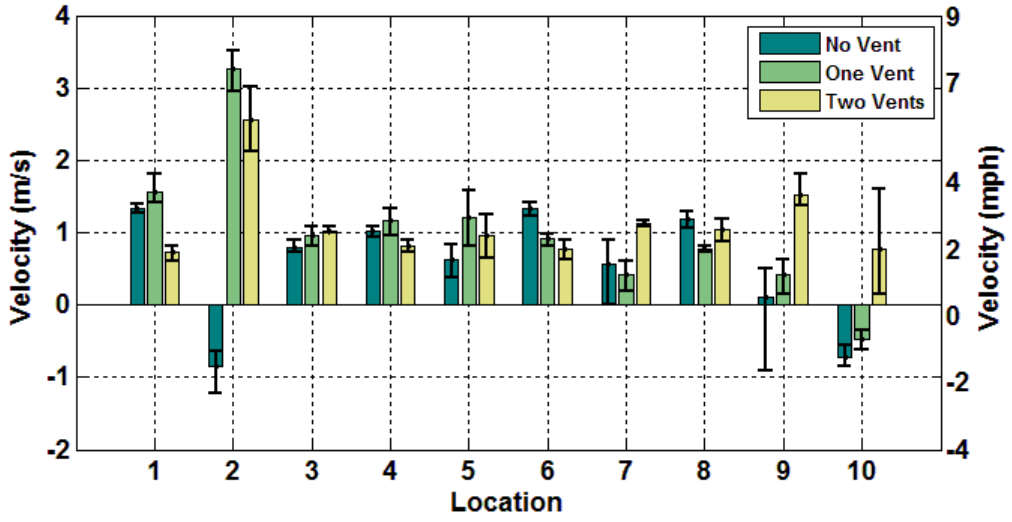

Figure 3-20: Mean steady state velocities measured in the ceiling vents versus the locations of the measurements for the 0.5 MW fires. The error bars represent the range of the steady state velocities.

In Figure 3-21 when the vents were closed in the 1 MW fires, the mean steady state velocities in the ceiling vent spanned from less than -1 m/s to above 2 m/s (-2 mph to 4 mph). With one vent open, the velocities ranged from -1 m/s to 5 m/s (-2 mph to 11 mph). With both vents opened, the velocities ranged from just less than 1 m/s to above 4 m/s (2 mph to 9 mph). Excluding the noticeable outlier, Location 2, the range of mean steady state velocities in the open vent in the experiments with one open vent was 1.5 m/s to 3 m/s (3.4 mph to 7 mph). Removing the Location 2 velocity, the velocity range was reduced to just less than 1 m/s to just above 2 m/s (2 mph to 4 mph) when both vents were opened.

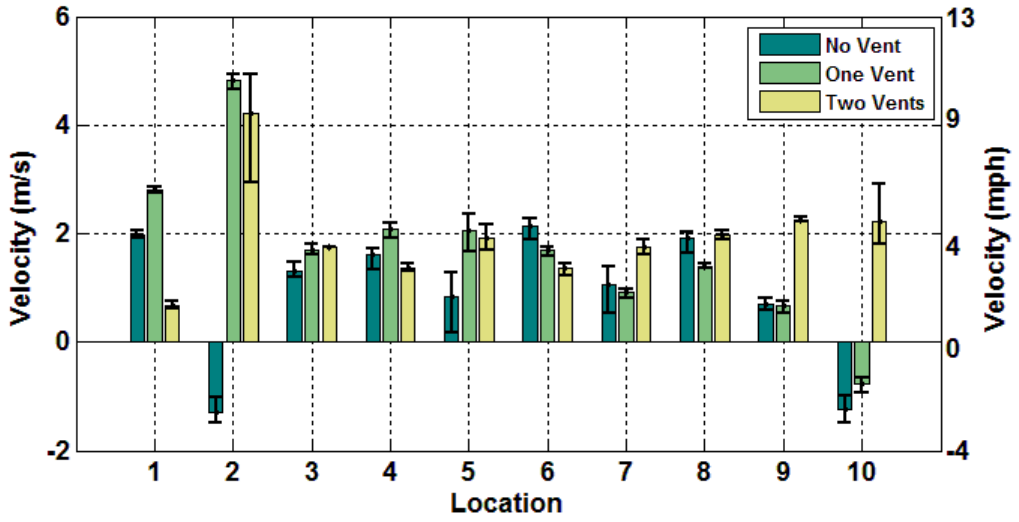

Figure 3-21: Mean steady state velocities measured in the ceiling vents versus the locations of the measurements for the 1 MW fires. The error bars represent the range of the steady state velocities.

In Figure 3-22, the fire size was doubled to 2 MW. When the vents were closed, the mean steady state velocities varied from less than -1 m/s to almost 3 m/s (-2 mph to 7 mph). The addition of one vent shifted the range to -1 m/s to 7 m/s (-2 mph to 16 mph). Excluding the locations in the closed vent, the range became 3 m/s to 7 m/s (7 mph to 16 mph). The range was 1 m/s to above 6 m/s (2 mph to 13 mph) with both vent opened.

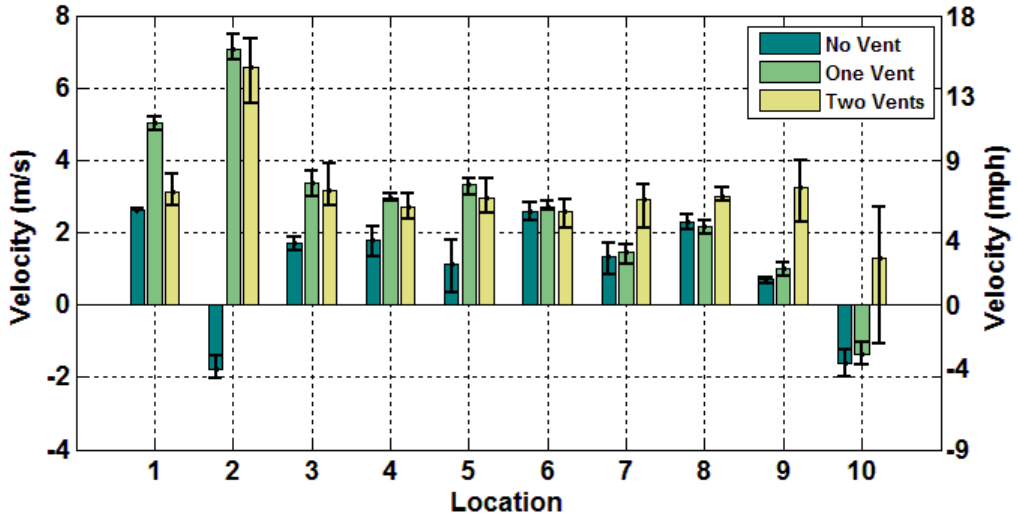

Figure 3-22: Mean steady state velocities measured in the ceiling vents versus the locations of the measurements for the 2 MW fires. The error bars represent the range of the steady state velocities.

4. Natural Gas Experiments vs. FDS Simulations

The Fire Dynamics Simulator (FDS) is a computer program developed by NIST to simulate the growth of a fire and the movement of smoke and heat through space and time based on input from a user. The input relates to such aspects as the location of objects, properties of the objects, fuel, measurement instrumentation, atmospheric conditions, and resolution of the calculations. The equations that determine the fluid movement in the simulations are the Navier-Stokes equations. Given input from the user, FDS is able to solve the equations through space and time. FDS outputs files numerically describe changes that occur. Software, called Smokeview (also developed by NIST), provides a visual simulation of the results provided by FDS. The measurement instrumentation can be included in the simulation to output measurements that are comparable to actual experiments.

FDS has been extensively verified and validated. "Verification is a check of the math, while Validation is a check of the physics" [37]. FDS is validated by comparing the simulation results to experimental results. Through verification and validation, the developers can determine how accurate the model is and what areas need the most improvement. FDS has been validated with numerous experiments using liquid fuel fires in a single room [38] but has not been validated for a vertical vent in a room with a gaseous fuel fire. This report is intended to, in part, determine the similarities and differences between the simulations and the natural gas experiments conducted here.

The dimensions and materials of the room and fuel and locations of the measurement instrumentations in the simulation identically matched those of the experiments with two exceptions. Given that the wooden frame of the room made minimal contact with the gypsum wallboard, its impact on the heat transfer through the wallboard was disregarded. The wooden frame was excluded from the simulation.

Given that the natural gas used in the experiments was greater than 94% methane (Natural Gas Composition & Properties), the gaseous fuel used in the simulation was given the properties of methane. The only materials used in the experiments were gypsum wallboard and cement board. The input parameters for the materials are presented in Table 4-1.

Table 4-1: FDS material input parameters

Gypsum Wallboard			
Thermal conductivity	0.16 W/m-K	1.1 Btu-in/ft^2-hr-°F	[39]
Density	676.0 kg/m^3	42.2 lb/ft^3	[39]
Specific heat	1.09 kJ/kg-K	0.260 Btu/lb-°F	[40]
Cement Board			
Thermal conductivity	0.183 W/m-K	1.27 Btu-in/ft^2-hr-°F	[41]
Density	923.0 kg/m^3	57.6 lb/ft^3	[41]
Specific heat	0.84 kJ/kg-K	0.201 Btu/lb-°F	[40]

Four FDS simulations were run. The input files are provided in Appendix C. Each simulation represented one set of continuously run experiments, such that the first FDS file represents Experiments 1-10 as mentioned in Section 3. The timing of HRR and vent changes in the simulations was set to match the experiments. The HRR used in the simulation was the gas flow based HRR because it was a more accurate method of measuring the HRR (See the uncertainties in Section 2.6). All of the FDS steady-state values shown in this report were collected from the output of the four simulations. The values were assembled from the last 90 s of data, before a vent was opened or closed or the fire size was changed. The last 90 s of data were averaged to create one steady-state value. The FDS simulations may or may not have been at steady state as defined in Section 3.

The FDS simulations were given a grid cell size of 10 cm. The grid cell size refers to the resolution of FDS's calculations. The area included in each simulation was divided into 10 cm × 10 cm × 10 cm cubes. In every simulation, FDS makes calculations representing each block in the simulation area and passes changing information to other blocks so those calculations can be conducted and the results can be appropriately adjusted with time. Making the grid cell size smaller relative to the simulation area increases the spatial resolution of a simulation. The cost of increasing the resolution is that it increases the number of calculations that need to be performed. This means that the simulation takes more time to run on the computer. A simulation with a very small grid could take months to run. Generally, that amount of resolution is not necessary or not necessary throughout the entirety of the simulation space for a room fire calculation. The difference in temperature estimates between a 10 cm, 20 cm, and a 40 cm grid cell can be seen in Figure 4-1. The simulated temperature output for the 40 cm varied noticeably from the 20 cm and much less so between 20 cm and 10 cm. If the cell size was reduced more, the difference between the temperatures produced from the 10 cm cell size would vary even less from the new cell size. Because the difference between the 10 cm cell size and any smaller grid cell size would be small, it would not be worth the significantly greater run time of the simulation with the smaller cell size. For that reason, a 10 cm grid cell size was chosen.

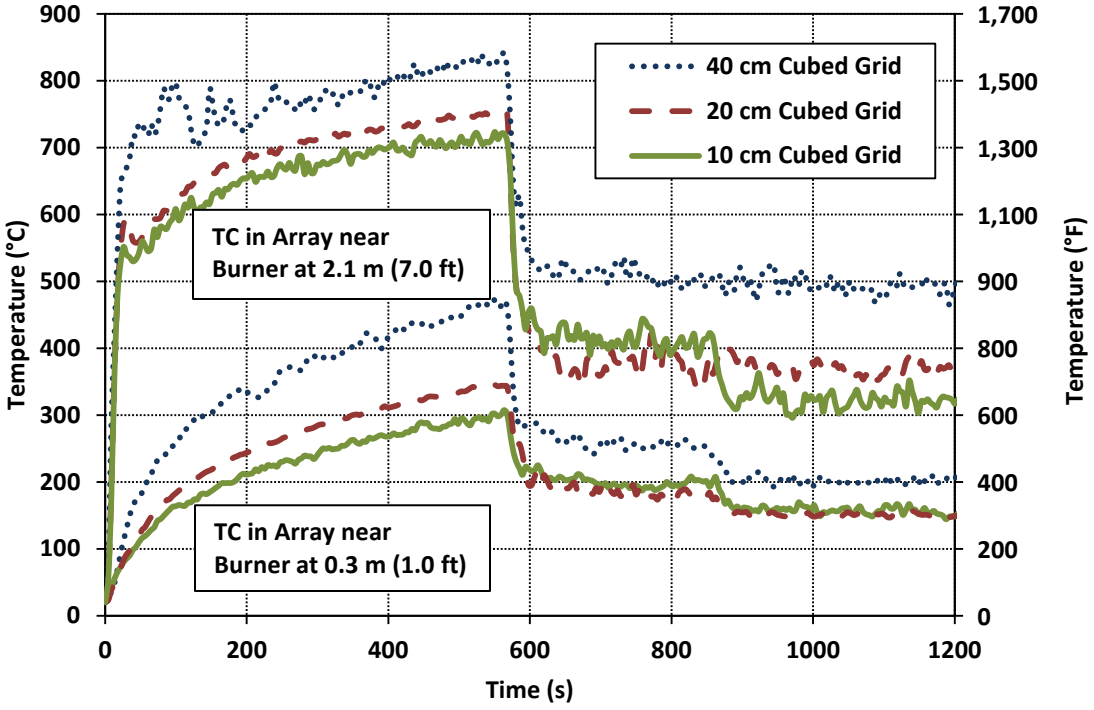

Figure 4-1: Temperature over time for two thermocouples near the burner, one at a height of 0.3 m (1.0 ft) and another at 2.1 m (7.0 ft), produced by three different FDS simulations each with the grid cell sizes - 10 cm, 20 cm, and 40 cm

In this section, the steady state data from the simulations is plotted against the steady state data from the experiments. The black line in the plots is where the data point would be if the results of the simulations perfectly matched the experiments. The dotted black lines indicate the expanded measurement uncertainty presented in Section 2.6 about the ideal model prediction. The data points that fall between the dotted lines are within the uncertainty and are considered to be correctly simulated by FDS. When the data points fall below the lines, FDS has under-predicted the data points, meaning FDS reported the values to be less than what was actually measured in the experiments. If the data points are above the lines, the data points were over-predicted by FDS (the simulated data point was greater than the value measured in the experiment).

4.1. Temperature

In the following sections, the temperature measurements within the room and in the openings to the room from the experiments that were collected in the natural gas experiments are compared to those produced by the FDS simulations.

4.1.1. Interior

The following three figures display the steady state simulation temperatures over the steady state experiment temperatures at the thermocouple array near the burner when the vents were closed, one vent was open, and two vents were open. In Figure 4-2 when the vents were closed, FDS over-predicted some of the temperatures at a height of 1.5 m (5.0 ft) and below. The temperatures were under-predicted by the simulations at a height of 2.1 m (7.0 ft) and 2.37 m (7.9 ft). The simulation temperatures were at most 50 °C (120 °F) less or more than the uncertainty in the measured temperatures.

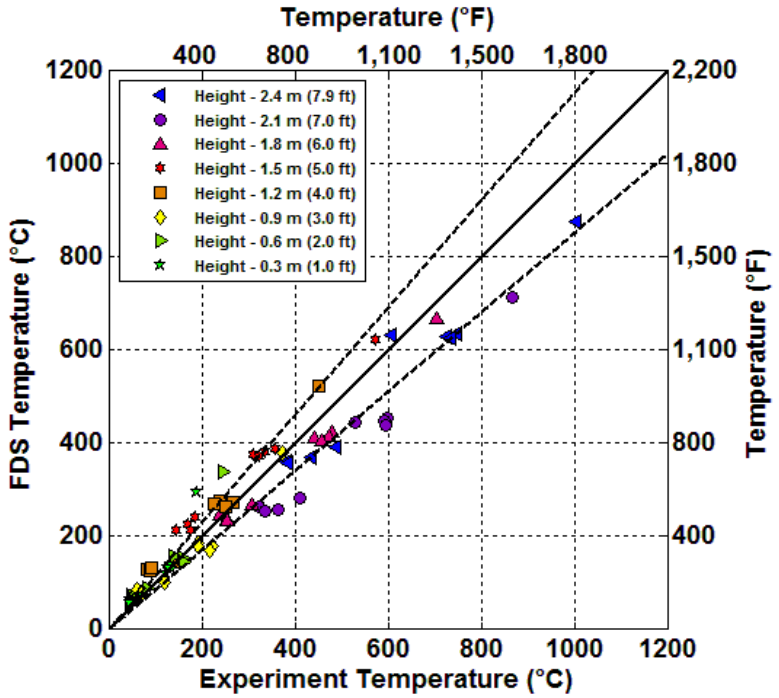

Figure 4-2: Steady state simulation temperatures versus the steady state natural gas experiment temperatures from the thermocouple array near the burner when both vents were closed. The dotted lines represent the expanded measurement uncertainty presented in Section 2.6 about the ideal model prediction.

Figure 4-3 shows the steady state temperatures when one vent was open. With one vent open, there was minimal over-prediction. However, above 300 °C (600 °F) in the experiments, all of the steady state temperatures are under-predicted by the simulations. The greatest deviation from the measurement uncertainty was 200 °C (400 °F) near the ceiling. This meant that the actual steady state temperature was at least 200 °C (400 °F) greater than what the steady state temperature was in the simulations.

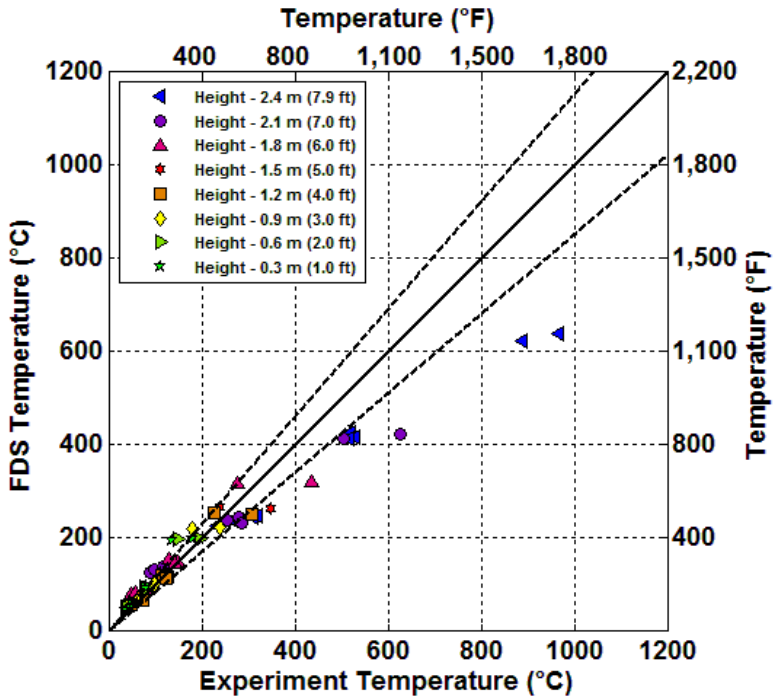

Figure 4-3 Steady state simulation temperatures versus the steady state natural gas experiment temperatures from the thermocouple array near the burner when one vent was open. The dotted lines represent the expanded measurement uncertainty presented in Section 2.6 about the ideal model prediction.

As in the previous figure, Figure 4-4 shows minimal over-prediction of the steady state temperatures by FDS, but as the steady state temperature increased above 200 °C (400 °F) in the experiments FDS increasingly under-predicted the temperatures. Near the ceiling when the steady state experiment temperature was about 1000 °C (1,800 °F), FDS was reporting temperatures at 500 °C (900 °F). This was 300 °C (600 °F) less than what can be attributed to the uncertainty of the measurement.

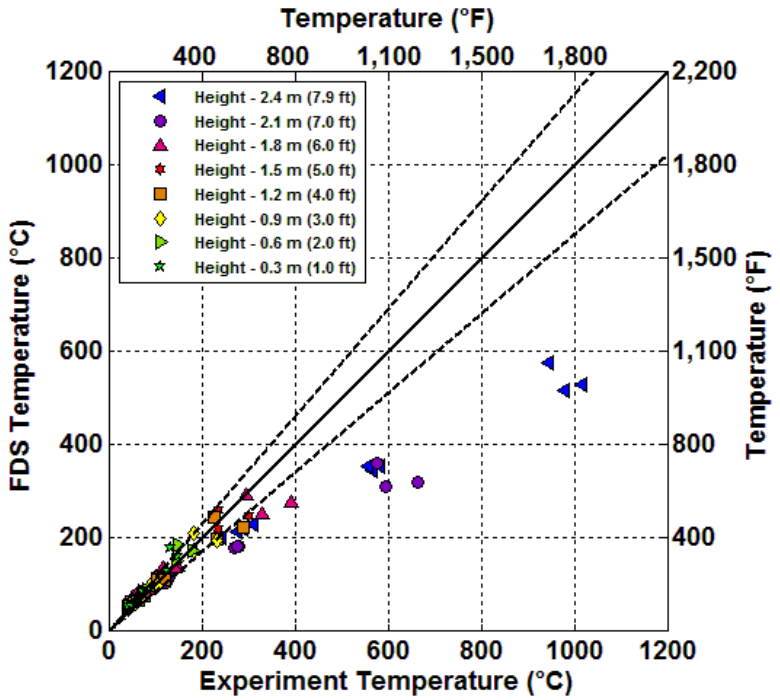

Figure 4-4: Steady state simulation temperatures versus the steady state natural gas experiment temperatures from the thermocouple array near the burner when both vents were open. The dotted lines represent the expanded measurement uncertainty presented in Section 2.6 about the ideal model prediction.

In Figure 4-5, Figure 4-6, and Figure 4-7, the steady state temperatures recorded by the thermocouple array near the doorway are compared to the steady state simulation temperatures when the vents were closed, one vent was open, and two vents were open. When the vents were closed, almost none of the steady state temperatures were under-predicted. All of the steady state temperatures at 1.2 m (4.0 ft) and most of the steady state temperatures at 2.4 m (7.9 ft) were over-predicted by the simulation. At 1.2 m (4.0 ft), there was likely a discrepancy in the simulation where the hot gas layer ended and the cooler lower layer of gases began from where it actually was located in the experiments. In the simulation, the steady state temperatures at 1.2 m (4.0 ft) behaved like the hotter, upper layer, while in the experiments the steady state temperatures behaved like the cooler, lower layer. The highest over-prediction was about 160 °C (320 °F) difference in temperature. Most of the over-predicted steady state temperatures were less than 80 °C (180 °F) different from the experiments.

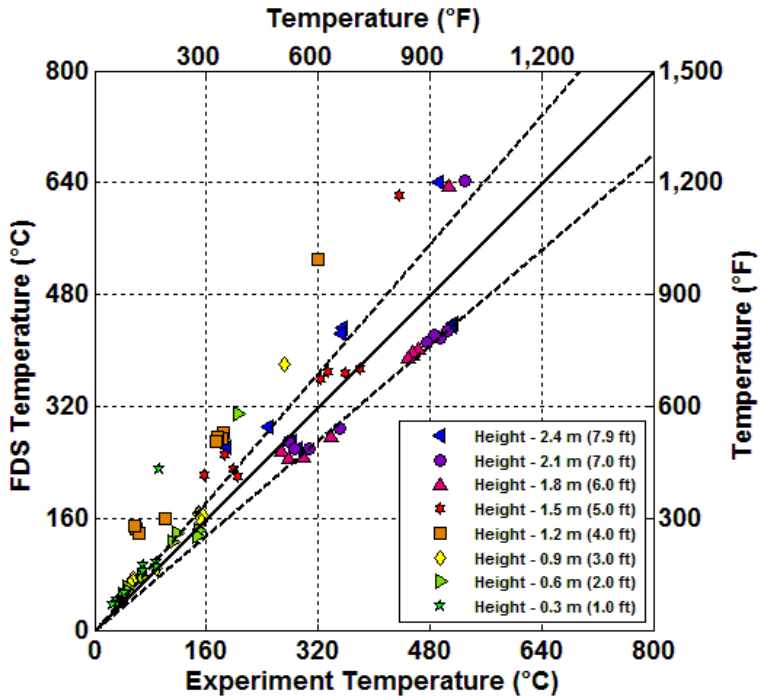

Figure 4-5: Steady state simulation temperatures versus the steady state natural gas experiment temperatures from the thermocouple array near the doorway when both vents were closed. The dotted lines represent the expanded measurement uncertainty presented in Section 2.6 about the ideal model prediction.

In Figure 4-6 when one vent was open, the simulations over-predicted some of the steady state temperatures. At the thermocouple closest to the ceiling, a number of the steady state temperatures were over-predicted. The greatest discrepancy between the simulations and the experiments was about 200 °C (400 °F). Most of the over-predicted values had a discrepancy less than 40 °C (100 °F).

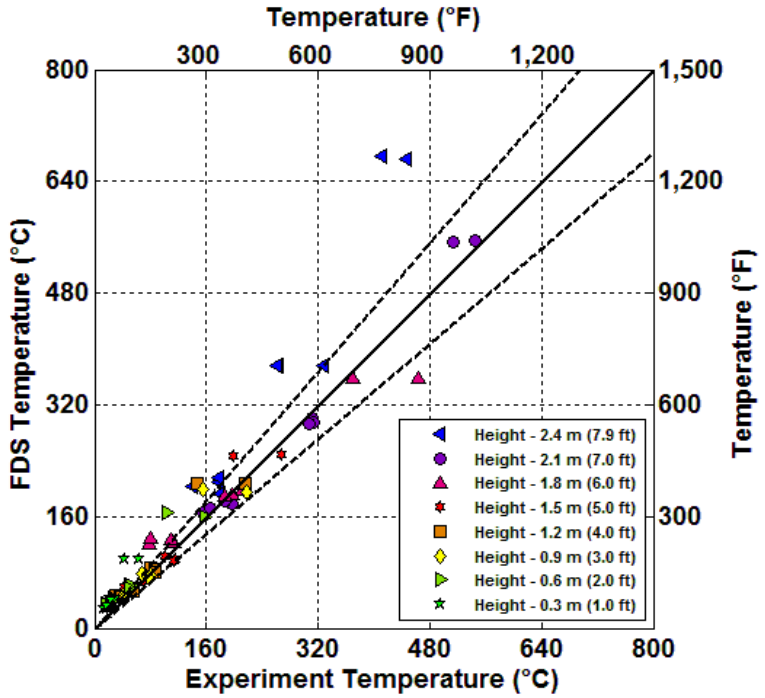

Figure 4-6: Steady state simulation temperatures versus the steady state natural gas experiment temperatures from the thermocouple array near the doorway when one vent was open. The dotted lines represent the expanded measurement uncertainty presented in Section 2.6 about the ideal model prediction.

When two vents were opened, again there were almost no under-predictions of the temperature (Figure 4-7). The higher temperatures recorded at 2.4 m (7.9 ft) were over-predicted by as much as 200 °C (400 °F). At 0.9 m (3.0 ft) and below the steady state temperatures were mostly over-predicted. The majority of the over-predicted simulation values varied less than 40 °C (100 °F) from the experiments.

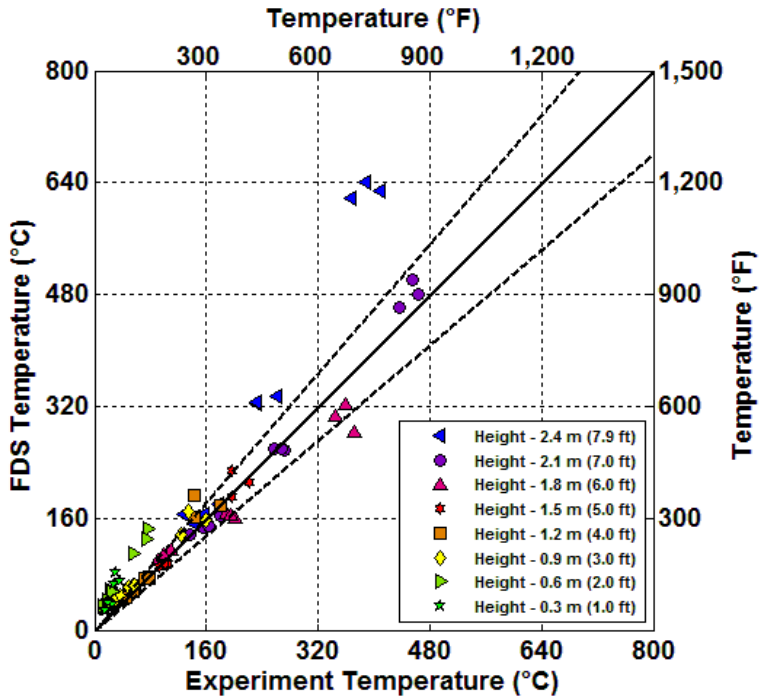

Figure 4-7 Steady state simulation temperatures versus the steady state natural gas experiment temperatures from the thermocouple array near the doorway when both vents were open. The dotted lines represent the expanded measurement uncertainty presented in Section 2.6 about the ideal model prediction.

4.1.2. Doorway

The experimental steady state temperatures from the doorway when the vents were closed, one vent was open, and two vents were open are plotted versus the simulation steady state temperatures in Figure 4-8, Figure 4-9, and Figure 4-10. When both vents were closed, the steady state temperatures from 0.5 m to 1.5 m (1.5 ft to 4.8 ft) were over-predicted by the simulations. The greatest discrepancy between the experimental and simulated steady state temperatures was about 200 °C (400 °F) at 1.3 m (4.2 ft). At the three highest locations almost all of the steady state temperatures from the experiments matched the temperatures from the simulations. Almost none of the steady state temperatures were under-predicted by the simulations.

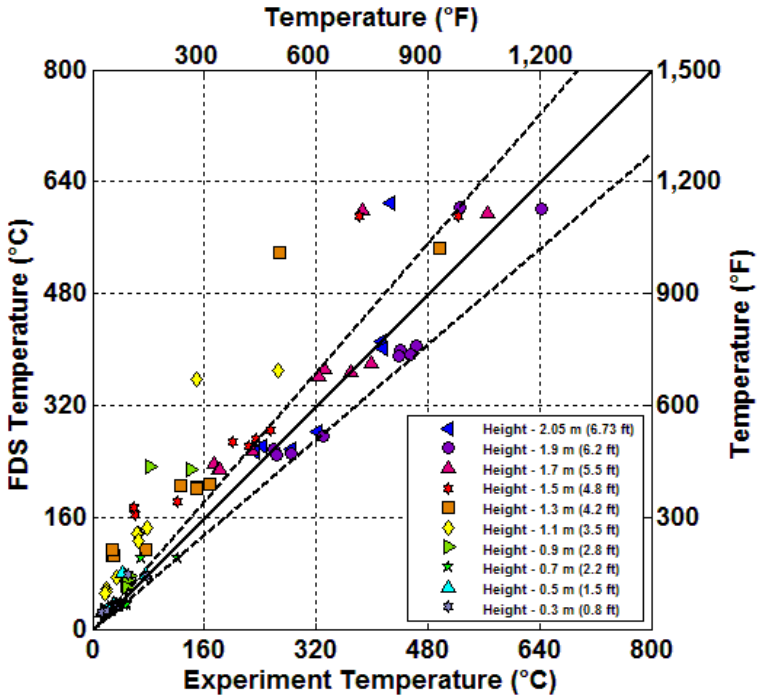

Figure 4-8: Steady state simulation temperatures versus the steady state natural gas experiment temperatures from the thermocouple array in the doorway when both vents were closed The dotted lines represent the expanded measurement uncertainty presented in Section 2.6 about the ideal model prediction.

In the figure below, the simulations both over-predicted and under-predicted the experiment steady state temperatures in the doorway when one vent was open. When the fire size was 0.5 MW, the steady state temperatures at 1.9 m and 2.05 m (6.2 ft and 6.73 ft) were over-predicted. The steady state temperatures were over-predicted by no more than 100 °C (200 °F). Overall there was much less over-prediction with the addition of the vent. However, there was some under-prediction from a height of 0.7 m to 1.7 m (2.2 ft to 5.5 ft) by as much as 100 °C (200 °F).

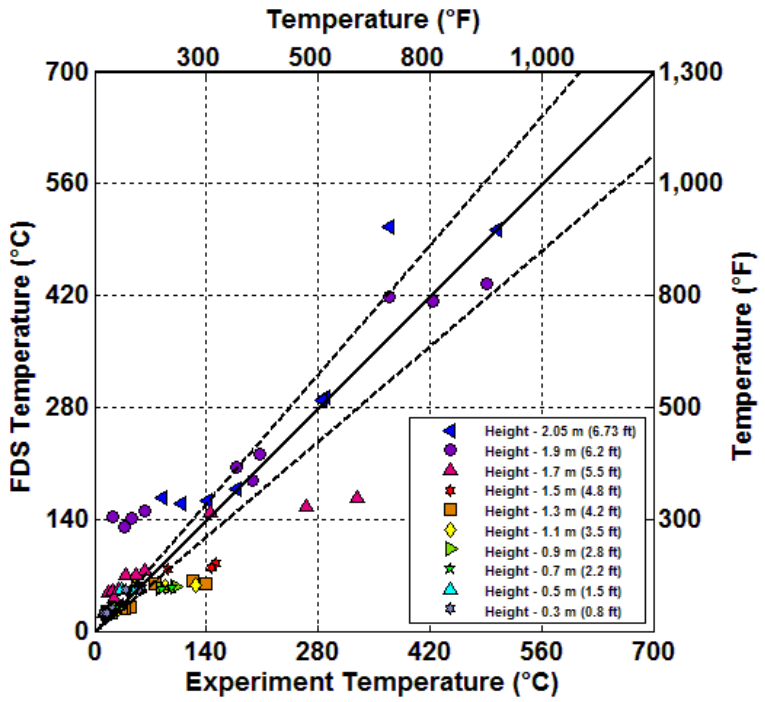

Figure 4-9: Steady state simulation temperatures versus the steady state natural gas experiment temperatures from the thermocouple array in the doorway when one vent was open. The dotted lines represent the expanded measurement uncertainty presented in Section 2.6 about the ideal model prediction.

In Figure 4-10, the simulations mildly under-predicted some steady state temperatures at heights of 0.7 m to 1.5 m (2.2 ft to 4.8 ft) when two vents were open. At most, the values were under-predicted by 25 °C (77 °F). At the two highest locations, all of the values were over-predicted. The steady state temperatures were severely over-predicted during the 2 MW fires at those heights. The simulations over-predicted the steady state temperatures by as much as 300 °C (600 °F). In the simulations, hot gases are coming out the doorway still while in the experiments the hot gases are fully exhausted by the two vents.

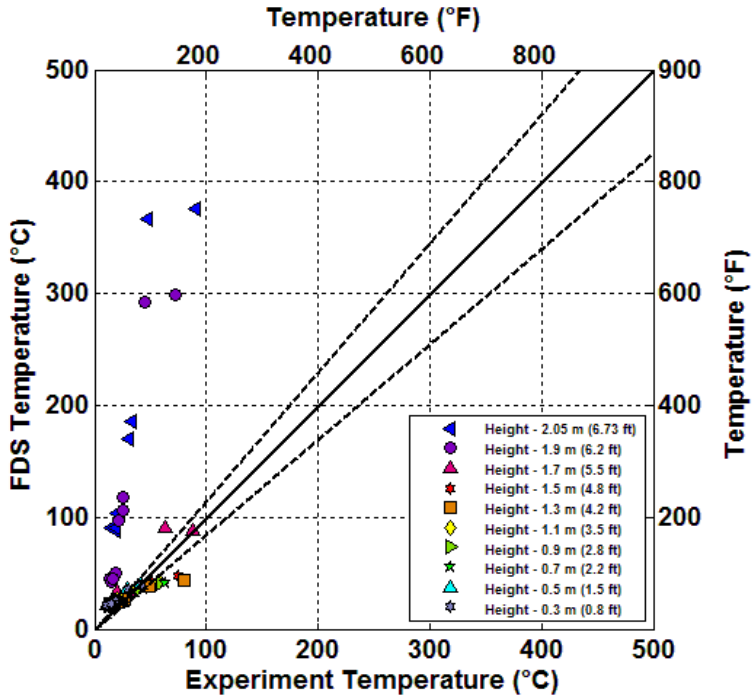

Figure 4-10: Steady state simulation temperatures versus the steady state natural gas experiment temperatures from the thermocouple array in the doorway when both vents were open. The dotted lines represent the expanded measurement uncertainty presented in Section 2.6 about the ideal model prediction.

4.1.3. Ceiling Vents

Figure 4-11, Figure 4-12, and Figure 4-13 show the experiment steady state temperatures versus the simulation steady state temperatures in the ceiling vent shaft when the vents were closed, one vent was open, and two vents were open. The first five locations were located in the half of the vent near the burner, which was the first vent opened. The last five locations were in the half of the vent closer to the doorway and were under the second vent door that was opened. When both vents were closed, almost all of the steady state temperatures were accurately predicted by FDS within the expanded measurement uncertainty. Some of the values were slightly under-predicted by no more than 25 °C (77 °F). No values were over-predicted.

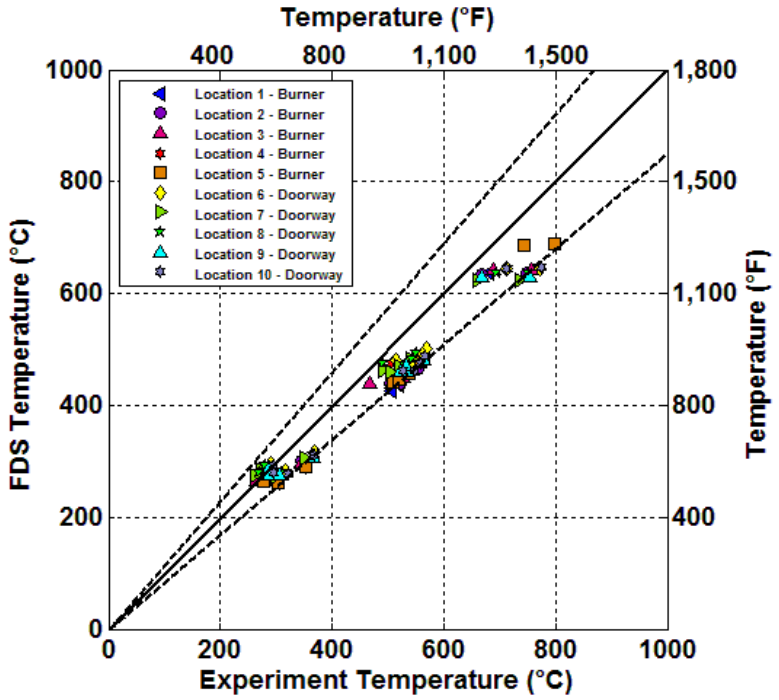

Figure 4-11: Steady state simulation temperatures versus the steady state natural gas experiment temperatures from the thermocouples in the ceiling vents when both vents were closed. The dotted lines represent the expanded measurement uncertainty presented in Section 2.6 about the ideal model prediction.

In Figure 4-12 when one vent was open, there were a few over-predicted and under-predicted steady state temperatures, but most of the temperatures were accurately simulated by FDS. Only four temperatures were over-predicted. More temperatures were under-predicted but most were under-predicted by 20 °C (70 °F) or less. The greatest deviation from the experiment steady state temperatures was about 120 °C (250 °F).

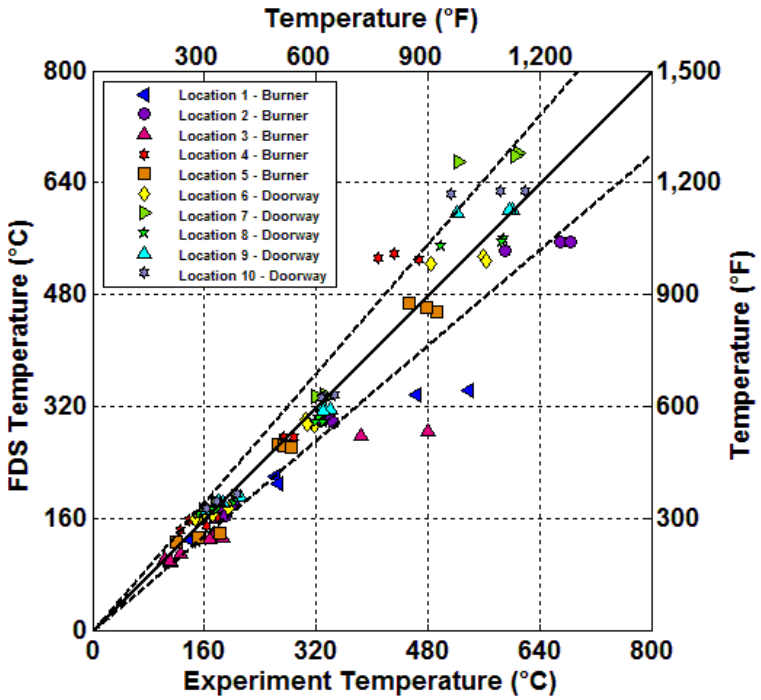

Figure 4-12: Steady state simulation temperatures versus the steady state natural gas experiment temperatures from the thermocouples in the ceiling vents when one vent was open. The dotted lines represent the expanded measurement uncertainty presented in Section 2.6 about the ideal model prediction.

In the following figure, there were a significant number of under-predicted steady state temperatures when the both vents were open. The most under-predicted value was under-predicted by 200 °C (400 °F). Few temperatures were over-predicted and they were just slightly over-predicted. Locations 5, 7, and 9 were most accurately predicted.

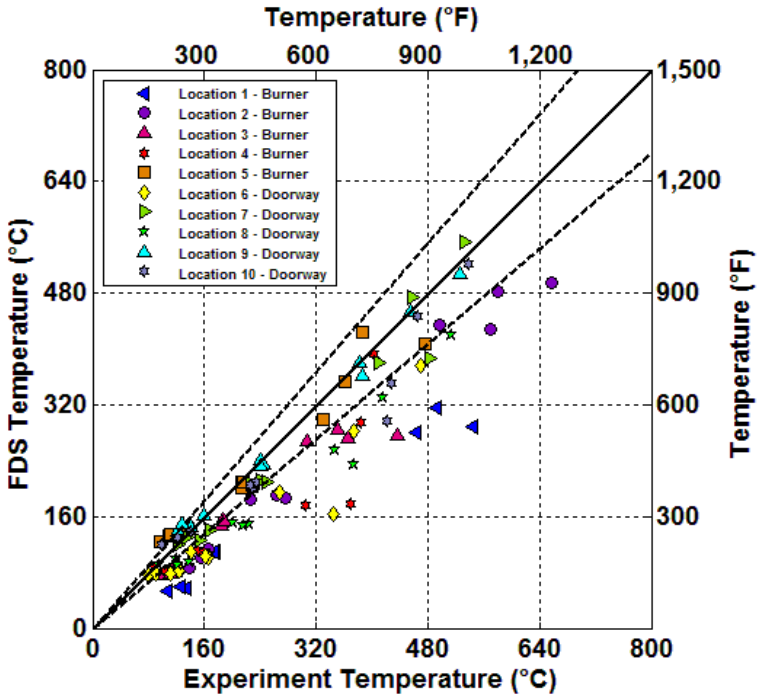

Figure 4-13: Steady state simulation temperatures versus the steady state natural gas experiment temperatures from the thermocouples in the ceiling vents when both vents were open. The dotted lines represent the expanded measurement uncertainty presented in Section 2.6 about the ideal model prediction.

4.2. Heat Flux

In Figure 4-14, Figure 4-15, and Figure 4-16 the steady state heat fluxes from the simulations are plotted over the steady state heat fluxes from the experiments when the ceiling vents were closed, one vent was open, and both vents were open. When both vents were open, most of the steady state heat fluxes were under-predicted. Some steady state heat fluxes were over-predicted and few were accurately simulated. The steady state heat fluxes were under-predicted by as much as 10 kW/m^2 and over-predicted by as much as almost 20 kW/m^2. The heat fluxes produced by FDS are a function of the wall temperature, which behaves similarly to the temperatures that were measured by the thermocouple arrays inside the room. Because it was known from Section 4.1.1, that the temperatures in the room from the experiments did not perfectly match the simulations, the heat fluxes also were not expected to match the simulation results. The simulated steady state heat fluxes deviated more from the measured heat steady state fluxes than the simulated steady state temperatures from the measured steady state temperatures. This was because the heat fluxes in FDS were calculated from the wall temperature to the fourth power. That means the uncertainty in the simulated wall temperatures is multiplied by itself four times. In general, heat flux is not simulated by FDS as accurately as temperature [38].

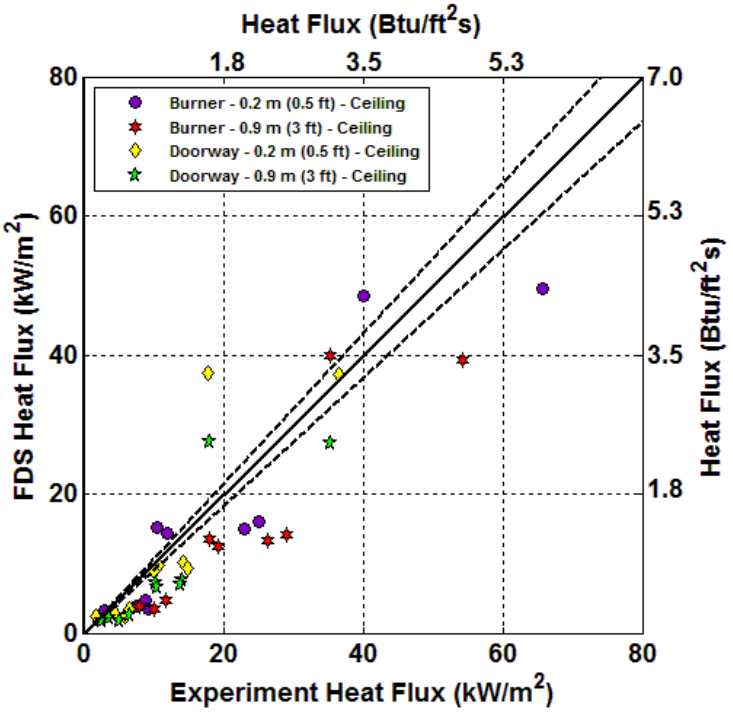

Figure 4-14 Steady state simulation heat fluxes versus the steady state natural gas experiment heat fluxes when both vents were closed. The dotted lines represent the expanded measurement uncertainty presented in Section 2.6 about the ideal model prediction.

In the figure below when one vent was open, again most of the steady state heat fluxes were under-predicted. The steady state heat fluxes were under-predicted by as much as 25 kW/m^2 and over-predicted by less than 10 kW/m^2. The highest measured steady state heat fluxes were less accurately simulated than when the vents were closed.

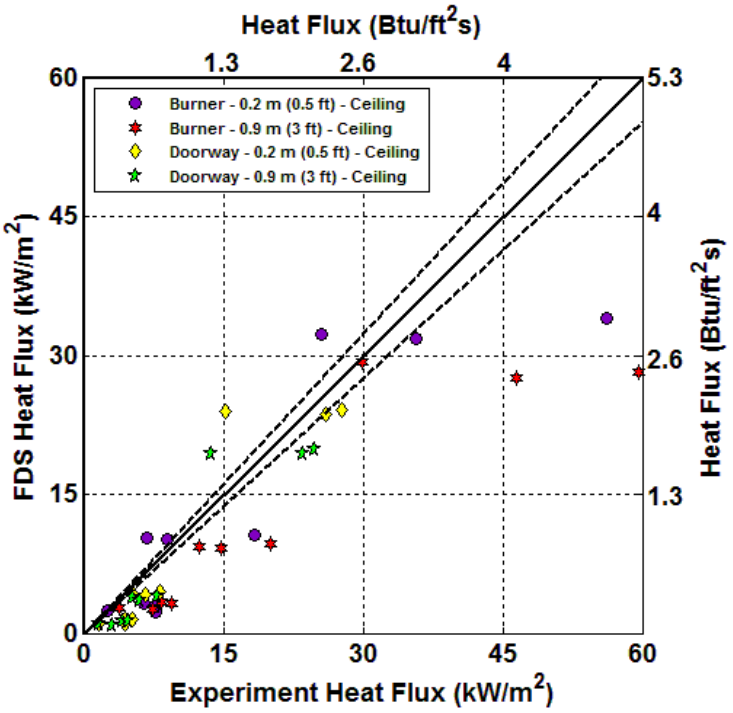

Figure 4-15: Steady state simulation heat fluxes versus the steady state natural gas experiment heat fluxes when one vent was open. The dotted lines represent the expanded measurement uncertainty presented in Section 2.6 about the ideal model prediction.

When both vents were open, the relationship between the measured steady state heat fluxes and the simulated heat fluxes shown in Figure 4-16 was similar to the relationship seen when one vent was open. Again, most of the values were under-predicted. The steady state heat fluxes were under-predicted by as much as 30 kW/m^2 and over-predicted by as much as 5 kW/m^2. When both vents were open, the highest steady state heat fluxes were more under-predicted than when one vent was open.

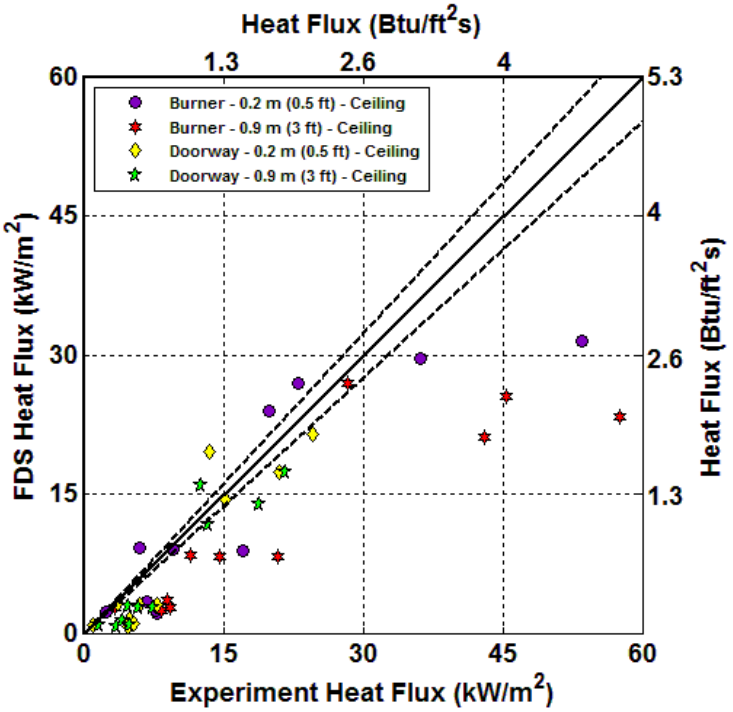

Figure 4-16: Steady state simulation heat fluxes versus the steady state natural gas experiment heat fluxes when both vents were open. The dotted lines represent the expanded measurement uncertainty presented in Section 2.6 about the ideal model prediction.

4.3. Velocity

The velocities recorded in the experiments are compared to the simulations in the following sections. As in the previous velocity section, a positive velocity indicated that gases were leaving the room and a negative velocity meant that the gases were entering the room. Besides just evaluating whether the experiment steady state velocities matched the quantity that was simulated by FDS, the direction of the gas movement is a key point of discussion.

4.3.1. Doorway

The next three figures show the steady state velocities collected within the doorway when the vents were closed, one vent was open, and two vents were open. In Figure 4-17 when the vents were closed, gases were flowing into and out of the room. Velocity measurements in general are much less steady than other measurements due to turbulence, so the steady state velocities were not expected to match the simulations as well as the temperatures did. The velocities were almost all under-predicted at heights from 0.3 m (0.8 ft) to 0.9 m (2.8 ft), and generally under-predicted by no more than 1 m/s (2 mph). At these heights, the gases were leaving the room in the experiments and the simulations. At 1.1 m and 1.3 m (3.5 ft and 4.2 ft), the experiment velocities were negative while the simulation velocities were positive. The simulation was predicting that gases were leaving the room at those two heights, when in reality gases were entering the room. This discrepancy resulted from the FDS simulating a deeper hot gas layer than actually existed. At the top four heights, most of the steady state velocities were under-predicted. The most under-predicted velocities was about 2 m/s (4 mph) greater than the simulations predicted.

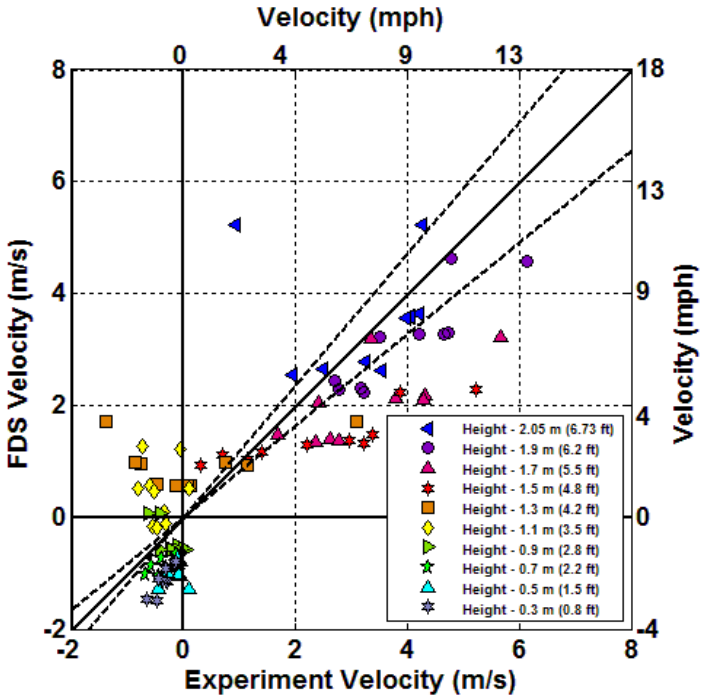

Figure 4-17: Steady state simulation velocities versus the steady state natural gas experiment velocities from the doorway when both vents were closed. The dotted lines represent the expanded measurement uncertainty presented in Section 2.6 about the ideal model prediction.

In Figure 4-18, most of the steady state velocities are negative in both the experiments and the simulations when one vent was open. This meant that both indicate that the single vent was exhausting most of the hot gases. Of the velocities that both the experiments and the simulations agree were negative, most were under-predicted. They were under-predicted by as much as 1.5 m/s (3.4 mph). Some were over-predicted by no more than 1 m/s (2 mph). There were six steady state velocities that were positive in both the experiments and simulations, indicating that the vent did not fully relieve all of the hot gases in either. In the simulations, almost all of the steady state velocities at 1.9 m and 2.05 m (6.2 ft and 6.73 ft) were positive. But in the experiments, most of the same steady state velocities were negative. Overall, the steady state velocities were over-predicted as much as 1.5 m/s (3 mph) and under-predicted by as much as 2 m/s (4 mph).

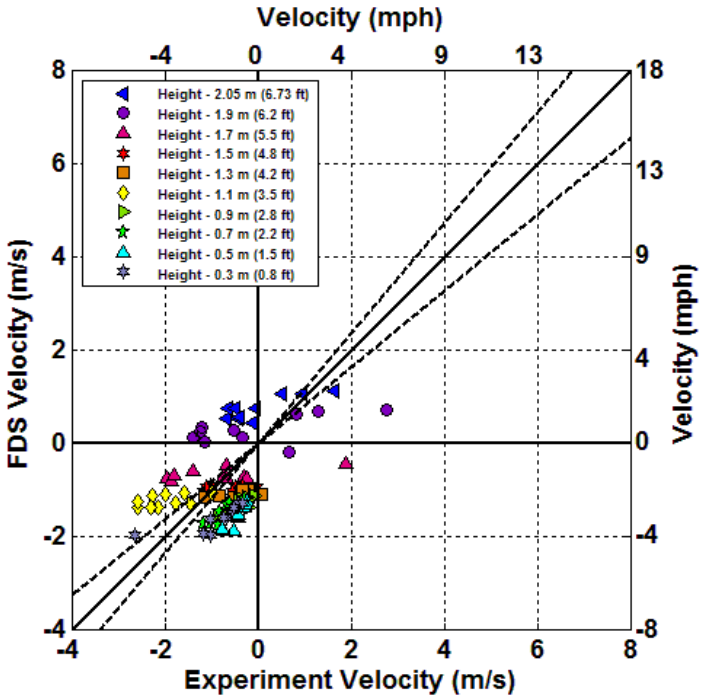

Figure 4-18 Steady state simulation velocities versus the steady state natural gas experiment velocities from the doorway when one vent was open. The dotted lines represent the expanded measurement uncertainty presented in Section 2.6 about the ideal model prediction.

When both vents were open, none of the velocities in the doorway were positive as is shown in Figure 4-19. In the simulations, there were positive velocities at 2.05 m (6.73 m). In the experiments, gases were only going into the room at the doorway. In the simulations, some of the hot gas layer was still exhausting through the doorway. The results of the simulations meant that the hot gas layer in the simulations was deeper than in the experiments. Those velocities were low, under 1 m/s (2 mph). The velocities were over-predicted by as much as 2 m/s (4 mph) and under-predicted by as much as 1.5 m/s (3 mph). Few of the steady state velocities from the experiments matched the steady state velocities from the simulations.

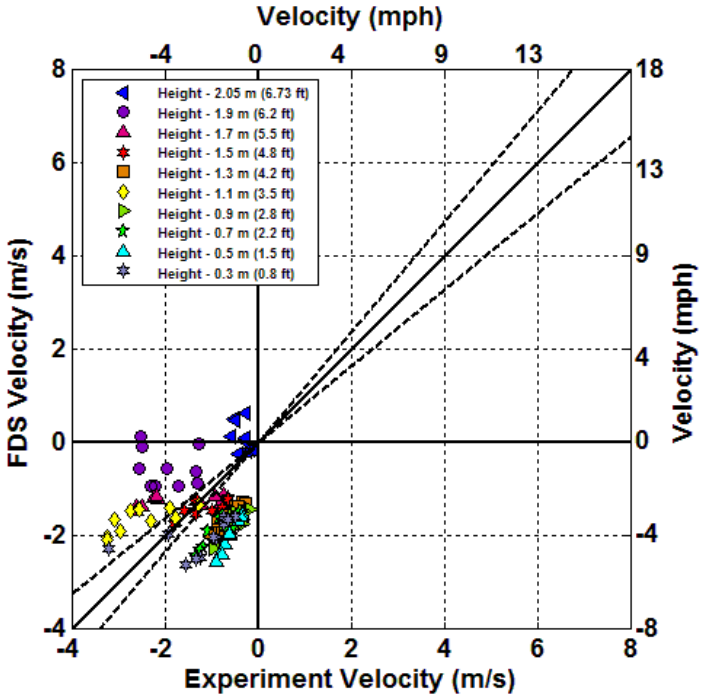

Figure 4-19: Steady state simulation velocities versus the steady state natural gas experiment velocities from the doorway when both vents were open. The dotted lines represent the expanded measurement uncertainty presented in Section 2.6 about the ideal model prediction.

4.3.2. Ceiling Vents

Figure 4-20, Figure 4-21, and Figure 4-22 show the experiment steady state velocities versus the simulation steady state velocities from the ceiling vent shaft when the vents were closed, one vent was open, and both vents were closed. When the vents were closed, few of the steady state velocities from the experiments matched the simulations. This was a result of there being a shaft in the ceiling. When the vents were closed, the gases in the shaft are rising, hitting the vent doors and recirculating in the shaft causing more turbulent movement of the gases. The movement of turbulent gases is difficult to predict in general as well as in FDS. This resulted in the steady state velocities from the experiments being generally inconsistent with the experiments. At Locations 1, 7, 9, and 10, FDS simulated the gases moving in the opposite direction then they were in the experiments. The steady state velocities at Locations 2, 5, and 10 were mostly over-predicted by as much as 2 m/s (4 mph). At the other locations, all of the steady state velocities were under-predicted by as much as 2.5 m/s (6 mph).

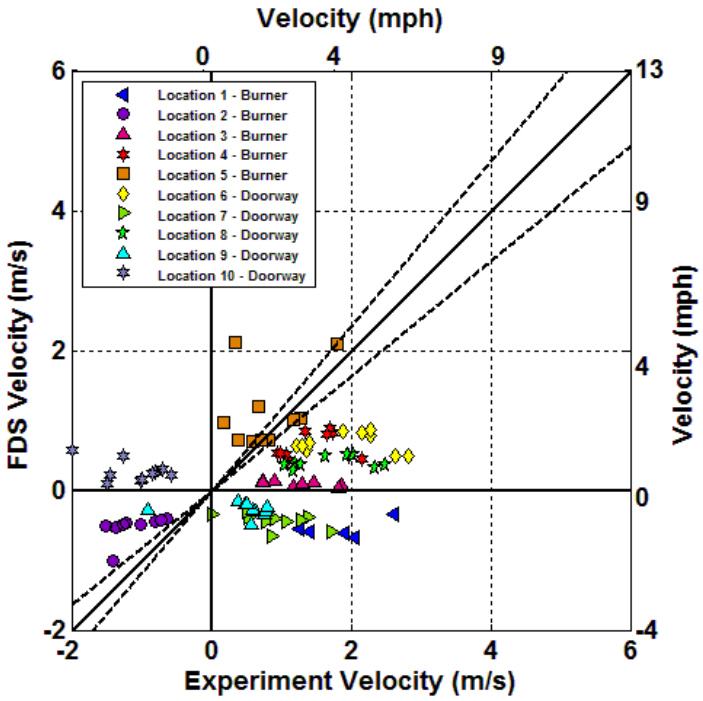

Figure 4-20: Steady state simulation velocities versus the steady state natural gas experiment velocities from the ceiling vents when both vents were closed. The dotted lines represent the expanded measurement uncertainty presented in Section 2.6 about the ideal model prediction.

With one vent open, the steady state velocities from the simulations are much more consistent with the experiment steady state velocities as is shown in Figure 4-21. The steady state velocities were over-predicted by less than 1 m/s (2 mph) and under-predicted by less than about 1 m/s (2 mph). The directions of all of the experiment velocities were correctly simulated by FDS. Overall, the steady-state velocities were fairly well simulated.

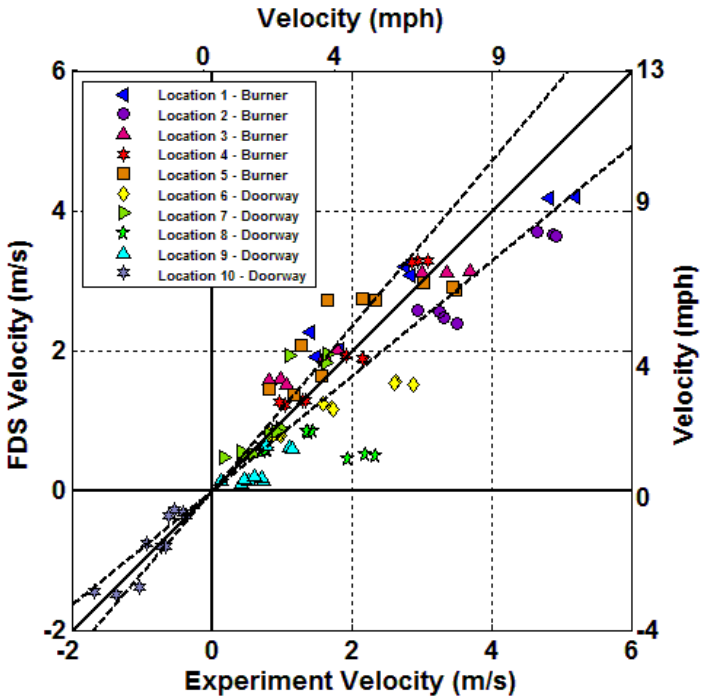

Figure 4-21: Steady state simulation velocities versus the steady state natural gas experiment velocities from the ceiling vents when one vent was open. The dotted lines represent the expanded measurement uncertainty presented in Section 2.6 about the ideal model prediction.

In Figure 4-22 when both vents were open, the simulation and experiment steady state velocities are also in much better agreement than when the vents were closed. All of the steady state velocities in the experiments were positive. In some of the simulations, FDS predicted that the steady-state velocities at Location 10 were negative. With the exception of some values at Locations 1 and 2, the steady state velocities were over-predicted and under-predicted by no more than 1 m/s (2 mph). Almost every value at those two locations were under-predicted and by more than any of the other locations. The great discrepancy between the simulation and experiment steady state velocities was 3 m/s (7 mph).

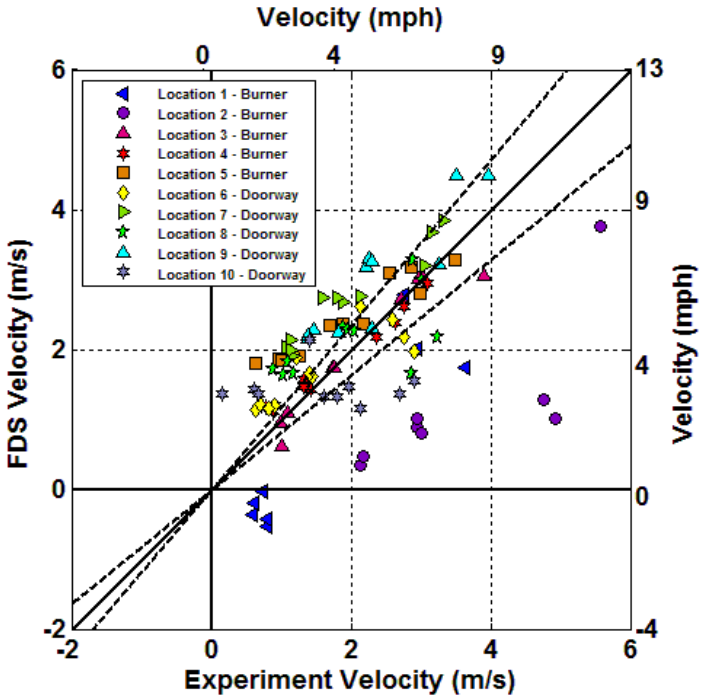

Figure 4-22: Steady state simulation velocities versus the steady state natural gas experiment velocities from the ceiling vents when both vents were open. The dotted lines represent the expanded measurement uncertainty presented in Section 2.6 about the ideal model prediction.

5. Sleeper Sofa Experiment Conditions & Results

Sleeper sofas are real fuels found in many houses. Unlike the natural gas experiments, burning sleeper sofas did not reach steady state, as was seen previously with the heat release rate data for the sleeper sofa presented in Figure 2-8 that was not contained by an enclosure. There was a slower initial development period due to the slow fire spread across the fuel followed by an intense peak in the fire growth. Sleeper sofas were burned in the last two experiments to assess how well the results from the controlled natural gas experiments compared to the results using furniture. In addition, two methods of extinguishing the fires were assessed. A pressurized water (labeled PW Ext. in the plots) fire extinguisher was applied to the upper layer and directly to the fire until it ran out of water. Then, a garden hose was used to extinguish what remained of the fire. Both were applied to the fires by an individual wearing full turnout gear. The different types of extinguishment were used to evaluate whether a pressurized water extinguisher could be used to suppress a room fire, an issue debated in the fire service [25]. This issue is not in line with the objectives of this study and will not be addressed in any detail in this report.

5.1. HRR

The HRRs measured by the calorimeter are presented in Figure 5-1 and Figure 5-2. The figures appear to indicate a strong increase in HRR after the first vent was opened. This is not accurate. During these experiments, when the vents were closed, the majority of the smoke exiting the structure was not contained by the calorimeter as seen in Figure 5-3, resulting in unrealistically, low HRRs. Given that most of the flow exhausted out the vents directly under the calorimeter and the velocity of the flow exiting the doorway was reduced, this allowed the smoke and hot gases to be captured properly by the calorimeter and the HRRs to be correctly reported.

In Experiment 32, the maximum HRR recorded was about 3.1 MW (2,900 Btu/s). Due to the enclosure effects, the sleeper sofa fire grew to be 1.1 MW (1,000 Btu/s) more than the fire size of the sleeper sofa in an open area (Figure 2-8). In Experiment 33, the fire size grew to 6.0 MW (5,700 Btu/s). While the change in fire size cannot be determined when the first vent is opened, in both experiments, the HRR dropped as a result of the second vent being opened. This indicated that the opening of the vents improved the conditions inside the room. Over the course of the vents being open, the HRR dropped 0.5 MW (500 Btu/s) in Experiment 33 and 2.0 MW (1,900 Btu/s) in Experiment 33.

When the pressurized water extinguisher was applied to the fire in Experiment 32, the HRR dropped significantly from 3000 kW (3,000 Btu/s) to about 500 kW (500 Btu/s). However, when the same pressurized water extinguisher was applied to the fire in Experiment 33, the HRR was barely affected.

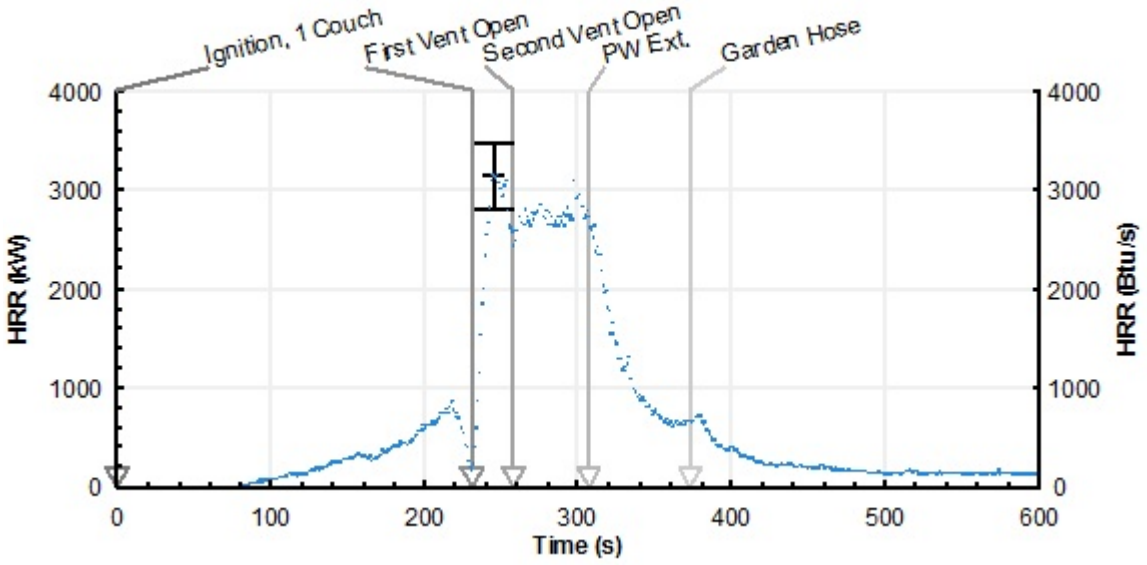

Figure 5-1: Plot of the calorimeter HRR in Experiment 32. The error bar represents the measurement uncertainty as presented in Section 2.6.

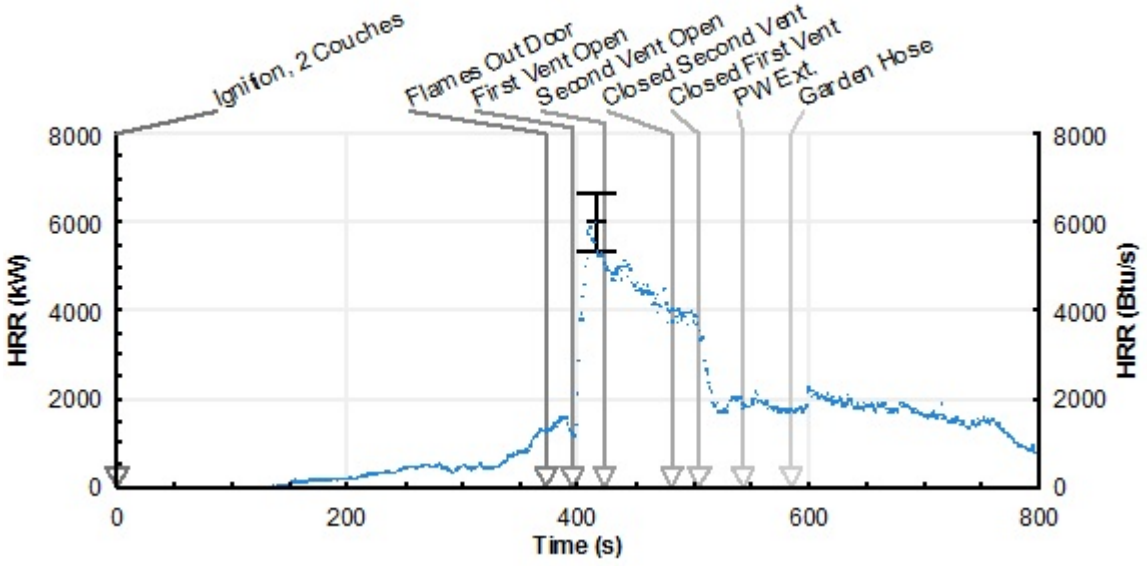

Figure 5-2: Plot of the calorimeter HRR in Experiment 33. The error bar represents the measurement uncertainty as presented in Section 2.6.

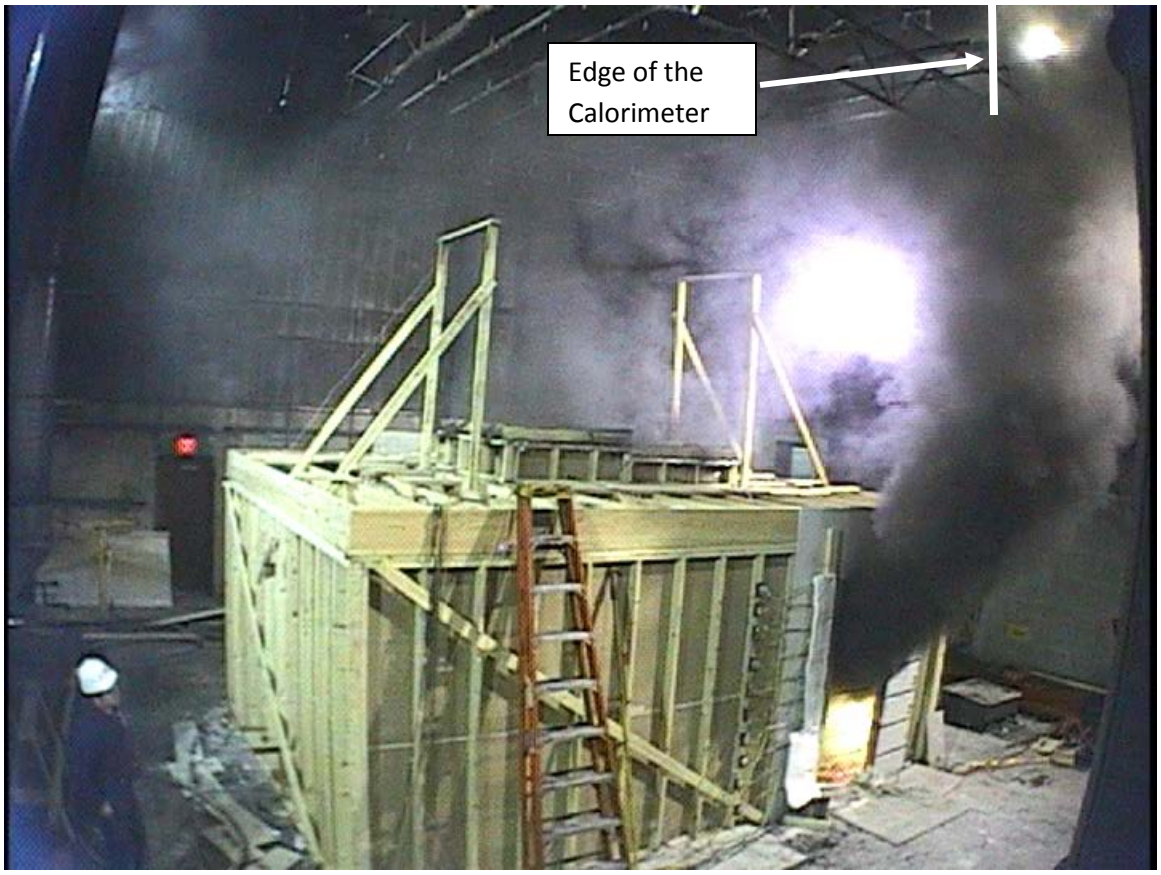

Figure 5-3: Photograph of the smoke escaping the calorimeter in Experiment 33

5.2. Temperature

In both experiments, temperature was measured within the room and at the vents to the room at the same locations as the natural gas experiments.

5.2.1. Interior Temperature

In Experiment 32, the interior temperatures, recorded by a thermocouple array near the sofa and another on the opposite side of the vent near the doorway, are presented in Figure 5-4 and Figure 5-5. Before any vents are opened, the temperatures recorded near the sofa peaked just below 900 °C (1,700 °F). The thermocouple closest to the ceiling, recording the highest temperature, showed relatively little variation in temperature after the first vent was opened. After the second was opened, all of the temperatures at the thermocouple array near the sofa began to increase. The temperature near the ceiling increased 100 °C (200 °F). The increase in temperatures was then halted by the pressurized water extinguisher. As the pressurized water extinguisher was applied, the temperatures originally spanning 900 °C (1,700 °F) all dropped to below 300 °C (600 °F). The pressurized water extinguisher successfully extinguished most of the fire.

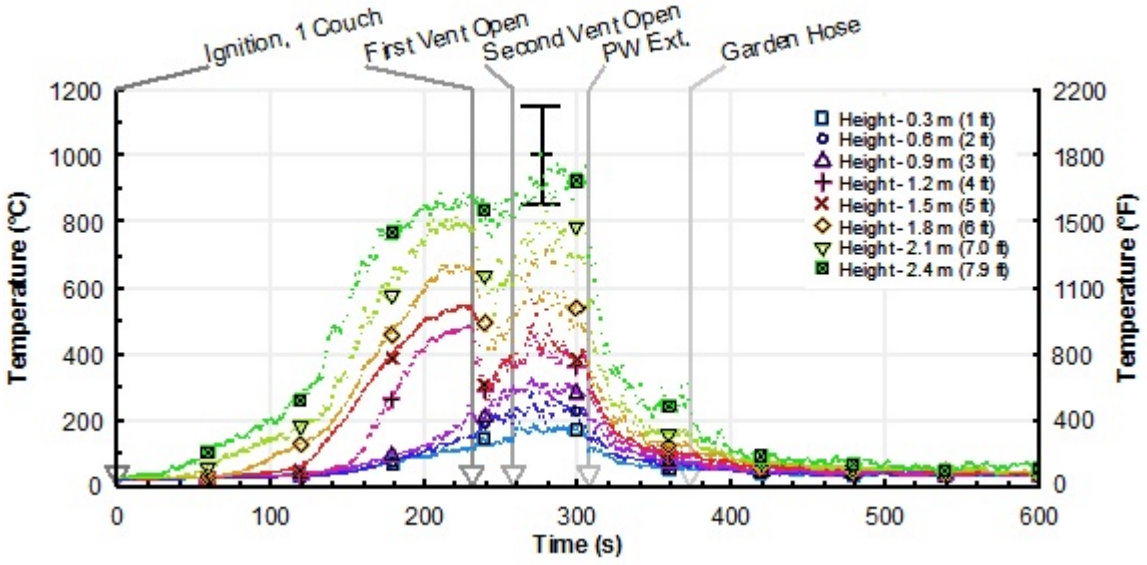

Figure 5-4: Plot of temperatures recorded by the thermocouple array near the sofa in Experiment 32. The error bar represents the expanded measurement uncertainty as presented in Section 2.6.

When the first vent was opened, the temperatures from thermocouple array near the doorway began to decrease. The highest temperature decreased from above 450 °C (840 °F) to below 400 °C (800 °F). After the second vent was opened, the three temperatures recorded closet to the ceiling, which previously were decreasing in temperature, became level at about 350 °C (660 °F). When the pressurized water extinguisher was applied all of the temperatures decreased. When the pressurized water extinguisher was out of water, all of the temperatures had fallen to below 200 °C (400 °F).

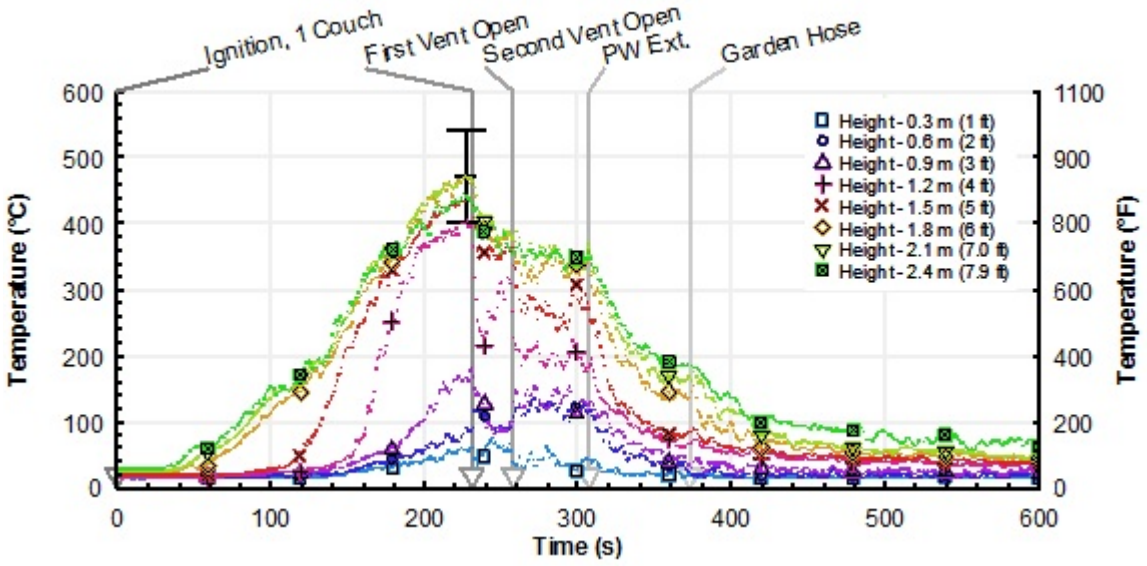

Figure 5-5: Plot of temperatures recorded by the thermocouple array near the doorway in Experiment 32. The error bar represents the expanded measurement uncertainty as presented in Section 2.6.

Figure 5-6 and Figure 5-7 show the temperatures collected at the thermocouple array near the sofas and near the doorway for Experiment 33. Before the first vent was opened, flames were coming out the doorway. The temperature reached 1700 °C (3,100 °F) at the thermocouple array near the sofas and 700 °C (1,300 °F) at the thermocouple array near the doorway. Every thermocouple in the room recorded temperatures greater than 200 °C (400 °F). After the first vent is opened, the temperatures near the sofas decrease, but only slightly. The opening of the second vent resulted in a greater decrease in temperatures, but it provided no improvement for the chances of survivability. Throughout the time the vents were open, the lowest thermocouples minimally decreased. The highest thermocouple decreased 700 °C (1,300 °F), which still left the temperature at 1000 °C (1,800 °F). At this point, the vents were closed causing the temperatures to increase again. All of the temperatures increased 200 °C to 300 °C (400 °F to 600 °F). At about 700 s (11 min. 40 s), the pressurized water extinguisher was applied to the upper layer and the fire. All of the temperatures then decreased 200 °C to 300 °C (400 °F to 600 °F). When the extinguisher's water supply was exhausted, the lowest temperature along the array was 400 °C (800 °F), still well above what is survivable by firefighters. Over the course of several more minutes, the fire was eventually extinguished with the garden hose.

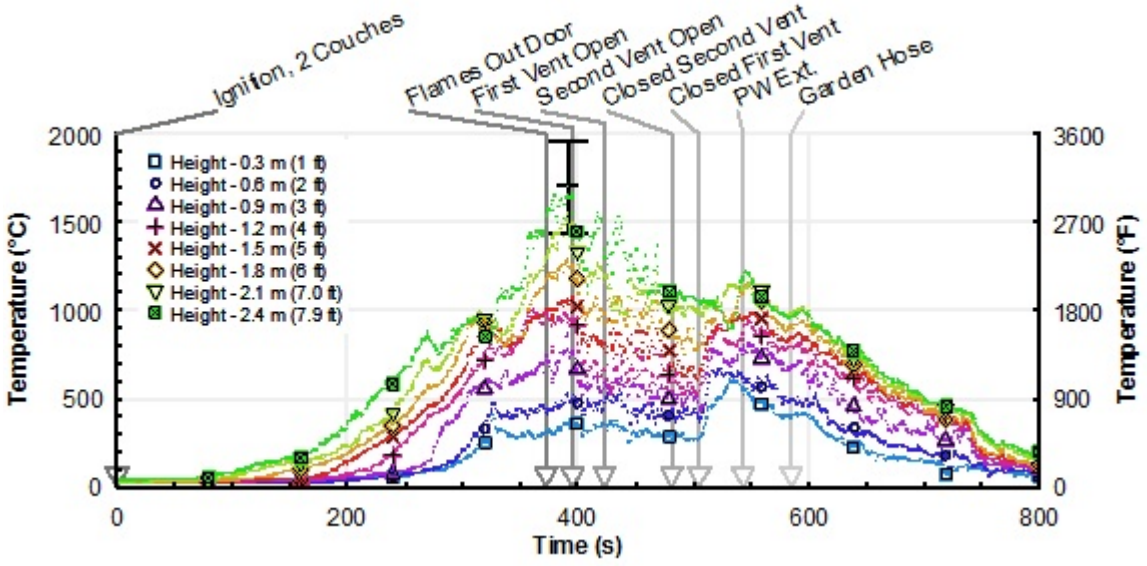

Figure 5-6: Plot of temperatures recorded by the thermocouple array near the sofas in Experiment 33. The error bar represents the expanded measurement uncertainty as presented in Section 2.6.

Before the first vent was opened, the temperatures in the thermocouple array near the doorway reached 700 °C (1,300 °F). The two lower layer thermocouples recorded temperatures between 200 °C (400 °F) and 300 °C (600 °F). After each vent was opened, the temperatures decreased. The highest temperature dropped from 700 °C (1,300 °F) to just above 500 °C (900 °F) after both vents were opened. Once the vents were closed, the temperatures quickly regained what was lost when the vents were open. At some locations on the thermocouple array, the temperatures exceeded what was recorded before the vents were opened. At this point, the pressurized water extinguisher was applied. The discharge minimally impacted the temperatures. All of the temperatures remained very high.

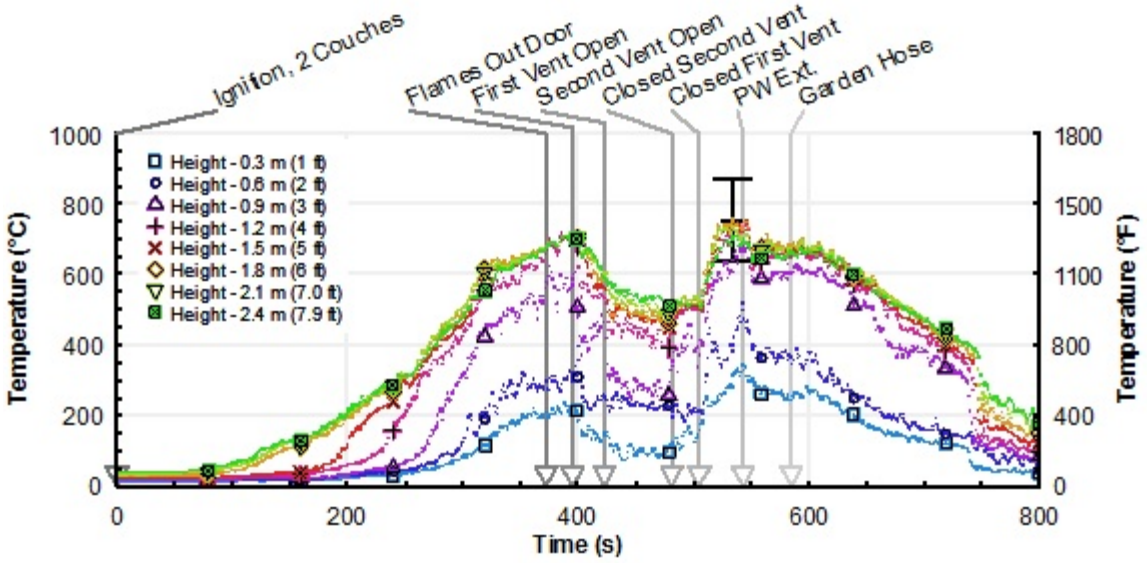

Figure 5-7: Plot of temperatures recorded by the thermocouple array near the doorway in Experiment 33. The error bar represents the expanded measurement uncertainty as presented in Section 2.6.

5.2.2. Vent Temperature

The temperatures recorded in the doorway and in the vents for Experiment 32 are provided in Figure 5-8 and Figure 5-9. The temperature in the doorway reached a maximum of 350 °C (660 °F). As the vents were opened, the temperatures of the gases exiting through the doorway decreased. All of the upper layer temperatures dropped to below 200 °C (400 °F) by the time the PW extinguisher was applied. The addition of the pressurized water extinguisher and the garden hose did not noticeably impact the already decreasing temperatures. Throughout the opening of the vents and the application of water, the temperatures in the upper layer decreased, but the location of the hot layer interface remained the same.

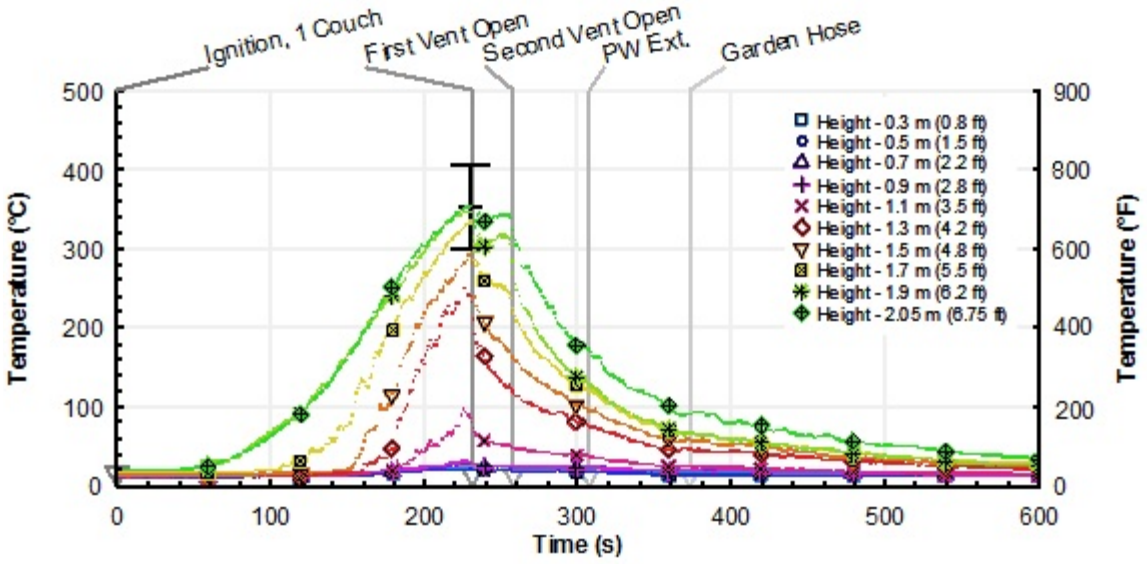

Figure 5-8: Plot of temperatures recorded by the thermocouples in the doorway for Experiment 32. The error bar represents the expanded measurement uncertainty as presented in Section 2.6.

In the vent, the thermocouples recorded temperatures between 400 °C and 500 °C (800 °F and 900 °F). With the exception of the temperatures from the two thermocouples closest to the fire, all of the temperatures became steady or decreased after the first vent was opened. The temperatures at the two thermocouples nearest to the fire increased about 100 °C (200 °F). The addition of the second vent caused one of the two to begin decreasing and the other to level out. When the pressurized water extinguisher was applied, all of the temperatures began decreasing more quickly. After the water in the extinguisher was exhausted, the temperatures ranged from 150 °C and 250 °C (300 °F and 480 °F).

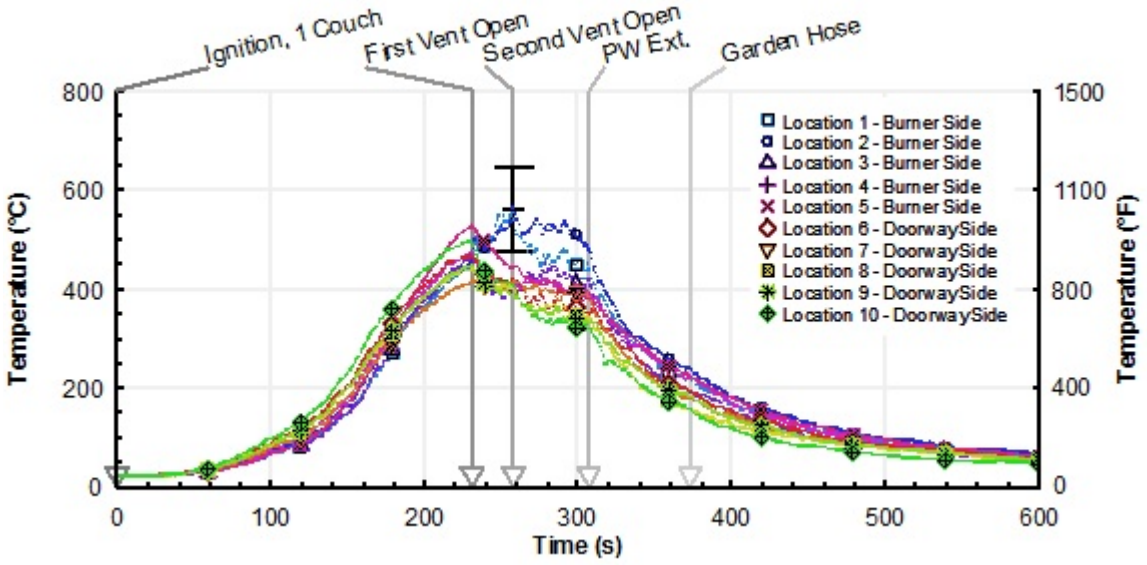

Figure 5-9: Plot of temperatures recorded by the thermocouples in the ceiling vent for Experiment 32. The error bar represents the expanded measurement uncertainty as presented in Section 2.6.

The temperatures recorded in the doorway and the vents in Experiment 33 are presented in Figure 5-10 and Figure 5-11. The temperatures reached above 600 °C (1,100 °F) before the vents were opened. The opening of the vents resulted in an immediate decrease in temperatures. By the time the vents were closed the temperatures had all dropped below 300 °C (600 °F). Once the vents were closed, the upper layer temperatures quickly returned to recording temperatures in excess of 500 °C (900 °F). Using the pressurized water extinguisher had little effect on the hot gases exiting through the door. Some of the thermocouples showed increasing temperatures as the PW extinguisher was being sprayed into the fire. After about a minute of using the garden hose, the temperatures began to decrease.

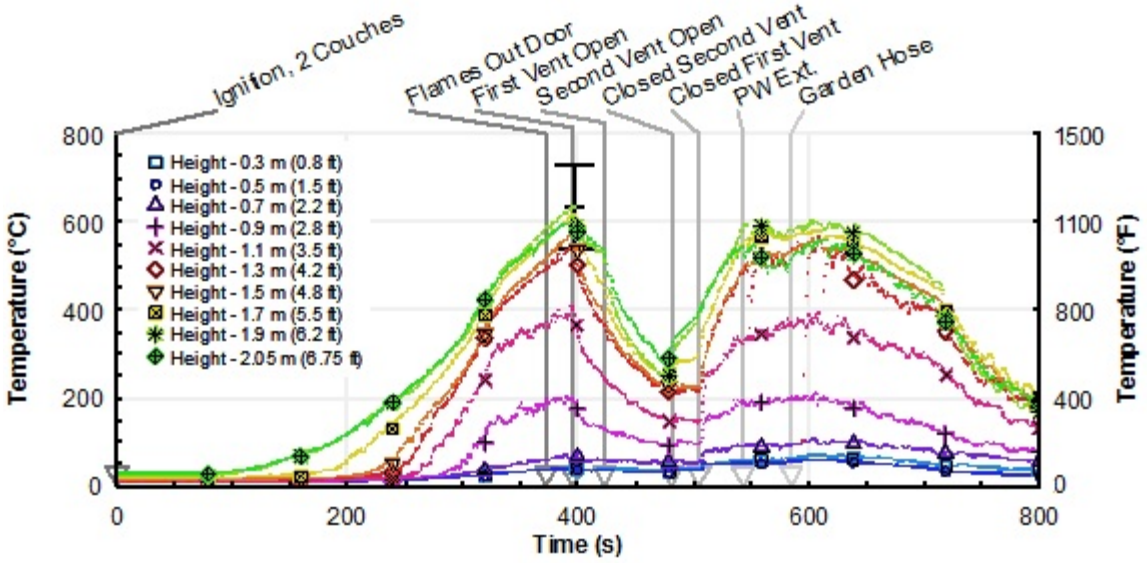

Figure 5-10: Plot of temperatures recorded by the thermocouples in the doorway for Experiment 33. The error bar represents the expanded measurement uncertainty as presented in Section 2.6.

Before any of the vents were opened, the temperatures recorded in the vents were between 700 °C and 900 °C (1,300 °F and 1,700 °F). Upon opening the first vent, the same two thermocouples from the previous experiment (the closest two to the burner, Location 1 and Location 2) showed a sudden increased in temperature while the others decreased in temperature. After the addition of the second vent, the temperatures at those two locations began to decrease. Before the vents were closed again, the temperature of the hot gases leaving the vents were still in excess of 500 °C (900 °F). When the pressurized water extinguisher was applied the temperatures in the vent were in the 700 °C to 800 °C (1,300 °F and 1,500 °F) range. The addition of the water barely caused a ripple in the vent temperatures.

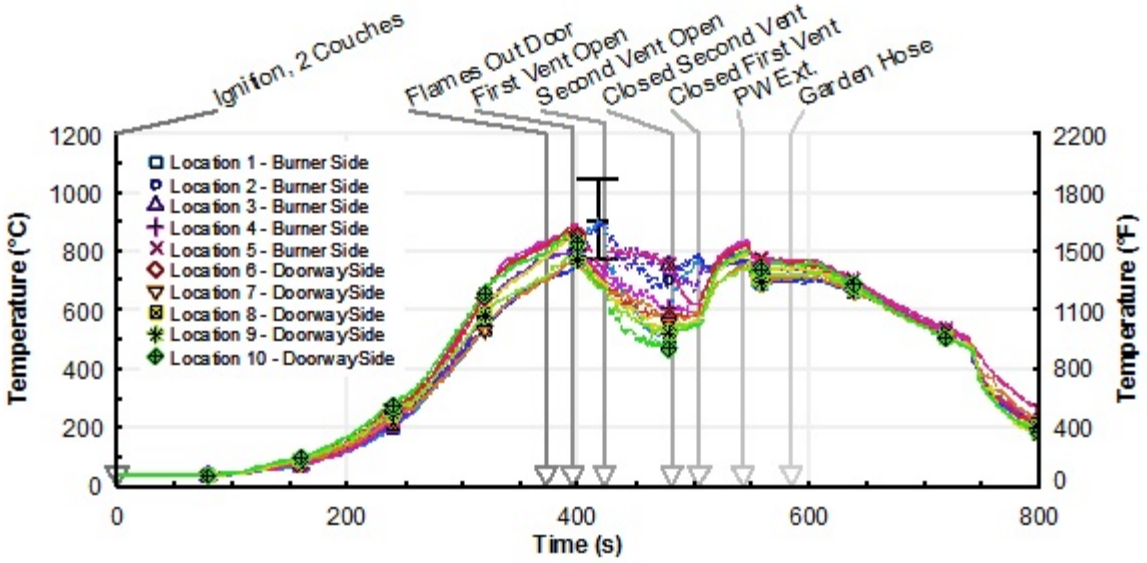

Figure 5-11: Plot of temperatures recorded by the thermocouples in the ceiling vent for Experiment 33. The error bar represents the expanded measurement uncertainty as presented in Section 2.6.

5.3. Heat Flux

The heat fluxes gathered from the interior of the room for Experiment 32 and Experiment 33 are provided in Figure 5-12 and Figure 5-13. In Experiment 32, the heat fluxes recorded on the side of the room closest to the fire stayed higher than the heat fluxes on the doorway side of the room throughout the experiment. Before the first vent was opened, the highest heat flux was about 30 kW/m^2 (2.6 Btu/ft^2-s). Afterward, the heat fluxes measured near the fire began increasing, while the heat fluxes from the doorway side began decreasing. The highest recorded heat flux was 60 kW/m^2 (5.3 Btu/ft^2-s). By the time the PW extinguisher was being applied, the heat flux measured near the burner facing the fire at 0.9 m (3.0 ft) was 55 kW/m^2 (4.8 Btu/ft^2-s). The application of the water caused the heat fluxes measured near the fire to drop immediately. At the end of the pressurized water extinguisher water supply, all of the heat fluxes measured in the room were below 10 kW/m^2 (0.9 Btu/ft^2-s).

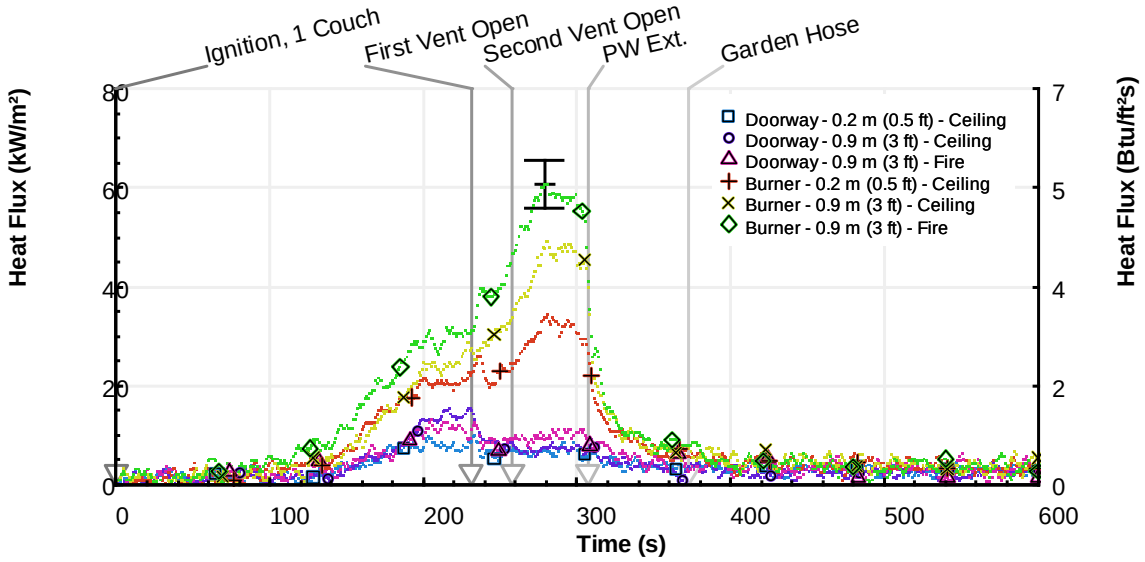

Figure 5-12: Plot of the heat fluxes from Experiment 32. The error bar represents the expanded measurement uncertainty as presented in Section 2.6.

Unlike in Experiment 32, the heat fluxes measured at a height of 0.9 m (3 ft) initially showed similar behavior and the heat fluxes measured near the floor showed similar behavior in Experiment 33. Before the first vent was opened, the heat flux gauges at a height of 0.9 m (3 ft) recorded heat fluxes between 30 kW/m^2 and 60 kW/m^2 (2.6 Btu/ft^2-s and 5.3 Btu/ft^2-s) while the lower heat flux gauges read about 10 kW/m^2 (0.9 Btu/ft^2-s). Afterward, the higher heat flux gauges recorded a decrease in heat flux. The heat fluxes near the floor increased at least 10 kW/m^2 (0.9 Btu/ft^2-s). After the second vent was opened, the behavior looked similar to the results of Experiment 33. All of the heat flux measurements near the fire were higher than the measurements near the doorway. Before the vents were closed, the burner side heat fluxes were between 25 kW/m^2 and 50 kW/m^2 (2.2 Btu/ft^2-s and 4.4 Btu/ft^2-s). The doorway side heat fluxes were between 15 kW/m^2 and 20 kW/m^2 (1.3 Btu/ft^2-s and 1.8 Btu/ft^2-s). When the vents were closed, the behavior shifted back to what was seen before the vents were opened. The heat fluxes measured at 0.9 m (3 ft) showed similar behavior and the heat fluxes measured near the floor showed similar behavior. Just before the pressurized water extinguisher was applied, the lower heat flux gauged read about 25 kW/m^2 (2.2 Btu/ft^2-s) and the higher heat flux gauges ranged from 45 kW/m^2 to 55 kW/m^2 (4.0 Btu/ft^2-s and 4.8 Btu/ft^2-s). The water applied to the fire by the extinguisher had no significant effect on the recorded heat fluxes. The use of the garden hose, however, did result in decreasing heat fluxes.

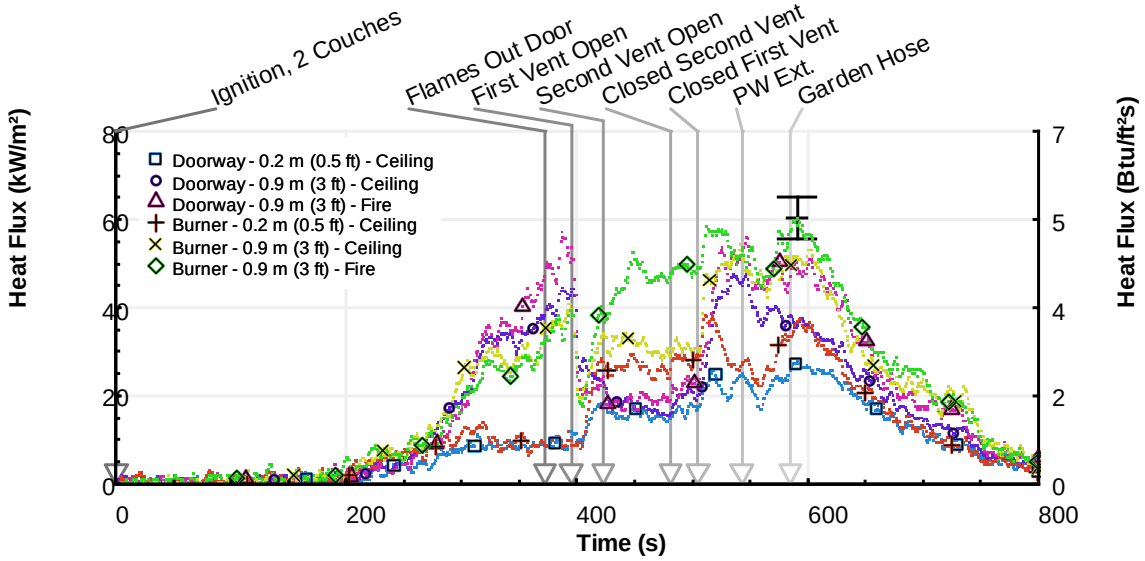

Figure 5-13: Plot of the heat fluxes from Experiment 33. The error bar represents the expanded measurement uncertainty as presented in Section 2.6.

5.4. Velocity

The velocities recorded by the bidirectional probes in the doorway in Experiment 32 are presented in Figure 5-14. The positive velocities measured by the three highest bidirectional probes indicated that the hot gases were exiting the room at those locations. The negative velocities indicate the heights at which the cool, fresh air was being entrained into the room. The highest velocity recorded in the gases exiting the room was 8 m/s (18 mph), before the vents were opened. The highest velocity recorded for the air coming into the room was on the order of 1 m/s (2 mph). After the first vent was opened, some of the hot gases were still exhausting through the doorway, but most of the gas flow was fresh air coming into the room. The velocity of the hot products of combustion exhausting through the doorway was reduced significantly. The highest velocities recorded near the top of the door during this period were about 2 m/s (4 mph). With the addition of the second vent, only fresh air was coming in through the door. All of the hot gases were exiting through the vents. The velocities of the gases coming into the room were between 1 m/s and 3 m/s (2 mph and 7 mph). When the pressurized water extinguisher water was applied to the fire, the velocities slowly decreased in magnitude. They decreased again when the garden hose was introduced.

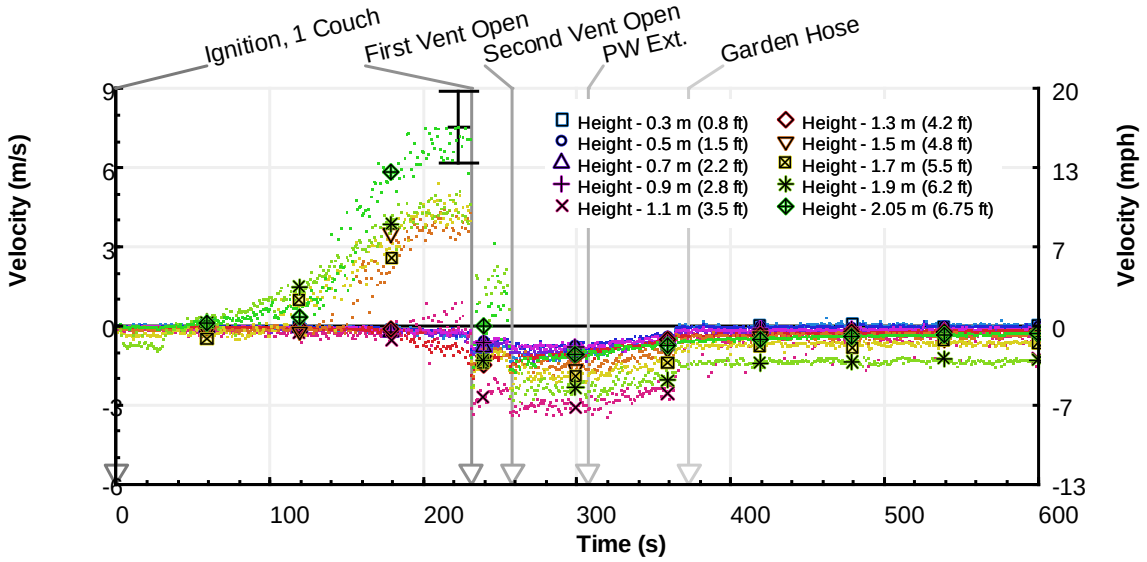

Figure 5-14: Plot of gas velocities in the doorway in Experiment 32. The error bar represents the expanded measurement uncertainty as presented in Section 2.6.

Figure 5-15 shows the velocities recorded in the vent during Experiment 32. During the time the vents are closed, the velocities reflect the movement of the hot gases inside the structures and are irrelevant to the analysis of the velocity of the gases exiting and entering the structure. When the first vent was open, the velocities measured in the burner side vent ranged from 2 m/s to 9 m/s (4 mph to 20 mph). The velocity measurement taken closest to the origin of the fire (Location 2) recorded the highest velocities and continued to record the highest velocities as the second vent was opened. The highest velocity recorded was 10 m/s (22 mph). When the second vent was opened, with the exception of Location 2, all of the velocities were between 3 m/s and 5 m/s (7 mph and 11 mph). As water was applied to the fire, all of the velocities decreased.

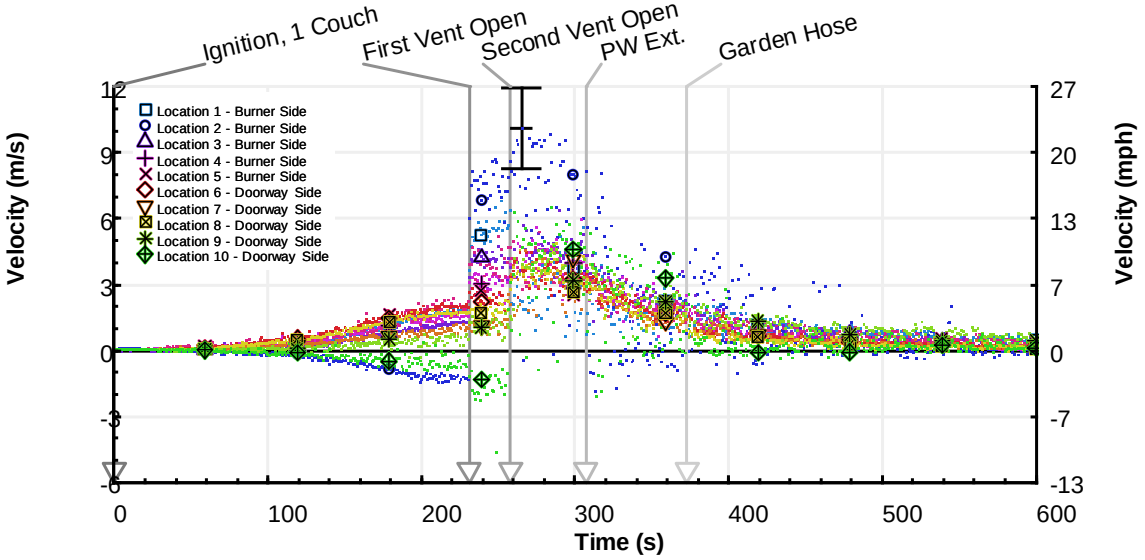

Figure 5-15: Plot of gas velocities in the ceiling vent in Experiment 32. The error bar represents the expanded measurement uncertainty as presented in Section 2.6.

The velocities recorded in the doorway in Experiment 33 are provided in Figure 5-16. The interface between the hot gases exiting the room and the cool air coming entering the room existed between 0.9 m and 1.1 m from the top of the door (2.8 ft and 3.5 ft). Before the first vent was opened, the highest magnitude velocity recorded exiting the room was 10 m/s (22 mph). Afterward, it decreased to 6 m/s (13 mph). At this point, the interface shifted to between 1.7 m and 1.9 m from the top of the doorway (5.5 ft and 6.2 ft). When the second vent was opened, no hot gases were exiting through the doorway. Fresh air with a velocity up to 4 m/s (9 mph) was coming through the doorway. After the vents were closed, the velocities quickly returned to how they were prior to the vents being open. The addition of the water from the pressurized water extinguisher had no impact on the gases moving in and out of the doorway. Only after a couple minutes of the garden hose being applied to the fire, the velocities begin to decrease in magnitude.

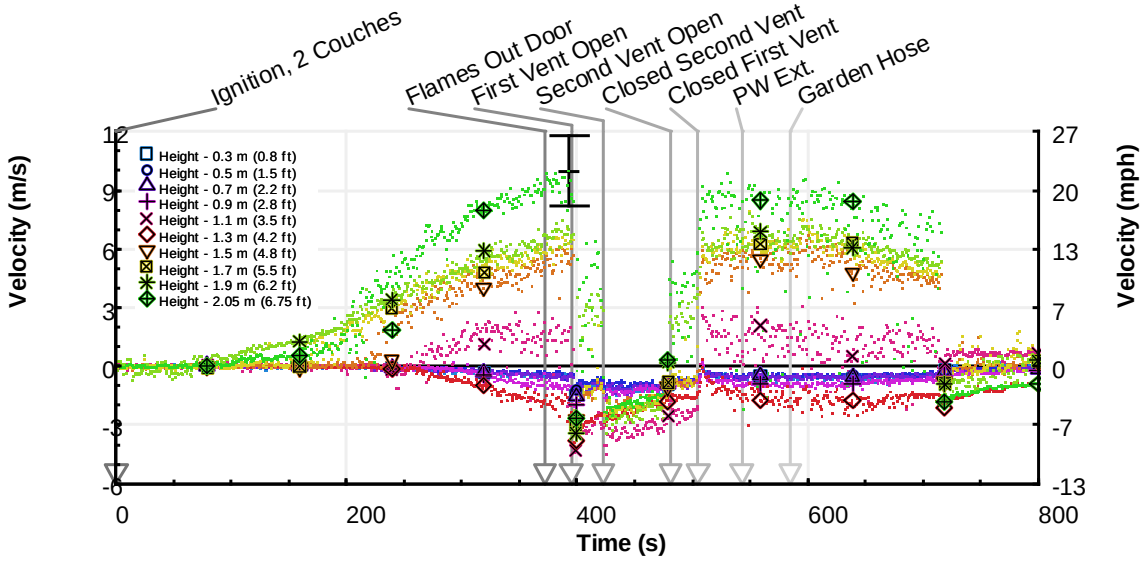

Figure 5-16: Plot of gas velocities in the doorway in Experiment 33. The error bar represents the expanded measurement uncertainty as presented in Section 2.6.

In Figure 5-17, the velocities collected from the ceiling vents in Experiment 33 are plotted. When the first vent was opened, the velocities in that vent ranged from 3 m/s to 12 m/s (7 mph and 27 mph). After the second vent was opened, all of the velocities ranged from 2 m/s to 12 m/s (4 mph to 27 mph). The highest velocities were recorded at the location closet to the origin of the fire, Location 2. When one or both of the vents were open, gases were exiting the vents.

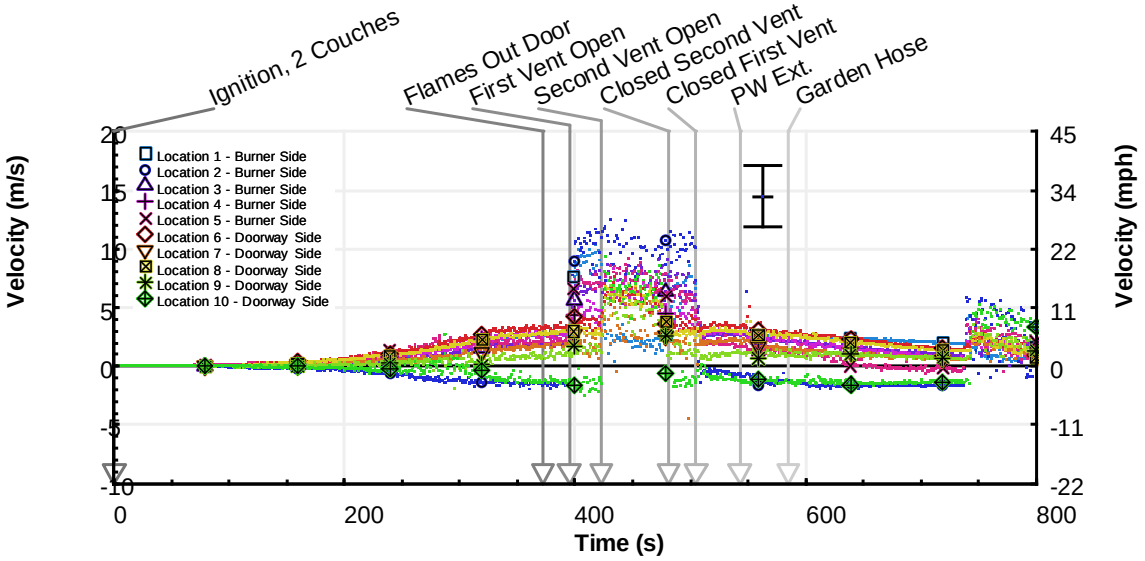

Figure 5-17: Plot of gas velocities in the ceiling vent in Experiment 33. The error bar represents the expanded measurement uncertainty as presented in Section 2.6.

6. Discussion

To evaluate how effective the ceiling vents were at relieving smoke and hot gases from the room, the analysis divided the room into two zones. The first zone is called the cold gas layer (CGL) and will be defined by where the cool air feeding the fire is located. The second zone is called the hot gas layer (HGL) and will be defined by where the hot gases produced by the fire are located. The location of the gas layer interface that divides the cold and hot gas layers can be calculated from the temperatures collected along the height of a room. Three gas layer heights were calculated from the temperatures from the thermocouple array near the burner, thermocouple array near the doorway, and the thermocouples in the door. Using the same temperatures, three HGL temperatures were calculated. The HGL temperature is the average temperature above the gas layer interface height. A rising gas layer interface height with an increasing ceiling vent size would mean the amount of hot gases and smoke had definitively decreased within the room. A decrease in the hot gas layer temperature as the vent size increased would indicate that the hot gas layer had become less hazardous.

The height of the gas layer interface was calculated using the following equations from Ref. [42].

$$(H - z_{int})T_h + z_{int}T_c = \int_0^H T(z)dz = I_1$$

$$(H - z_{int})\frac{1}{T_h} + z_{int}\frac{1}{T_c} = \int_0^H \frac{1}{T(z)}dz = I_2$$

$$z_{int} = \frac{T_c(I_1 I_2 - H^2)}{I_1 + I_2 T_c{}^2 - 2T_c H}$$

Where H was the height of the room or the doorway depending on the vertical temperatures used, T(z) was the temperature data collected over the height of the room, T_h was the HGL temperature, T_c was the cold gas layer, and z_{int} was the interface height. The HGL temperature was determined from:

$$(H - z_{int})T_h = \int_{z_{int}}^H T(z)dz \quad [42]$$

6.1. Effects of Vents

The average gas layer heights calculated from the steady-state temperatures from the thermocouple array near the burner, thermocouple array near the doorway, and the thermocouples in the doorway from the natural gas experiments are presented in Figure 6-1, Figure 6-2, and Figure 6-3. At the location near the burner (Figure 6-1), the average gas layer interface height increases at every fire size between when the vents were closed and one vent was opened. The increase in the height meant the ceiling vent was able to exhaust at least 0.3 m (1.0 ft) of the hot gas layer when the when the fire size was between 0.5 MW and 2 MW. The addition of the second vent had no impact on the depth of the HGL for any of the fire sizes.

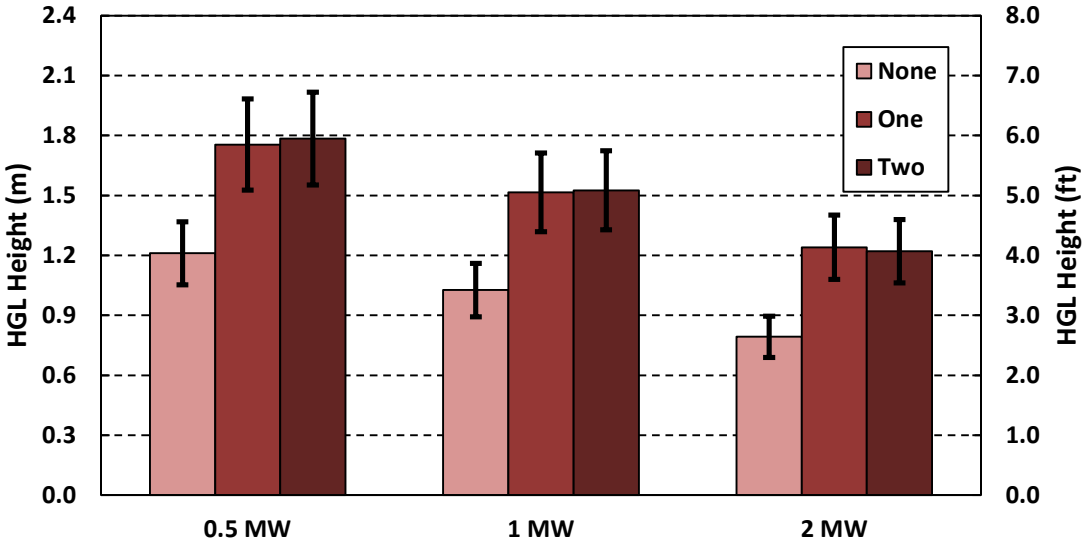

Figure 6-1: Bar graph of the average gas layer interface height from the steady-state 0.5 MW, 1 MW, and 2 MW fires with the vents closed, one vent opened , and two vents opened based on the temperatures from the thermocouple array near the burner. The error bar represents the expanded measurement uncertainty as presented in Section 2.6.

In Figure 6-2 at 0.5 MW and 1 MW, there was no significant increase in the interface height. At 2 MW, the interface height slightly increased with the changing ventilation conditions. At each fire size, the change in the interface height was less than 0.3 m (1 ft) as the ventilation changed.

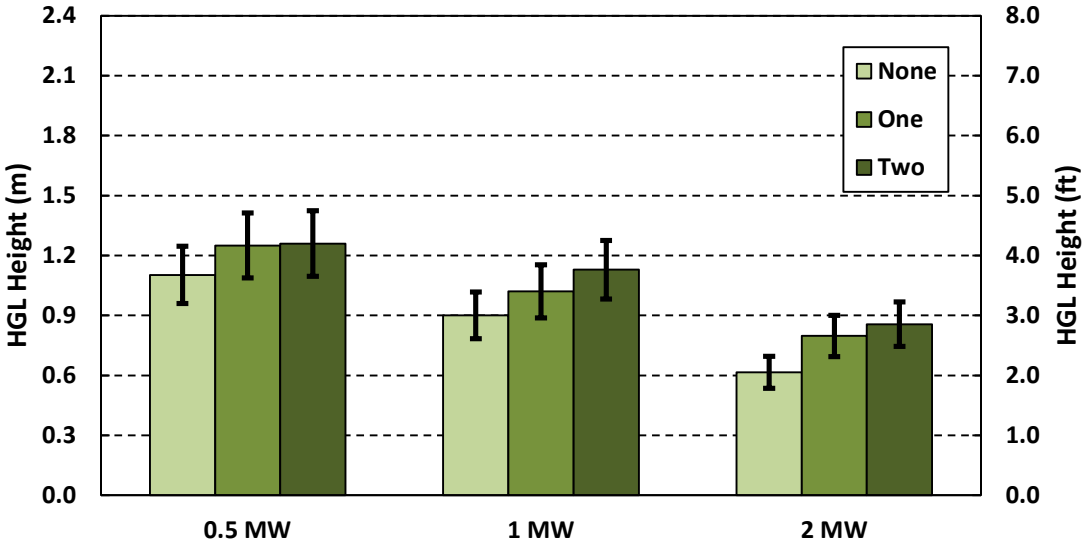

Figure 6-2: Bar graph of the average gas layer interface height from the steady-state 0.5 MW, 1 MW, and 2 MW fires with the vents closed, one vent opened , and two vents opened based on the temperatures from the thermocouple array near the doorway. The error bar represents the expanded measurement uncertainty as presented in Section 2.6.

In Figure 6-3, the average steady state HGL interface height in the doorway was plotted only for the experiments with the vents closed and one open vent. When both vents were opened, there was no hot gas layer, as can be seen in Figure 3-8 through Figure 3-10. Therefore, there was no interface when the two vents were open. With all three fire sizes, the average gas interface height increased when the conditions changed from no open vents to one open vent. This indicated that the HGL was reduced at each fire size. At each fire size, the interface height rose at least 0.3 m (1.0 ft) with the addition of the first vent.

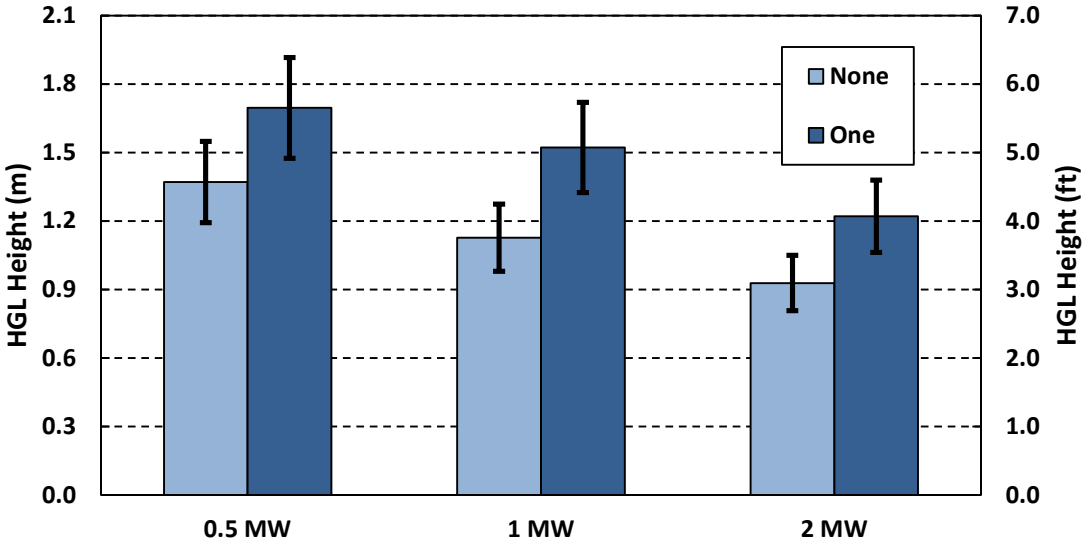

Figure 6-3: Bar graph of the average gas layer interface height from the steady-state 0.5 MW, 1 MW, and 2 MW fires with the vents closed, one vent opened , and two vents opened based on the temperatures from the thermocouples in the doorway. The error bar represents the expanded measurement uncertainty as presented in Section 2.6.

In the following three figures, the average HGL temperatures calculated from the thermocouple array near the burner, thermocouple array near the doorway, and the thermocouples in the doorway for the natural gas experiments are presented. In Figure 6-4, the HGL temperatures from the location near the burner decreased at every fire size when the conditions changed from no open vents to one open vent. At 2 MW, the temperature dropped over 200 °C (400 °F). The addition of the second vent had no impact on the hot gas layer temperature, which was consistent with the discussion in Section 3.2.1.

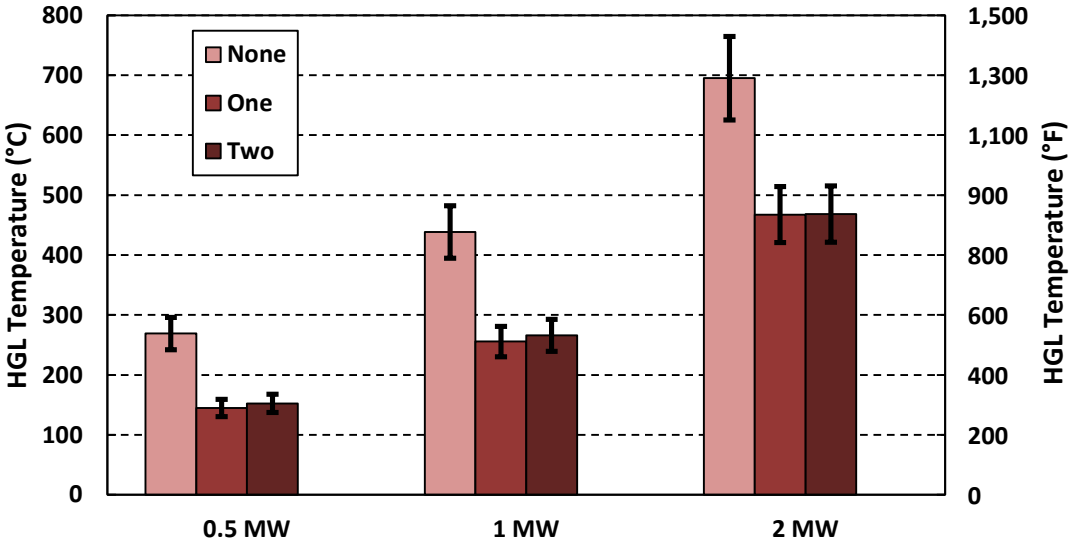

Figure 6-4: Bar graph of the HGL temperatures from the steady-state 0.5 MW, 1 MW, and 2 MW fires with the vents closed, one vent opened, and two vents opened based on the temperatures from the thermocouple array near the burner. The error bar represents the expanded measurement uncertainty as presented in Section 2.6.

At the location near the burner, the average HGL temperatures, shown in Figure 6-5, decreased significantly when one vent was opened. At 2 MW, the change in the average HGL temperature was almost 200 °C (400 °F). Changing conditions from one open vent to two open vents, there was no decrease in temperature for any of the fire sizes.

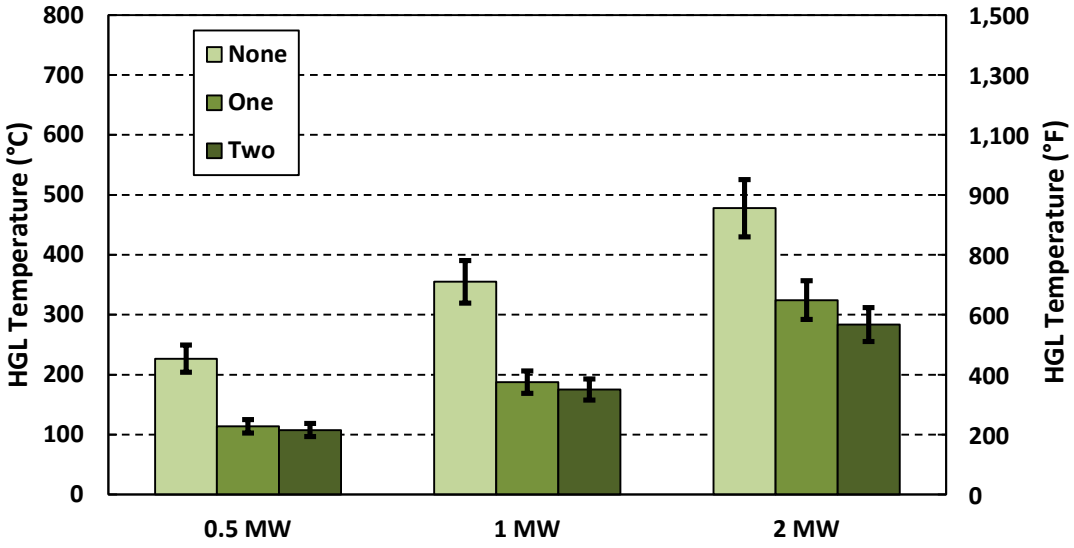

Figure 6-5: Bar graph of the average HGL temperatures from the steady-state 0.5 MW, 1 MW, and 2 MW fires with the vents closed, one vent opened, and two vents opened based on the temperatures from the thermocouple array near the doorway. The error bar represents the expanded measurement uncertainty as presented in Section 2.6.

At the doorway, the average HGL temperature was reduced with the addition of one vent and again with the second vent (Figure 6-6). When both vents were open, a HGL no longer existed. This was confirmed by the average HGL temperature being about or under 50 °C (120 °F).

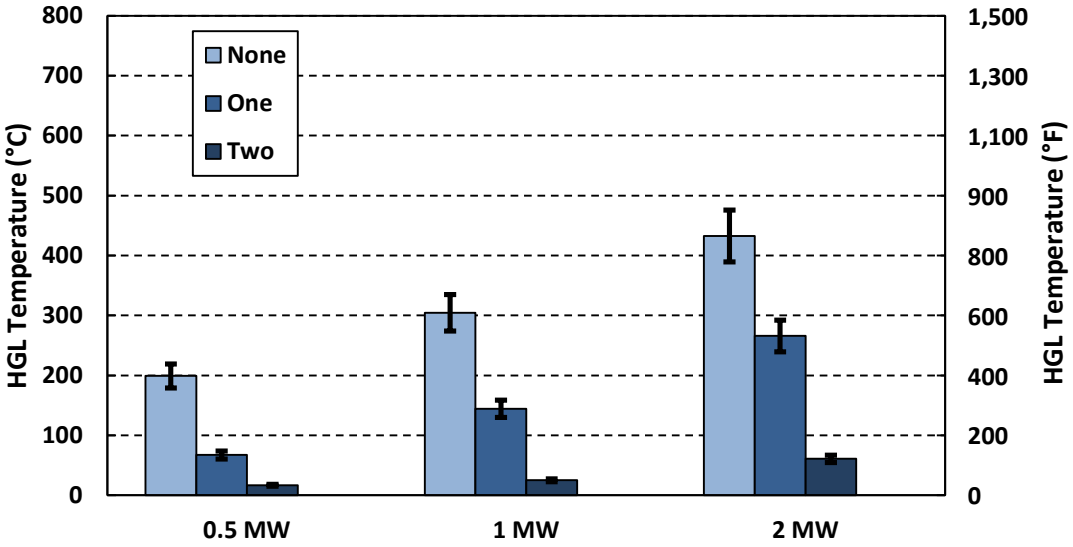

Figure 6-6: Bar graph of the average HGL temperatures from the steady-state 0.5 MW, 1 MW, and 2 MW fires with the vents closed, one vent opened , and two vents opened based on the temperatures from the thermocouples in the doorway. The error bar represents the expanded measurement uncertainty as presented in Section 2.6.

6.2. Comparison of Natural Gas Experiments and FDS Simulations

From the steady state temperatures collected near the burner, near the doorway, and in the doorway, the average HGL interface height and HGL temperature was calculated for each fire size at each of the three locations for both the experiments and the FDS simulations. The average interface heights from the experiments are plotted against the interface heights from the simulations in Figure 6-7 (near the burner), Figure 6-8 (near the doorway), and Figure 6-9 (in the doorway). At the locations inside the compartment, all of the average interface heights are well predicted. Inside the doorway, the average interface heights are also well-predicted when the vents were closed and one vent was opened. However, at the same location, when two vents were open, there was a large discrepancy. In the experiments, there was no HGL in the doorway. That being said, why then was the reported average interface height about 0.80 m (2.62 ft) and not the height of the doorway – 2.08 m (6.82 ft)? This is a limitation of the calculation used to get the interface height. As long as there is a temperature difference across the height of the doorway, there is an interface height produced by the calculation, even if the temperature difference across the doorway height is 5 °C (9 °F). Even if hot gases are no longer flowing through the doorway, there is a temperature gradient across the height of the room from the stored heat energy being released by the walls (as a result of being exposed to the fire for so long). Based on all of the information discussed so far, it was known that gases were only flowing into the room whenever two vents were open. In contrast, when two vents were open in the simulations, some hot gases were still flowing out the door as was seen in Figure 4-9 and Figure 4-19. The high interface heights of about 1.6 m to 1.8 m (5.2 ft to 5.9 ft) reflect that.

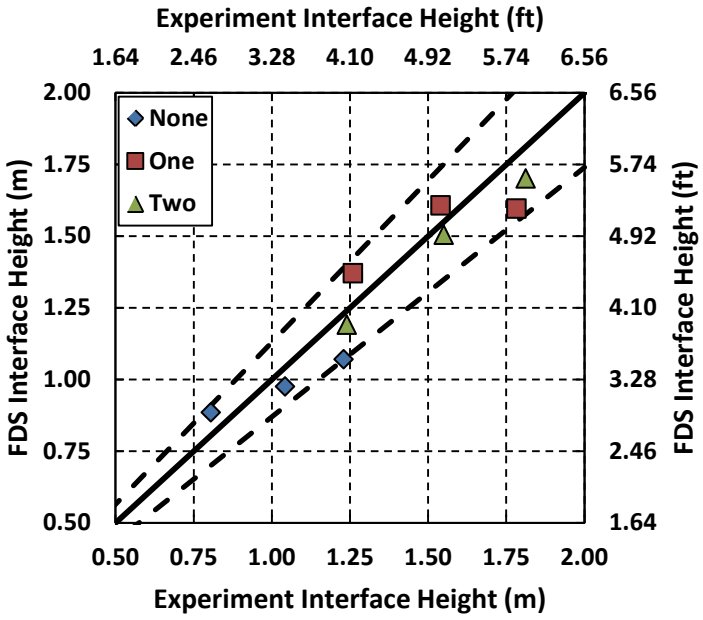

Figure 6-7: Average interface heights for each fire size based on the steady state temperatures from the thermocouple array near the burner for the experiments versus the simulations when no vents were open, one vent was open, and two vents were open. The dotted lines represent the expanded measurement uncertainty presented in Section 2.6 about the ideal model prediction.

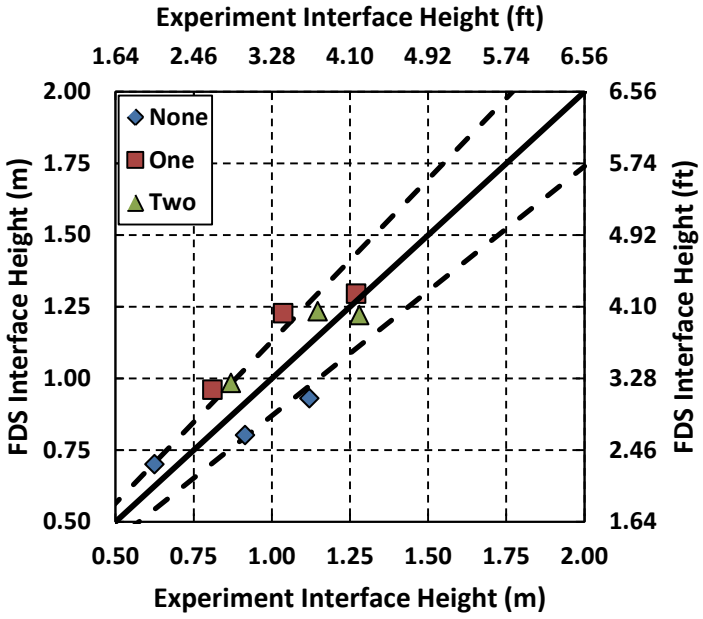

Figure 6-8: Average interface heights for each fire size based on the steady state temperatures from the thermocouple array near the doorway for the experiments versus the simulations when no vents were open, one vent was open, and two vents were open. The dotted lines represent the expanded measurement uncertainty presented in Section 2.6 about the ideal model prediction.

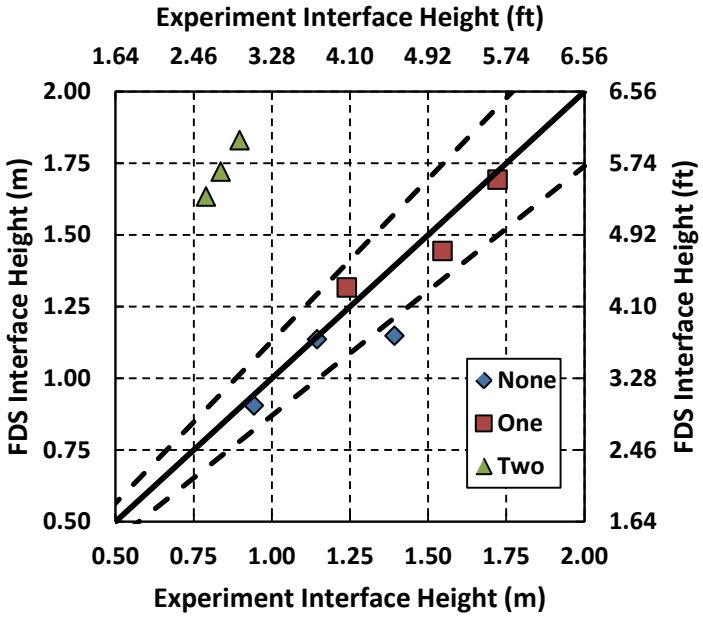

Figure 6-9: Average interface heights for each fire size based on the steady state temperatures from the thermocouples in the doorway for the experiments versus the simulations when no vents were open, one vent was open, and two vents were open. The dotted lines represent the expanded measurement uncertainty presented in Section 2.6 about the ideal model prediction.

The next three figures are plots of the measured HGL temperatures versus the simulated HGL temperatures evaluated near the burner, near the doorway, and in the doorway. In Figure 6-10, the HGL temperatures are well predicted when the vents were closed at the location near the burner. When one vent was open when the fire size was 2 MW, the HGL temperature was slightly under-predicted. When two vents were open, all of the HGL temperatures were under-predicted. The deviation from the measured HGL temperatures also increased with fire size. This matched the trend seen in the steady state temperatures measured in the thermocouple array near the burner (Figure 4-4). At 2 MW when both vents were open, the HGL temperature was under-predicted by about 125 °C (257 °F). At the location near the doorway, shown in Figure 6-11, the HGL temperatures were well simulated. In the doorway, the HGL temperatures were also well simulated when the vents were closed, but the HGL temperatures were over-predicted when one vent was open and two vents were open. At 2 MW when both vents were open, the HGL temperature was over-predicted by more than 200 °C (400 °F). This was because in the simulations hot gases were still flowing out of the doorway while in the experiments the two vents fully exhausted the hot gases. When two vents were open, the deviation from the measured HGL temperatures increased with an increase in fire size.

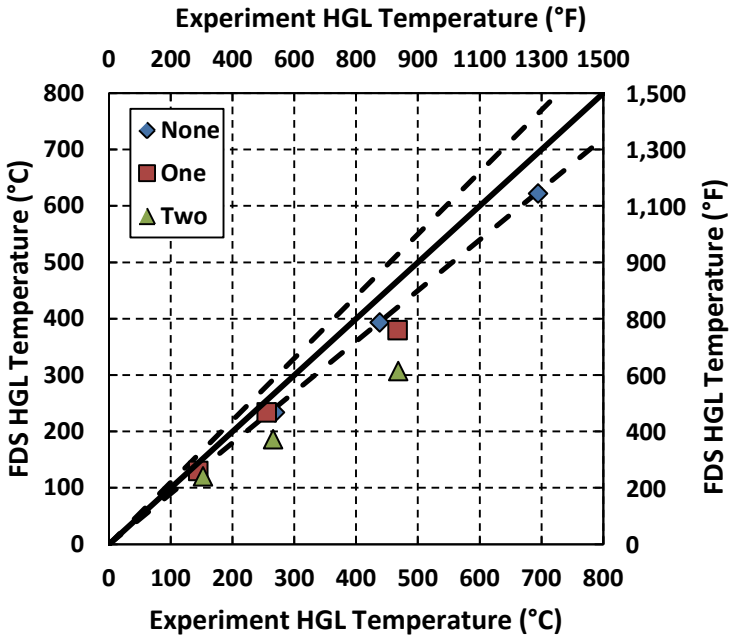

Figure 6-10: Average HGL temperatures for each fire size based on the steady state temperatures from the thermocouple array near the burner for the experiments versus the simulations when no vents were open, one vent was open, and two vents were open. The dotted lines represent the expanded measurement uncertainty presented in Section 2.6 about the ideal model prediction.

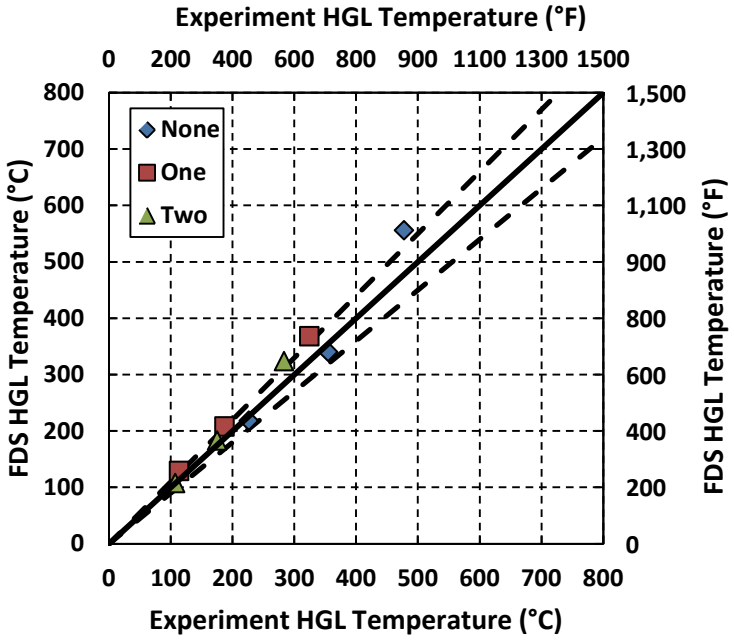

Figure 6-11: Average HGL temperatures for each fire size based on the steady state temperatures from the thermocouple array near the doorway for the experiments versus the simulations when no vents were open, one vent was open, and two vents were open. The dotted lines represent the expanded measurement uncertainty presented in Section 2.6 about the ideal model prediction.

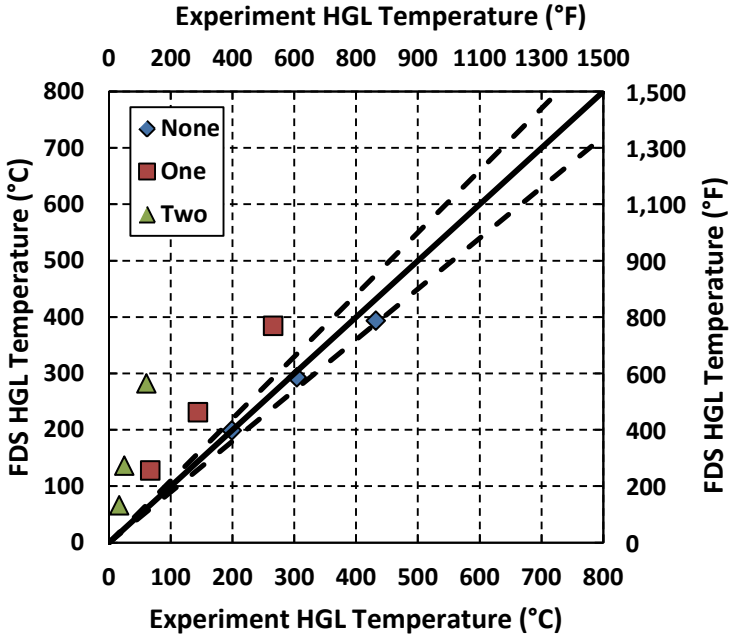

Figure 6-12: Average HGL temperatures for each fire size based on the steady state temperatures from the thermocouples in the doorway for the experiments versus the simulations when no vents were open, one vent was open, and two vents were open. The dotted lines represent the expanded measurement uncertainty presented in Section 2.6 about the ideal model prediction.

6.3. Comparison of Natural Gas Experiments and Sleeper Sofa Experiments

In the next six figures, the interface heights and HGL temperatures presented are based on the steady state temperatures from the 2 MW, natural gas fires and the instantaneous temperatures measured 10 s before the vent conditions were changed in the experiments with the sleeper sofas. In Figure 6-13 through Figure 6-15, the gas layer interface height is presented for the locations near the burner, near the doorway, and in the doorway. At the location near the burner, opening a vent improved conditions significantly in the 2 MW fires, almost 0.5 m (1.5 ft). Two vents had no impact on the interface height at 2 MW. Neither the single vent nor the combination of vents impacted the interface height in the experiment with one sleeper sofa or two sleeper sofas. With two sleeper sofas, the CGL was only 0.8 m (2.5 ft) high.

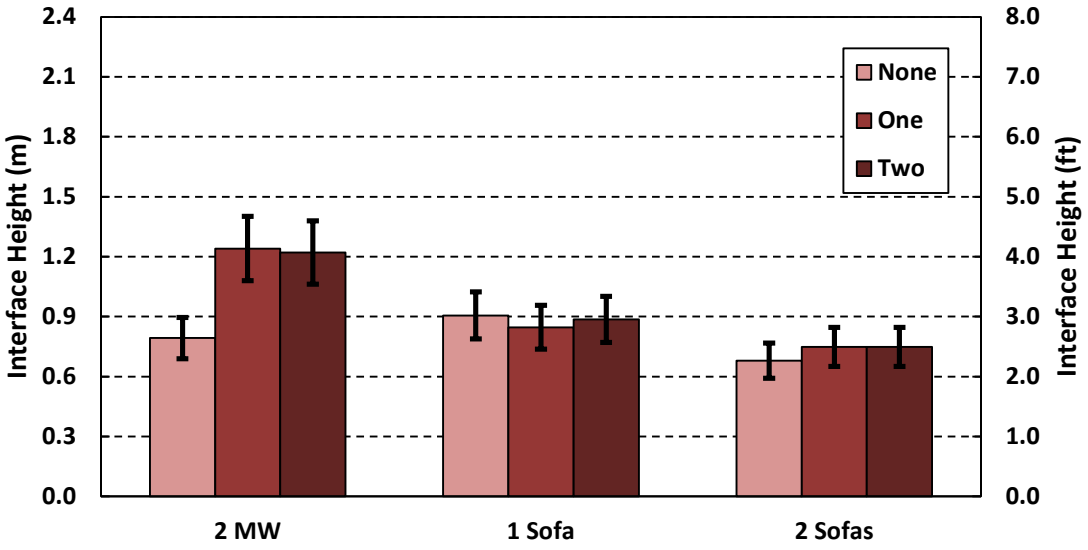

Figure 6-13: Bar graph of the HGL height from the steady-state 2 MW natural gas experiments, one sleeper sofa, and two sleeper sofas fires with the vents closed, one vent opened, and two vents opened based on the temperatures from the thermocouple array near the burner. The error bar represents the expanded measurement uncertainty as presented in Section 2.6.

In Figure 6-14 at the location near the doorway, the interface height increased as one vent was opened and then two vents were opened. In the experiment where the fuel was a single sleeper sofa, the interface slightly increased when one vent was opened and then the interface decreased when two vents were opened. When two sleeper sofas were burning, the interface height decreased slightly when the first vent was opened and decreased more after the second vent was opened. The decrease in the interface height means that the HGL increased slightly after the vents were opened. Near the doorway when the two sleeper sofas were burning the CGL was 0.6 m (2.0 ft).

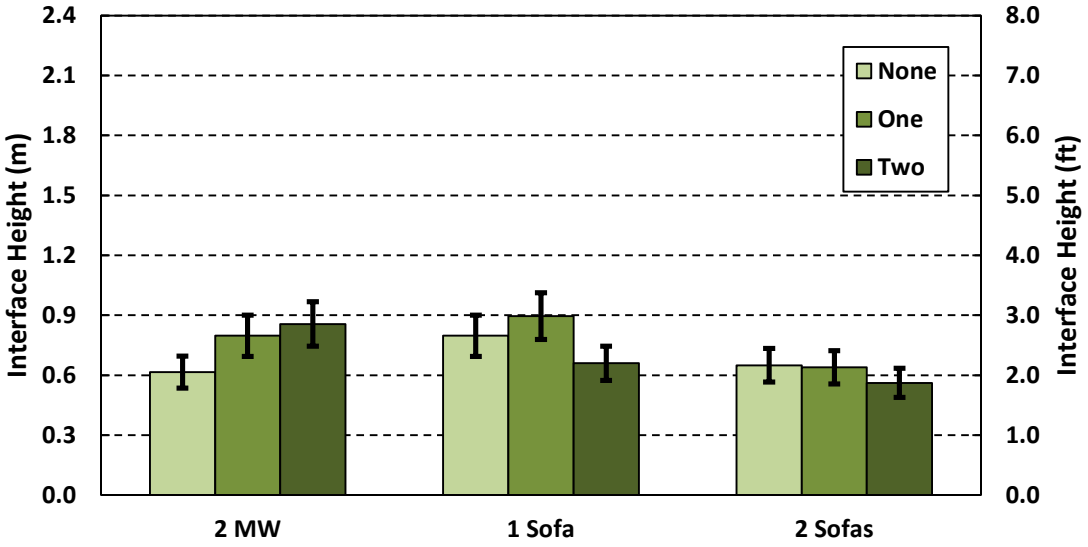

Figure 6-14: Bar graph of the HGL height from the steady-state 2 MW natural gas experiments, one sleeper sofa, and two sleeper sofas fires with the vents closed, one vent opened, and two vents opened based on the temperatures from the thermocouple array near the doorway. The error bar represents the expanded measurement uncertainty as presented in Section 2.6.

In the doorway at 2 MW, the gas layer interface height, shown in Figure 6-15, increased 0.3 m (1 ft) when one vent was opened. The interface heights in sofas experiments were unaffected by the changes in ventilation. With two sleeper sofas burning, the cool, fresh air was coming in through less than 0.9 m (3.0 ft) of the doorway.

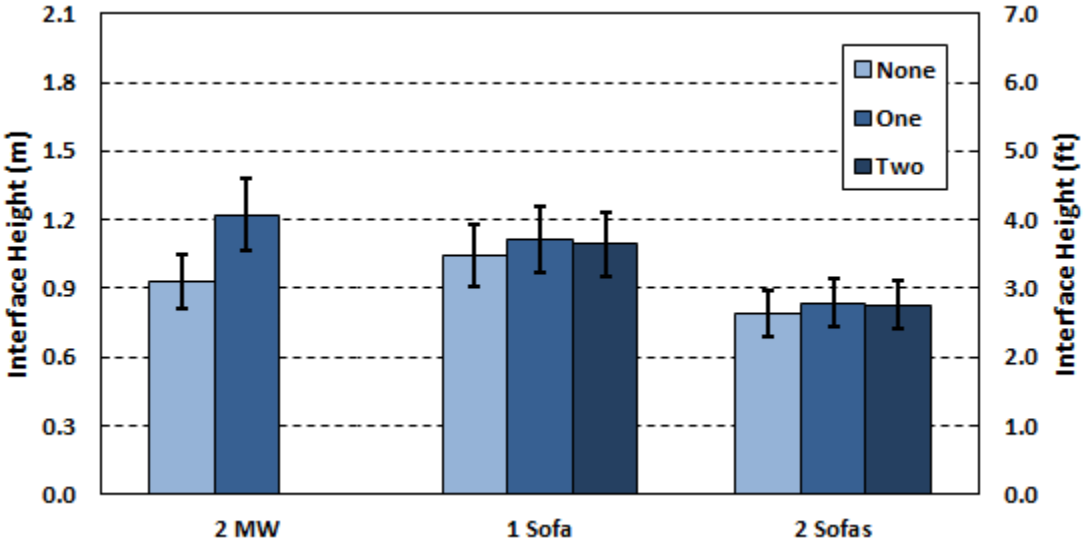

Figure 6-15: Bar graph of the HGL height from the steady-state 2 MW natural gas experiments, one sleeper sofa, and two sleeper sofas fires with the vents closed, one vent opened, and two vents opened based on the temperatures from the thermocouples in the doorway. The error bar represents the expanded measurement uncertainty as presented in Section 2.6.

The next three figures display the HGL temperatures calculated near the burner, near the doorway, and in the doorway. In Figure 6-16 at the location near the burner, opening one vent reduced the temperature. In the 2 MW fires, transitioning from one open vent to two open vents did not change the HGL temperature. In the one sleeper sofa experiment, the same change in ventilation increased the HGL temperature. With two sofas burning, the temperature decreased changing the conditions from one open vent to two. In this experiment, the HGL temperature was reduced 300 °C (600 °F) between when the vents were closed and two vents were opened. Even with the large reduction in temperature, in all of the fires presented the HGL temperature near the burner was at temperatures that would be quickly lethal to firefighters.

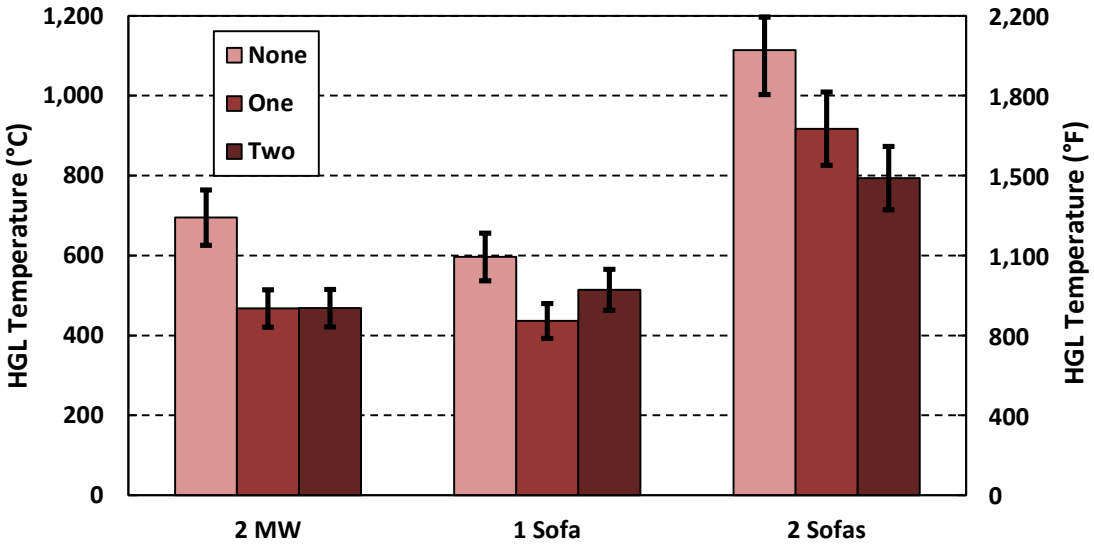

Figure 6-16: Bar graph of the HGL temperature from the steady-state 2 MW natural gas experiments, one sleeper sofa, and two sleeper sofas fires with the vents closed, one vent opened, and two vents opened based on the temperatures from the thermocouple array near the burner. The error bar represents the expanded measurement uncertainty as presented in Section 2.6.

At the location near the doorway, the HGL temperatures in Figure 6-17 were significantly less than the HGL temperatures on the other side of the vent in Figure 6-16. In each of the sleeper sofa experiments, opening one vent decreased the HGL temperature and opening a second vent further decreased the temperature. The two vents were able to cool the HGL in the three different fire conditions, but all of the temperatures were still above 260 °C (500 °F). This is the temperature that a firefighter's turnout gear is tested to withstand for only five minutes and there are less fire resistant pieces of a firefighter's uniform [35].

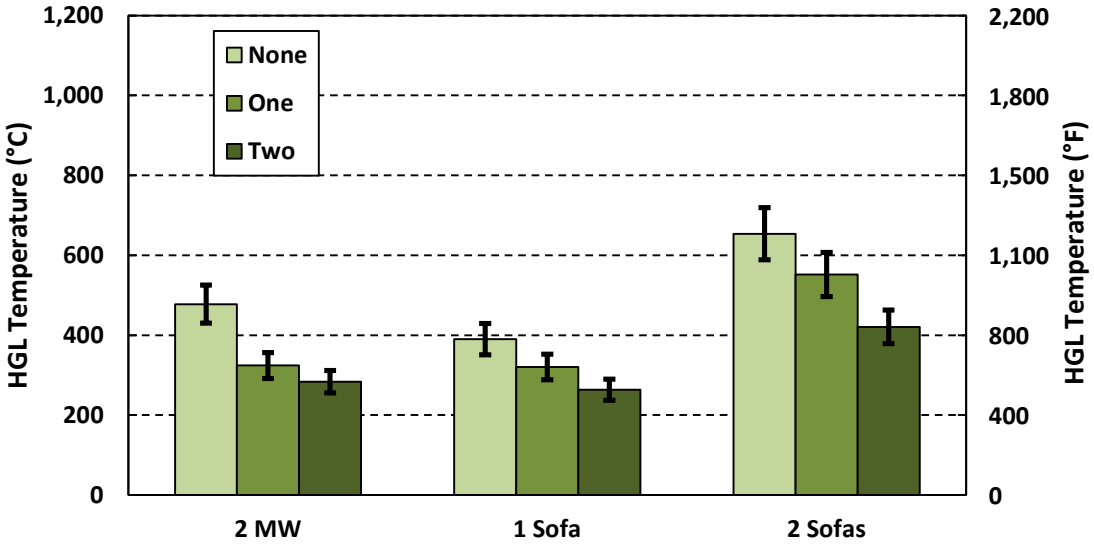

Figure 6-17: Bar graph of the HGL temperature from the steady-state 2 MW natural gas experiments, one sleeper sofa, and two sleeper sofas fires with the vents closed, one vent opened, and two vents opened based on the temperatures from the thermocouple array near the doorway. The error bar represents the expanded measurement uncertainty as presented in Section 2.6.

In Figure 6-18, the HGL temperatures for each of the sleeper sofa experiments determined from within the doorway did not significantly decrease when changing the conditions from no open vents to one open vent. But, the decrease in temperature ranged from 200 °C to almost 400 °C (400 °F to 800 °F) between when there were no vents and two open vents for each fire presented. With two open vents, the HGL temperatures from the sleeper sofa experiments were above the boiling point of water – 100 °C (212 °F).

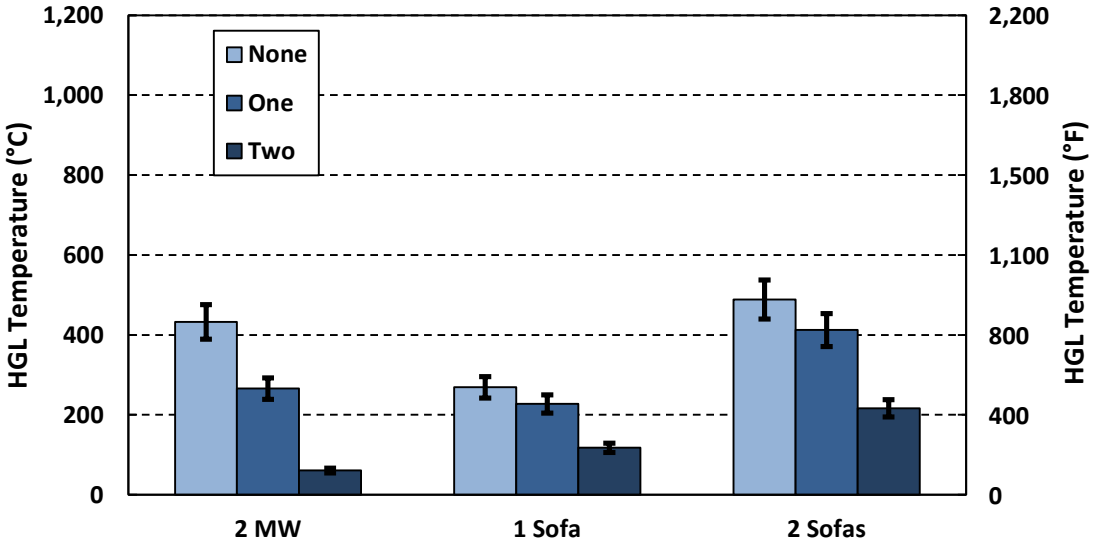

Figure 6-18: Bar graph of the HGL temperature from the steady-state 2 MW natural gas experiments, one sleeper sofa, and two sleeper sofas fires with the vents closed, one vent opened, and two vents opened based on the temperatures from the thermocouples in the doorway. The error bar represents the expanded measurement uncertainty as presented in Section 2.6.

7. Summary

In this study, thirty-three full-scale fire experiments were conducted in a room with an open doorway. In thirty-one of the experiments, the fire was fueled by natural gas. The fire size was varied between 0.5 MW, 1 MW, and 2 MW. In addition to varying the fire size, two 1.2 m × 1.2 m (4.0 ft × 4.0 ft) ceiling vents were opened and closed. The natural gas fires used a constant fuel flow, allowing the conditions in the room to reach nearly steady state. In the last two experiments, a sleeper sofa was ignited. In one experiment, there was only one sleeper sofa. In the other experiment, there were two sleeper sofas. When the sofas appeared to reach a maximum fire size, one vent was opened, shortly followed by the opening of the second vent.

The average steady state hot gas layer interface height and hot gas layer temperature was calculated for each of the experiments at three locations for the purpose of determining whether or not the average hot gas layer interface height increased and the average hot gas layer temperature decreased, reducing the threat to life. In the natural gas experiments, one open vent increased the average steady state hot gas layer interface height near the burner for all three fire sizes (meaning the hot gas layer depth was reduced), while the second vent had an insignificant impact. The average steady state hot gas layer interface height was increased by 0.3 m to 0.6 m (1.0 ft to 2.0 ft). Near the doorway, when one vent was opened, the average steady state interface height increased for all fire sizes, but the increase was less than 0.3 m (1.0 ft). Only in the 1 MW and 2 MW fires did the second vent affect the hot gas layer. In the doorway, one vent increased the average steady state interface height at least 0.3 m (1.0 ft) for each fire size. Two vents were able to completely exhaust the average steady state hot gas layer in the doorway for all three fire sizes. No hot gases flowed through the doorway as confirmed by the average steady state hot gas layer temperatures, which were near the temperature of the exterior of the room. The addition of the first vent and then the addition of the second vent decreased the average steady state hot gas layer temperature at all locations and for all fire sizes.

After completing the natural gas experiments, simulations were developed to match the experiments, including the instrumentation, using the National Institute of Standards and Technology's Fire Dynamics Simulator. The average steady state hot gas layer interface calculated from the simulations near the burner, near the doorway, and in the doorway were within the uncertainty of the measured average steady state hot gas layer interface height for all of the fire sizes and vent conditions except for the interface heights in the doorway when both vents were open. The interface heights were strongly over-predicted in the doorway when both vents were open. This resulted from the simulations predicting that there was always a hot gas layer in the doorway, while, in the experiments, there was no hot gas layer when both vents were open. The average steady state hot gas layer temperatures were also calculated from the results of the simulations. The average steady state hot gas layer temperatures were well simulated near the doorway for all of the fires sizes and vent conditions. Near the burner, the average steady state hot gas layer temperatures were significantly under-predicted when two vents were open. In the doorway, the average steady state hot gas layer temperatures were over-predicted when one vent was open and two vents were open. The average steady state hot gas layer temperatures were increasingly under-predicted or over-predicted with an increased in fire size. The rest of the average steady state hot gas layer temperatures were fairly well simulated by the Fire Dynamics Simulator.

While both one open vent and two open vents contributed to reducing the hot gas layer depth and temperature in the natural gas experiments, neither one nor two vents were capable of significantly impacting the average gas layer interface height in the sleeper sofa experiments. The vents did contribute to reducing the average hot gas layer temperatures. Near the doorway and in the doorway, the reduction in hot gas layer temperature between no open vents and one open vent matched or was surpassed by the reduction between one open vent and two open vents in both of the sleeper sofa experiments. With two open vents in the experiment with two sofas, the cold gas layer at the doorway was less than 0.9 m (3.0 ft), making the hot gas layer about 1.2 m (4.0 ft) deep. Through the upper 1.2 m (4.0 ft) of the door, temperatures still averaged over 200 °C (400 °F) after a minute of the two 1.2 m × 1.2 m (4.0 ft × 4.0 ft) ceiling vents being open.

In conclusion, one 1.2 m × 1.2 m (4.0 ft × 4.0 ft) ceiling vent was not sufficient to prevent the hot gas layer from flowing through the doorway in any of the fires. This means that if this room had been part of the house the hot gas layer would still have been flowing into the house. Two open vents, creating a 2.4 m × 1.2 m (8.0 ft × 4.0 ft) opening in the ceiling, fully exhausted the hot gas layer at 0.5 MW, 1 MW, and 2 MW. The simulations produced by the Fire Dynamics Simulator reproduced the hot gas layer interface height for all of the natural gas fires and vent conditions close to or within the experimental uncertainty except when both vents were open in the doorway. In this case, the steady state hot gas layer interface height was severely over-predicted. When two vents were open, the simulated steady state hot gas layer temperatures were over-predicted and deviated the most from the measured temperatures. The steady state hot gas layer temperatures were under-predicted near the burner and over-predicted in the doorway. The deviation increased in both cases with an increase in fire size. In the sleeper sofa experiments, there was little change in the depth of the hot gas layer in the doorway with one and then two vents. But both one vent and two vents decreased the temperature of the hot gas layer.

8. Conclusions

The findings of this study impact firefighters and the ability of researchers to address questions raised by the fire service through computer fire modeling. After evaluating vertical ventilation in well controlled, natural gas fires, comparing the results to computer simulations, and evaluating vertical ventilation in less predictable furniture fires, the following conclusions were reached:

One 1.2 m × 1.2 m (4.0 ft × 4.0 ft) vent did not fully exhaust the smoke and hot gas layer in any of the fires. If this was the intended goal of the minimum vent size requirement (which was never explained in the firefighter training textbook [24]), it was never achieved. Another possible goal could have been to reduce the smoke and hot gases flowing through the doorway. When treating this room as a part of a larger structure, reducing the hazard to the rest of the building may be valuable to firefighters and building occupants located in other areas of a building. The vent was effective in meeting this goal for the smaller fires (2 MW in size or less), but did not significantly decrease either the hot gas layer depth or temperature when two sofas were burning.

Two 1.2 m × 1.2 m (4.0 ft × 4.0 ft) vents did fully exhaust the smoke and hot gas layer for the natural gas fires. If the goal of venting is to fully exhaust the hot gas layer, then for the fires 2 MW in size or less, this goal was achieved. If the goal was to reduce the flow of the smoke and hot gases through the doorway, then doubling the vent size did achieve this goal. But the double vent size would only partly reduce the hazard to firefighters and building occupants within the building and outside the room of origin. When two sofas were burning with both vents open, the temperatures in the doorway decreased but were still not low enough for firefighters to safely walk or crawl into the room.

Given that two 1.2 m × 1.2 m (4.0 ft × 4.0 ft) vents, which were 11% of the total area of the ceiling, were not able to relieve enough of the hazards created by two sofas burning to permit firefighters to safely enter the room, there may be a limit to the usefulness of vertical ventilation as a firefighting tactic. As a fire grows and extends beyond the room of origin, more and more vents would be necessary to control the smoke and hot gases. As more vents are needed, either more firefighters will be needed to open or cut vents in the roof or each firefighter will spend more time standing on top of a structure that is burning underneath them.

The Fire Dynamics Simulator used to simulate the natural gas experiments needs to be validated further before it can be used to accurately simulate conditions in a structure fire with vertical ventilation. The hot gas layer depth was generally well predicted, but the temperatures of the hot gas layer in the doorway were being increasingly over-predicted when two vents were open and the fire size was increased. If the results in the doorway are incorrect, then that error will be propagated throughout a multi-room structure.

Appendices

Appendix A. Natural Gas Composition & Properties

The table below was provided by Nicor Gas Company

Table 8-1: Table of Natural Gas Properties

January 5, 2012 Percent by Volume at 14.73 PSIA and 60 Degrees F.

		Northern Natural Gas Pipeline	
Date of Sample:		Dec-11 (Avg)	
Moisture		Dry	
Nitrogen	N2	1.67	%
Carbon Dioxide	CO2	0.88	
Methane	CH4	94.62	
Ethane	C2H6	2.44	
Propane	C3H8	0.30	
Butanes - I	C4H10	0.03	
Butanes - N	C4H10	0.04	
Pentanes - I	C5H12	0.01	
Pentanes - N	C5H12	0.01	
Hexane & Others	C6+	0.01	
Helium	He	0.00	
Heptanes	C7	0.00	
Hydrogen	H2	0.00	
Oxygen	O2	0.00	
		100.00	%
BTU Per Cubic Foot			
By Calorimeter		1014	
Calculated from Analysis		1012	
Specific Gravity			
Determined by Balance		0.587	
Calculated		0.585	

Appendix B. Raw Steady State Experiment Data

Table 1-2: Steady state temperatures (°C) at 0.03 m from the ceiling on the thermocouple array near the burner

Experiment #	Fire Size (MW)	# of Open Vents	Temperature	Standard Deviation
1	0.5	0	383	20
2	0.5	1	233	37
3	0.5	2	242	35
4	0.5	0	387	33
5	1	0	749	41
6	1	1	522	60
7	1	2	566	73
8	1	0	607	131
9	2	0	-	-
10	2	1	-	-
11	2	0	1006	26
12	2	1	888	63
13	2	2	944	79
14	0.5	0	436	26
15	0.5	1	272	41
16	0.5	2	277	40
17	1	0	728	38
18	1	1	529	48
19	1	2	582	56
20	1	0	735	42
21	1	1	516	57
22	1	2	558	55
23	0.5	2	311	31
24	0.5	1	321	51
25	0.5	0	489	45
26	0.5	1	311	36
27	0.5	2	290	40
28	2	2	979	67
29	2	0	1022	18
30	2	1	967	47
31	2	2	1018	38

Table 1-3: Steady state temperatures (°C) at 0.3 m from the ceiling on the thermocouple array near the burner

Experiment #	Fire Size (MW)	# of Open Vents	Temperature	Standard Deviation
1	0.5	0	322	12
2	0.5	1	89	16
3	0.5	2	94	13
4	0.5	0	337	17
5	1	0	600	30
6	1	1	279	39
7	1	2	271	36
8	1	0	531	65
9	2	0	-	-
10	2	1	-	-
11	2	0	868	28
12	2	1	504	55
13	2	2	575	80
14	0.5	0	363	15
15	0.5	1	97	14
16	0.5	2	108	15
17	1	0	593	26
18	1	1	287	43
19	1	2	279	41
20	1	0	595	29
21	1	1	255	39
22	1	2	276	42
23	0.5	2	131	14
24	0.5	1	116	15
25	0.5	0	410	17
26	0.5	1	119	14
27	0.5	2	122	20
28	2	2	596	73
29	2	0	912	25
30	2	1	627	67
31	2	2	664	70

Table 1-4: Steady state temperatures (°C) at 0.6 m from the ceiling on the thermocouple array near the burner

Experiment #	Fire Size (MW)	# of Open Vents	Temperature	Standard Deviation
1	0.5	0	240	6
2	0.5	1	49	2
3	0.5	2	53	4
4	0.5	0	256	8
5	1	0	478	8
6	1	1	131	7
7	1	2	119	7
8	1	0	443	13
9	2	0	-	-
10	2	1	-	-
11	2	0	705	17
12	2	1	277	13
13	2	2	295	22
14	0.5	0	254	9
15	0.5	1	58	4
16	0.5	2	59	4
17	1	0	474	13
18	1	1	150	8
19	1	2	148	12
20	1	0	458	14
21	1	1	142	5
22	1	2	141	7
23	0.5	2	87	6
24	0.5	1	83	6
25	0.5	0	309	8
26	0.5	1	81	5
27	0.5	2	73	6
28	2	2	329	25
29	2	0	797	15
30	2	1	435	29
31	2	2	393	30

Table 1-5: Steady state temperatures (°C) at 0.9 m from the ceiling on the thermocouple array near the burner

Experiment #	Fire Size (MW)	# of Open Vents	Temperature	Standard Deviation
1	0.5	0	170	7
2	0.5	1	41	1
3	0.5	2	43	4
4	0.5	0	176	8
5	1	0	357	12
6	1	1	112	5
7	1	2	101	11
8	1	0	311	20
9	2	0	-	-
10	2	1	-	-
11	2	0	573	15
12	2	1	238	12
13	2	2	236	14
14	0.5	0	145	6
15	0.5	1	45	3
16	0.5	2	44	3
17	1	0	337	10
18	1	1	122	10
19	1	2	114	10
20	1	0	324	12
21	1	1	121	7
22	1	2	113	8
23	0.5	2	69	4
24	0.5	1	70	4
25	0.5	0	185	7
26	0.5	1	68	4
27	0.5	2	58	6
28	2	2	237	14
29	2	0	718	16
30	2	1	349	16
31	2	2	301	15

Table 1-6: Steady state temperatures (°C) at 1.2 m from the ceiling on the thermocouple array near the burner

Experiment #	Fire Size (MW)	# of Open Vents	Temperature	Standard Deviation
1	0.5	0	83	3
2	0.5	1	46	2
3	0.5	2	48	3
4	0.5	0	90	4
5	1	0	240	8
6	1	1	114	5
7	1	2	103	9
8	1	0	226	11
9	2	0	-	-
10	2	1	-	-
11	2	0	452	19
12	2	1	226	13
13	2	2	227	15
14	0.5	0	92	3
15	0.5	1	49	2
16	0.5	2	49	3
17	1	0	267	8
18	1	1	125	8
19	1	2	119	8
20	1	0	250	9
21	1	1	123	7
22	1	2	121	9
23	0.5	2	75	5
24	0.5	1	74	4
25	0.5	0	145	6
26	0.5	1	72	4
27	0.5	2	63	4
28	2	2	232	15
29	2	0	597	18
30	2	1	308	15
31	2	2	288	18

Table 1-7: Steady state temperatures (°C) at 1.5 m from the ceiling on the thermocouple array near the burner

Experiment #	Fire Size (MW)	# of Open Vents	Temperature	Standard Deviation
1	0.5	0	62	3
2	0.5	1	41	2
3	0.5	2	43	3
4	0.5	0	69	4
5	1	0	193	8
6	1	1	99	5
7	1	2	88	6
8	1	0	191	10
9	2	0	-	-
10	2	1	-	-
11	2	0	374	15
12	2	1	180	8
13	2	2	183	11
14	0.5	0	69	4
15	0.5	1	42	2
16	0.5	2	47	3
17	1	0	225	10
18	1	1	98	5
19	1	2	103	9
20	1	0	219	10
21	1	1	99	5
22	1	2	105	12
23	0.5	2	67	5
24	0.5	1	62	4
25	0.5	0	119	6
26	0.5	1	60	3
27	0.5	2	57	4
28	2	2	183	11
29	2	0	527	14
30	2	1	239	12
31	2	2	232	20

Table 1-8: Steady state temperatures (°C) at 1.8 m from the ceiling on the thermocouple array near the burner

Experiment #	Fire Size (MW)	# of Open Vents	Temperature	Standard Deviation
1	0.5	0	48	3
2	0.5	1	36	2
3	0.5	2	40	2
4	0.5	0	52	2
5	1	0	139	7
6	1	1	78	3
7	1	2	75	3
8	1	0	140	7
9	2	0	-	-
10	2	1	-	-
11	2	0	245	10
12	2	1	149	7
13	2	2	149	7
14	0.5	0	49	2
15	0.5	1	39	2
16	0.5	2	42	2
17	1	0	159	8
18	1	1	81	3
19	1	2	84	5
20	1	0	161	9
21	1	1	83	3
22	1	2	83	6
23	0.5	2	58	3
24	0.5	1	53	3
25	0.5	0	84	3
26	0.5	1	52	2
27	0.5	2	50	3
28	2	2	147	6
29	2	0	391	16
30	2	1	197	7
31	2	2	180	11

Table 1-9: Steady state temperatures (°C) at 2.1 m from the ceiling on the thermocouple array near the burner

Experiment #	Fire Size (MW)	# of Open Vents	Temperature	Standard Deviation
1	0.5	0	47	1
2	0.5	1	37	3
3	0.5	2	42	2
4	0.5	0	50	2
5	1	0	133	4
6	1	1	79	4
7	1	2	75	3
8	1	0	137	7
9	2	0	-	-
10	2	1	-	-
11	2	0	191	9
12	2	1	137	7
13	2	2	133	10
14	0.5	0	46	3
15	0.5	1	38	3
16	0.5	2	41	3
17	1	0	128	5
18	1	1	78	4
19	1	2	73	4
20	1	0	124	4
21	1	1	78	4
22	1	2	73	3
23	0.5	2	53	3
24	0.5	1	50	3
25	0.5	0	74	3
26	0.5	1	49	2
27	0.5	2	47	2
28	2	2	125	5
29	2	0	315	9
30	2	1	181	8
31	2	2	147	6

Table 1-10: Steady state temperatures (°C) at 0.03 m from the ceiling on the thermocouple array near the doorway

Experiment #	Fire Size (MW)	# of Open Vents	Temperature	Standard Deviation
1	0.5	0	282	5
2	0.5	1	180	7
3	0.5	2	145	6
4	0.5	0	290	6
5	1	0	514	13
6	1	1	329	18
7	1	2	261	9
8	1	0	511	20
9	2	0	-	-
10	2	1	-	-
11	2	0	493	14
12	2	1	412	5
13	2	2	388	19
14	0.5	0	188	3
15	0.5	1	141	3
16	0.5	2	129	1
17	1	0	356	5
18	1	1	263	3
19	1	2	233	2
20	1	0	353	4
21	1	1	262	2
22	1	2	233	3
23	0.5	2	179	2
24	0.5	1	178	2
25	0.5	0	250	2
26	0.5	1	178	2
27	0.5	2	156	2
28	2	2	369	4
29	2	0	570	10
30	2	1	447	3
31	2	2	408	2

Table 1-11: Steady state temperatures (°C) at 0.3 m from the ceiling on the thermocouple array near the doorway

Experiment #	Fire Size (MW)	# of Open Vents	Temperature	Standard Deviation
1	0.5	0	279	4
2	0.5	1	155	8
3	0.5	2	137	5
4	0.5	0	287	4
5	1	0	505	12
6	1	1	311	14
7	1	2	258	8
8	1	0	495	21
9	2	0	-	-
10	2	1	-	-
11	2	0	530	11
12	2	1	514	23
13	2	2	455	33
14	0.5	0	308	4
15	0.5	1	167	10
16	0.5	2	154	7
17	1	0	486	12
18	1	1	313	18
19	1	2	272	9
20	1	0	477	8
21	1	1	308	17
22	1	2	267	9
23	0.5	2	180	10
24	0.5	1	197	9
25	0.5	0	351	4
26	0.5	1	187	12
27	0.5	2	164	8
28	2	2	437	13
29	2	0	657	32
30	2	1	545	12
31	2	2	463	15

Table 1-12: Steady state temperatures (°C) at 0.6 m from the ceiling on the thermocouple array near the doorway

Experiment #	Fire Size (MW)	# of Open Vents	Temperature	Standard Deviation
1	0.5	0	269	5
2	0.5	1	79	10
3	0.5	2	91	13
4	0.5	0	277	6
5	1	0	463	8
6	1	1	212	21
7	1	2	200	22
8	1	0	456	15
9	2	0	-	-
10	2	1	-	-
11	2	0	507	10
12	2	1	369	24
13	2	2	359	39
14	0.5	0	298	8
15	0.5	1	81	14
16	0.5	2	100	12
17	1	0	455	13
18	1	1	198	22
19	1	2	190	31
20	1	0	449	12
21	1	1	186	23
22	1	2	195	27
23	0.5	2	109	18
24	0.5	1	114	13
25	0.5	0	338	7
26	0.5	1	109	13
27	0.5	2	99	15
28	2	2	373	31
29	2	0	636	35
30	2	1	464	25
31	2	2	344	43

Table 1-13: Steady state temperatures (°C) at 0.9 m from the ceiling on the thermocouple array near the doorway

Experiment #	Fire Size (MW)	# of Open Vents	Temperature	Standard Deviation
1	0.5	0	198	8
2	0.5	1	43	3
3	0.5	2	47	5
4	0.5	0	206	8
5	1	0	380	11
6	1	1	102	10
7	1	2	92	8
8	1	0	360	18
9	2	0	-	-
10	2	1	-	-
11	2	0	437	11
12	2	1	198	4
13	2	2	196	8
14	0.5	0	157	11
15	0.5	1	49	3
16	0.5	2	52	3
17	1	0	335	15
18	1	1	115	4
19	1	2	105	7
20	1	0	325	17
21	1	1	113	4
22	1	2	101	5
23	0.5	2	72	4
24	0.5	1	71	3
25	0.5	0	187	11
26	0.5	1	70	2
27	0.5	2	62	4
28	2	2	196	9
29	2	0	583	36
30	2	1	267	9
31	2	2	222	9

Table 1-14: Steady state temperatures (°C) at 1.2 m from the ceiling on the thermocouple array near the doorway

Experiment #	Fire Size (MW)	# of Open Vents	Temperature	Standard Deviation
1	0.5	0	60	2
2	0.5	1	31	3
3	0.5	2	36	5
4	0.5	0	63	3
5	1	0	184	6
6	1	1	81	4
7	1	2	72	5
8	1	0	182	12
9	2	0	-	-
10	2	1	-	-
11	2	0	319	18
12	2	1	147	4
13	2	2	142	7
14	0.5	0	57	3
15	0.5	1	36	3
16	0.5	2	40	4
17	1	0	176	5
18	1	1	87	3
19	1	2	78	5
20	1	0	175	6
21	1	1	87	3
22	1	2	78	4
23	0.5	2	56	4
24	0.5	1	53	3
25	0.5	0	101	3
26	0.5	1	55	2
27	0.5	2	44	5
28	2	2	144	6
29	2	0	513	15
30	2	1	215	6
31	2	2	180	6

Table 1-15: Steady state temperatures (°C) at 1.5 m from the ceiling on the thermocouple array near the doorway

Experiment #	Fire Size (MW)	# of Open Vents	Temperature	Standard Deviation
1	0.5	0	55	2
2	0.5	1	23	3
3	0.5	2	22	4
4	0.5	0	56	2
5	1	0	150	3
6	1	1	68	4
7	1	2	49	7
8	1	0	148	7
9	2	0	-	-
10	2	1	-	-
11	2	0	271	13
12	2	1	155	7
13	2	2	135	16
14	0.5	0	51	2
15	0.5	1	26	4
16	0.5	2	21	4
17	1	0	154	5
18	1	1	80	4
19	1	2	55	8
20	1	0	154	6
21	1	1	79	3
22	1	2	57	8
23	0.5	2	36	5
24	0.5	1	43	5
25	0.5	0	89	2
26	0.5	1	46	4
27	0.5	2	28	5
28	2	2	124	7
29	2	0	467	9
30	2	1	218	7
31	2	2	159	7

Table 1-16: Steady state temperatures (°C) at 1.8 m from the ceiling on the thermocouple array near the doorway

Experiment #	Fire Size (MW)	# of Open Vents	Temperature	Standard Deviation
1	0.5	0	47	2
2	0.5	1	18	2
3	0.5	2	16	2
4	0.5	0	50	2
5	1	0	148	4
6	1	1	48	6
7	1	2	26	3
8	1	0	147	9
9	2	0	-	-
10	2	1	-	-
11	2	0	206	19
12	2	1	104	5
13	2	2	76	23
14	0.5	0	40	2
15	0.5	1	15	2
16	0.5	2	12	1
17	1	0	118	6
18	1	1	51	4
19	1	2	21	6
20	1	0	112	5
21	1	1	48	6
22	1	2	23	4
23	0.5	2	17	3
24	0.5	1	26	5
25	0.5	0	67	3
26	0.5	1	25	5
27	0.5	2	18	3
28	2	2	54	13
29	2	0	305	39
30	2	1	158	11
31	2	2	75	18

Table 1-17: Steady state temperatures (°C) at 2.1 m from the ceiling on the thermocouple array near the doorway

Experiment #	Fire Size (MW)	# of Open Vents	Temperature	Standard Deviation
1	0.5	0	32	2
2	0.5	1	18	1
3	0.5	2	17	2
4	0.5	0	34	2
5	1	0	88	4
6	1	1	30	3
7	1	2	26	2
8	1	0	89	5
9	2	0	-	-
10	2	1	-	-
11	2	0	94	6
12	2	1	43	9
13	2	2	31	9
14	0.5	0	25	2
15	0.5	1	13	1
16	0.5	2	14	1
17	1	0	70	6
18	1	1	21	3
19	1	2	19	2
20	1	0	71	6
21	1	1	23	3
22	1	2	21	2
23	0.5	2	18	2
24	0.5	1	18	2
25	0.5	0	42	3
26	0.5	1	18	2
27	0.5	2	16	1
28	2	2	27	2
29	2	0	202	12
30	2	1	64	11
31	2	2	36	2

Table 1-18: Steady state temperatures (°C) at 0.03 m from the top of the doorway

Experiment #	Fire Size (MW)	# of Open Vents	Temperature	Standard Deviation
1	0.5	0	244	5
2	0.5	1	108	5
3	0.5	2	15	1
4	0.5	0	232	9
5	1	0	-	-
6	1	1	-	-
7	1	2	-	-
8	1	0	-	-
9	2	0	-	-
10	2	1	-	-
11	2	0	426	10
12	2	1	368	4
13	2	2	-	-
14	0.5	0	285	2
15	0.5	1	142	3
16	0.5	2	19	2
17	1	0	414	7
18	1	1	288	4
19	1	2	34	3
20	1	0	416	8
21	1	1	285	3
22	1	2	31	1
23	0.5	2	21	1
24	0.5	1	84	41
25	0.5	0	322	6
26	0.5	1	177	5
27	0.5	2	18	0
28	2	2	48	4
29	2	0	504	65
30	2	1	504	7
31	2	2	91	11

Table 1-19: Steady state temperatures (°C) at 0.2 m from the top of the doorway

Experiment #	Fire Size (MW)	# of Open Vents	Temperature	Standard Deviation
1	0.5	0	260	2
2	0.5	1	23	2
3	0.5	2	13	0
4	0.5	0	264	3
5	1	0	463	4
6	1	1	198	14
7	1	2	21	1
8	1	0	454	14
9	2	0	644	7
10	2	1	491	32
11	2	0	526	10
12	2	1	368	10
13	2	2	-	-
14	0.5	0	284	3
15	0.5	1	47	4
16	0.5	2	15	1
17	1	0	440	4
18	1	1	206	7
19	1	2	26	1
20	1	0	438	4
21	1	1	177	12
22	1	2	26	1
23	0.5	2	19	0
24	0.5	1	37	11
25	0.5	0	331	3
26	0.5	1	64	4
27	0.5	2	17	0
28	2	2	45	3
29	2	0	625	12
30	2	1	424	16
31	2	2	72	6

Table 1-20: Steady state temperatures (°C) at 0.4 m from the top of the doorway

Experiment #	Fire Size (MW)	# of Open Vents	Temperature	Standard Deviation
1	0.5	0	173	4
2	0.5	1	17	0
3	0.5	2	15	0
4	0.5	0	181	8
5	1	0	400	9
6	1	1	39	6
7	1	2	20	0
8	1	0	369	13
9	2	0	565	8
10	2	1	329	44
11	2	0	387	12
12	2	1	146	9
13	2	2	-	-
14	0.5	0	182	6
15	0.5	1	23	1
16	0.5	2	16	0
17	1	0	333	10
18	1	1	62	5
19	1	2	31	1
20	1	0	325	11
21	1	1	51	2
22	1	2	33	0
23	0.5	2	24	1
24	0.5	1	24	1
25	0.5	0	228	5
26	0.5	1	30	1
27	0.5	2	20	0
28	2	2	64	1
29	2	0	545	7
30	2	1	265	21
31	2	2	87	4

Table 1-21: Steady state temperatures (°C) at 0.6 m from the top of the doorway

Experiment #	Fire Size (MW)	# of Open Vents	Temperature	Standard Deviation
1	0.5	0	59	1
2	0.5	1	16	0
3	0.5	2	15	0
4	0.5	0	62	3
5	1	0	255	2
6	1	1	47	6
7	1	2	23	1
8	1	0	201	17
9	2	0	524	18
10	2	1	153	47
11	2	0	383	11
12	2	1	91	8
13	2	2	-	-
14	0.5	0	59	3
15	0.5	1	17	1
16	0.5	2	15	0
17	1	0	233	10
18	1	1	43	3
19	1	2	26	0
20	1	0	223	7
21	1	1	39	1
22	1	2	29	1
23	0.5	2	22	0
24	0.5	1	22	0
25	0.5	0	123	2
26	0.5	1	24	1
27	0.5	2	18	0
28	2	2	52	1
29	2	0	487	20
30	2	1	147	16
31	2	2	74	3

Table 1-22: Steady state temperatures (°C) at 0.8 m from the top of the doorway

Experiment #	Fire Size (MW)	# of Open Vents	Temperature	Standard Deviation
1	0.5	0	29	0
2	0.5	1	16	0
3	0.5	2	15	0
4	0.5	0	31	1
5	1	0	167	5
6	1	1	44	5
7	1	2	26	1
8	1	0	127	16
9	2	0	498	17
10	2	1	123	42
11	2	0	268	11
12	2	1	76	6
13	2	2	-	-
14	0.5	0	27	1
15	0.5	1	16	0
16	0.5	2	14	0
17	1	0	150	8
18	1	1	37	2
19	1	2	25	1
20	1	0	149	6
21	1	1	34	1
22	1	2	27	1
23	0.5	2	20	1
24	0.5	1	20	0
25	0.5	0	76	2
26	0.5	1	21	1
27	0.5	2	17	0
28	2	2	48	1
29	2	0	419	31
30	2	1	139	12
31	2	2	80	4

Table 1-23: Steady state temperatures (°C) at 1.0 m from the top of the doorway

Experiment #	Fire Size (MW)	# of Open Vents	Temperature	Standard Deviation
1	0.5	0	20	0
2	0.5	1	14	0
3	0.5	2	14	0
4	0.5	0	21	0
5	1	0	79	4
6	1	1	30	2
7	1	2	21	0
8	1	0	66	10
9	2	0	266	10
10	2	1	127	21
11	2	0	148	10
12	2	1	50	3
13	2	2	-	-
14	0.5	0	17	0
15	0.5	1	13	0
16	0.5	2	13	0
17	1	0	63	4
18	1	1	26	1
19	1	2	20	0
20	1	0	66	2
21	1	1	27	0
22	1	2	22	0
23	0.5	2	18	0
24	0.5	1	18	0
25	0.5	0	34	1
26	0.5	1	18	0
27	0.5	2	16	0
28	2	2	39	1
29	2	0	236	23
30	2	1	89	5
31	2	2	58	1

Table 1-24: Steady state temperatures (°C) at 1.2 m from the top of the doorway

Experiment #	Fire Size (MW)	# of Open Vents	Temperature	Standard Deviation
1	0.5	0	20	0
2	0.5	1	15	0
3	0.5	2	14	0
4	0.5	0	20	0
5	1	0	52	2
6	1	1	29	1
7	1	2	22	0
8	1	0	46	3
9	2	0	141	10
10	2	1	101	9
11	2	0	82	5
12	2	1	52	2
13	2	2	-	-
14	0.5	0	18	0
15	0.5	1	14	0
16	0.5	2	13	0
17	1	0	48	2
18	1	1	27	1
19	1	2	21	1
20	1	0	48	1
21	1	1	28	0
22	1	2	23	0
23	0.5	2	19	1
24	0.5	1	18	0
25	0.5	0	28	1
26	0.5	1	19	0
27	0.5	2	16	0
28	2	2	40	1
29	2	0	123	12
30	2	1	83	2
31	2	2	60	1

Table 1-25: Steady state temperatures (°C) at 1.4 m from the top of the doorway

Experiment #	Fire Size (MW)	# of Open Vents	Temperature	Standard Deviation
1	0.5	0	20	0
2	0.5	1	15	0
3	0.5	2	14	0
4	0.5	0	20	0
5	1	0	50	1
6	1	1	30	1
7	1	2	23	0
8	1	0	44	3
9	2	0	123	10
10	2	1	98	8
11	2	0	69	4
12	2	1	54	3
13	2	2	-	-
14	0.5	0	18	0
15	0.5	1	15	0
16	0.5	2	14	0
17	1	0	48	2
18	1	1	29	1
19	1	2	23	1
20	1	0	49	2
21	1	1	30	1
22	1	2	25	1
23	0.5	2	20	1
24	0.5	1	19	0
25	0.5	0	28	0
26	0.5	1	20	0
27	0.5	2	17	0
28	2	2	44	2
29	2	0	110	11
30	2	1	85	2
31	2	2	63	2

Table 1-26: Steady state temperatures (°C) at 1.6 m from the top of the doorway

Experiment #	Fire Size (MW)	# of Open Vents	Temperature	Standard Deviation
1	0.5	0	15	0
2	0.5	1	13	0
3	0.5	2	12	0
4	0.5	0	15	0
5	1	0	31	1
6	1	1	20	0
7	1	2	17	0
8	1	0	30	1
9	2	0	75	4
10	2	1	56	3
11	2	0	42	2
12	2	1	33	0
13	2	2	-	-
14	0.5	0	14	0
15	0.5	1	12	0
16	0.5	2	11	0
17	1	0	30	1
18	1	1	20	0
19	1	2	17	0
20	1	0	32	1
21	1	1	22	0
22	1	2	18	0
23	0.5	2	16	0
24	0.5	1	16	0
25	0.5	0	20	0
26	0.5	1	16	0
27	0.5	2	14	0
28	2	2	30	0
29	2	0	73	5
30	2	1	51	1
31	2	2	40	1

Table 1-27: Steady state temperatures (°C) at 1.8 m from the top of the doorway

Experiment #	Fire Size (MW)	# of Open Vents	Temperature	Standard Deviation
1	0.5	0	16	0
2	0.5	1	13	0
3	0.5	2	13	0
4	0.5	0	16	0
5	1	0	34	1
6	1	1	22	1
7	1	2	18	0
8	1	0	32	2
9	2	0	77	4
10	2	1	60	3
11	2	0	52	2
12	2	1	40	1
13	2	2	-	-
14	0.5	0	15	0
15	0.5	1	12	0
16	0.5	2	12	0
17	1	0	32	1
18	1	1	21	0
19	1	2	17	0
20	1	0	34	1
21	1	1	23	0
22	1	2	19	0
23	0.5	2	16	0
24	0.5	1	16	0
25	0.5	0	22	0
26	0.5	1	16	0
27	0.5	2	15	0
28	2	2	31	0
29	2	0	76	5
30	2	1	55	1
31	2	2	42	1

Table 1-28: Steady state velocities (m/s) at 0.03 m from the top of the doorway

Experiment #	Fire Size (MW)	# of Open Vents	Velocity	Standard Deviation
1	0.5	0	-2.5	2.30
2	0.5	1	0.4	0.09
3	0.5	2	0.2	0.08
4	0.5	0	-2.0	2.55
5	1	0	-4.2	1.79
6	1	1	0.0	0.17
7	1	2	0.3	0.12
8	1	0	-4.0	1.93
9	2	0	-4.3	1.75
10	2	1	-1.6	0.89
11	2	0	-0.9	3.14
12	2	1	-0.5	0.70
13	2	2	0.5	0.79
14	0.5	0	-3.5	1.60
15	0.5	1	0.7	0.13
16	0.5	2	0.4	0.11
17	1	0	-4.1	2.86
18	1	1	0.7	0.20
19	1	2	0.6	0.10
20	1	0	-4.0	2.66
21	1	1	0.5	0.21
22	1	2	0.3	0.10
23	0.5	2	0.2	0.08
24	0.5	1	0.1	0.16
25	0.5	0	-3.2	2.22
26	0.5	1	0.4	0.14
27	0.5	2	0.1	0.08
28	2	2	0.3	0.41
29	2	0	-3.9	3.61
30	2	1	-0.9	1.03
31	2	2	0.5	0.15

Table 1-29: Steady state velocities (m/s) at 0.2 m from the top of the doorway

Experiment #	Fire Size (MW)	# of Open Vents	Velocity	Standard Deviation
1	0.5	0	-3.2	0.16
2	0.5	1	0.5	0.40
3	0.5	2	1.3	0.19
4	0.5	0	-3.2	0.19
5	1	0	-4.7	0.23
6	1	1	-0.7	0.61
7	1	2	1.3	0.22
8	1	0	-4.7	0.26
9	2	0	-6.1	0.22
10	2	1	-2.8	0.34
11	2	0	-4.8	0.27
12	2	1	-0.8	0.70
13	2	2	1.3	1.70
14	0.5	0	-2.8	0.25
15	0.5	1	1.2	0.34
16	0.5	2	1.7	0.22
17	1	0	-4.2	0.30
18	1	1	0.3	0.76
19	1	2	1.9	0.20
20	1	0	-3.5	0.27
21	1	1	1.2	0.74
22	1	2	2.5	0.19
23	0.5	2	2.3	0.15
24	0.5	1	1.4	0.65
25	0.5	0	-2.7	0.21
26	0.5	1	1.2	0.58
27	0.5	2	2.2	0.19
28	2	2	2.5	0.49
29	2	0	-5.2	0.25
30	2	1	-1.3	0.40
31	2	2	2.5	0.23

Table 1-30: Steady state velocities (m/s) at 0.4 m from the top of the doorway

Experiment #	Fire Size (MW)	# of Open Vents	Velocity	Standard Deviation
1	0.5	0	-2.6	0.24
2	0.5	1	0.3	0.16
3	0.5	2	0.7	0.17
4	0.5	0	-2.8	0.22
5	1	0	-4.3	0.22
6	1	1	0.2	0.24
7	1	2	0.8	0.14
8	1	0	-4.3	0.21
9	2	0	-5.7	0.20
10	2	1	-1.9	0.52
11	2	0	-3.4	0.27
12	2	1	1.4	0.61
13	2	2	2.2	0.77
14	0.5	0	-2.4	0.30
15	0.5	1	0.7	0.16
16	0.5	2	0.9	0.12
17	1	0	-3.8	0.26
18	1	1	0.7	0.15
19	1	2	1.2	0.13
20	1	0	-2.4	0.24
21	1	1	2.0	0.16
22	1	2	2.5	0.12
23	0.5	2	2.2	0.13
24	0.5	1	1.9	0.20
25	0.5	0	-1.7	0.22
26	0.5	1	1.8	0.17
27	0.5	2	2.2	0.18
28	2	2	2.6	0.36
29	2	0	-4.0	0.21
30	2	1	0.7	0.91
31	2	2	2.6	0.16

Table 1-31: Steady state velocities (m/s) at 0.6 m from the top of the doorway

Experiment #	Fire Size (MW)	# of Open Vents	Velocity	Standard Deviation
1	0.5	0	-0.7	0.52
2	0.5	1	0.3	0.13
3	0.5	2	0.6	0.14
4	0.5	0	-1.1	0.62
5	1	0	-3.4	0.24
6	1	1	0.4	0.15
7	1	2	0.8	0.12
8	1	0	-3.2	0.22
9	2	0	-5.2	0.22
10	2	1	0.0	0.43
11	2	0	-3.9	0.34
12	2	1	1.0	0.17
13	2	2	1.3	0.43
14	0.5	0	-0.3	0.34
15	0.5	1	0.5	0.12
16	0.5	2	0.7	0.13
17	1	0	-3.0	0.30
18	1	1	0.5	0.12
19	1	2	1.0	0.11
20	1	0	-2.2	0.31
21	1	1	1.2	0.11
22	1	2	1.6	0.13
23	0.5	2	1.4	0.11
24	0.5	1	1.1	0.20
25	0.5	0	-1.4	0.44
26	0.5	1	1.0	0.12
27	0.5	2	1.3	0.16
28	2	2	1.8	0.18
29	2	0	-4.2	0.26
30	2	1	1.1	0.17
31	2	2	1.8	0.15

Table 1-32: Steady state velocities (m/s) at 0.8 m from the top of the doorway

Experiment #	Fire Size (MW)	# of Open Vents	Velocity	Standard Deviation
1	0.5	0	0.1	0.02
2	0.5	1	-0.2	0.05
3	0.5	2	-0.3	0.06
4	0.5	0	0.1	0.03
5	1	0	1.1	0.09
6	1	1	-0.2	0.07
7	1	2	-0.5	0.08
8	1	0	0.7	0.14
9	2	0	3.1	0.12
10	2	1	0.1	0.26
11	2	0	1.4	0.11
12	2	1	0.8	0.09
13	2	2	0.9	0.12
14	0.5	0	0.1	0.02
15	0.5	1	0.2	0.04
16	0.5	2	0.3	0.05
17	1	0	0.8	0.08
18	1	1	0.4	0.05
19	1	2	0.5	0.05
20	1	0	0.9	0.07
21	1	1	0.5	0.05
22	1	2	0.6	0.06
23	0.5	2	0.5	0.05
24	0.5	1	0.4	0.07
25	0.5	0	0.5	0.06
26	0.5	1	0.3	0.05
27	0.5	2	0.4	0.06
28	2	2	0.9	0.09
29	2	0	1.8	0.21
30	2	1	1.1	0.12
31	2	2	1.0	0.08

Table 1-33: Steady state velocities (m/s) at 1.0 m from the top of the doorway

Experiment #	Fire Size (MW)	# of Open Vents	Velocity	Standard Deviation
1	0.5	0	-0.3	0.11
2	0.5	1	-1.0	0.14
3	0.5	2	-1.3	0.12
4	0.5	0	-0.6	0.10
5	1	0	-0.6	0.19
6	1	1	-1.4	0.13
7	1	2	-1.8	0.14
8	1	0	-0.8	0.18
9	2	0	-0.7	0.67
10	2	1	-2.1	0.14
11	2	0	0.0	0.38
12	2	1	2.6	0.33
13	2	2	3.0	0.38
14	0.5	0	0.5	0.41
15	0.5	1	1.6	0.23
16	0.5	2	1.9	0.20
17	1	0	-0.1	0.34
18	1	1	1.8	0.17
19	1	2	2.3	0.16
20	1	0	0.5	0.32
21	1	1	2.6	0.22
22	1	2	3.1	0.18
23	0.5	2	2.7	0.17
24	0.5	1	2.3	0.33
25	0.5	0	0.3	0.18
26	0.5	1	2.0	0.46
27	0.5	2	2.5	0.18
28	2	2	3.2	0.25
29	2	0	-0.5	0.32
30	2	1	2.3	0.47
31	2	2	3.2	0.21

Table 1-34: Steady state velocities (m/s) at 1.2 m from the top of the doorway

Experiment #	Fire Size (MW)	# of Open Vents	Velocity	Standard Deviation
1	0.5	0	0.0	0.04
2	0.5	1	0.1	0.05
3	0.5	2	0.2	0.06
4	0.5	0	0.0	0.04
5	1	0	0.1	0.05
6	1	1	0.2	0.06
7	1	2	0.3	0.09
8	1	0	0.0	0.05
9	2	0	0.4	0.08
10	2	1	0.7	0.15
11	2	0	0.6	0.06
12	2	1	0.8	0.08
13	2	2	0.9	0.15
14	0.5	0	0.1	0.03
15	0.5	1	0.2	0.08
16	0.5	2	0.3	0.07
17	1	0	0.3	0.05
18	1	1	0.4	0.07
19	1	2	0.5	0.08
20	1	0	0.4	0.05
21	1	1	0.6	0.08
22	1	2	0.7	0.09
23	0.5	2	0.6	0.07
24	0.5	1	0.4	0.10
25	0.5	0	0.2	0.04
26	0.5	1	0.4	0.06
27	0.5	2	0.5	0.07
28	2	2	0.9	0.11
29	2	0	0.7	0.08
30	2	1	0.9	0.10
31	2	2	1.0	0.11

Table 1-35: Steady state velocities (m/s) at 1.4 m from the top of the doorway

Experiment #	Fire Size (MW)	# of Open Vents	Velocity	Standard Deviation
1	0.5	0	0.1	0.05
2	0.5	1	0.2	0.08
3	0.5	2	0.3	0.09
4	0.5	0	0.1	0.06
5	1	0	0.2	0.06
6	1	1	0.4	0.09
7	1	2	0.5	0.12
8	1	0	0.1	0.07
9	2	0	0.4	0.10
10	2	1	0.9	0.18
11	2	0	0.7	0.09
12	2	1	1.0	0.12
13	2	2	1.2	0.20
14	0.5	0	0.1	0.05
15	0.5	1	0.3	0.07
16	0.5	2	0.4	0.09
17	1	0	0.3	0.07
18	1	1	0.5	0.10
19	1	2	0.7	0.12
20	1	0	0.6	0.07
21	1	1	0.8	0.11
22	1	2	1.1	0.14
23	0.5	2	0.8	0.11
24	0.5	1	0.7	0.13
25	0.5	0	0.4	0.05
26	0.5	1	0.6	0.11
27	0.5	2	0.8	0.10
28	2	2	1.2	0.13
29	2	0	0.9	0.08
30	2	1	1.2	0.14
31	2	2	1.3	0.14

Table 1-36: Steady state velocities (m/s) at 1.6 m from the top of the doorway

Experiment #	Fire Size (MW)	# of Open Vents	Velocity	Standard Deviation
1	0.5	0	-0.1	0.04
2	0.5	1	-0.2	0.07
3	0.5	2	-0.4	0.08
4	0.5	0	-0.1	0.05
5	1	0	-0.1	0.05
6	1	1	-0.4	0.09
7	1	2	-0.6	0.10
8	1	0	-0.1	0.05
9	2	0	0.1	0.07
10	2	1	-0.5	0.15
11	2	0	0.5	0.07
12	2	1	0.7	0.10
13	2	2	0.8	0.14
14	0.5	0	0.1	0.04
15	0.5	1	0.2	0.06
16	0.5	2	0.3	0.08
17	1	0	0.3	0.06
18	1	1	0.4	0.09
19	1	2	0.6	0.10
20	1	0	0.3	0.06
21	1	1	0.4	0.07
22	1	2	0.6	0.13
23	0.5	2	0.4	0.09
24	0.5	1	0.3	0.12
25	0.5	0	0.1	0.05
26	0.5	1	0.3	0.09
27	0.5	2	0.4	0.10
28	2	2	0.8	0.11
29	2	0	0.6	0.06
30	2	1	0.8	0.10
31	2	2	0.9	0.09

Table 1-37: Steady state velocities (m/s) at 1.8 m from the top of the doorway

Experiment #	Fire Size (MW)	# of Open Vents	Velocity	Standard Deviation
1	0.5	0	-0.1	0.08
2	0.5	1	-0.4	0.14
3	0.5	2	-0.7	0.18
4	0.5	0	-0.2	0.08
5	1	0	-0.3	0.10
6	1	1	-1.0	0.35
7	1	2	-1.9	0.68
8	1	0	-0.3	0.11
9	2	0	-0.5	0.17
10	2	1	-2.7	0.78
11	2	0	0.7	0.09
12	2	1	1.0	0.12
13	2	2	1.2	0.24
14	0.5	0	0.1	0.05
15	0.5	1	0.3	0.09
16	0.5	2	0.5	0.09
17	1	0	0.4	0.07
18	1	1	0.7	0.09
19	1	2	0.9	0.13
20	1	0	0.5	0.09
21	1	1	0.7	0.10
22	1	2	1.0	0.13
23	0.5	2	0.7	0.10
24	0.5	1	0.5	0.12
25	0.5	0	0.3	0.08
26	0.5	1	0.5	0.08
27	0.5	2	0.6	0.10
28	2	2	1.3	0.16
29	2	0	0.8	0.08
30	2	1	1.2	0.11
31	2	2	1.5	0.11

Table 1-38: Steady state temperatures (°C) at location #1 in the ceiling vent

Experiment #	Fire Size (MW)	# of Open Vents	Temperature	Standard Deviation
1	0.5	0	-	-
2	0.5	1	-	-
3	0.5	2	-	-
4	0.5	0	-	-
5	1	0	-	-
6	1	1	-	-
7	1	2	-	-
8	1	0	-	-
9	2	0	-	-
10	2	1	-	-
11	2	0	680	5
12	2	1	463	18
13	2	2	493	70
14	0.5	0	298	3
15	0.5	1	148	6
16	0.5	2	107	13
17	1	0	520	5
18	1	1	261	13
19	1	2	176	19
20	1	0	507	4
21	1	1	266	13
22	1	2	174	23
23	0.5	2	134	9
24	0.5	1	141	14
25	0.5	0	346	3
26	0.5	1	156	7
27	0.5	2	125	9
28	2	2	464	37
29	2	0	734	29
30	2	1	538	21
31	2	2	545	33

Table 1-39: Steady state temperatures (°C) at location #2 in the ceiling vent

Experiment #	Fire Size (MW)	# of Open Vents	Temperature	Standard Deviation
1	0.5	0	282	2
2	0.5	1	174	4
3	0.5	2	122	5
4	0.5	0	279	4
5	1	0	552	3
6	1	1	327	8
7	1	2	226	10
8	1	0	523	16
9	2	0	749	13
10	2	1	671	27
11	2	0	668	4
12	2	1	590	22
13	2	2	579	43
14	0.5	0	293	2
15	0.5	1	187	4
16	0.5	2	139	5
17	1	0	516	5
18	1	1	341	8
19	1	2	264	8
20	1	0	505	4
21	1	1	344	7
22	1	2	276	10
23	0.5	2	167	4
24	0.5	1	191	16
25	0.5	0	344	3
26	0.5	1	200	5
27	0.5	2	155	6
28	2	2	497	28
29	2	0	725	26
30	2	1	684	19
31	2	2	570	30

Table 1-40: Steady state temperatures (°C) at location #3 in the ceiling vent

Experiment #	Fire Size (MW)	# of Open Vents	Temperature	Standard Deviation
1	0.5	0	284	1
2	0.5	1	103	4
3	0.5	2	100	6
4	0.5	0	264	7
5	1	0	543	3
6	1	1	171	13
7	1	2	187	8
8	1	0	467	23
9	2	0	757	16
10	2	1	481	29
11	2	0	688	5
12	2	1	272	9
13	2	2	365	71
14	0.5	0	298	3
15	0.5	1	126	5
16	0.5	2	111	4
17	1	0	528	6
18	1	1	187	6
19	1	2	185	6
20	1	0	507	5
21	1	1	168	7
22	1	2	189	6
23	0.5	2	120	3
24	0.5	1	112	7
25	0.5	0	346	4
26	0.5	1	111	3
27	0.5	2	113	3
28	2	2	308	12
29	2	0	725	36
30	2	1	385	13
31	2	2	350	10

Table 1-41: Steady state temperatures (°C) at location #4 in the ceiling vent

Experiment #	Fire Size (MW)	# of Open Vents	Temperature	Standard Deviation
1	0.5	0	294	2
2	0.5	1	126	4
3	0.5	2	89	4
4	0.5	0	283	6
5	1	0	567	3
6	1	1	273	10
7	1	2	152	6
8	1	0	505	23
9	2	0	769	14
10	2	1	431	39
11	2	0	714	6
12	2	1	409	15
13	2	2	385	45
14	0.5	0	320	3
15	0.5	1	163	3
16	0.5	2	104	2
17	1	0	565	5
18	1	1	288	7
19	1	2	167	6
20	1	0	543	4
21	1	1	270	8
22	1	2	160	5
23	0.5	2	122	3
24	0.5	1	139	15
25	0.5	0	370	3
26	0.5	1	178	4
27	0.5	2	115	3
28	2	2	304	7
29	2	0	754	29
30	2	1	468	16
31	2	2	369	11

Table 1-42: Steady state temperatures (°C) at location #5 in the ceiling vent

Experiment #	Fire Size (MW)	# of Open Vents	Temperature	Standard Deviation
1	0.5	0	285	1
2	0.5	1	120	3
3	0.5	2	98	6
4	0.5	0	277	6
5	1	0	558	2
6	1	1	266	7
7	1	2	214	13
8	1	0	509	18
9	2	0	798	18
10	2	1	453	49
11	2	0	743	5
12	2	1	494	7
13	2	2	476	52
14	0.5	0	302	3
15	0.5	1	151	3
16	0.5	2	109	2
17	1	0	538	5
18	1	1	274	6
19	1	2	213	5
20	1	0	519	4
21	1	1	284	7
22	1	2	215	5
23	0.5	2	137	4
24	0.5	1	150	13
25	0.5	0	353	3
26	0.5	1	181	2
27	0.5	2	111	2
28	2	2	330	8
29	2	0	764	33
30	2	1	479	6
31	2	2	361	6

Table 1-43: Steady state temperatures (°C) at location #6 in the ceiling vent

Experiment #	Fire Size (MW)	# of Open Vents	Temperature	Standard Deviation
1	0.5	0	291	1
2	0.5	1	148	2
3	0.5	2	80	3
4	0.5	0	285	5
5	1	0	570	3
6	1	1	306	7
7	1	2	140	6
8	1	0	515	24
9	2	0	771	14
10	2	1	559	28
11	2	0	711	7
12	2	1	484	5
13	2	2	375	77
14	0.5	0	316	2
15	0.5	1	173	2
16	0.5	2	91	4
17	1	0	561	7
18	1	1	317	3
19	1	2	165	7
20	1	0	542	4
21	1	1	308	3
22	1	2	161	8
23	0.5	2	124	7
24	0.5	1	157	24
25	0.5	0	369	3
26	0.5	1	195	2
27	0.5	2	111	8
28	2	2	267	10
29	2	0	756	28
30	2	1	564	5
31	2	2	345	17

Table 1-44: Steady state temperatures (°C) at location #7 in the ceiling vent

Experiment #	Fire Size (MW)	# of Open Vents	Temperature	Standard Deviation
1	0.5	0	273	1
2	0.5	1	160	2
3	0.5	2	122	4
4	0.5	0	261	5
5	1	0	540	3
6	1	1	335	11
7	1	2	227	8
8	1	0	490	21
9	2	0	737	15
10	2	1	610	25
11	2	0	659	7
12	2	1	524	8
13	2	2	458	37
14	0.5	0	297	2
15	0.5	1	181	3
16	0.5	2	135	4
17	1	0	519	7
18	1	1	333	3
19	1	2	241	6
20	1	0	503	3
21	1	1	320	3
22	1	2	249	10
23	0.5	2	168	7
24	0.5	1	175	10
25	0.5	0	350	3
26	0.5	1	205	3
27	0.5	2	153	4
28	2	2	409	14
29	2	0	704	28
30	2	1	606	6
31	2	2	483	17

Table 1-45: Steady state temperatures (°C) at location #8 in the ceiling vent

Experiment #	Fire Size (MW)	# of Open Vents	Temperature	Standard Deviation
1	0.5	0	279	1
2	0.5	1	153	2
3	0.5	2	95	6
4	0.5	0	270	6
5	1	0	550	2
6	1	1	323	9
7	1	2	201	8
8	1	0	490	26
9	2	0	752	14
10	2	1	589	27
11	2	0	695	8
12	2	1	498	4
13	2	2	415	50
14	0.5	0	309	2
15	0.5	1	178	1
16	0.5	2	120	7
17	1	0	543	8
18	1	1	330	3
19	1	2	225	7
20	1	0	530	3
21	1	1	321	2
22	1	2	216	7
23	0.5	2	139	6
24	0.5	1	170	12
25	0.5	0	365	2
26	0.5	1	203	2
27	0.5	2	122	8
28	2	2	347	11
29	2	0	738	32
30	2	1	587	4
31	2	2	373	16

Table 1-46: Steady state temperatures (°C) at location #9 in the ceiling vent

Experiment #	Fire Size (MW)	# of Open Vents	Temperature	Standard Deviation
1	0.5	0	288	2
2	0.5	1	163	2
3	0.5	2	122	5
4	0.5	0	287	4
5	1	0	563	4
6	1	1	331	8
7	1	2	240	5
8	1	0	534	22
9	2	0	755	14
10	2	1	602	22
11	2	0	668	6
12	2	1	522	6
13	2	2	456	39
14	0.5	0	306	3
15	0.5	1	186	2
16	0.5	2	141	2
17	1	0	532	5
18	1	1	341	3
19	1	2	244	7
20	1	0	523	4
21	1	1	330	3
22	1	2	240	5
23	0.5	2	159	5
24	0.5	1	180	9
25	0.5	0	365	2
26	0.5	1	211	3
27	0.5	2	128	14
28	2	2	387	10
29	2	0	715	32
30	2	1	597	4
31	2	2	382	15

Table 1-47: Steady state temperatures (°C) at location #10 in the ceiling vent

Experiment #	Fire Size (MW)	# of Open Vents	Temperature	Standard Deviation
1	0.5	0	297	1
2	0.5	1	163	0
3	0.5	2	99	4
4	0.5	0	296	4
5	1	0	566	3
6	1	1	347	11
7	1	2	230	6
8	1	0	528	23
9	2	0	776	15
10	2	1	620	30
11	2	0	713	6
12	2	1	513	5
13	2	2	465	27
14	0.5	0	322	2
15	0.5	1	183	2
16	0.5	2	120	7
17	1	0	559	5
18	1	1	332	4
19	1	2	235	9
20	1	0	548	4
21	1	1	327	3
22	1	2	225	8
23	0.5	2	141	3
24	0.5	1	179	18
25	0.5	0	368	3
26	0.5	1	207	2
27	0.5	2	122	6
28	2	2	421	19
29	2	0	751	30
30	2	1	585	4
31	2	2	429	17

Table 1-48: Steady state velocities (m/s) at location #1 in the ceiling vent

Experiment #	Fire Size (MW)	# of Open Vents	Velocity	Standard Deviation
1	0.5	0	-	-
2	0.5	1	-	-
3	0.5	2	-	-
4	0.5	0	-	-
5	1	0	-	-
6	1	1	-	-
7	1	2	-	-
8	1	0	-	-
9	2	0	-	-
10	2	1	-	-
11	2	0	2.6	0.07
12	2	1	4.8	0.48
13	2	2	2.8	1.54
14	0.5	0	1.3	0.03
15	0.5	1	1.5	0.32
16	0.5	2	0.6	0.53
17	1	0	2.1	0.04
18	1	1	2.8	0.40
19	1	2	0.6	0.79
20	1	0	1.9	0.04
21	1	1	2.8	0.47
22	1	2	0.7	0.84
23	0.5	2	0.8	0.56
24	0.5	1	1.4	0.58
25	0.5	0	1.4	0.03
26	0.5	1	1.8	0.39
27	0.5	2	0.8	0.55
28	2	2	3.0	1.28
29	2	0	2.7	0.09
30	2	1	5.2	0.43
31	2	2	3.6	1.33

Table 1-49: Steady state velocities (m/s) at location #2 in the ceiling vent

Experiment #	Fire Size (MW)	# of Open Vents	Velocity	Standard Deviation
1	0.5	0	-0.6	0.05
2	0.5	1	3.5	1.00
3	0.5	2	2.1	1.76
4	0.5	0	-0.8	0.06
5	1	0	-1.4	0.07
6	1	1	4.9	1.06
7	1	2	2.9	2.04
8	1	0	-1.5	0.08
9	2	0	-2.0	0.08
10	2	1	7.5	0.69
11	2	0	-1.4	0.08
12	2	1	6.8	0.98
13	2	2	5.6	3.33
14	0.5	0	-0.7	0.06
15	0.5	1	3.3	1.23
16	0.5	2	2.2	1.76
17	1	0	-1.3	0.06
18	1	1	4.7	1.45
19	1	2	4.8	1.58
20	1	0	-1.0	0.05
21	1	1	4.9	1.44
22	1	2	4.9	1.47
23	0.5	2	2.9	1.80
24	0.5	1	3.3	1.60
25	0.5	0	-1.2	0.06
26	0.5	1	2.9	1.49
27	0.5	2	3.0	1.81
28	2	2	7.1	1.19
29	2	0	-2.0	0.12
30	2	1	6.9	1.73
31	2	2	7.4	1.17

Table 1-50: Steady state velocities (m/s) at location #3 in the ceiling vent

Experiment #	Fire Size (MW)	# of Open Vents	Velocity	Standard Deviation
1	0.5	0	0.9	0.04
2	0.5	1	0.8	0.27
3	0.5	2	1.0	0.44
4	0.5	0	0.7	0.04
5	1	0	1.5	0.04
6	1	1	1.8	0.35
7	1	2	1.7	0.59
8	1	0	1.2	0.07
9	2	0	1.9	0.08
10	2	1	3.7	0.64
11	2	0	1.8	0.05
12	2	1	3.0	0.34
13	2	2	3.0	0.52
14	0.5	0	-	-
15	0.5	1	-	-
16	0.5	2	-	-
17	1	0	-	-
18	1	1	-	-
19	1	2	-	-
20	1	0	1.3	0.05
21	1	1	1.6	0.30
22	1	2	1.8	0.46
23	0.5	2	1.1	0.34
24	0.5	1	1.0	0.30
25	0.5	0	0.7	0.04
26	0.5	1	1.1	0.29
27	0.5	2	1.0	0.45
28	2	2	2.7	0.48
29	2	0	1.5	0.06
30	2	1	3.4	0.56
31	2	2	3.0	0.56

Table 1-51: Steady state velocities (m/s) at location #4 in the ceiling vent

Experiment #	Fire Size (MW)	# of Open Vents	Velocity	Standard Deviation
1	0.5	0	1.1	0.04
2	0.5	1	1.0	0.22
3	0.5	2	0.7	0.28
4	0.5	0	0.9	0.07
5	1	0	1.7	0.08
6	1	1	2.2	0.28
7	1	2	1.3	0.46
8	1	0	1.3	0.09
9	2	0	2.0	0.09
10	2	1	2.9	0.42
11	2	0	2.1	0.11
12	2	1	3.1	0.34
13	2	2	2.8	0.60
14	0.5	0	1.1	0.05
15	0.5	1	1.3	0.16
16	0.5	2	0.8	0.32
17	1	0	1.7	0.12
18	1	1	2.2	0.26
19	1	2	1.4	0.38
20	1	0	1.7	0.10
21	1	1	1.9	0.24
22	1	2	1.3	0.45
23	0.5	2	0.9	0.39
24	0.5	1	1.0	0.26
25	0.5	0	1.0	0.06
26	0.5	1	1.3	0.20
27	0.5	2	0.9	0.45
28	2	2	2.4	0.62
29	2	0	1.3	0.08
30	2	1	2.9	0.39
31	2	2	2.6	0.74

Table 1-52: Steady state velocities (m/s) at location #5 in the ceiling vent

Experiment #	Fire Size (MW)	# of Open Vents	Velocity	Standard Deviation
1	0.5	0	0.6	0.08
2	0.5	1	0.8	0.49
3	0.5	2	0.6	0.36
4	0.5	0	0.4	0.09
5	1	0	0.7	0.11
6	1	1	1.7	0.91
7	1	2	1.7	0.61
8	1	0	0.2	0.14
9	2	0	0.4	0.21
10	2	1	3.0	0.59
11	2	0	1.8	0.17
12	2	1	3.5	0.75
13	2	2	3.5	0.95
14	0.5	0	0.8	0.07
15	0.5	1	1.2	0.41
16	0.5	2	1.0	0.38
17	1	0	1.3	0.10
18	1	1	2.2	0.61
19	1	2	1.9	0.54
20	1	0	1.2	0.10
21	1	1	2.3	0.59
22	1	2	2.2	0.59
23	0.5	2	1.3	0.37
24	0.5	1	1.3	0.51
25	0.5	0	0.7	0.09
26	0.5	1	1.6	0.49
27	0.5	2	1.0	0.36
28	2	2	3.0	0.54
29	2	0	1.2	0.17
30	2	1	3.5	0.54
31	2	2	2.9	0.53

Table 1-53: Steady state velocities (m/s) at location #6 in the ceiling vent

Experiment #	Fire Size (MW)	# of Open Vents	Velocity	Standard Deviation
1	0.5	0	1.4	0.05
2	0.5	1	0.9	0.09
3	0.5	2	0.6	0.24
4	0.5	0	1.2	0.06
5	1	0	2.3	0.07
6	1	1	1.7	0.14
7	1	2	1.2	0.35
8	1	0	1.9	0.11
9	2	0	2.6	0.06
10	2	1	2.9	0.24
11	2	0	2.8	0.08
12	2	1	2.6	0.20
13	2	2	2.8	0.41
14	0.5	0	1.4	0.04
15	0.5	1	1.0	0.10
16	0.5	2	0.7	0.22
17	1	0	2.3	0.09
18	1	1	1.7	0.16
19	1	2	1.5	0.33
20	1	0	2.2	0.07
21	1	1	1.6	0.16
22	1	2	1.4	0.40
23	0.5	2	0.9	0.34
24	0.5	1	0.8	0.19
25	0.5	0	1.3	0.05
26	0.5	1	1.0	0.11
27	0.5	2	0.8	0.39
28	2	2	2.1	0.54
29	2	0	2.3	0.09
30	2	1	2.6	0.19
31	2	2	2.6	0.62

Table 1-54: Steady state velocities (m/s) at location #7 in the ceiling vent

Experiment #	Fire Size (MW)	# of Open Vents	Velocity	Standard Deviation
1	0.5	0	0.8	0.03
2	0.5	1	0.5	0.13
3	0.5	2	1.2	0.32
4	0.5	0	0.5	0.04
5	1	0	1.1	0.07
6	1	1	0.8	0.19
7	1	2	1.9	0.66
8	1	0	0.5	0.11
9	2	0	0.9	0.08
10	2	1	1.1	0.41
11	2	0	1.7	0.07
12	2	1	1.6	0.26
13	2	2	3.1	1.14
14	0.5	0	0.9	0.03
15	0.5	1	0.6	0.09
16	0.5	2	1.1	0.31
17	1	0	1.4	0.05
18	1	1	1.0	0.13
19	1	2	1.6	0.61
20	1	0	1.3	0.07
21	1	1	0.9	0.14
22	1	2	1.8	0.57
23	0.5	2	1.1	0.46
24	0.5	1	0.4	0.31
25	0.5	0	0.0	0.06
26	0.5	1	0.2	0.10
27	0.5	2	1.1	0.53
28	2	2	3.2	0.70
29	2	0	1.4	0.10
30	2	1	1.7	0.32
31	2	2	3.3	0.87

Table 1-55: Steady state velocities (m/s) at location #8 in the ceiling vent

Experiment #	Fire Size (MW)	# of Open Vents	Velocity	Standard Deviation
1	0.5	0	1.2	0.04
2	0.5	1	0.7	0.08
3	0.5	2	0.9	0.24
4	0.5	0	1.1	0.04
5	1	0	2.0	0.08
6	1	1	1.4	0.11
7	1	2	1.9	0.33
8	1	0	1.6	0.12
9	2	0	2.3	0.08
10	2	1	2.3	0.14
11	2	0	2.5	0.13
12	2	1	2.2	0.15
13	2	2	3.2	0.68
14	0.5	0	1.3	0.03
15	0.5	1	0.8	0.09
16	0.5	2	1.1	0.25
17	1	0	2.0	0.08
18	1	1	1.4	0.11
19	1	2	2.1	0.33
20	1	0	2.0	0.07
21	1	1	1.4	0.12
22	1	2	2.0	0.29
23	0.5	2	1.2	0.26
24	0.5	1	0.7	0.27
25	0.5	0	1.2	0.04
26	0.5	1	0.8	0.08
27	0.5	2	1.0	0.30
28	2	2	2.9	0.42
29	2	0	2.1	0.09
30	2	1	1.9	0.15
31	2	2	3.0	0.44

Table 1-56: Steady state velocities (m/s) at location #9 in the ceiling vent

Experiment #	Fire Size (MW)	# of Open Vents	Velocity	Standard Deviation
1	0.5	0	0.4	0.07
2	0.5	1	0.4	0.22
3	0.5	2	1.4	0.31
4	0.5	0	0.5	0.08
5	1	0	0.6	0.13
6	1	1	0.5	0.23
7	1	2	2.2	0.76
8	1	0	0.6	0.15
9	2	0	0.6	0.12
10	2	1	1.1	0.33
11	2	0	0.8	0.14
12	2	1	1.2	0.26
13	2	2	3.3	1.33
14	0.5	0	0.5	0.06
15	0.5	1	0.5	0.11
16	0.5	2	1.5	0.41
17	1	0	0.8	0.11
18	1	1	0.7	0.19
19	1	2	2.3	0.45
20	1	0	0.8	0.07
21	1	1	0.7	0.17
22	1	2	2.3	0.58
23	0.5	2	1.8	0.39
24	0.5	1	0.6	0.46
25	0.5	0	-0.9	0.35
26	0.5	1	0.1	0.15
27	0.5	2	1.4	0.51
28	2	2	3.5	0.82
29	2	0	0.8	0.12
30	2	1	0.8	0.22
31	2	2	4.0	0.54

Table 1-57: Steady state velocities (m/s) at location #10 in the ceiling vent

Experiment #	Fire Size (MW)	# of Open Vents	Velocity	Standard Deviation
1	0.5	0	-0.7	0.04
2	0.5	1	-0.5	0.18
3	0.5	2	0.2	0.76
4	0.5	0	-0.8	0.05
5	1	0	-1.4	0.06
6	1	1	-0.9	0.29
7	1	2	1.8	1.97
8	1	0	-1.5	0.07
9	2	0	-2.0	0.06
10	2	1	-1.7	0.53
11	2	0	-1.3	0.08
12	2	1	-1.0	0.44
13	2	2	2.1	3.14
14	0.5	0	-0.6	0.06
15	0.5	1	-0.4	0.19
16	0.5	2	1.6	1.48
17	1	0	-1.0	0.08
18	1	1	-0.7	0.34
19	1	2	2.9	1.53
20	1	0	-1.0	0.10
21	1	1	-0.6	0.25
22	1	2	2.0	1.58
23	0.5	2	0.6	0.96
24	0.5	1	-0.4	0.63
25	0.5	0	-0.9	0.03
26	0.5	1	-0.6	0.43
27	0.5	2	0.7	1.16
28	2	2	2.7	2.42
29	2	0	-1.6	0.09
30	2	1	-1.4	0.39
31	2	2	1.4	2.43

Table 1-58: Steady state heat fluxes (kW/m^2) at the floor facing the ceiling near the burner

Experiment #	Fire Size (MW)	# of Open Vents	Heat Flux	Standard Deviation
1	0.5	0	8	1.1
2	0.5	1	8	1.1
3	0.5	2	8	0.8
4	0.5	0	9	0.9
5	1	0	25	1.0
6	1	1	18	1.1
7	1	2	17	0.8
8	1	0	23	4.1
9	2	0	66	4.2
10	2	1	56	1.6
11	2	0	40	1.8
12	2	1	36	1.2
13	2	2	36	1.4
14	0.5	0	3	0.9
15	0.5	1	3	1.2
16	0.5	2	2	1.0
17	1	0	11	0.9
18	1	1	7	1.0
19	1	2	6	0.8
20	1	0	12	1.0
21	1	1	9	0.9
22	1	2	10	1.2
23	0.5	2	7	1.0
24	0.5	1	6	0.9
25	0.5	0	9	1.1
26	0.5	1	8	0.8
27	0.5	2	8	0.8
28	2	2	20	1.0
29	2	0	31	1.4
30	2	1	25	1.1
31	2	2	23	1.1

Table 1-59: Steady state heat fluxes (kW/m^2) 0.9 m above the floor facing the ceiling near the burner

Experiment #	Fire Size (MW)	# of Open Vents	Heat Flux	Standard Deviation
1	0.5	0	8	1.2
2	0.5	1	7	1.1
3	0.5	2	8	1.2
4	0.5	0	10	1.4
5	1	0	29	1.7
6	1	1	20	1.3
7	1	2	21	1.1
8	1	0	26	3.9
9	2	0	35	2.2
10	2	1	30	1.3
11	2	0	54	2.8
12	2	1	47	2.1
13	2	2	45	2.6
14	0.5	0	4	1.2
15	0.5	1	4	1.0
16	0.5	2	3	1.1
17	1	0	18	1.6
18	1	1	12	1.1
19	1	2	11	0.8
20	1	0	19	1.0
21	1	1	15	1.0
22	1	2	15	1.0
23	0.5	2	9	1.1
24	0.5	1	8	0.9
25	0.5	0	12	1.0
26	0.5	1	10	1.1
27	0.5	2	9	1.2
28	2	2	43	1.8
29	2	0	63	1.9
30	2	1	60	1.3
31	2	2	58	1.7

Table 1-60: Steady state heat fluxes (kW/m^2) 0.9 m above the floor facing the fire near the burner

Experiment #	Fire Size (MW)	# of Open Vents	Heat Flux	Standard Deviation
1	0.5	0	11	0.9
2	0.5	1	12	1.0
3	0.5	2	12	1.1
4	0.5	0	14	1.0
5	1	0	35	1.2
6	1	1	32	1.7
7	1	2	30	1.2
8	1	0	35	3.5
9	2	0	24	0.9
10	2	1	24	1.3
11	2	0	48	2.4
12	2	1	53	1.5
13	2	2	53	2.6
14	0.5	0	6	1.1
15	0.5	1	8	1.2
16	0.5	2	8	1.2
17	1	0	33	1.7
18	1	1	27	1.2
19	1	2	23	1.3
20	1	0	32	1.7
21	1	1	28	1.4
22	1	2	25	1.4
23	0.5	2	12	1.1
24	0.5	1	13	1.3
25	0.5	0	15	1.2
26	0.5	1	14	1.1
27	0.5	2	12	1.2
28	2	2	57	1.6
29	2	0	79	2.8
30	2	1	78	1.5
31	2	2	65	2.1

Table 1-61: Steady state heat fluxes (kW/m^2) at the floor facing the ceiling near the doorway

Experiment #	Fire Size (MW)	# of Open Vents	Heat Flux	Standard Deviation
1	0.5	0	4	1.0
2	0.5	1	4	0.9
3	0.5	2	5	1.0
4	0.5	0	6	0.9
5	1	0	14	0.8
6	1	1	8	0.7
7	1	2	8	0.8
8	1	0	15	1.4
9	2	0	37	1.7
10	2	1	28	1.3
11	2	0	18	0.9
12	2	1	15	0.9
13	2	2	14	1.4
14	0.5	0	2	0.9
15	0.5	1	2	0.9
16	0.5	2	1	0.6
17	1	0	11	1.0
18	1	1	5	0.6
19	1	2	4	0.8
20	1	0	10	0.9
21	1	1	7	0.6
22	1	2	6	0.9
23	0.5	2	5	0.8
24	0.5	1	4	0.9
25	0.5	0	7	0.7
26	0.5	1	5	0.8
27	0.5	2	5	0.8
28	2	2	15	0.9
29	2	0	36	1.8
30	2	1	26	0.9
31	2	2	21	0.9

Table 1-62: Steady state heat fluxes (kW/m^2) 0.9 m above the floor facing the ceiling near the doorway

Experiment #	Fire Size (MW)	# of Open Vents	Heat Flux	Standard Deviation
1	0.5	0	4	0.9
2	0.5	1	3	0.7
3	0.5	2	4	0.7
4	0.5	0	5	0.7
5	1	0	14	0.6
6	1	1	8	0.8
7	1	2	7	0.7
8	1	0	14	1.0
9	2	0	35	1.8
10	2	1	25	1.6
11	2	0	18	0.8
12	2	1	14	0.6
13	2	2	13	1.0
14	0.5	0	3	0.8
15	0.5	1	2	0.7
16	0.5	2	2	0.6
17	1	0	10	0.7
18	1	1	5	0.8
19	1	2	5	0.7
20	1	0	10	0.6
21	1	1	6	0.5
22	1	2	6	0.8
23	0.5	2	4	0.7
24	0.5	1	4	0.6
25	0.5	0	6	0.6
26	0.5	1	5	0.9
27	0.5	2	5	0.7
28	2	2	13	0.5
29	2	0	37	2.4
30	2	1	24	0.8
31	2	2	19	0.8

Table 1-63: Steady state heat fluxes (kW/m^2) 0.9 m above the floor facing the fire near the doorway

Experiment #	Fire Size (MW)	# of Open Vents	Heat Flux	Standard Deviation
1	0.5	0	6	0.6
2	0.5	1	5	0.8
3	0.5	2	6	1.0
4	0.5	0	7	1.2
5	1	0	18	0.8
6	1	1	13	1.2
7	1	2	12	1.1
8	1	0	18	0.9
9	2	0	45	2.2
10	2	1	35	2.2
11	2	0	23	1.4
12	2	1	21	1.2
13	2	2	20	1.7
14	0.5	0	2	1.0
15	0.5	1	2	0.8
16	0.5	2	2	1.2
17	1	0	13	1.2
18	1	1	8	0.8
19	1	2	6	1.0
20	1	0	14	0.9
21	1	1	9	1.0
22	1	2	9	1.1
23	0.5	2	6	1.1
24	0.5	1	7	1.0
25	0.5	0	8	1.2
26	0.5	1	7	1.2
27	0.5	2	7	1.2
28	2	2	22	1.0
29	2	0	47	1.5
30	2	1	35	1.3
31	2	2	29	1.1

Table 1-64: Steady state calorimeter HRRs (kW)

Experiment #	Fire Size (MW)	# of Open Vents	Calorimeter HRR	Standard Deviation
1	0.5	0	450	30
2	0.5	1	494	32
3	0.5	2	515	28
4	0.5	0	390	34
5	1	0	1088	48
6	1	1	1340	62
7	1	2	1247	45
8	1	0	926	62
9	2	0	1863	154
10	2	1	2914	150
11	2	0	1718	112
12	2	1	2401	95
13	2	2	2361	90
14	0.5	0	389	26
15	0.5	1	519	28
16	0.5	2	494	30
17	1	0	798	49
18	1	1	1097	50
19	1	2	1077	43
20	1	0	759	46
21	1	1	1021	41
22	1	2	976	43
23	0.5	2	421	23
24	0.5	1	422	29
25	0.5	0	337	29
26	0.5	1	464	27
27	0.5	2	453	26
28	2	2	2094	105
29	2	0	869	225
30	2	1	2419	99
31	2	2	2333	92

Appendix C. FDS Files

EX1_11_10cmGrid.fds

Generated by PyroSim - Version 2012.1.0605
Aug 23, 2012 2:43:45 PM

```
&HEAD CHID='EX1_11_10cmGrid'/
&TIME T_END=5000.0/
&DUMP RENDER_FILE='EX1_11_10cmGrid.ge1', DT_RESTART=300.0, PLOT3D_QUANTITY(1:4)='OPTICAL
DENSITY','PRESSURE','TEMPERATURE','VELOCITY'/

&MESH ID='MESH', IJK=20,20,20, XB=-1.0,1.0,0.0,2.0,0.0,2.0/
&MESH ID='MESH02', IJK=20,20,20, XB=1.0,3.0,0.0,2.0,0.0,2.0/
&MESH ID='MESH0202', IJK=20,20,20, XB=5.0,7.0,0.0,2.0,0.0,2.0/
&MESH ID='MESH03', IJK=20,20,20, XB=3.0,5.0,0.0,2.0,0.0,2.0/
&MESH ID='MESH0203', IJK=20,20,20, XB=1.0,3.0,2.0,4.0,0.0,2.0/
&MESH ID='MESH04', IJK=20,20,20, XB=-1.0,1.0,2.0,4.0,0.0,2.0/
&MESH ID='MESH020202', IJK=20,20,20, XB=5.0,7.0,2.0,4.0,0.0,2.0/
&MESH ID='MESH0302', IJK=20,20,20, XB=3.0,5.0,2.0,4.0,0.0,2.0/
&MESH ID='MESH0204', IJK=20,20,20, XB=1.0,3.0,4.0,6.0,0.0,2.0/
&MESH ID='MESH05', IJK=20,20,20, XB=-1.0,1.0,4.0,6.0,0.0,2.0/
&MESH ID='MESH020203', IJK=20,20,20, XB=5.0,7.0,4.0,6.0,0.0,2.0/
&MESH ID='MESH0303', IJK=20,20,20, XB=3.0,5.0,4.0,6.0,0.0,2.0/
&MESH ID='MESH0205', IJK=20,20,20, XB=1.0,3.0,6.0,8.0,0.0,2.0/
&MESH ID='MESH06', IJK=20,20,20, XB=-1.0,1.0,6.0,8.0,0.0,2.0/
&MESH ID='MESH020204', IJK=20,20,20, XB=5.0,7.0,6.0,8.0,0.0,2.0/
&MESH ID='MESH0304', IJK=20,20,20, XB=3.0,5.0,6.0,8.0,0.0,2.0/
&MESH ID='MESH0206', IJK=20,20,20, XB=1.0,3.0,0.0,2.0,2.0,4.0/
&MESH ID='MESH07', IJK=20,20,20, XB=-1.0,1.0,0.0,2.0,2.0,4.0/
&MESH ID='MESH020205', IJK=20,20,20, XB=5.0,7.0,0.0,2.0,2.0,4.0/
&MESH ID='MESH0305', IJK=20,20,20, XB=3.0,5.0,0.0,2.0,2.0,4.0/
&MESH ID='MESH020302', IJK=20,20,20, XB=1.0,3.0,2.0,4.0,2.0,4.0/
&MESH ID='MESH0402', IJK=20,20,20, XB=-1.0,1.0,2.0,4.0,2.0,4.0/
&MESH ID='MESH02020202', IJK=20,20,20, XB=5.0,7.0,2.0,4.0,2.0,4.0/
&MESH ID='MESH030202', IJK=20,20,20, XB=3.0,5.0,2.0,4.0,2.0,4.0/
&MESH ID='MESH020402', IJK=20,20,20, XB=1.0,3.0,4.0,6.0,2.0,4.0/
&MESH ID='MESH0502', IJK=20,20,20, XB=-1.0,1.0,4.0,6.0,2.0,4.0/
&MESH ID='MESH02020302', IJK=20,20,20, XB=5.0,7.0,4.0,6.0,2.0,4.0/
&MESH ID='MESH030302', IJK=20,20,20, XB=3.0,5.0,4.0,6.0,2.0,4.0/
&MESH ID='MESH020502', IJK=20,20,20, XB=1.0,3.0,6.0,8.0,2.0,4.0/
&MESH ID='MESH0602', IJK=20,20,20, XB=-1.0,1.0,6.0,8.0,2.0,4.0/
&MESH ID='MESH02020402', IJK=20,20,20, XB=5.0,7.0,6.0,8.0,2.0,4.0/
&MESH ID='MESH030402', IJK=20,20,20, XB=3.0,5.0,6.0,8.0,2.0,4.0/

&REAC ID='METHANE',
    FYI='Methane Properties',
```

C=1.0,
H=4.0,
O=0.0,
N=0.0/

&RAMP ID='4x8 CTRL_RAMP', T=1839.75, F=-1.0/
&RAMP ID='4x8 CTRL_RAMP', T=1840.25, F=1.0/
&RAMP ID='4x8 CTRL_RAMP', T=2167.75, F=1.0/
&RAMP ID='4x8 CTRL_RAMP', T=2168.25, F=-1.0/
&RAMP ID='4x8 CTRL_RAMP', T=3169.75, F=-1.0/
&RAMP ID='4x8 CTRL_RAMP', T=3170.25, F=1.0/
&RAMP ID='4x8 CTRL_RAMP', T=3603.75, F=1.0/
&RAMP ID='4x8 CTRL_RAMP', T=3604.25, F=-1.0/
&RAMP ID='4x8 CTRL_RAMP', T=4283.75, F=-1.0/
&RAMP ID='4x8 CTRL_RAMP', T=4284.25, F=1.0/
&RAMP ID='4x4 CTRL_RAMP', T=1214.75, F=-1.0/
&RAMP ID='4x4 CTRL_RAMP', T=1215.25, F=1.0/
&RAMP ID='4x4 CTRL_RAMP', T=2167.75, F=1.0/
&RAMP ID='4x4 CTRL_RAMP', T=2168.25, F=-1.0/
&RAMP ID='4x4 CTRL_RAMP', T=2954.75, F=-1.0/
&RAMP ID='4x4 CTRL_RAMP', T=2955.25, F=1.0/
&RAMP ID='4x4 CTRL_RAMP', T=3603.75, F=1.0/
&RAMP ID='4x4 CTRL_RAMP', T=3604.25, F=-1.0/
&RAMP ID='4x4 CTRL_RAMP', T=4152.75, F=-1.0/
&RAMP ID='4x4 CTRL_RAMP', T=4153.25, F=1.0/
&RAMP ID='4x8 CTRLReverse_RAMP', T=-0.25, F=-1.0/
&RAMP ID='4x8 CTRLReverse_RAMP', T=0.25, F=1.0/
&RAMP ID='4x8 CTRLReverse_RAMP', T=1839.75, F=1.0/
&RAMP ID='4x8 CTRLReverse_RAMP', T=1840.25, F=-1.0/
&RAMP ID='4x8 CTRLReverse_RAMP', T=2167.75, F=-1.0/
&RAMP ID='4x8 CTRLReverse_RAMP', T=2168.25, F=1.0/
&RAMP ID='4x8 CTRLReverse_RAMP', T=3169.75, F=1.0/
&RAMP ID='4x8 CTRLReverse_RAMP', T=3170.25, F=-1.0/
&RAMP ID='4x8 CTRLReverse_RAMP', T=3603.75, F=-1.0/
&RAMP ID='4x8 CTRLReverse_RAMP', T=3604.25, F=1.0/
&RAMP ID='4x8 CTRLReverse_RAMP', T=4283.75, F=1.0/
&RAMP ID='4x8 CTRLReverse_RAMP', T=4284.25, F=-1.0/
&DEVC ID='0_TC1_25mmBC', QUANTITY='THERMOCOUPLE', XYZ=3.15,1.9,2.35/
&DEVC ID='10_TC2_610mmBC', QUANTITY='THERMOCOUPLE', XYZ=3.15,6.19,1.8/
&DEVC ID='11_TC2_915mmBC', QUANTITY='THERMOCOUPLE', XYZ=3.15,6.19,1.5/
&DEVC ID='12_TC2_1220mmBC', QUANTITY='THERMOCOUPLE', XYZ=3.15,6.19,1.2/
&DEVC ID='13_TC2_1520mmBC', QUANTITY='THERMOCOUPLE', XYZ=3.15,6.19,0.9/
&DEVC ID='14_TC2_1830mmBC', QUANTITY='THERMOCOUPLE', XYZ=3.15,6.19,0.6/
&DEVC ID='15_TC2_2130mmBC', QUANTITY='THERMOCOUPLE', XYZ=3.15,6.19,0.3/
&DEVC ID='16_Door_TC1', QUANTITY='THERMOCOUPLE', XYZ=5.3,5.25,1.97/
&DEVC ID='17_Door_TC2', QUANTITY='THERMOCOUPLE', XYZ=5.3,5.25,1.8/

&DEVC ID='18_Door_TC3', QUANTITY='THERMOCOUPLE', XYZ=5.3,5.25,1.6/
&DEVC ID='19_Door_TC4', QUANTITY='THERMOCOUPLE', XYZ=5.3,5.25,1.4/
&DEVC ID='1_TC1_305mmBC', QUANTITY='THERMOCOUPLE', XYZ=3.15,1.91,2.08/
&DEVC ID='20_Door_TC5', QUANTITY='THERMOCOUPLE', XYZ=5.3,5.25,1.2/
&DEVC ID='21_Door_TC6', QUANTITY='THERMOCOUPLE', XYZ=5.3,5.25,1.0/
&DEVC ID='22_Door_TC7', QUANTITY='THERMOCOUPLE', XYZ=5.3,5.25,0.8/
&DEVC ID='23_Door_TC8', QUANTITY='THERMOCOUPLE', XYZ=5.3,5.25,0.6/
&DEVC ID='24_Door_TC9', QUANTITY='THERMOCOUPLE', XYZ=5.3,5.25,0.4/
&DEVC ID='25_Door_TC10', QUANTITY='THERMOCOUPLE', XYZ=5.3,5.25,0.2/
&DEVC ID='26_Door_BDP1', QUANTITY='U-VELOCITY', XYZ=5.3,5.25,1.97, ORIENTATION=1.0,0.0,0.0/
&DEVC ID='27_Door_BDP2', QUANTITY='U-VELOCITY', XYZ=5.3,5.25,1.8, ORIENTATION=1.0,0.0,0.0/
&DEVC ID='28_Door_BDP3', QUANTITY='U-VELOCITY', XYZ=5.3,5.25,1.6, ORIENTATION=1.0,0.0,0.0/
&DEVC ID='29_Door_BDP4', QUANTITY='U-VELOCITY', XYZ=5.3,5.25,1.4, ORIENTATION=1.0,0.0,0.0/
&DEVC ID='2_TC1_610mmBC', QUANTITY='THERMOCOUPLE', XYZ=3.15,1.91,1.78/
&DEVC ID='30_Door_BDP5', QUANTITY='U-VELOCITY', XYZ=5.3,5.25,1.2, ORIENTATION=1.0,0.0,0.0/
&DEVC ID='31_Door_BDP6', QUANTITY='U-VELOCITY', XYZ=5.3,5.25,1.0, ORIENTATION=1.0,0.0,0.0/
&DEVC ID='32_Door_BDP7', QUANTITY='U-VELOCITY', XYZ=5.3,5.25,0.8, ORIENTATION=1.0,0.0,0.0/
&DEVC ID='33_Door_BDP8', QUANTITY='U-VELOCITY', XYZ=5.3,5.25,0.6, ORIENTATION=1.0,0.0,0.0/
&DEVC ID='34_Door_BDP9', QUANTITY='U-VELOCITY', XYZ=5.3,5.25,0.4, ORIENTATION=1.0,0.0,0.0/
&DEVC ID='35_Door_BDP10', QUANTITY='U-VELOCITY', XYZ=5.3,5.25,0.2, ORIENTATION=1.0,0.0,0.0/
&DEVC ID='36_VENT_TC1', QUANTITY='THERMOCOUPLE', XYZ=2.7,4.65,2.73/
&DEVC ID='37_VENT_TC2', QUANTITY='THERMOCOUPLE', XYZ=3.15,4.65,2.73/
&DEVC ID='38_VENT_TC3', QUANTITY='THERMOCOUPLE', XYZ=3.15,4.2,2.73/
&DEVC ID='39_VENT_TC4', QUANTITY='THERMOCOUPLE', XYZ=2.7,3.45,2.73/
&DEVC ID='3_TC1_915mmBC', QUANTITY='THERMOCOUPLE', XYZ=3.15,1.91,1.48/
&DEVC ID='40_VENT_TC5', QUANTITY='THERMOCOUPLE', XYZ=3.15,3.45,2.73/
&DEVC ID='41_VENT_TC6', QUANTITY='THERMOCOUPLE', XYZ=3.15,3.9,2.73/
&DEVC ID='42_VENT_TC7', QUANTITY='THERMOCOUPLE', XYZ=3.15,5.1,2.73/
&DEVC ID='43_VENT_TC8', QUANTITY='THERMOCOUPLE', XYZ=3.15,3.0,2.73/
&DEVC ID='44_VENT_TC9', QUANTITY='THERMOCOUPLE', XYZ=3.6,4.65,2.73/
&DEVC ID='45_VENT_TC10', QUANTITY='THERMOCOUPLE', XYZ=3.6,3.45,2.73/
&DEVC ID='46_Vent_BDP1', QUANTITY='W-VELOCITY', XYZ=2.7,4.65,2.73, ORIENTATION=0.0,0.0,1.0/
&DEVC ID='47_Vent_BDP2', QUANTITY='W-VELOCITY', XYZ=3.15,4.65,2.73, ORIENTATION=0.0,0.0,1.0/
&DEVC ID='48_Vent_BDP3', QUANTITY='W-VELOCITY', XYZ=3.15,4.2,2.73, ORIENTATION=0.0,0.0,1.0/
&DEVC ID='49_Vent_BDP4', QUANTITY='W-VELOCITY', XYZ=2.7,3.45,2.73, ORIENTATION=0.0,0.0,1.0/
&DEVC ID='4_TC1_1220mmBC', QUANTITY='THERMOCOUPLE', XYZ=3.15,1.91,1.18/
&DEVC ID='50_Vent_BDP5', QUANTITY='W-VELOCITY', XYZ=3.15,3.45,2.73, ORIENTATION=0.0,0.0,1.0/
&DEVC ID='51_Vent_BDP6', QUANTITY='W-VELOCITY', XYZ=3.15,3.9,2.73, ORIENTATION=0.0,0.0,1.0/
&DEVC ID='52_Vent_BDP7', QUANTITY='W-VELOCITY', XYZ=3.15,5.1,2.73, ORIENTATION=0.0,0.0,1.0/
&DEVC ID='53_Vent_BDP8', QUANTITY='W-VELOCITY', XYZ=3.15,3.0,2.73, ORIENTATION=0.0,0.0,1.0/
&DEVC ID='54_Vent_BDP9', QUANTITY='W-VELOCITY', XYZ=3.6,4.65,2.73, ORIENTATION=0.0,0.0,1.0/
&DEVC ID='55_Vent_BDP10', QUANTITY='W-VELOCITY', XYZ=3.6,3.45,2.73, ORIENTATION=0.0,0.0,1.0/
&DEVC ID='56_HF_B3FTCEIL', QUANTITY='GAUGE HEAT FLUX', XYZ=3.15,1.6,0.93, IOR=3/
&DEVC ID='58_HF_BFLCEIL', QUANTITY='GAUGE HEAT FLUX', XYZ=3.15,2.05,0.17, IOR=3/
&DEVC ID='59_HF_DR3FTCEIL', QUANTITY='GAUGE HEAT FLUX', XYZ=3.15,6.49,0.95, IOR=3/
&DEVC ID='5_TC1_1520mmBC', QUANTITY='THERMOCOUPLE', XYZ=3.15,1.91,0.88/

```
&DEVC ID='61_HF_FLCEIL', QUANTITY='GAUGE HEAT FLUX', XYZ=3.15,6.04,0.17, IOR=3/
&DEVC ID='6_TC1_1830mmBC', QUANTITY='THERMOCOUPLE', XYZ=3.15,1.91,0.58/
&DEVC ID='7_TC1_2130mmBC', QUANTITY='THERMOCOUPLE', XYZ=3.15,1.91,0.28/
&DEVC ID='8_TC2_25mmBC', QUANTITY='THERMOCOUPLE', XYZ=3.15,6.19,2.37/
&DEVC ID='9_TC2_305mmBC', QUANTITY='THERMOCOUPLE', XYZ=3.15,6.19,2.1/
&DEVC ID='HRR', QUANTITY='HRR', XB=-1.0,7.0,0.0,8.0,0.0,4.0/
&DEVC ID='SMOKE LAYER HT DOORWAY', QUANTITY='LAYER HEIGHT', XB=5.3,5.3,5.25,5.25,0.0,2.0/
&DEVC ID='SMOKE LAYER HT FIRE Burner', QUANTITY='LAYER HEIGHT', XB=3.15,3.15,1.91,1.91,0.0,2.4/
&DEVC ID='SMOKE LAYER HT FIRE Door', QUANTITY='LAYER HEIGHT', XB=3.15,3.15,6.19,6.19,0.0,2.4/
&DEVC ID='SMOKE LAYER TEMP Burner', QUANTITY='UPPER TEMPERATURE', XB=3.15,3.15,1.91,1.91,0.0,2.4/
&DEVC ID='SMOKE LAYER TEMP Door', QUANTITY='UPPER TEMPERATURE', XB=3.15,3.15,6.19,6.19,0.0,2.4/
&DEVC ID='TIME', QUANTITY='TIME', XYZ=-1.0,0.0,0.0/
&CTRL ID='4x8 CTRL', FUNCTION_TYPE='CUSTOM', RAMP_ID='4x8 CTRL_RAMP', LATCH=.FALSE., INPUT_ID='TIME'/
&CTRL ID='4x4 CTRL', FUNCTION_TYPE='CUSTOM', RAMP_ID='4x4 CTRL_RAMP', LATCH=.FALSE., INPUT_ID='TIME'/
&CTRL ID='4x8 CTRLReverse', FUNCTION_TYPE='CUSTOM', RAMP_ID='4x8 CTRLReverse_RAMP', LATCH=.FALSE.,
INPUT_ID='TIME'/

&MATL ID='Drywall',
    SPECIFIC_HEAT=1.09,
    CONDUCTIVITY=0.16,
    DENSITY=676.0/
&MATL ID='CementBoard',
    SPECIFIC_HEAT=0.84,
    CONDUCTIVITY=0.183,
    DENSITY=923.0/

&SURF ID='Burner',
    COLOR='RED',
    HRRPUA=3788.0,
    RAMP_Q='Burner_RAMP_Q'/
&RAMP ID='Burner_RAMP_Q', T=0.0, F=0.197/
&RAMP ID='Burner_RAMP_Q', T=2473.0, F=0.197/
&RAMP ID='Burner_RAMP_Q', T=2474.0, F=0.462/
&RAMP ID='Burner_RAMP_Q', T=3839.0, F=0.462/
&RAMP ID='Burner_RAMP_Q', T=3840.0, F=1.0/
&SURF ID='Drywall',
    RGB=146,202,166,
    MATL_ID(1,1)='Drywall',
    MATL_MASS_FRACTION(1,1)=1.0,
    THICKNESS(1)=0.01/
&SURF ID='CementBoard',
    RGB=146,202,166,
    MATL_ID(1,1)='CementBoard',
    MATL_MASS_FRACTION(1,1)=1.0,
    THICKNESS(1)=0.016/
```

&OBST XB=1.02,1.782,1.02,1.782,0.0,0.54, RGB=255,0,51, SURF_ID='INERT'/ Burner
&OBST XB=0.9,5.4,0.9,1.0,0.0,2.4, RGB=255,255,204, SURF_ID='Drywall'/ Bottom Wall (Min X)
&OBST XB=5.3,5.4,0.9,7.2,0.0,2.4, RGB=255,255,204, SURF_ID='Drywall'/ Right Wall (Max Y)
&OBST XB=0.9,5.4,7.1,7.2,0.0,2.4, RGB=255,255,204, SURF_ID='Drywall'/ Top Wall (Max X)
&OBST XB=0.9,1.0,0.9,7.2,0.0,2.4, RGB=255,255,204, SURF_ID='Drywall'/ Left Wall (Min Y)
&OBST XB=0.9,5.4,0.9,7.2,2.4,2.5, RGB=255,255,204, SURF_ID='Drywall'/ Ceiling
&OBST XB=2.55,3.75,2.85,2.86,2.45,3.03, RGB=255,255,204, SURF_ID='Drywall'/ Bottom Wall (Min X)
&OBST XB=3.74,3.75,2.85,5.25,2.45,3.03, RGB=255,255,204, SURF_ID='Drywall'/ Right Wall (Max Y)
&OBST XB=2.55,3.75,5.24,5.25,2.45,3.03, RGB=255,255,204, SURF_ID='Drywall'/ Top Wall (Max X)
&OBST XB=2.55,2.56,2.85,5.25,2.45,3.03, RGB=255,255,204, SURF_ID='Drywall'/ Left Wall (Min Y)
&OBST XB=2.55,3.75,4.05,5.25,3.03,3.04, RGB=255,255,204, SURF_ID='Drywall'/ Left Vent Door
&OBST XB=2.55,3.75,2.85,2.86,3.03,3.13, RGB=255,255,204, SURF_ID='Drywall'/ Bottom Wall (Min X)
&OBST XB=3.74,3.75,2.85,4.05,3.03,3.13, RGB=255,255,204, SURF_ID='Drywall'/ Right Wall (Max Y)
&OBST XB=2.55,2.56,2.85,4.05,3.03,3.13, RGB=255,255,204, SURF_ID='Drywall'/ Left Wall (Min Y)
&OBST XB=2.55,3.75,4.04,4.05,3.03,3.13, RGB=255,255,204, SURF_ID='Drywall', CTRL_ID='4x8 CTRLReverse'/ Top Wall (Max X)
&OBST XB=2.55,3.75,2.85,4.05,3.13,3.14, RGB=255,255,204, SURF_ID='Drywall'/ Right Vent Door
&OBST XB=1.0,3.4,1.0,1.02,0.0,2.4, RGB=255,255,204, SURF_ID='CementBoard'/ CementBoardX
&OBST XB=1.0,1.02,1.0,3.4,0.0,2.4, RGB=255,255,204, SURF_ID='CementBoard'/ CementBoardY
&OBST XB=1.0,2.55,1.0,3.4,2.38,2.4, RGB=255,255,204, SURF_ID='CementBoard'/ CementBoardZ1
&OBST XB=2.55,3.4,1.0,2.85,2.38,2.4, RGB=255,255,204, SURF_ID='CementBoard'/ CementBoardZ2
&OBST XB=-1.0,7.0,0.0,8.0,0.0,0.02, RGB=255,255,204, SURF_ID='CementBoard'/ Floor
&OBST XB=3.05,3.25,1.95,2.15,0.0,0.17, SURF_ID='INERT'/ HFBaseL1
&OBST XB=3.05,3.25,5.94,6.14,0.0,0.17, SURF_ID='INERT'/ HFBaseR1
&OBST XB=3.05,3.25,1.5,1.7,0.83,0.93, SURF_ID='INERT'/ HFBaseL1
&OBST XB=3.05,3.25,6.39,6.59,0.83,0.95, SURF_ID='INERT'/ HFBaseR1

&HOLE XB=5.3,5.4,4.8,5.7,0.0,2.0/ Fire Room Door
&HOLE XB=2.55,3.75,2.85,5.25,2.4,2.5/ 4x8
&HOLE XB=2.55,3.75,4.05,5.25,3.03,3.04, CTRL_ID='4x8 CTRL'/ 4x4Right
&HOLE XB=2.55,3.75,2.85,4.05,3.13,3.14, CTRL_ID='4x4 CTRL'/ 4x4Left

&VENT SURF_ID='OPEN', XB=-1.0,-1.0,0.0,2.0,0.0,2.0, COLOR='INVISIBLE'/ Vent Min X for MESH
&VENT SURF_ID='OPEN', XB=1.0,1.0,0.0,2.0,0.0,2.0, COLOR='INVISIBLE'/ Vent Max X for MESH
&VENT SURF_ID='OPEN', XB=-1.0,1.0,0.0,0.0,0.0,2.0, COLOR='INVISIBLE'/ Vent Min Y for MESH
&VENT SURF_ID='OPEN', XB=-1.0,1.0,2.0,2.0,0.0,2.0, COLOR='INVISIBLE'/ Vent Max Y for MESH
&VENT SURF_ID='OPEN', XB=-1.0,1.0,0.0,2.0,2.0,2.0, COLOR='INVISIBLE'/ Vent Max Z for MESH
&VENT SURF_ID='OPEN', XB=3.0,3.0,0.0,2.0,0.0,2.0, COLOR='INVISIBLE'/ Vent Max X for MESH02
&VENT SURF_ID='OPEN', XB=1.0,3.0,0.0,0.0,0.0,2.0, COLOR='INVISIBLE'/ Vent Min Y for MESH02
&VENT SURF_ID='OPEN', XB=1.0,3.0,2.0,2.0,0.0,2.0, COLOR='INVISIBLE'/ Vent Max Y for MESH02
&VENT SURF_ID='OPEN', XB=1.0,3.0,0.0,2.0,2.0,2.0, COLOR='INVISIBLE'/ Vent Max Z for MESH02
&VENT SURF_ID='OPEN', XB=7.0,7.0,0.0,2.0,0.0,2.0, COLOR='INVISIBLE'/ Vent Max X for MESH0202
&VENT SURF_ID='OPEN', XB=5.0,7.0,0.0,0.0,0.0,2.0, COLOR='INVISIBLE'/ Vent Min Y for MESH0202
&VENT SURF_ID='OPEN', XB=5.0,7.0,2.0,2.0,0.0,2.0, COLOR='INVISIBLE'/ Vent Max Y for MESH0202
&VENT SURF_ID='OPEN', XB=5.0,7.0,0.0,2.0,2.0,2.0, COLOR='INVISIBLE'/ Vent Max Z for MESH0202
&VENT SURF_ID='OPEN', XB=5.0,5.0,0.0,2.0,0.0,2.0, COLOR='INVISIBLE'/ Vent Max X for MESH03

&VENT SURF_ID='OPEN', XB=3.0,5.0,0.0,0.0,0.0,2.0, COLOR='INVISIBLE'/ Vent Min Y for MESH03
&VENT SURF_ID='OPEN', XB=3.0,5.0,2.0,2.0,0.0,2.0, COLOR='INVISIBLE'/ Vent Max Y for MESH03
&VENT SURF_ID='OPEN', XB=3.0,5.0,0.0,2.0,2.0,2.0, COLOR='INVISIBLE'/ Vent Max Z for MESH03
&VENT SURF_ID='OPEN', XB=3.0,3.0,2.0,4.0,0.0,2.0, COLOR='INVISIBLE'/ Vent Max X for MESH0203
&VENT SURF_ID='OPEN', XB=1.0,3.0,4.0,4.0,0.0,2.0, COLOR='INVISIBLE'/ Vent Max Y for MESH0203
&VENT SURF_ID='OPEN', XB=1.0,3.0,2.0,4.0,2.0,2.0, COLOR='INVISIBLE'/ Vent Max Z for MESH0203
&VENT SURF_ID='OPEN', XB=-1.0,-1.0,2.0,4.0,0.0,2.0, COLOR='INVISIBLE'/ Vent Min X for MESH04
&VENT SURF_ID='OPEN', XB=1.0,1.0,2.0,4.0,0.0,2.0, COLOR='INVISIBLE'/ Vent Max X for MESH04
&VENT SURF_ID='OPEN', XB=-1.0,1.0,4.0,4.0,0.0,2.0, COLOR='INVISIBLE'/ Vent Max Y for MESH04
&VENT SURF_ID='OPEN', XB=-1.0,1.0,2.0,4.0,2.0,2.0, COLOR='INVISIBLE'/ Vent Max Z for MESH04
&VENT SURF_ID='OPEN', XB=7.0,7.0,2.0,4.0,0.0,2.0, COLOR='INVISIBLE'/ Vent Max X for MESH020202
&VENT SURF_ID='OPEN', XB=5.0,7.0,4.0,4.0,0.0,2.0, COLOR='INVISIBLE'/ Vent Max Y for MESH020202
&VENT SURF_ID='OPEN', XB=5.0,7.0,2.0,4.0,2.0,2.0, COLOR='INVISIBLE'/ Vent Max Z for MESH020202
&VENT SURF_ID='OPEN', XB=5.0,5.0,2.0,4.0,0.0,2.0, COLOR='INVISIBLE'/ Vent Max X for MESH0302
&VENT SURF_ID='OPEN', XB=3.0,5.0,4.0,4.0,0.0,2.0, COLOR='INVISIBLE'/ Vent Max Y for MESH0302
&VENT SURF_ID='OPEN', XB=3.0,5.0,2.0,4.0,2.0,2.0, COLOR='INVISIBLE'/ Vent Max Z for MESH0302
&VENT SURF_ID='OPEN', XB=3.0,3.0,4.0,6.0,0.0,2.0, COLOR='INVISIBLE'/ Vent Max X for MESH0204
&VENT SURF_ID='OPEN', XB=1.0,3.0,6.0,6.0,0.0,2.0, COLOR='INVISIBLE'/ Vent Max Y for MESH0204
&VENT SURF_ID='OPEN', XB=1.0,3.0,4.0,6.0,2.0,2.0, COLOR='INVISIBLE'/ Vent Max Z for MESH0204
&VENT SURF_ID='OPEN', XB=-1.0,-1.0,4.0,6.0,0.0,2.0, COLOR='INVISIBLE'/ Vent Min X for MESH05
&VENT SURF_ID='OPEN', XB=1.0,1.0,4.0,6.0,0.0,2.0, COLOR='INVISIBLE'/ Vent Max X for MESH05
&VENT SURF_ID='OPEN', XB=-1.0,1.0,6.0,6.0,0.0,2.0, COLOR='INVISIBLE'/ Vent Max Y for MESH05
&VENT SURF_ID='OPEN', XB=-1.0,1.0,4.0,6.0,2.0,2.0, COLOR='INVISIBLE'/ Vent Max Z for MESH05
&VENT SURF_ID='OPEN', XB=7.0,7.0,4.0,6.0,0.0,2.0, COLOR='INVISIBLE'/ Vent Max X for MESH020203
&VENT SURF_ID='OPEN', XB=5.0,7.0,6.0,6.0,0.0,2.0, COLOR='INVISIBLE'/ Vent Max Y for MESH020203
&VENT SURF_ID='OPEN', XB=5.0,7.0,4.0,6.0,2.0,2.0, COLOR='INVISIBLE'/ Vent Max Z for MESH020203
&VENT SURF_ID='OPEN', XB=5.0,5.0,4.0,6.0,0.0,2.0, COLOR='INVISIBLE'/ Vent Max X for MESH0303
&VENT SURF_ID='OPEN', XB=3.0,5.0,6.0,6.0,0.0,2.0, COLOR='INVISIBLE'/ Vent Max Y for MESH0303
&VENT SURF_ID='OPEN', XB=3.0,5.0,4.0,6.0,2.0,2.0, COLOR='INVISIBLE'/ Vent Max Z for MESH0303
&VENT SURF_ID='OPEN', XB=3.0,3.0,6.0,8.0,0.0,2.0, COLOR='INVISIBLE'/ Vent Max X for MESH0205
&VENT SURF_ID='OPEN', XB=1.0,3.0,8.0,8.0,0.0,2.0, COLOR='INVISIBLE'/ Vent Max Y for MESH0205
&VENT SURF_ID='OPEN', XB=1.0,3.0,6.0,8.0,2.0,2.0, COLOR='INVISIBLE'/ Vent Max Z for MESH0205
&VENT SURF_ID='OPEN', XB=-1.0,-1.0,6.0,8.0,0.0,2.0, COLOR='INVISIBLE'/ Vent Min X for MESH06
&VENT SURF_ID='OPEN', XB=1.0,1.0,6.0,8.0,0.0,2.0, COLOR='INVISIBLE'/ Vent Max X for MESH06
&VENT SURF_ID='OPEN', XB=-1.0,1.0,8.0,8.0,0.0,2.0, COLOR='INVISIBLE'/ Vent Max Y for MESH06
&VENT SURF_ID='OPEN', XB=-1.0,1.0,6.0,8.0,2.0,2.0, COLOR='INVISIBLE'/ Vent Max Z for MESH06
&VENT SURF_ID='OPEN', XB=7.0,7.0,6.0,8.0,0.0,2.0, COLOR='INVISIBLE'/ Vent Max X for MESH020204
&VENT SURF_ID='OPEN', XB=5.0,7.0,8.0,8.0,0.0,2.0, COLOR='INVISIBLE'/ Vent Max Y for MESH020204
&VENT SURF_ID='OPEN', XB=5.0,7.0,6.0,8.0,2.0,2.0, COLOR='INVISIBLE'/ Vent Max Z for MESH020204
&VENT SURF_ID='OPEN', XB=5.0,5.0,6.0,8.0,0.0,2.0, COLOR='INVISIBLE'/ Vent Max X for MESH0304
&VENT SURF_ID='OPEN', XB=3.0,5.0,8.0,8.0,0.0,2.0, COLOR='INVISIBLE'/ Vent Max Y for MESH0304
&VENT SURF_ID='OPEN', XB=3.0,5.0,6.0,8.0,2.0,2.0, COLOR='INVISIBLE'/ Vent Max Z for MESH0304
&VENT SURF_ID='OPEN', XB=3.0,3.0,0.0,2.0,2.0,4.0, COLOR='INVISIBLE'/ Vent Max X for MESH0206
&VENT SURF_ID='OPEN', XB=1.0,3.0,0.0,0.0,2.0,4.0, COLOR='INVISIBLE'/ Vent Min Y for MESH0206
&VENT SURF_ID='OPEN', XB=1.0,3.0,2.0,2.0,2.0,4.0, COLOR='INVISIBLE'/ Vent Max Y for MESH0206
&VENT SURF_ID='OPEN', XB=1.0,3.0,0.0,2.0,4.0,4.0, COLOR='INVISIBLE'/ Vent Max Z for MESH0206

&VENT SURF_ID='OPEN', XB=-1.0,-1.0,0.0,2.0,2.0,4.0, COLOR='INVISIBLE'/ Vent Min X for MESH07
&VENT SURF_ID='OPEN', XB=1.0,1.0,0.0,2.0,2.0,4.0, COLOR='INVISIBLE'/ Vent Max X for MESH07
&VENT SURF_ID='OPEN', XB=-1.0,1.0,0.0,0.0,2.0,4.0, COLOR='INVISIBLE'/ Vent Min Y for MESH07
&VENT SURF_ID='OPEN', XB=-1.0,1.0,2.0,2.0,2.0,4.0, COLOR='INVISIBLE'/ Vent Max Y for MESH07
&VENT SURF_ID='OPEN', XB=-1.0,1.0,0.0,2.0,4.0,4.0, COLOR='INVISIBLE'/ Vent Max Z for MESH07
&VENT SURF_ID='OPEN', XB=7.0,7.0,0.0,2.0,2.0,4.0, COLOR='INVISIBLE'/ Vent Max X for MESH020205
&VENT SURF_ID='OPEN', XB=5.0,7.0,0.0,0.0,2.0,4.0, COLOR='INVISIBLE'/ Vent Min Y for MESH020205
&VENT SURF_ID='OPEN', XB=5.0,7.0,2.0,2.0,2.0,4.0, COLOR='INVISIBLE'/ Vent Max Y for MESH020205
&VENT SURF_ID='OPEN', XB=5.0,7.0,0.0,2.0,4.0,4.0, COLOR='INVISIBLE'/ Vent Max Z for MESH020205
&VENT SURF_ID='OPEN', XB=5.0,5.0,0.0,2.0,2.0,4.0, COLOR='INVISIBLE'/ Vent Max X for MESH0305
&VENT SURF_ID='OPEN', XB=3.0,5.0,0.0,0.0,2.0,4.0, COLOR='INVISIBLE'/ Vent Min Y for MESH0305
&VENT SURF_ID='OPEN', XB=3.0,5.0,2.0,2.0,2.0,4.0, COLOR='INVISIBLE'/ Vent Max Y for MESH0305
&VENT SURF_ID='OPEN', XB=3.0,5.0,0.0,2.0,4.0,4.0, COLOR='INVISIBLE'/ Vent Max Z for MESH0305
&VENT SURF_ID='OPEN', XB=3.0,3.0,2.0,4.0,2.0,4.0, COLOR='INVISIBLE'/ Vent Max X for MESH020302
&VENT SURF_ID='OPEN', XB=1.0,3.0,4.0,4.0,2.0,4.0, COLOR='INVISIBLE'/ Vent Max Y for MESH020302
&VENT SURF_ID='OPEN', XB=1.0,3.0,2.0,4.0,4.0,4.0, COLOR='INVISIBLE'/ Vent Max Z for MESH020302
&VENT SURF_ID='OPEN', XB=-1.0,-1.0,2.0,4.0,2.0,4.0, COLOR='INVISIBLE'/ Vent Min X for MESH0402
&VENT SURF_ID='OPEN', XB=1.0,1.0,2.0,4.0,2.0,4.0, COLOR='INVISIBLE'/ Vent Max X for MESH0402
&VENT SURF_ID='OPEN', XB=-1.0,1.0,4.0,4.0,2.0,4.0, COLOR='INVISIBLE'/ Vent Max Y for MESH0402
&VENT SURF_ID='OPEN', XB=-1.0,1.0,2.0,4.0,4.0,4.0, COLOR='INVISIBLE'/ Vent Max Z for MESH0402
&VENT SURF_ID='OPEN', XB=7.0,7.0,2.0,4.0,2.0,4.0, COLOR='INVISIBLE'/ Vent Max X for MESH02020202
&VENT SURF_ID='OPEN', XB=5.0,7.0,4.0,4.0,2.0,4.0, COLOR='INVISIBLE'/ Vent Max Y for MESH02020202
&VENT SURF_ID='OPEN', XB=5.0,7.0,2.0,4.0,4.0,4.0, COLOR='INVISIBLE'/ Vent Max Z for MESH02020202
&VENT SURF_ID='OPEN', XB=5.0,5.0,2.0,4.0,2.0,4.0, COLOR='INVISIBLE'/ Vent Max X for MESH030202
&VENT SURF_ID='OPEN', XB=3.0,5.0,4.0,4.0,2.0,4.0, COLOR='INVISIBLE'/ Vent Max Y for MESH030202
&VENT SURF_ID='OPEN', XB=3.0,5.0,2.0,4.0,4.0,4.0, COLOR='INVISIBLE'/ Vent Max Z for MESH030202
&VENT SURF_ID='OPEN', XB=3.0,3.0,4.0,6.0,2.0,4.0, COLOR='INVISIBLE'/ Vent Max X for MESH020402
&VENT SURF_ID='OPEN', XB=1.0,3.0,6.0,6.0,2.0,4.0, COLOR='INVISIBLE'/ Vent Max Y for MESH020402
&VENT SURF_ID='OPEN', XB=1.0,3.0,4.0,6.0,4.0,4.0, COLOR='INVISIBLE'/ Vent Max Z for MESH020402
&VENT SURF_ID='OPEN', XB=-1.0,-1.0,4.0,6.0,2.0,4.0, COLOR='INVISIBLE'/ Vent Min X for MESH0502
&VENT SURF_ID='OPEN', XB=1.0,1.0,4.0,6.0,2.0,4.0, COLOR='INVISIBLE'/ Vent Max X for MESH0502
&VENT SURF_ID='OPEN', XB=-1.0,1.0,6.0,6.0,2.0,4.0, COLOR='INVISIBLE'/ Vent Max Y for MESH0502
&VENT SURF_ID='OPEN', XB=-1.0,1.0,4.0,6.0,4.0,4.0, COLOR='INVISIBLE'/ Vent Max Z for MESH0502
&VENT SURF_ID='OPEN', XB=7.0,7.0,4.0,6.0,2.0,4.0, COLOR='INVISIBLE'/ Vent Max X for MESH02020302
&VENT SURF_ID='OPEN', XB=5.0,7.0,6.0,6.0,2.0,4.0, COLOR='INVISIBLE'/ Vent Max Y for MESH02020302
&VENT SURF_ID='OPEN', XB=5.0,7.0,4.0,6.0,4.0,4.0, COLOR='INVISIBLE'/ Vent Max Z for MESH02020302
&VENT SURF_ID='OPEN', XB=5.0,5.0,4.0,6.0,2.0,4.0, COLOR='INVISIBLE'/ Vent Max X for MESH030302
&VENT SURF_ID='OPEN', XB=3.0,5.0,6.0,6.0,2.0,4.0, COLOR='INVISIBLE'/ Vent Max Y for MESH030302
&VENT SURF_ID='OPEN', XB=3.0,5.0,4.0,6.0,4.0,4.0, COLOR='INVISIBLE'/ Vent Max Z for MESH030302
&VENT SURF_ID='OPEN', XB=3.0,3.0,6.0,8.0,2.0,4.0, COLOR='INVISIBLE'/ Vent Max X for MESH020502
&VENT SURF_ID='OPEN', XB=1.0,3.0,8.0,8.0,2.0,4.0, COLOR='INVISIBLE'/ Vent Max Y for MESH020502
&VENT SURF_ID='OPEN', XB=1.0,3.0,6.0,8.0,4.0,4.0, COLOR='INVISIBLE'/ Vent Max Z for MESH020502
&VENT SURF_ID='OPEN', XB=-1.0,-1.0,6.0,8.0,2.0,4.0, COLOR='INVISIBLE'/ Vent Min X for MESH0602
&VENT SURF_ID='OPEN', XB=1.0,1.0,6.0,8.0,2.0,4.0, COLOR='INVISIBLE'/ Vent Max X for MESH0602
&VENT SURF_ID='OPEN', XB=-1.0,1.0,8.0,8.0,2.0,4.0, COLOR='INVISIBLE'/ Vent Max Y for MESH0602
&VENT SURF_ID='OPEN', XB=-1.0,1.0,6.0,8.0,4.0,4.0, COLOR='INVISIBLE'/ Vent Max Z for MESH0602

```
&VENT SURF_ID='OPEN', XB=7.0,7.0,6.0,8.0,2.0,4.0, COLOR='INVISIBLE'/ Vent Max X for MESH02020402
&VENT SURF_ID='OPEN', XB=5.0,7.0,8.0,8.0,2.0,4.0, COLOR='INVISIBLE'/ Vent Max Y for MESH02020402
&VENT SURF_ID='OPEN', XB=5.0,7.0,6.0,8.0,4.0,4.0, COLOR='INVISIBLE'/ Vent Max Z for MESH02020402
&VENT SURF_ID='OPEN', XB=5.0,5.0,6.0,8.0,2.0,4.0, COLOR='INVISIBLE'/ Vent Max X for MESH030402
&VENT SURF_ID='OPEN', XB=3.0,5.0,8.0,8.0,2.0,4.0, COLOR='INVISIBLE'/ Vent Max Y for MESH030402
&VENT SURF_ID='OPEN', XB=3.0,5.0,6.0,8.0,4.0,4.0, COLOR='INVISIBLE'/ Vent Max Z for MESH030402
&VENT SURF_ID='Burner', XB=1.02,1.782,1.02,1.782,0.54,0.54/ Vent

&SLCF QUANTITY='TEMPERATURE', PBY=5.25/
&SLCF QUANTITY='TEMPERATURE', PBX=3.15/
&SLCF QUANTITY='VELOCITY', VECTOR=.TRUE., PBY=5.25/
&SLCF QUANTITY='VELOCITY', VECTOR=.TRUE., PBX=3.15/
&SLCF QUANTITY='PRESSURE', PBX=3.15/
&SLCF QUANTITY='PRESSURE', PBY=5.25/
&SLCF QUANTITY='VELOCITY', VECTOR=.TRUE., PBZ=2.5/


&TAIL /
```

EX12_14_10cmGrid.fds

Generated by PyroSim - Version 2012.1.0605
Aug 23, 2012 3:30:09 PM

```
&HEAD CHID='EX12_14_10cmGrid'/
&TIME T_END=4334.0/
&DUMP RENDER_FILE='EX12_14_10cmGrid.ge1', DT_RESTART=300.0, PLOT3D_QUANTITY(1:4)='OPTICAL
DENSITY','PRESSURE','TEMPERATURE','VELOCITY'/

&MESH ID='MESH', IJK=20,20,20, XB=-1.0,1.0,0.0,2.0,0.0,2.0/
&MESH ID='MESH02', IJK=20,20,20, XB=1.0,3.0,0.0,2.0,0.0,2.0/
&MESH ID='MESH0202', IJK=20,20,20, XB=5.0,7.0,0.0,2.0,0.0,2.0/
&MESH ID='MESH03', IJK=20,20,20, XB=3.0,5.0,0.0,2.0,0.0,2.0/
&MESH ID='MESH0203', IJK=20,20,20, XB=1.0,3.0,2.0,4.0,0.0,2.0/
&MESH ID='MESH04', IJK=20,20,20, XB=-1.0,1.0,2.0,4.0,0.0,2.0/
&MESH ID='MESH020202', IJK=20,20,20, XB=5.0,7.0,2.0,4.0,0.0,2.0/
&MESH ID='MESH0302', IJK=20,20,20, XB=3.0,5.0,2.0,4.0,0.0,2.0/
&MESH ID='MESH0204', IJK=20,20,20, XB=1.0,3.0,4.0,6.0,0.0,2.0/
&MESH ID='MESH05', IJK=20,20,20, XB=-1.0,1.0,4.0,6.0,0.0,2.0/
&MESH ID='MESH020203', IJK=20,20,20, XB=5.0,7.0,4.0,6.0,0.0,2.0/
&MESH ID='MESH0303', IJK=20,20,20, XB=3.0,5.0,4.0,6.0,0.0,2.0/
&MESH ID='MESH0205', IJK=20,20,20, XB=1.0,3.0,6.0,8.0,0.0,2.0/
&MESH ID='MESH06', IJK=20,20,20, XB=-1.0,1.0,6.0,8.0,0.0,2.0/
&MESH ID='MESH020204', IJK=20,20,20, XB=5.0,7.0,6.0,8.0,0.0,2.0/
&MESH ID='MESH0304', IJK=20,20,20, XB=3.0,5.0,6.0,8.0,0.0,2.0/
&MESH ID='MESH0206', IJK=20,20,20, XB=1.0,3.0,0.0,2.0,2.0,4.0/
&MESH ID='MESH07', IJK=20,20,20, XB=-1.0,1.0,0.0,2.0,2.0,4.0/
&MESH ID='MESH020205', IJK=20,20,20, XB=5.0,7.0,0.0,2.0,2.0,4.0/
&MESH ID='MESH0305', IJK=20,20,20, XB=3.0,5.0,0.0,2.0,2.0,4.0/
&MESH ID='MESH020302', IJK=20,20,20, XB=1.0,3.0,2.0,4.0,2.0,4.0/
&MESH ID='MESH0402', IJK=20,20,20, XB=-1.0,1.0,2.0,4.0,2.0,4.0/
&MESH ID='MESH02020202', IJK=20,20,20, XB=5.0,7.0,2.0,4.0,2.0,4.0/
&MESH ID='MESH030202', IJK=20,20,20, XB=3.0,5.0,2.0,4.0,2.0,4.0/
&MESH ID='MESH020402', IJK=20,20,20, XB=1.0,3.0,4.0,6.0,2.0,4.0/
&MESH ID='MESH0502', IJK=20,20,20, XB=-1.0,1.0,4.0,6.0,2.0,4.0/
&MESH ID='MESH02020302', IJK=20,20,20, XB=5.0,7.0,4.0,6.0,2.0,4.0/
&MESH ID='MESH030302', IJK=20,20,20, XB=3.0,5.0,4.0,6.0,2.0,4.0/
&MESH ID='MESH020502', IJK=20,20,20, XB=1.0,3.0,6.0,8.0,2.0,4.0/
&MESH ID='MESH0602', IJK=20,20,20, XB=-1.0,1.0,6.0,8.0,2.0,4.0/
&MESH ID='MESH02020402', IJK=20,20,20, XB=5.0,7.0,6.0,8.0,2.0,4.0/
&MESH ID='MESH030402', IJK=20,20,20, XB=3.0,5.0,6.0,8.0,2.0,4.0/

&REAC ID='METHANE',
    FYI='Methane Properties',
    C=1.0,
    H=4.0,
```

O=0.0,
N=0.0/

&DEVC ID='0_TC1_25mmBC', QUANTITY='THERMOCOUPLE', XYZ=3.15,1.9,2.35/
&DEVC ID='10_TC2_610mmBC', QUANTITY='THERMOCOUPLE', XYZ=3.15,6.19,1.8/
&DEVC ID='11_TC2_915mmBC', QUANTITY='THERMOCOUPLE', XYZ=3.15,6.19,1.5/
&DEVC ID='12_TC2_1220mmBC', QUANTITY='THERMOCOUPLE', XYZ=3.15,6.19,1.2/
&DEVC ID='13_TC2_1520mmBC', QUANTITY='THERMOCOUPLE', XYZ=3.15,6.19,0.9/
&DEVC ID='14_TC2_1830mmBC', QUANTITY='THERMOCOUPLE', XYZ=3.15,6.19,0.6/
&DEVC ID='15_TC2_2130mmBC', QUANTITY='THERMOCOUPLE', XYZ=3.15,6.19,0.3/
&DEVC ID='16_Door_TC1', QUANTITY='THERMOCOUPLE', XYZ=5.3,5.25,1.97/
&DEVC ID='17_Door_TC2', QUANTITY='THERMOCOUPLE', XYZ=5.3,5.25,1.8/
&DEVC ID='18_Door_TC3', QUANTITY='THERMOCOUPLE', XYZ=5.3,5.25,1.6/
&DEVC ID='19_Door_TC4', QUANTITY='THERMOCOUPLE', XYZ=5.3,5.25,1.4/
&DEVC ID='1_TC1_305mmBC', QUANTITY='THERMOCOUPLE', XYZ=3.15,1.91,2.08/
&DEVC ID='20_Door_TC5', QUANTITY='THERMOCOUPLE', XYZ=5.3,5.25,1.2/
&DEVC ID='21_Door_TC6', QUANTITY='THERMOCOUPLE', XYZ=5.3,5.25,1.0/
&DEVC ID='22_Door_TC7', QUANTITY='THERMOCOUPLE', XYZ=5.3,5.25,0.8/
&DEVC ID='23_Door_TC8', QUANTITY='THERMOCOUPLE', XYZ=5.3,5.25,0.6/
&DEVC ID='24_Door_TC9', QUANTITY='THERMOCOUPLE', XYZ=5.3,5.25,0.4/
&DEVC ID='25_Door_TC10', QUANTITY='THERMOCOUPLE', XYZ=5.3,5.25,0.2/
&DEVC ID='26_Door_BDP1', QUANTITY='U-VELOCITY', XYZ=5.3,5.25,1.97, ORIENTATION=1.0,0.0,0.0/
&DEVC ID='27_Door_BDP2', QUANTITY='U-VELOCITY', XYZ=5.3,5.25,1.8, ORIENTATION=1.0,0.0,0.0/
&DEVC ID='28_Door_BDP3', QUANTITY='U-VELOCITY', XYZ=5.3,5.25,1.6, ORIENTATION=1.0,0.0,0.0/
&DEVC ID='29_Door_BDP4', QUANTITY='U-VELOCITY', XYZ=5.3,5.25,1.4, ORIENTATION=1.0,0.0,0.0/
&DEVC ID='2_TC1_610mmBC', QUANTITY='THERMOCOUPLE', XYZ=3.15,1.91,1.78/
&DEVC ID='30_Door_BDP5', QUANTITY='U-VELOCITY', XYZ=5.3,5.25,1.2, ORIENTATION=1.0,0.0,0.0/
&DEVC ID='31_Door_BDP6', QUANTITY='U-VELOCITY', XYZ=5.3,5.25,1.0, ORIENTATION=1.0,0.0,0.0/
&DEVC ID='32_Door_BDP7', QUANTITY='U-VELOCITY', XYZ=5.3,5.25,0.8, ORIENTATION=1.0,0.0,0.0/
&DEVC ID='33_Door_BDP8', QUANTITY='U-VELOCITY', XYZ=5.3,5.25,0.6, ORIENTATION=1.0,0.0,0.0/
&DEVC ID='34_Door_BDP9', QUANTITY='U-VELOCITY', XYZ=5.3,5.25,0.4, ORIENTATION=1.0,0.0,0.0/
&DEVC ID='35_Door_BDP10', QUANTITY='U-VELOCITY', XYZ=5.3,5.25,0.2, ORIENTATION=1.0,0.0,0.0/
&DEVC ID='36_VENT_TC1', QUANTITY='THERMOCOUPLE', XYZ=2.7,4.65,2.73/
&DEVC ID='37_VENT_TC2', QUANTITY='THERMOCOUPLE', XYZ=3.15,4.65,2.73/
&DEVC ID='38_VENT_TC3', QUANTITY='THERMOCOUPLE', XYZ=3.15,4.2,2.73/
&DEVC ID='39_VENT_TC4', QUANTITY='THERMOCOUPLE', XYZ=2.7,3.45,2.73/
&DEVC ID='3_TC1_915mmBC', QUANTITY='THERMOCOUPLE', XYZ=3.15,1.91,1.48/
&DEVC ID='40_VENT_TC5', QUANTITY='THERMOCOUPLE', XYZ=3.15,3.45,2.73/
&DEVC ID='41_VENT_TC6', QUANTITY='THERMOCOUPLE', XYZ=3.15,3.9,2.73/
&DEVC ID='42_VENT_TC7', QUANTITY='THERMOCOUPLE', XYZ=3.15,5.1,2.73/
&DEVC ID='43_VENT_TC8', QUANTITY='THERMOCOUPLE', XYZ=3.15,3.0,2.73/
&DEVC ID='44_VENT_TC9', QUANTITY='THERMOCOUPLE', XYZ=3.6,4.65,2.73/
&DEVC ID='45_VENT_TC10', QUANTITY='THERMOCOUPLE', XYZ=3.6,3.45,2.73/
&DEVC ID='46_Vent_BDP1', QUANTITY='W-VELOCITY', XYZ=2.7,4.65,2.73, ORIENTATION=0.0,0.0,1.0/
&DEVC ID='47_Vent_BDP2', QUANTITY='W-VELOCITY', XYZ=3.15,4.65,2.73, ORIENTATION=0.0,0.0,1.0/
&DEVC ID='48_Vent_BDP3', QUANTITY='W-VELOCITY', XYZ=3.15,4.2,2.73, ORIENTATION=0.0,0.0,1.0/

```
&DEVC ID='49_Vent_BDP4', QUANTITY='W-VELOCITY', XYZ=2.7,3.45,2.73, ORIENTATION=0.0,0.0,1.0/
&DEVC ID='4_TC1_1220mmBC', QUANTITY='THERMOCOUPLE', XYZ=3.15,1.91,1.18/
&DEVC ID='50_Vent_BDP5', QUANTITY='W-VELOCITY', XYZ=3.15,3.45,2.73, ORIENTATION=0.0,0.0,1.0/
&DEVC ID='51_Vent_BDP6', QUANTITY='W-VELOCITY', XYZ=3.15,3.9,2.73, ORIENTATION=0.0,0.0,1.0/
&DEVC ID='52_Vent_BDP7', QUANTITY='W-VELOCITY', XYZ=3.15,5.1,2.73, ORIENTATION=0.0,0.0,1.0/
&DEVC ID='53_Vent_BDP8', QUANTITY='W-VELOCITY', XYZ=3.15,3.0,2.73, ORIENTATION=0.0,0.0,1.0/
&DEVC ID='54_Vent_BDP9', QUANTITY='W-VELOCITY', XYZ=3.6,4.65,2.73, ORIENTATION=0.0,0.0,1.0/
&DEVC ID='55_Vent_BDP10', QUANTITY='W-VELOCITY', XYZ=3.6,3.45,2.73, ORIENTATION=0.0,0.0,1.0/
&DEVC ID='56_HF_B3FTCEIL', QUANTITY='GAUGE HEAT FLUX', XYZ=3.15,1.6,0.93, IOR=3/
&DEVC ID='58_HF_BFLCEIL', QUANTITY='GAUGE HEAT FLUX', XYZ=3.15,2.05,0.17, IOR=3/
&DEVC ID='59_HF_DR3FTCEIL', QUANTITY='GAUGE HEAT FLUX', XYZ=3.15,6.49,0.95, IOR=3/
&DEVC ID='5_TC1_1520mmBC', QUANTITY='THERMOCOUPLE', XYZ=3.15,1.91,0.88/
&DEVC ID='61_HF_FLCEIL', QUANTITY='GAUGE HEAT FLUX', XYZ=3.15,6.04,0.17, IOR=3/
&DEVC ID='6_TC1_1830mmBC', QUANTITY='THERMOCOUPLE', XYZ=3.15,1.91,0.58/
&DEVC ID='7_TC1_2130mmBC', QUANTITY='THERMOCOUPLE', XYZ=3.15,1.91,0.28/
&DEVC ID='8_TC2_25mmBC', QUANTITY='THERMOCOUPLE', XYZ=3.15,6.19,2.37/
&DEVC ID='9_TC2_305mmBC', QUANTITY='THERMOCOUPLE', XYZ=3.15,6.19,2.1/
&DEVC ID='HRR', QUANTITY='HRR', XB=-1.0,7.0,0.0,8.0,0.0,4.0/
&DEVC ID='SMOKE LAYER HT DOORWAY', QUANTITY='LAYER HEIGHT', XB=5.3,5.3,5.25,5.25,0.0,2.0/
&DEVC ID='SMOKE LAYER HT FIRE Burner', QUANTITY='LAYER HEIGHT', XB=3.15,3.15,1.91,1.91,0.0,2.4/
&DEVC ID='SMOKE LAYER HT FIRE Door', QUANTITY='LAYER HEIGHT', XB=3.15,3.15,6.19,6.19,0.0,2.4/
&DEVC ID='SMOKE LAYER TEMP Burner', QUANTITY='UPPER TEMPERATURE', XB=3.15,3.15,1.91,1.91,0.0,2.4/
&DEVC ID='SMOKE LAYER TEMP Door', QUANTITY='UPPER TEMPERATURE', XB=3.15,3.15,6.19,6.19,0.0,2.4/
&DEVC ID='TIMER', QUANTITY='TIME', XYZ=-1.0,0.0,0.0, SETPOINT=859.0/
&DEVC ID='TIMER2', QUANTITY='TIME', XYZ=-1.0,0.0,0.0, SETPOINT=565.0/
&DEVC ID='TIMER3', QUANTITY='TIME', XYZ=-1.0,0.0,0.0, SETPOINT=859.0, INITIAL_STATE=.TRUE./
&MATL ID='Drywall',
    SPECIFIC_HEAT=1.09,
    CONDUCTIVITY=0.16,
    DENSITY=676.0/
&MATL ID='CementBoard',
    SPECIFIC_HEAT=0.84,
    CONDUCTIVITY=0.183,
    DENSITY=923.0/

&SURF ID='Burner',
    COLOR='RED',
    HRRPUA=3712.0/
&SURF ID='Drywall',
    RGB=146,202,166,
    MATL_ID(1,1)='Drywall',
    MATL_ID(2,1)='Drywall',
    MATL_MASS_FRACTION(1,1)=1.0,
    MATL_MASS_FRACTION(2,1)=1.0,
    THICKNESS(1:2)=0.01,0.01/
&SURF ID='CementBoard',
```

```
    RGB=146,202,166,
    MATL_ID(1,1)='CementBoard',
    MATL_MASS_FRACTION(1,1)=1.0,
    THICKNESS(1)=0.016/

&OBST XB=1.02,1.782,1.02,1.782,0.0,0.54, RGB=255,0,51, SURF_ID='INERT'/ Burner
&OBST XB=0.9,5.4,0.9,1.0,0.0,2.4, RGB=255,255,204, SURF_ID='Drywall'/ Bottom Wall (Min X)
&OBST XB=5.3,5.4,0.9,7.2,0.0,2.4, RGB=255,255,204, SURF_ID='Drywall'/ Right Wall (Max Y)
&OBST XB=0.9,5.4,7.1,7.2,0.0,2.4, RGB=255,255,204, SURF_ID='Drywall'/ Top Wall (Max X)
&OBST XB=0.9,1.0,0.9,7.2,0.0,2.4, RGB=255,255,204, SURF_ID='Drywall'/ Left Wall (Min Y)
&OBST XB=0.9,5.4,0.9,7.2,2.4,2.5, RGB=255,255,204, SURF_ID='Drywall'/ Ceiling
&OBST XB=2.55,3.75,2.85,2.86,2.45,3.03, RGB=255,255,204, SURF_ID='Drywall'/ Bottom Wall (Min X)
&OBST XB=3.74,3.75,2.85,5.25,2.45,3.03, RGB=255,255,204, SURF_ID='Drywall'/ Right Wall (Max Y)
&OBST XB=2.55,3.75,5.24,5.25,2.45,3.03, RGB=255,255,204, SURF_ID='Drywall'/ Top Wall (Max X)
&OBST XB=2.55,2.56,2.85,5.25,2.45,3.03, RGB=255,255,204, SURF_ID='Drywall'/ Left Wall (Min Y)
&OBST XB=2.55,3.75,4.05,5.25,3.03,3.04, RGB=255,255,204, SURF_ID='Drywall'/ Left Vent Door
&OBST XB=2.55,3.75,2.85,2.86,3.03,3.13, RGB=255,255,204, SURF_ID='Drywall'/ Bottom Wall (Min X)
&OBST XB=3.74,3.75,2.85,4.05,3.03,3.13, RGB=255,255,204, SURF_ID='Drywall'/ Right Wall (Max Y)
&OBST XB=2.55,2.56,2.85,4.05,3.03,3.13, RGB=255,255,204, SURF_ID='Drywall'/ Left Wall (Min Y)
&OBST XB=2.55,3.75,4.04,4.05,3.03,3.13, RGB=255,255,204, SURF_ID='Drywall', DEVC_ID='TIMER3'/ Top Wall
(Max X)
&OBST XB=2.55,3.75,2.85,4.05,3.13,3.14, RGB=255,255,204, SURF_ID='Drywall'/ Right Vent Door
&OBST XB=1.0,2.2,1.0,1.02,0.0,2.4, RGB=255,255,204, SURF_ID='CementBoard'/ CementBoardX
&OBST XB=1.0,1.02,1.0,2.2,0.0,2.4, RGB=255,255,204, SURF_ID='CementBoard'/ CementBoardY
&OBST XB=-1.0,7.0,0.0,8.0,0.0,0.02, RGB=255,255,204, SURF_ID='CementBoard'/ Floor
&OBST XB=3.05,3.25,1.95,2.15,0.0,0.17, SURF_ID='INERT'/ HFBaseL1
&OBST XB=3.05,3.25,5.94,6.14,0.0,0.17, SURF_ID='INERT'/ HFBaseR1
&OBST XB=3.05,3.25,1.5,1.7,0.83,0.93, SURF_ID='INERT'/ HFBaseL1
&OBST XB=3.05,3.25,6.39,6.59,0.83,0.95, SURF_ID='INERT'/ HFBaseR1
&OBST XB=0.9,5.4,0.9,7.2,2.38,2.4, RGB=255,255,204, SURF_ID='CementBoard'/ Ceiling Cement
&OBST XB=2.2,5.3,1.0,1.02,0.6,2.4, RGB=255,255,204, SURF_ID='CementBoard'/ CementBoardX2
&OBST XB=1.0,1.02,2.2,3.7,0.6,2.4, RGB=255,255,204, SURF_ID='CementBoard'/ CementBoardY2
&OBST XB=5.28,5.3,1.0,2.2,1.4,2.4, RGB=255,255,204, SURF_ID='CementBoard'/ CementBoardY3

&HOLE XB=5.3,5.4,4.8,5.7,0.0,2.0/ Fire Room Door
&HOLE XB=2.55,3.75,2.85,5.25,2.35,2.5/ 4x8
&HOLE XB=2.55,3.75,4.05,5.25,3.03,3.04, DEVC_ID='TIMER'/ 4x4Right
&HOLE XB=2.55,3.75,2.85,4.05,3.13,3.14, DEVC_ID='TIMER2'/ 4x4Left

&VENT SURF_ID='OPEN', XB=-1.0,-1.0,0.0,2.0,0.0,2.0, COLOR='INVISIBLE'/ Vent Min X for MESH
&VENT SURF_ID='OPEN', XB=1.0,1.0,0.0,2.0,0.0,2.0, COLOR='INVISIBLE'/ Vent Max X for MESH
&VENT SURF_ID='OPEN', XB=-1.0,1.0,0.0,0.0,0.0,2.0, COLOR='INVISIBLE'/ Vent Min Y for MESH
&VENT SURF_ID='OPEN', XB=-1.0,1.0,2.0,2.0,0.0,2.0, COLOR='INVISIBLE'/ Vent Max Y for MESH
&VENT SURF_ID='OPEN', XB=-1.0,1.0,0.0,2.0,2.0,2.0, COLOR='INVISIBLE'/ Vent Max Z for MESH
&VENT SURF_ID='OPEN', XB=3.0,3.0,0.0,2.0,0.0,2.0, COLOR='INVISIBLE'/ Vent Max X for MESH02
&VENT SURF_ID='OPEN', XB=1.0,3.0,0.0,0.0,0.0,2.0, COLOR='INVISIBLE'/ Vent Min Y for MESH02
```

&VENT SURF_ID='OPEN', XB=1.0,3.0,2.0,2.0,0.0,2.0, COLOR='INVISIBLE'/ Vent Max Y for MESH02
&VENT SURF_ID='OPEN', XB=1.0,3.0,0.0,2.0,2.0,2.0, COLOR='INVISIBLE'/ Vent Max Z for MESH02
&VENT SURF_ID='OPEN', XB=7.0,7.0,0.0,2.0,0.0,2.0, COLOR='INVISIBLE'/ Vent Max X for MESH0202
&VENT SURF_ID='OPEN', XB=5.0,7.0,0.0,0.0,0.0,2.0, COLOR='INVISIBLE'/ Vent Min Y for MESH0202
&VENT SURF_ID='OPEN', XB=5.0,7.0,2.0,2.0,0.0,2.0, COLOR='INVISIBLE'/ Vent Max Y for MESH0202
&VENT SURF_ID='OPEN', XB=5.0,7.0,0.0,2.0,2.0,2.0, COLOR='INVISIBLE'/ Vent Max Z for MESH0202
&VENT SURF_ID='OPEN', XB=5.0,5.0,0.0,2.0,0.0,2.0, COLOR='INVISIBLE'/ Vent Max X for MESH03
&VENT SURF_ID='OPEN', XB=3.0,5.0,0.0,0.0,0.0,2.0, COLOR='INVISIBLE'/ Vent Min Y for MESH03
&VENT SURF_ID='OPEN', XB=3.0,5.0,2.0,2.0,0.0,2.0, COLOR='INVISIBLE'/ Vent Max Y for MESH03
&VENT SURF_ID='OPEN', XB=3.0,5.0,0.0,2.0,2.0,2.0, COLOR='INVISIBLE'/ Vent Max Z for MESH03
&VENT SURF_ID='OPEN', XB=3.0,3.0,2.0,4.0,0.0,2.0, COLOR='INVISIBLE'/ Vent Max X for MESH0203
&VENT SURF_ID='OPEN', XB=1.0,3.0,4.0,4.0,0.0,2.0, COLOR='INVISIBLE'/ Vent Max Y for MESH0203
&VENT SURF_ID='OPEN', XB=1.0,3.0,2.0,4.0,2.0,2.0, COLOR='INVISIBLE'/ Vent Max Z for MESH0203
&VENT SURF_ID='OPEN', XB=-1.0,-1.0,2.0,4.0,0.0,2.0, COLOR='INVISIBLE'/ Vent Min X for MESH04
&VENT SURF_ID='OPEN', XB=1.0,1.0,2.0,4.0,0.0,2.0, COLOR='INVISIBLE'/ Vent Max X for MESH04
&VENT SURF_ID='OPEN', XB=-1.0,1.0,4.0,4.0,0.0,2.0, COLOR='INVISIBLE'/ Vent Max Y for MESH04
&VENT SURF_ID='OPEN', XB=-1.0,1.0,2.0,4.0,2.0,2.0, COLOR='INVISIBLE'/ Vent Max Z for MESH04
&VENT SURF_ID='OPEN', XB=7.0,7.0,2.0,4.0,0.0,2.0, COLOR='INVISIBLE'/ Vent Max X for MESH020202
&VENT SURF_ID='OPEN', XB=5.0,7.0,4.0,4.0,0.0,2.0, COLOR='INVISIBLE'/ Vent Max Y for MESH020202
&VENT SURF_ID='OPEN', XB=5.0,7.0,2.0,4.0,2.0,2.0, COLOR='INVISIBLE'/ Vent Max Z for MESH020202
&VENT SURF_ID='OPEN', XB=5.0,5.0,2.0,4.0,0.0,2.0, COLOR='INVISIBLE'/ Vent Max X for MESH0302
&VENT SURF_ID='OPEN', XB=3.0,5.0,4.0,4.0,0.0,2.0, COLOR='INVISIBLE'/ Vent Max Y for MESH0302
&VENT SURF_ID='OPEN', XB=3.0,5.0,2.0,4.0,2.0,2.0, COLOR='INVISIBLE'/ Vent Max Z for MESH0302
&VENT SURF_ID='OPEN', XB=3.0,3.0,4.0,6.0,0.0,2.0, COLOR='INVISIBLE'/ Vent Max X for MESH0204
&VENT SURF_ID='OPEN', XB=1.0,3.0,6.0,6.0,0.0,2.0, COLOR='INVISIBLE'/ Vent Max Y for MESH0204
&VENT SURF_ID='OPEN', XB=1.0,3.0,4.0,6.0,2.0,2.0, COLOR='INVISIBLE'/ Vent Max Z for MESH0204
&VENT SURF_ID='OPEN', XB=-1.0,-1.0,4.0,6.0,0.0,2.0, COLOR='INVISIBLE'/ Vent Min X for MESH05
&VENT SURF_ID='OPEN', XB=1.0,1.0,4.0,6.0,0.0,2.0, COLOR='INVISIBLE'/ Vent Max X for MESH05
&VENT SURF_ID='OPEN', XB=-1.0,1.0,6.0,6.0,0.0,2.0, COLOR='INVISIBLE'/ Vent Max Y for MESH05
&VENT SURF_ID='OPEN', XB=-1.0,1.0,4.0,6.0,2.0,2.0, COLOR='INVISIBLE'/ Vent Max Z for MESH05
&VENT SURF_ID='OPEN', XB=7.0,7.0,4.0,6.0,0.0,2.0, COLOR='INVISIBLE'/ Vent Max X for MESH020203
&VENT SURF_ID='OPEN', XB=5.0,7.0,6.0,6.0,0.0,2.0, COLOR='INVISIBLE'/ Vent Max Y for MESH020203
&VENT SURF_ID='OPEN', XB=5.0,7.0,4.0,6.0,2.0,2.0, COLOR='INVISIBLE'/ Vent Max Z for MESH020203
&VENT SURF_ID='OPEN', XB=5.0,5.0,4.0,6.0,0.0,2.0, COLOR='INVISIBLE'/ Vent Max X for MESH0303
&VENT SURF_ID='OPEN', XB=3.0,5.0,6.0,6.0,0.0,2.0, COLOR='INVISIBLE'/ Vent Max Y for MESH0303
&VENT SURF_ID='OPEN', XB=3.0,5.0,4.0,6.0,2.0,2.0, COLOR='INVISIBLE'/ Vent Max Z for MESH0303
&VENT SURF_ID='OPEN', XB=3.0,3.0,6.0,8.0,0.0,2.0, COLOR='INVISIBLE'/ Vent Max X for MESH0205
&VENT SURF_ID='OPEN', XB=1.0,3.0,8.0,8.0,0.0,2.0, COLOR='INVISIBLE'/ Vent Max Y for MESH0205
&VENT SURF_ID='OPEN', XB=1.0,3.0,6.0,8.0,2.0,2.0, COLOR='INVISIBLE'/ Vent Max Z for MESH0205
&VENT SURF_ID='OPEN', XB=-1.0,-1.0,6.0,8.0,0.0,2.0, COLOR='INVISIBLE'/ Vent Min X for MESH06
&VENT SURF_ID='OPEN', XB=1.0,1.0,6.0,8.0,0.0,2.0, COLOR='INVISIBLE'/ Vent Max X for MESH06
&VENT SURF_ID='OPEN', XB=-1.0,1.0,8.0,8.0,0.0,2.0, COLOR='INVISIBLE'/ Vent Max Y for MESH06
&VENT SURF_ID='OPEN', XB=-1.0,1.0,6.0,8.0,2.0,2.0, COLOR='INVISIBLE'/ Vent Max Z for MESH06
&VENT SURF_ID='OPEN', XB=7.0,7.0,6.0,8.0,0.0,2.0, COLOR='INVISIBLE'/ Vent Max X for MESH020204
&VENT SURF_ID='OPEN', XB=5.0,7.0,8.0,8.0,0.0,2.0, COLOR='INVISIBLE'/ Vent Max Y for MESH020204
&VENT SURF_ID='OPEN', XB=5.0,7.0,6.0,8.0,2.0,2.0, COLOR='INVISIBLE'/ Vent Max Z for MESH020204

&VENT SURF_ID='OPEN', XB=5.0,5.0,6.0,8.0,0.0,2.0, COLOR='INVISIBLE'/ Vent Max X for MESH0304
&VENT SURF_ID='OPEN', XB=3.0,5.0,8.0,8.0,0.0,2.0, COLOR='INVISIBLE'/ Vent Max Y for MESH0304
&VENT SURF_ID='OPEN', XB=3.0,5.0,6.0,8.0,2.0,2.0, COLOR='INVISIBLE'/ Vent Max Z for MESH0304
&VENT SURF_ID='OPEN', XB=3.0,3.0,0.0,2.0,2.0,4.0, COLOR='INVISIBLE'/ Vent Max X for MESH0206
&VENT SURF_ID='OPEN', XB=1.0,3.0,0.0,0.0,2.0,4.0, COLOR='INVISIBLE'/ Vent Min Y for MESH0206
&VENT SURF_ID='OPEN', XB=1.0,3.0,2.0,2.0,2.0,4.0, COLOR='INVISIBLE'/ Vent Max Y for MESH0206
&VENT SURF_ID='OPEN', XB=1.0,3.0,0.0,2.0,4.0,4.0, COLOR='INVISIBLE'/ Vent Max Z for MESH0206
&VENT SURF_ID='OPEN', XB=-1.0,-1.0,0.0,2.0,2.0,4.0, COLOR='INVISIBLE'/ Vent Min X for MESH07
&VENT SURF_ID='OPEN', XB=1.0,1.0,0.0,2.0,2.0,4.0, COLOR='INVISIBLE'/ Vent Max X for MESH07
&VENT SURF_ID='OPEN', XB=-1.0,1.0,0.0,0.0,2.0,4.0, COLOR='INVISIBLE'/ Vent Min Y for MESH07
&VENT SURF_ID='OPEN', XB=-1.0,1.0,2.0,2.0,2.0,4.0, COLOR='INVISIBLE'/ Vent Max Y for MESH07
&VENT SURF_ID='OPEN', XB=-1.0,1.0,0.0,2.0,4.0,4.0, COLOR='INVISIBLE'/ Vent Max Z for MESH07
&VENT SURF_ID='OPEN', XB=7.0,7.0,0.0,2.0,2.0,4.0, COLOR='INVISIBLE'/ Vent Max X for MESH020205
&VENT SURF_ID='OPEN', XB=5.0,7.0,0.0,0.0,2.0,4.0, COLOR='INVISIBLE'/ Vent Min Y for MESH020205
&VENT SURF_ID='OPEN', XB=5.0,7.0,2.0,2.0,2.0,4.0, COLOR='INVISIBLE'/ Vent Max Y for MESH020205
&VENT SURF_ID='OPEN', XB=5.0,7.0,0.0,2.0,4.0,4.0, COLOR='INVISIBLE'/ Vent Max Z for MESH020205
&VENT SURF_ID='OPEN', XB=5.0,5.0,0.0,2.0,2.0,4.0, COLOR='INVISIBLE'/ Vent Max X for MESH0305
&VENT SURF_ID='OPEN', XB=3.0,5.0,0.0,0.0,2.0,4.0, COLOR='INVISIBLE'/ Vent Min Y for MESH0305
&VENT SURF_ID='OPEN', XB=3.0,5.0,2.0,2.0,2.0,4.0, COLOR='INVISIBLE'/ Vent Max Y for MESH0305
&VENT SURF_ID='OPEN', XB=3.0,5.0,0.0,2.0,4.0,4.0, COLOR='INVISIBLE'/ Vent Max Z for MESH0305
&VENT SURF_ID='OPEN', XB=3.0,3.0,2.0,4.0,2.0,4.0, COLOR='INVISIBLE'/ Vent Max X for MESH020302
&VENT SURF_ID='OPEN', XB=1.0,3.0,4.0,4.0,2.0,4.0, COLOR='INVISIBLE'/ Vent Max Y for MESH020302
&VENT SURF_ID='OPEN', XB=1.0,3.0,2.0,4.0,4.0,4.0, COLOR='INVISIBLE'/ Vent Max Z for MESH020302
&VENT SURF_ID='OPEN', XB=-1.0,-1.0,2.0,4.0,2.0,4.0, COLOR='INVISIBLE'/ Vent Min X for MESH0402
&VENT SURF_ID='OPEN', XB=1.0,1.0,2.0,4.0,2.0,4.0, COLOR='INVISIBLE'/ Vent Max X for MESH0402
&VENT SURF_ID='OPEN', XB=-1.0,1.0,4.0,4.0,2.0,4.0, COLOR='INVISIBLE'/ Vent Max Y for MESH0402
&VENT SURF_ID='OPEN', XB=-1.0,1.0,2.0,4.0,4.0,4.0, COLOR='INVISIBLE'/ Vent Max Z for MESH0402
&VENT SURF_ID='OPEN', XB=7.0,7.0,2.0,4.0,2.0,4.0, COLOR='INVISIBLE'/ Vent Max X for MESH02020202
&VENT SURF_ID='OPEN', XB=5.0,7.0,4.0,4.0,2.0,4.0, COLOR='INVISIBLE'/ Vent Max Y for MESH02020202
&VENT SURF_ID='OPEN', XB=5.0,7.0,2.0,4.0,4.0,4.0, COLOR='INVISIBLE'/ Vent Max Z for MESH02020202
&VENT SURF_ID='OPEN', XB=5.0,5.0,2.0,4.0,2.0,4.0, COLOR='INVISIBLE'/ Vent Max X for MESH030202
&VENT SURF_ID='OPEN', XB=3.0,5.0,4.0,4.0,2.0,4.0, COLOR='INVISIBLE'/ Vent Max Y for MESH030202
&VENT SURF_ID='OPEN', XB=3.0,5.0,2.0,4.0,4.0,4.0, COLOR='INVISIBLE'/ Vent Max Z for MESH030202
&VENT SURF_ID='OPEN', XB=3.0,3.0,4.0,6.0,2.0,4.0, COLOR='INVISIBLE'/ Vent Max X for MESH020402
&VENT SURF_ID='OPEN', XB=1.0,3.0,6.0,6.0,2.0,4.0, COLOR='INVISIBLE'/ Vent Max Y for MESH020402
&VENT SURF_ID='OPEN', XB=1.0,3.0,4.0,6.0,4.0,4.0, COLOR='INVISIBLE'/ Vent Max Z for MESH020402
&VENT SURF_ID='OPEN', XB=-1.0,-1.0,4.0,6.0,2.0,4.0, COLOR='INVISIBLE'/ Vent Min X for MESH0502
&VENT SURF_ID='OPEN', XB=1.0,1.0,4.0,6.0,2.0,4.0, COLOR='INVISIBLE'/ Vent Max X for MESH0502
&VENT SURF_ID='OPEN', XB=-1.0,1.0,6.0,6.0,2.0,4.0, COLOR='INVISIBLE'/ Vent Max Y for MESH0502
&VENT SURF_ID='OPEN', XB=-1.0,1.0,4.0,6.0,4.0,4.0, COLOR='INVISIBLE'/ Vent Max Z for MESH0502
&VENT SURF_ID='OPEN', XB=7.0,7.0,4.0,6.0,2.0,4.0, COLOR='INVISIBLE'/ Vent Max X for MESH02020302
&VENT SURF_ID='OPEN', XB=5.0,7.0,6.0,6.0,2.0,4.0, COLOR='INVISIBLE'/ Vent Max Y for MESH02020302
&VENT SURF_ID='OPEN', XB=5.0,7.0,4.0,6.0,4.0,4.0, COLOR='INVISIBLE'/ Vent Max Z for MESH02020302
&VENT SURF_ID='OPEN', XB=5.0,5.0,4.0,6.0,2.0,4.0, COLOR='INVISIBLE'/ Vent Max X for MESH030302
&VENT SURF_ID='OPEN', XB=3.0,5.0,6.0,6.0,2.0,4.0, COLOR='INVISIBLE'/ Vent Max Y for MESH030302
&VENT SURF_ID='OPEN', XB=3.0,5.0,4.0,6.0,4.0,4.0, COLOR='INVISIBLE'/ Vent Max Z for MESH030302

```
&VENT SURF_ID='OPEN', XB=3.0,3.0,6.0,8.0,2.0,4.0, COLOR='INVISIBLE'/ Vent Max X for MESH020502
&VENT SURF_ID='OPEN', XB=1.0,3.0,8.0,8.0,2.0,4.0, COLOR='INVISIBLE'/ Vent Max Y for MESH020502
&VENT SURF_ID='OPEN', XB=1.0,3.0,6.0,8.0,4.0,4.0, COLOR='INVISIBLE'/ Vent Max Z for MESH020502
&VENT SURF_ID='OPEN', XB=-1.0,-1.0,6.0,8.0,2.0,4.0, COLOR='INVISIBLE'/ Vent Min X for MESH0602
&VENT SURF_ID='OPEN', XB=1.0,1.0,6.0,8.0,2.0,4.0, COLOR='INVISIBLE'/ Vent Max X for MESH0602
&VENT SURF_ID='OPEN', XB=-1.0,1.0,8.0,8.0,2.0,4.0, COLOR='INVISIBLE'/ Vent Max Y for MESH0602
&VENT SURF_ID='OPEN', XB=-1.0,1.0,6.0,8.0,4.0,4.0, COLOR='INVISIBLE'/ Vent Max Z for MESH0602
&VENT SURF_ID='OPEN', XB=7.0,7.0,6.0,8.0,2.0,4.0, COLOR='INVISIBLE'/ Vent Max X for MESH02020402
&VENT SURF_ID='OPEN', XB=5.0,7.0,8.0,8.0,2.0,4.0, COLOR='INVISIBLE'/ Vent Max Y for MESH02020402
&VENT SURF_ID='OPEN', XB=5.0,7.0,6.0,8.0,4.0,4.0, COLOR='INVISIBLE'/ Vent Max Z for MESH02020402
&VENT SURF_ID='OPEN', XB=5.0,5.0,6.0,8.0,2.0,4.0, COLOR='INVISIBLE'/ Vent Max X for MESH030402
&VENT SURF_ID='OPEN', XB=3.0,5.0,8.0,8.0,2.0,4.0, COLOR='INVISIBLE'/ Vent Max Y for MESH030402
&VENT SURF_ID='OPEN', XB=3.0,5.0,6.0,8.0,4.0,4.0, COLOR='INVISIBLE'/ Vent Max Z for MESH030402
&VENT SURF_ID='Burner', XB=1.02,1.782,1.02,1.782,0.54,0.54/ Vent

&SLCF QUANTITY='TEMPERATURE', PBY=5.25/
&SLCF QUANTITY='TEMPERATURE', PBX=3.15/
&SLCF QUANTITY='VELOCITY', VECTOR=.TRUE., PBY=5.25/
&SLCF QUANTITY='VELOCITY', VECTOR=.TRUE., PBX=3.15/
&SLCF QUANTITY='PRESSURE', PBX=3.15/
&SLCF QUANTITY='PRESSURE', PBY=5.25/
&SLCF QUANTITY='VELOCITY', VECTOR=.TRUE., PBZ=2.5/


&TAIL /
```

EX15_20_10cmGrid.fds

Generated by PyroSim - Version 2012.1.0605

Aug 23, 2012 3:05:22 PM

```
&HEAD CHID='EX15_20_10cmGrid'/
&TIME T_END=4334.0/
&DUMP RENDER_FILE='EX15_20_10cmGrid.ge1', DT_RESTART=300.0, PLOT3D_QUANTITY(1:4)='OPTICAL
DENSITY','PRESSURE','TEMPERATURE','VELOCITY'/

&MESH ID='MESH', IJK=20,20,20, XB=-1.0,1.0,0.0,2.0,0.0,2.0/
&MESH ID='MESH02', IJK=20,20,20, XB=1.0,3.0,0.0,2.0,0.0,2.0/
&MESH ID='MESH0202', IJK=20,20,20, XB=5.0,7.0,0.0,2.0,0.0,2.0/
&MESH ID='MESH03', IJK=20,20,20, XB=3.0,5.0,0.0,2.0,0.0,2.0/
&MESH ID='MESH0203', IJK=20,20,20, XB=1.0,3.0,2.0,4.0,0.0,2.0/
&MESH ID='MESH04', IJK=20,20,20, XB=-1.0,1.0,2.0,4.0,0.0,2.0/
&MESH ID='MESH020202', IJK=20,20,20, XB=5.0,7.0,2.0,4.0,0.0,2.0/
&MESH ID='MESH0302', IJK=20,20,20, XB=3.0,5.0,2.0,4.0,0.0,2.0/
&MESH ID='MESH0204', IJK=20,20,20, XB=1.0,3.0,4.0,6.0,0.0,2.0/
&MESH ID='MESH05', IJK=20,20,20, XB=-1.0,1.0,4.0,6.0,0.0,2.0/
&MESH ID='MESH020203', IJK=20,20,20, XB=5.0,7.0,4.0,6.0,0.0,2.0/
&MESH ID='MESH0303', IJK=20,20,20, XB=3.0,5.0,4.0,6.0,0.0,2.0/
&MESH ID='MESH0205', IJK=20,20,20, XB=1.0,3.0,6.0,8.0,0.0,2.0/
&MESH ID='MESH06', IJK=20,20,20, XB=-1.0,1.0,6.0,8.0,0.0,2.0/
&MESH ID='MESH020204', IJK=20,20,20, XB=5.0,7.0,6.0,8.0,0.0,2.0/
&MESH ID='MESH0304', IJK=20,20,20, XB=3.0,5.0,6.0,8.0,0.0,2.0/
&MESH ID='MESH0206', IJK=20,20,20, XB=1.0,3.0,0.0,2.0,2.0,4.0/
&MESH ID='MESH07', IJK=20,20,20, XB=-1.0,1.0,0.0,2.0,2.0,4.0/
&MESH ID='MESH020205', IJK=20,20,20, XB=5.0,7.0,0.0,2.0,2.0,4.0/
&MESH ID='MESH0305', IJK=20,20,20, XB=3.0,5.0,0.0,2.0,2.0,4.0/
&MESH ID='MESH020302', IJK=20,20,20, XB=1.0,3.0,2.0,4.0,2.0,4.0/
&MESH ID='MESH0402', IJK=20,20,20, XB=-1.0,1.0,2.0,4.0,2.0,4.0/
&MESH ID='MESH02020202', IJK=20,20,20, XB=5.0,7.0,2.0,4.0,2.0,4.0/
&MESH ID='MESH030202', IJK=20,20,20, XB=3.0,5.0,2.0,4.0,2.0,4.0/
&MESH ID='MESH020402', IJK=20,20,20, XB=1.0,3.0,4.0,6.0,2.0,4.0/
&MESH ID='MESH0502', IJK=20,20,20, XB=-1.0,1.0,4.0,6.0,2.0,4.0/
&MESH ID='MESH02020302', IJK=20,20,20, XB=5.0,7.0,4.0,6.0,2.0,4.0/
&MESH ID='MESH030302', IJK=20,20,20, XB=3.0,5.0,4.0,6.0,2.0,4.0/
&MESH ID='MESH020502', IJK=20,20,20, XB=1.0,3.0,6.0,8.0,2.0,4.0/
&MESH ID='MESH0602', IJK=20,20,20, XB=-1.0,1.0,6.0,8.0,2.0,4.0/
&MESH ID='MESH02020402', IJK=20,20,20, XB=5.0,7.0,6.0,8.0,2.0,4.0/
&MESH ID='MESH030402', IJK=20,20,20, XB=3.0,5.0,6.0,8.0,2.0,4.0/

&REAC ID='METHANE',
    FYI='Methane Properties',
    C=1.0,
    H=4.0,
```

```
    O=0.0,
    N=0.0/

&RAMP ID='4x8 CTRL_RAMP', T=815.75, F=-1.0/
&RAMP ID='4x8 CTRL_RAMP', T=816.25, F=1.0/
&RAMP ID='4x8 CTRL_RAMP', T=1152.75, F=1.0/
&RAMP ID='4x8 CTRL_RAMP', T=1153.25, F=-1.0/
&RAMP ID='4x8 CTRL_RAMP', T=1935.75, F=-1.0/
&RAMP ID='4x8 CTRL_RAMP', T=1936.25, F=1.0/
&RAMP ID='4x4 CTRL_RAMP', T=452.75, F=-1.0/
&RAMP ID='4x4 CTRL_RAMP', T=453.25, F=1.0/
&RAMP ID='4x4 CTRL_RAMP', T=1152.75, F=1.0/
&RAMP ID='4x4 CTRL_RAMP', T=1153.25, F=-1.0/
&RAMP ID='4x4 CTRL_RAMP', T=1639.75, F=-1.0/
&RAMP ID='4x4 CTRL_RAMP', T=1640.25, F=1.0/
&RAMP ID='4x8 CTRLReverse_RAMP', T=-0.25, F=-1.0/
&RAMP ID='4x8 CTRLReverse_RAMP', T=0.25, F=1.0/
&RAMP ID='4x8 CTRLReverse_RAMP', T=815.75, F=1.0/
&RAMP ID='4x8 CTRLReverse_RAMP', T=816.25, F=-1.0/
&RAMP ID='4x8 CTRLReverse_RAMP', T=1152.75, F=-1.0/
&RAMP ID='4x8 CTRLReverse_RAMP', T=1153.25, F=1.0/
&RAMP ID='4x8 CTRLReverse_RAMP', T=1935.75, F=1.0/
&RAMP ID='4x8 CTRLReverse_RAMP', T=1936.25, F=-1.0/
&DEVC ID='0_TC1_25mmBC', QUANTITY='THERMOCOUPLE', XYZ=3.15,1.9,2.35/
&DEVC ID='10_TC2_610mmBC', QUANTITY='THERMOCOUPLE', XYZ=3.15,6.19,1.8/
&DEVC ID='11_TC2_915mmBC', QUANTITY='THERMOCOUPLE', XYZ=3.15,6.19,1.5/
&DEVC ID='12_TC2_1220mmBC', QUANTITY='THERMOCOUPLE', XYZ=3.15,6.19,1.2/
&DEVC ID='13_TC2_1520mmBC', QUANTITY='THERMOCOUPLE', XYZ=3.15,6.19,0.9/
&DEVC ID='14_TC2_1830mmBC', QUANTITY='THERMOCOUPLE', XYZ=3.15,6.19,0.6/
&DEVC ID='15_TC2_2130mmBC', QUANTITY='THERMOCOUPLE', XYZ=3.15,6.19,0.3/
&DEVC ID='16_Door_TC1', QUANTITY='THERMOCOUPLE', XYZ=5.3,5.25,1.97/
&DEVC ID='17_Door_TC2', QUANTITY='THERMOCOUPLE', XYZ=5.3,5.25,1.8/
&DEVC ID='18_Door_TC3', QUANTITY='THERMOCOUPLE', XYZ=5.3,5.25,1.6/
&DEVC ID='19_Door_TC4', QUANTITY='THERMOCOUPLE', XYZ=5.3,5.25,1.4/
&DEVC ID='1_TC1_305mmBC', QUANTITY='THERMOCOUPLE', XYZ=3.15,1.91,2.08/
&DEVC ID='20_Door_TC5', QUANTITY='THERMOCOUPLE', XYZ=5.3,5.25,1.2/
&DEVC ID='21_Door_TC6', QUANTITY='THERMOCOUPLE', XYZ=5.3,5.25,1.0/
&DEVC ID='22_Door_TC7', QUANTITY='THERMOCOUPLE', XYZ=5.3,5.25,0.8/
&DEVC ID='23_Door_TC8', QUANTITY='THERMOCOUPLE', XYZ=5.3,5.25,0.6/
&DEVC ID='24_Door_TC9', QUANTITY='THERMOCOUPLE', XYZ=5.3,5.25,0.4/
&DEVC ID='25_Door_TC10', QUANTITY='THERMOCOUPLE', XYZ=5.3,5.25,0.2/
&DEVC ID='26_Door_BDP1', QUANTITY='U-VELOCITY', XYZ=5.3,5.25,1.97, ORIENTATION=1.0,0.0,0.0/
&DEVC ID='27_Door_BDP2', QUANTITY='U-VELOCITY', XYZ=5.3,5.25,1.8, ORIENTATION=1.0,0.0,0.0/
&DEVC ID='28_Door_BDP3', QUANTITY='U-VELOCITY', XYZ=5.3,5.25,1.6, ORIENTATION=1.0,0.0,0.0/
&DEVC ID='29_Door_BDP4', QUANTITY='U-VELOCITY', XYZ=5.3,5.25,1.4, ORIENTATION=1.0,0.0,0.0/
&DEVC ID='2_TC1_610mmBC', QUANTITY='THERMOCOUPLE', XYZ=3.15,1.91,1.78/
```

&DEVC ID='30_Door_BDP5', QUANTITY='U-VELOCITY', XYZ=5.3,5.25,1.2, ORIENTATION=1.0,0.0,0.0/
&DEVC ID='31_Door_BDP6', QUANTITY='U-VELOCITY', XYZ=5.3,5.25,1.0, ORIENTATION=1.0,0.0,0.0/
&DEVC ID='32_Door_BDP7', QUANTITY='U-VELOCITY', XYZ=5.3,5.25,0.8, ORIENTATION=1.0,0.0,0.0/
&DEVC ID='33_Door_BDP8', QUANTITY='U-VELOCITY', XYZ=5.3,5.25,0.6, ORIENTATION=1.0,0.0,0.0/
&DEVC ID='34_Door_BDP9', QUANTITY='U-VELOCITY', XYZ=5.3,5.25,0.4, ORIENTATION=1.0,0.0,0.0/
&DEVC ID='35_Door_BDP10', QUANTITY='U-VELOCITY', XYZ=5.3,5.25,0.2, ORIENTATION=1.0,0.0,0.0/
&DEVC ID='36_VENT_TC1', QUANTITY='THERMOCOUPLE', XYZ=2.7,4.65,2.73/
&DEVC ID='37_VENT_TC2', QUANTITY='THERMOCOUPLE', XYZ=3.15,4.65,2.73/
&DEVC ID='38_VENT_TC3', QUANTITY='THERMOCOUPLE', XYZ=3.15,4.2,2.73/
&DEVC ID='39_VENT_TC4', QUANTITY='THERMOCOUPLE', XYZ=2.7,3.45,2.73/
&DEVC ID='3_TC1_915mmBC', QUANTITY='THERMOCOUPLE', XYZ=3.15,1.91,1.48/
&DEVC ID='40_VENT_TC5', QUANTITY='THERMOCOUPLE', XYZ=3.15,3.45,2.73/
&DEVC ID='41_VENT_TC6', QUANTITY='THERMOCOUPLE', XYZ=3.15,3.9,2.73/
&DEVC ID='42_VENT_TC7', QUANTITY='THERMOCOUPLE', XYZ=3.15,5.1,2.73/
&DEVC ID='43_VENT_TC8', QUANTITY='THERMOCOUPLE', XYZ=3.15,3.0,2.73/
&DEVC ID='44_VENT_TC9', QUANTITY='THERMOCOUPLE', XYZ=3.6,4.65,2.73/
&DEVC ID='45_VENT_TC10', QUANTITY='THERMOCOUPLE', XYZ=3.6,3.45,2.73/
&DEVC ID='46_Vent_BDP1', QUANTITY='W-VELOCITY', XYZ=2.7,4.65,2.73, ORIENTATION=0.0,0.0,1.0/
&DEVC ID='47_Vent_BDP2', QUANTITY='W-VELOCITY', XYZ=3.15,4.65,2.73, ORIENTATION=0.0,0.0,1.0/
&DEVC ID='48_Vent_BDP3', QUANTITY='W-VELOCITY', XYZ=3.15,4.2,2.73, ORIENTATION=0.0,0.0,1.0/
&DEVC ID='49_Vent_BDP4', QUANTITY='W-VELOCITY', XYZ=2.7,3.45,2.73, ORIENTATION=0.0,0.0,1.0/
&DEVC ID='4_TC1_1220mmBC', QUANTITY='THERMOCOUPLE', XYZ=3.15,1.91,1.18/
&DEVC ID='50_Vent_BDP5', QUANTITY='W-VELOCITY', XYZ=3.15,3.45,2.73, ORIENTATION=0.0,0.0,1.0/
&DEVC ID='51_Vent_BDP6', QUANTITY='W-VELOCITY', XYZ=3.15,3.9,2.73, ORIENTATION=0.0,0.0,1.0/
&DEVC ID='52_Vent_BDP7', QUANTITY='W-VELOCITY', XYZ=3.15,5.1,2.73, ORIENTATION=0.0,0.0,1.0/
&DEVC ID='53_Vent_BDP8', QUANTITY='W-VELOCITY', XYZ=3.15,3.0,2.73, ORIENTATION=0.0,0.0,1.0/
&DEVC ID='54_Vent_BDP9', QUANTITY='W-VELOCITY', XYZ=3.6,4.65,2.73, ORIENTATION=0.0,0.0,1.0/
&DEVC ID='55_Vent_BDP10', QUANTITY='W-VELOCITY', XYZ=3.6,3.45,2.73, ORIENTATION=0.0,0.0,1.0/
&DEVC ID='56_HF_B3FTCEIL', QUANTITY='GAUGE HEAT FLUX', XYZ=3.15,1.6,0.93, IOR=3/
&DEVC ID='58_HF_BFLCEIL', QUANTITY='GAUGE HEAT FLUX', XYZ=3.15,2.05,0.17, IOR=3/
&DEVC ID='59_HF_DR3FTCEIL', QUANTITY='GAUGE HEAT FLUX', XYZ=3.15,6.49,0.95, IOR=3/
&DEVC ID='5_TC1_1520mmBC', QUANTITY='THERMOCOUPLE', XYZ=3.15,1.91,0.88/
&DEVC ID='61_HF_FLCEIL', QUANTITY='GAUGE HEAT FLUX', XYZ=3.15,6.04,0.17, IOR=3/
&DEVC ID='6_TC1_1830mmBC', QUANTITY='THERMOCOUPLE', XYZ=3.15,1.91,0.58/
&DEVC ID='7_TC1_2130mmBC', QUANTITY='THERMOCOUPLE', XYZ=3.15,1.91,0.28/
&DEVC ID='8_TC2_25mmBC', QUANTITY='THERMOCOUPLE', XYZ=3.15,6.19,2.37/
&DEVC ID='9_TC2_305mmBC', QUANTITY='THERMOCOUPLE', XYZ=3.15,6.19,2.1/
&DEVC ID='HRR', QUANTITY='HRR', XB=-1.0,7.0,0.0,8.0,0.0,4.0/
&DEVC ID='SMOKE LAYER HT DOORWAY', QUANTITY='LAYER HEIGHT', XB=5.3,5.3,5.25,5.25,0.0,2.0/
&DEVC ID='SMOKE LAYER HT FIRE Burner', QUANTITY='LAYER HEIGHT', XB=3.15,3.15,1.91,1.91,0.0,2.4/
&DEVC ID='SMOKE LAYER HT FIRE Door', QUANTITY='LAYER HEIGHT', XB=3.15,3.15,6.19,6.19,0.0,2.4/
&DEVC ID='SMOKE LAYER TEMP Burner', QUANTITY='UPPER TEMPERATURE', XB=3.15,3.15,1.91,1.91,0.0,2.4/
&DEVC ID='SMOKE LAYER TEMP Door', QUANTITY='UPPER TEMPERATURE', XB=3.15,3.15,6.19,6.19,0.0,2.4/
&DEVC ID='TIME', QUANTITY='TIME', XYZ=-1.0,0.0,0.0/
&CTRL ID='4x8 CTRL', FUNCTION_TYPE='CUSTOM', RAMP_ID='4x8 CTRL_RAMP', LATCH=.FALSE., INPUT_ID='TIME'/
&CTRL ID='4x4 CTRL', FUNCTION_TYPE='CUSTOM', RAMP_ID='4x4 CTRL_RAMP', LATCH=.FALSE., INPUT_ID='TIME'/

```
&CTRL ID='4x8 CTRLReverse', FUNCTION_TYPE='CUSTOM', RAMP_ID='4x8 CTRLReverse_RAMP', LATCH=.FALSE.,
INPUT_ID='TIME'/

&MATL ID='Drywall',
    SPECIFIC_HEAT=1.09,
    CONDUCTIVITY=0.16,
    DENSITY=676.0/
&MATL ID='CementBoard',
    SPECIFIC_HEAT=0.84,
    CONDUCTIVITY=0.183,
    DENSITY=923.0/

&SURF ID='Burner',
    COLOR='RED',
    HRRPUA=1735.0,
    RAMP_Q='Burner_RAMP_Q'/
&RAMP ID='Burner_RAMP_Q', T=0.0, F=0.475/
&RAMP ID='Burner_RAMP_Q', T=1152.0, F=0.475/
&RAMP ID='Burner_RAMP_Q', T=1153.0, F=1.0/
&SURF ID='Drywall',
    RGB=146,202,166,
    MATL_ID(1,1)='Drywall',
    MATL_ID(2,1)='Drywall',
    MATL_MASS_FRACTION(1,1)=1.0,
    MATL_MASS_FRACTION(2,1)=1.0,
    THICKNESS(1:2)=0.01,0.01/
&SURF ID='CementBoard',
    RGB=146,202,166,
    MATL_ID(1,1)='CementBoard',
    MATL_MASS_FRACTION(1,1)=1.0,
    THICKNESS(1)=0.016/

&OBST XB=1.02,1.782,1.02,1.782,0.0,0.54, RGB=255,0,51, SURF_ID='INERT'/ Burner
&OBST XB=0.9,5.4,0.9,1.0,0.0,2.4, RGB=255,255,204, SURF_ID='Drywall'/ Bottom Wall (Min X)
&OBST XB=5.3,5.4,0.9,7.2,0.0,2.4, RGB=255,255,204, SURF_ID='Drywall'/ Right Wall (Max Y)
&OBST XB=0.9,5.4,7.1,7.2,0.0,2.4, RGB=255,255,204, SURF_ID='Drywall'/ Top Wall (Max X)
&OBST XB=0.9,1.0,0.9,7.2,0.0,2.4, RGB=255,255,204, SURF_ID='Drywall'/ Left Wall (Min Y)
&OBST XB=0.9,5.4,0.9,7.2,2.4,2.5, RGB=255,255,204, SURF_ID='Drywall'/ Ceiling
&OBST XB=2.55,3.75,2.85,2.86,2.45,3.03, RGB=255,255,204, SURF_ID='Drywall'/ Bottom Wall (Min X)
&OBST XB=3.74,3.75,2.85,5.25,2.45,3.03, RGB=255,255,204, SURF_ID='Drywall'/ Right Wall (Max Y)
&OBST XB=2.55,3.75,5.24,5.25,2.45,3.03, RGB=255,255,204, SURF_ID='Drywall'/ Top Wall (Max X)
&OBST XB=2.55,2.56,2.85,5.25,2.45,3.03, RGB=255,255,204, SURF_ID='Drywall'/ Left Wall (Min Y)
&OBST XB=2.55,3.75,4.05,5.25,3.03,3.04, RGB=255,255,204, SURF_ID='Drywall'/ Left Vent Door
&OBST XB=2.55,3.75,2.85,2.86,3.03,3.13, RGB=255,255,204, SURF_ID='Drywall'/ Bottom Wall (Min X)
&OBST XB=3.74,3.75,2.85,4.05,3.03,3.13, RGB=255,255,204, SURF_ID='Drywall'/ Right Wall (Max Y)
&OBST XB=2.55,2.56,2.85,4.05,3.03,3.13, RGB=255,255,204, SURF_ID='Drywall'/ Left Wall (Min Y)
```

&OBST XB=2.55,3.75,4.04,4.05,3.03,3.13, RGB=255,255,204, SURF_ID='Drywall', CTRL_ID='4x8 CTRLReverse'/ Top Wall (Max X)
&OBST XB=2.55,3.75,2.85,4.05,3.13,3.14, RGB=255,255,204, SURF_ID='Drywall'/ Right Vent Door
&OBST XB=1.0,2.2,1.0,1.02,0.0,2.4, RGB=255,255,204, SURF_ID='CementBoard'/ CementBoardX
&OBST XB=1.0,1.02,1.0,2.2,0.0,2.4, RGB=255,255,204, SURF_ID='CementBoard'/ CementBoardY
&OBST XB=-1.0,7.0,0.0,8.0,0.0,0.02, RGB=255,255,204, SURF_ID='CementBoard'/ Floor
&OBST XB=3.05,3.25,1.95,2.15,0.0,0.17, SURF_ID='INERT'/ HFBaseL1
&OBST XB=3.05,3.25,5.94,6.14,0.0,0.17, SURF_ID='INERT'/ HFBaseR1
&OBST XB=3.05,3.25,1.5,1.7,0.83,0.93, SURF_ID='INERT'/ HFBaseL1
&OBST XB=3.05,3.25,6.39,6.59,0.83,0.95, SURF_ID='INERT'/ HFBaseR1
&OBST XB=0.9,5.4,0.9,7.2,2.38,2.4, RGB=255,255,204, SURF_ID='CementBoard'/ Ceiling Cement
&OBST XB=2.2,5.3,1.0,1.02,0.6,2.4, RGB=255,255,204, SURF_ID='CementBoard'/ CementBoardX2
&OBST XB=1.0,1.02,2.2,3.7,0.6,2.4, RGB=255,255,204, SURF_ID='CementBoard'/ CementBoardY2
&OBST XB=5.28,5.3,1.0,2.2,1.4,2.4, RGB=255,255,204, SURF_ID='CementBoard'/ CementBoardY3

&HOLE XB=5.3,5.4,4.8,5.7,0.0,2.0/ Fire Room Door
&HOLE XB=2.55,3.75,2.85,5.25,2.35,2.5/ 4x8
&HOLE XB=2.55,3.75,4.05,5.25,3.03,3.04, CTRL_ID='4x8 CTRL'/ 4x4Right
&HOLE XB=2.55,3.75,2.85,4.05,3.13,3.14, CTRL_ID='4x4 CTRL'/ 4x4Left

&VENT SURF_ID='OPEN', XB=-1.0,-1.0,0.0,2.0,0.0,2.0, COLOR='INVISIBLE'/ Vent Min X for MESH
&VENT SURF_ID='OPEN', XB=1.0,1.0,0.0,2.0,0.0,2.0, COLOR='INVISIBLE'/ Vent Max X for MESH
&VENT SURF_ID='OPEN', XB=-1.0,1.0,0.0,0.0,0.0,2.0, COLOR='INVISIBLE'/ Vent Min Y for MESH
&VENT SURF_ID='OPEN', XB=-1.0,1.0,2.0,2.0,0.0,2.0, COLOR='INVISIBLE'/ Vent Max Y for MESH
&VENT SURF_ID='OPEN', XB=-1.0,1.0,0.0,2.0,2.0,2.0, COLOR='INVISIBLE'/ Vent Max Z for MESH
&VENT SURF_ID='OPEN', XB=3.0,3.0,0.0,2.0,0.0,2.0, COLOR='INVISIBLE'/ Vent Max X for MESH02
&VENT SURF_ID='OPEN', XB=1.0,3.0,0.0,0.0,0.0,2.0, COLOR='INVISIBLE'/ Vent Min Y for MESH02
&VENT SURF_ID='OPEN', XB=1.0,3.0,2.0,2.0,0.0,2.0, COLOR='INVISIBLE'/ Vent Max Y for MESH02
&VENT SURF_ID='OPEN', XB=1.0,3.0,0.0,2.0,2.0,2.0, COLOR='INVISIBLE'/ Vent Max Z for MESH02
&VENT SURF_ID='OPEN', XB=7.0,7.0,0.0,2.0,0.0,2.0, COLOR='INVISIBLE'/ Vent Max X for MESH0202
&VENT SURF_ID='OPEN', XB=5.0,7.0,0.0,0.0,0.0,2.0, COLOR='INVISIBLE'/ Vent Min Y for MESH0202
&VENT SURF_ID='OPEN', XB=5.0,7.0,2.0,2.0,0.0,2.0, COLOR='INVISIBLE'/ Vent Max Y for MESH0202
&VENT SURF_ID='OPEN', XB=5.0,7.0,0.0,2.0,2.0,2.0, COLOR='INVISIBLE'/ Vent Max Z for MESH0202
&VENT SURF_ID='OPEN', XB=5.0,5.0,0.0,2.0,0.0,2.0, COLOR='INVISIBLE'/ Vent Max X for MESH03
&VENT SURF_ID='OPEN', XB=3.0,5.0,0.0,0.0,0.0,2.0, COLOR='INVISIBLE'/ Vent Min Y for MESH03
&VENT SURF_ID='OPEN', XB=3.0,5.0,2.0,2.0,0.0,2.0, COLOR='INVISIBLE'/ Vent Max Y for MESH03
&VENT SURF_ID='OPEN', XB=3.0,5.0,0.0,2.0,2.0,2.0, COLOR='INVISIBLE'/ Vent Max Z for MESH03
&VENT SURF_ID='OPEN', XB=3.0,3.0,2.0,4.0,0.0,2.0, COLOR='INVISIBLE'/ Vent Max X for MESH0203
&VENT SURF_ID='OPEN', XB=1.0,3.0,4.0,4.0,0.0,2.0, COLOR='INVISIBLE'/ Vent Max Y for MESH0203
&VENT SURF_ID='OPEN', XB=1.0,3.0,2.0,4.0,2.0,2.0, COLOR='INVISIBLE'/ Vent Max Z for MESH0203
&VENT SURF_ID='OPEN', XB=-1.0,-1.0,2.0,4.0,0.0,2.0, COLOR='INVISIBLE'/ Vent Min X for MESH04
&VENT SURF_ID='OPEN', XB=1.0,1.0,2.0,4.0,0.0,2.0, COLOR='INVISIBLE'/ Vent Max X for MESH04
&VENT SURF_ID='OPEN', XB=-1.0,1.0,4.0,4.0,0.0,2.0, COLOR='INVISIBLE'/ Vent Max Y for MESH04
&VENT SURF_ID='OPEN', XB=-1.0,1.0,2.0,4.0,2.0,2.0, COLOR='INVISIBLE'/ Vent Max Z for MESH04
&VENT SURF_ID='OPEN', XB=7.0,7.0,2.0,4.0,0.0,2.0, COLOR='INVISIBLE'/ Vent Max X for MESH020202
&VENT SURF_ID='OPEN', XB=5.0,7.0,4.0,4.0,0.0,2.0, COLOR='INVISIBLE'/ Vent Max Y for MESH020202

&VENT SURF_ID='OPEN', XB=5.0,7.0,2.0,4.0,2.0,2.0, COLOR='INVISIBLE'/ Vent Max Z for MESH020202
&VENT SURF_ID='OPEN', XB=5.0,5.0,2.0,4.0,0.0,2.0, COLOR='INVISIBLE'/ Vent Max X for MESH0302
&VENT SURF_ID='OPEN', XB=3.0,5.0,4.0,4.0,0.0,2.0, COLOR='INVISIBLE'/ Vent Max Y for MESH0302
&VENT SURF_ID='OPEN', XB=3.0,5.0,2.0,4.0,2.0,2.0, COLOR='INVISIBLE'/ Vent Max Z for MESH0302
&VENT SURF_ID='OPEN', XB=3.0,3.0,4.0,6.0,0.0,2.0, COLOR='INVISIBLE'/ Vent Max X for MESH0204
&VENT SURF_ID='OPEN', XB=1.0,3.0,6.0,6.0,0.0,2.0, COLOR='INVISIBLE'/ Vent Max Y for MESH0204
&VENT SURF_ID='OPEN', XB=1.0,3.0,4.0,6.0,2.0,2.0, COLOR='INVISIBLE'/ Vent Max Z for MESH0204
&VENT SURF_ID='OPEN', XB=-1.0,-1.0,4.0,6.0,0.0,2.0, COLOR='INVISIBLE'/ Vent Min X for MESH05
&VENT SURF_ID='OPEN', XB=1.0,1.0,4.0,6.0,0.0,2.0, COLOR='INVISIBLE'/ Vent Max X for MESH05
&VENT SURF_ID='OPEN', XB=-1.0,1.0,6.0,6.0,0.0,2.0, COLOR='INVISIBLE'/ Vent Max Y for MESH05
&VENT SURF_ID='OPEN', XB=-1.0,1.0,4.0,6.0,2.0,2.0, COLOR='INVISIBLE'/ Vent Max Z for MESH05
&VENT SURF_ID='OPEN', XB=7.0,7.0,4.0,6.0,0.0,2.0, COLOR='INVISIBLE'/ Vent Max X for MESH020203
&VENT SURF_ID='OPEN', XB=5.0,7.0,6.0,6.0,0.0,2.0, COLOR='INVISIBLE'/ Vent Max Y for MESH020203
&VENT SURF_ID='OPEN', XB=5.0,7.0,4.0,6.0,2.0,2.0, COLOR='INVISIBLE'/ Vent Max Z for MESH020203
&VENT SURF_ID='OPEN', XB=5.0,5.0,4.0,6.0,0.0,2.0, COLOR='INVISIBLE'/ Vent Max X for MESH0303
&VENT SURF_ID='OPEN', XB=3.0,5.0,6.0,6.0,0.0,2.0, COLOR='INVISIBLE'/ Vent Max Y for MESH0303
&VENT SURF_ID='OPEN', XB=3.0,5.0,4.0,6.0,2.0,2.0, COLOR='INVISIBLE'/ Vent Max Z for MESH0303
&VENT SURF_ID='OPEN', XB=3.0,3.0,6.0,8.0,0.0,2.0, COLOR='INVISIBLE'/ Vent Max X for MESH0205
&VENT SURF_ID='OPEN', XB=1.0,3.0,8.0,8.0,0.0,2.0, COLOR='INVISIBLE'/ Vent Max Y for MESH0205
&VENT SURF_ID='OPEN', XB=1.0,3.0,6.0,8.0,2.0,2.0, COLOR='INVISIBLE'/ Vent Max Z for MESH0205
&VENT SURF_ID='OPEN', XB=-1.0,-1.0,6.0,8.0,0.0,2.0, COLOR='INVISIBLE'/ Vent Min X for MESH06
&VENT SURF_ID='OPEN', XB=1.0,1.0,6.0,8.0,0.0,2.0, COLOR='INVISIBLE'/ Vent Max X for MESH06
&VENT SURF_ID='OPEN', XB=-1.0,1.0,8.0,8.0,0.0,2.0, COLOR='INVISIBLE'/ Vent Max Y for MESH06
&VENT SURF_ID='OPEN', XB=-1.0,1.0,6.0,8.0,2.0,2.0, COLOR='INVISIBLE'/ Vent Max Z for MESH06
&VENT SURF_ID='OPEN', XB=7.0,7.0,6.0,8.0,0.0,2.0, COLOR='INVISIBLE'/ Vent Max X for MESH020204
&VENT SURF_ID='OPEN', XB=5.0,7.0,8.0,8.0,0.0,2.0, COLOR='INVISIBLE'/ Vent Max Y for MESH020204
&VENT SURF_ID='OPEN', XB=5.0,7.0,6.0,8.0,2.0,2.0, COLOR='INVISIBLE'/ Vent Max Z for MESH020204
&VENT SURF_ID='OPEN', XB=5.0,5.0,6.0,8.0,0.0,2.0, COLOR='INVISIBLE'/ Vent Max X for MESH0304
&VENT SURF_ID='OPEN', XB=3.0,5.0,8.0,8.0,0.0,2.0, COLOR='INVISIBLE'/ Vent Max Y for MESH0304
&VENT SURF_ID='OPEN', XB=3.0,5.0,6.0,8.0,2.0,2.0, COLOR='INVISIBLE'/ Vent Max Z for MESH0304
&VENT SURF_ID='OPEN', XB=3.0,3.0,0.0,2.0,2.0,4.0, COLOR='INVISIBLE'/ Vent Max X for MESH0206
&VENT SURF_ID='OPEN', XB=1.0,3.0,0.0,0.0,2.0,4.0, COLOR='INVISIBLE'/ Vent Min Y for MESH0206
&VENT SURF_ID='OPEN', XB=1.0,3.0,2.0,2.0,2.0,4.0, COLOR='INVISIBLE'/ Vent Max Y for MESH0206
&VENT SURF_ID='OPEN', XB=1.0,3.0,0.0,2.0,4.0,4.0, COLOR='INVISIBLE'/ Vent Max Z for MESH0206
&VENT SURF_ID='OPEN', XB=-1.0,-1.0,0.0,2.0,2.0,4.0, COLOR='INVISIBLE'/ Vent Min X for MESH07
&VENT SURF_ID='OPEN', XB=1.0,1.0,0.0,2.0,2.0,4.0, COLOR='INVISIBLE'/ Vent Max X for MESH07
&VENT SURF_ID='OPEN', XB=-1.0,1.0,0.0,0.0,2.0,4.0, COLOR='INVISIBLE'/ Vent Min Y for MESH07
&VENT SURF_ID='OPEN', XB=-1.0,1.0,2.0,2.0,2.0,4.0, COLOR='INVISIBLE'/ Vent Max Y for MESH07
&VENT SURF_ID='OPEN', XB=-1.0,1.0,0.0,2.0,4.0,4.0, COLOR='INVISIBLE'/ Vent Max Z for MESH07
&VENT SURF_ID='OPEN', XB=7.0,7.0,0.0,2.0,2.0,4.0, COLOR='INVISIBLE'/ Vent Max X for MESH020205
&VENT SURF_ID='OPEN', XB=5.0,7.0,0.0,0.0,2.0,4.0, COLOR='INVISIBLE'/ Vent Min Y for MESH020205
&VENT SURF_ID='OPEN', XB=5.0,7.0,2.0,2.0,2.0,4.0, COLOR='INVISIBLE'/ Vent Max Y for MESH020205
&VENT SURF_ID='OPEN', XB=5.0,7.0,0.0,2.0,4.0,4.0, COLOR='INVISIBLE'/ Vent Max Z for MESH020205
&VENT SURF_ID='OPEN', XB=5.0,5.0,0.0,2.0,2.0,4.0, COLOR='INVISIBLE'/ Vent Max X for MESH0305
&VENT SURF_ID='OPEN', XB=3.0,5.0,0.0,0.0,2.0,4.0, COLOR='INVISIBLE'/ Vent Min Y for MESH0305
&VENT SURF_ID='OPEN', XB=3.0,5.0,2.0,2.0,2.0,4.0, COLOR='INVISIBLE'/ Vent Max Y for MESH0305

```
&VENT SURF_ID='OPEN', XB=3.0,5.0,0.0,2.0,4.0,4.0, COLOR='INVISIBLE'/ Vent Max Z for MESH0305
&VENT SURF_ID='OPEN', XB=3.0,3.0,2.0,4.0,2.0,4.0, COLOR='INVISIBLE'/ Vent Max X for MESH020302
&VENT SURF_ID='OPEN', XB=1.0,3.0,4.0,4.0,2.0,4.0, COLOR='INVISIBLE'/ Vent Max Y for MESH020302
&VENT SURF_ID='OPEN', XB=1.0,3.0,2.0,4.0,4.0,4.0, COLOR='INVISIBLE'/ Vent Max Z for MESH020302
&VENT SURF_ID='OPEN', XB=-1.0,-1.0,2.0,4.0,2.0,4.0, COLOR='INVISIBLE'/ Vent Min X for MESH0402
&VENT SURF_ID='OPEN', XB=1.0,1.0,2.0,4.0,2.0,4.0, COLOR='INVISIBLE'/ Vent Max X for MESH0402
&VENT SURF_ID='OPEN', XB=-1.0,1.0,4.0,4.0,2.0,4.0, COLOR='INVISIBLE'/ Vent Max Y for MESH0402
&VENT SURF_ID='OPEN', XB=-1.0,1.0,2.0,4.0,4.0,4.0, COLOR='INVISIBLE'/ Vent Max Z for MESH0402
&VENT SURF_ID='OPEN', XB=7.0,7.0,2.0,4.0,2.0,4.0, COLOR='INVISIBLE'/ Vent Max X for MESH02020202
&VENT SURF_ID='OPEN', XB=5.0,7.0,4.0,4.0,2.0,4.0, COLOR='INVISIBLE'/ Vent Max Y for MESH02020202
&VENT SURF_ID='OPEN', XB=5.0,7.0,2.0,4.0,4.0,4.0, COLOR='INVISIBLE'/ Vent Max Z for MESH02020202
&VENT SURF_ID='OPEN', XB=5.0,5.0,2.0,4.0,2.0,4.0, COLOR='INVISIBLE'/ Vent Max X for MESH030202
&VENT SURF_ID='OPEN', XB=3.0,5.0,4.0,4.0,2.0,4.0, COLOR='INVISIBLE'/ Vent Max Y for MESH030202
&VENT SURF_ID='OPEN', XB=3.0,5.0,2.0,4.0,4.0,4.0, COLOR='INVISIBLE'/ Vent Max Z for MESH030202
&VENT SURF_ID='OPEN', XB=3.0,3.0,4.0,6.0,2.0,4.0, COLOR='INVISIBLE'/ Vent Max X for MESH020402
&VENT SURF_ID='OPEN', XB=1.0,3.0,6.0,6.0,2.0,4.0, COLOR='INVISIBLE'/ Vent Max Y for MESH020402
&VENT SURF_ID='OPEN', XB=1.0,3.0,4.0,6.0,4.0,4.0, COLOR='INVISIBLE'/ Vent Max Z for MESH020402
&VENT SURF_ID='OPEN', XB=-1.0,-1.0,4.0,6.0,2.0,4.0, COLOR='INVISIBLE'/ Vent Min X for MESH0502
&VENT SURF_ID='OPEN', XB=1.0,1.0,4.0,6.0,2.0,4.0, COLOR='INVISIBLE'/ Vent Max X for MESH0502
&VENT SURF_ID='OPEN', XB=-1.0,1.0,6.0,6.0,2.0,4.0, COLOR='INVISIBLE'/ Vent Max Y for MESH0502
&VENT SURF_ID='OPEN', XB=-1.0,1.0,4.0,6.0,4.0,4.0, COLOR='INVISIBLE'/ Vent Max Z for MESH0502
&VENT SURF_ID='OPEN', XB=7.0,7.0,4.0,6.0,2.0,4.0, COLOR='INVISIBLE'/ Vent Max X for MESH02020302
&VENT SURF_ID='OPEN', XB=5.0,7.0,6.0,6.0,2.0,4.0, COLOR='INVISIBLE'/ Vent Max Y for MESH02020302
&VENT SURF_ID='OPEN', XB=5.0,7.0,4.0,6.0,4.0,4.0, COLOR='INVISIBLE'/ Vent Max Z for MESH02020302
&VENT SURF_ID='OPEN', XB=5.0,5.0,4.0,6.0,2.0,4.0, COLOR='INVISIBLE'/ Vent Max X for MESH030302
&VENT SURF_ID='OPEN', XB=3.0,5.0,6.0,6.0,2.0,4.0, COLOR='INVISIBLE'/ Vent Max Y for MESH030302
&VENT SURF_ID='OPEN', XB=3.0,5.0,4.0,6.0,4.0,4.0, COLOR='INVISIBLE'/ Vent Max Z for MESH030302
&VENT SURF_ID='OPEN', XB=3.0,3.0,6.0,8.0,2.0,4.0, COLOR='INVISIBLE'/ Vent Max X for MESH020502
&VENT SURF_ID='OPEN', XB=1.0,3.0,8.0,8.0,2.0,4.0, COLOR='INVISIBLE'/ Vent Max Y for MESH020502
&VENT SURF_ID='OPEN', XB=1.0,3.0,6.0,8.0,4.0,4.0, COLOR='INVISIBLE'/ Vent Max Z for MESH020502
&VENT SURF_ID='OPEN', XB=-1.0,-1.0,6.0,8.0,2.0,4.0, COLOR='INVISIBLE'/ Vent Min X for MESH0602
&VENT SURF_ID='OPEN', XB=1.0,1.0,6.0,8.0,2.0,4.0, COLOR='INVISIBLE'/ Vent Max X for MESH0602
&VENT SURF_ID='OPEN', XB=-1.0,1.0,8.0,8.0,2.0,4.0, COLOR='INVISIBLE'/ Vent Max Y for MESH0602
&VENT SURF_ID='OPEN', XB=-1.0,1.0,6.0,8.0,4.0,4.0, COLOR='INVISIBLE'/ Vent Max Z for MESH0602
&VENT SURF_ID='OPEN', XB=7.0,7.0,6.0,8.0,2.0,4.0, COLOR='INVISIBLE'/ Vent Max X for MESH02020402
&VENT SURF_ID='OPEN', XB=5.0,7.0,8.0,8.0,2.0,4.0, COLOR='INVISIBLE'/ Vent Max Y for MESH02020402
&VENT SURF_ID='OPEN', XB=5.0,7.0,6.0,8.0,4.0,4.0, COLOR='INVISIBLE'/ Vent Max Z for MESH02020402
&VENT SURF_ID='OPEN', XB=5.0,5.0,6.0,8.0,2.0,4.0, COLOR='INVISIBLE'/ Vent Max X for MESH030402
&VENT SURF_ID='OPEN', XB=3.0,5.0,8.0,8.0,2.0,4.0, COLOR='INVISIBLE'/ Vent Max Y for MESH030402
&VENT SURF_ID='OPEN', XB=3.0,5.0,6.0,8.0,4.0,4.0, COLOR='INVISIBLE'/ Vent Max Z for MESH030402
&VENT SURF_ID='Burner', XB=1.02,1.782,1.02,1.782,0.54,0.54/ Vent

&SLCF QUANTITY='TEMPERATURE', PBY=5.25/
&SLCF QUANTITY='TEMPERATURE', PBX=3.15/
&SLCF QUANTITY='VELOCITY', VECTOR=.TRUE., PBY=5.25/
&SLCF QUANTITY='VELOCITY', VECTOR=.TRUE., PBX=3.15/
```

```
&SLCF QUANTITY='PRESSURE', PBX=3.15/
&SLCF QUANTITY='PRESSURE', PBY=5.25/
&SLCF QUANTITY='VELOCITY', VECTOR=.TRUE., PBZ=2.5/


&TAIL /
```

EX21_32_10cmGrid.fds

Generated by PyroSim - Version 2012.1.0605
Aug 23, 2012 3:16:43 PM

```
&HEAD CHID='EX21_32_10cmGrid'/
&TIME T_END=4334.0/
&DUMP RENDER_FILE='EX21_32_10cmGrid.ge1', DT_RESTART=300.0, PLOT3D_QUANTITY(1:4)='OPTICAL
DENSITY','PRESSURE','TEMPERATURE','VELOCITY'/

&MESH ID='MESH', IJK=20,20,20, XB=-1.0,1.0,0.0,2.0,0.0,2.0/
&MESH ID='MESH02', IJK=20,20,20, XB=1.0,3.0,0.0,2.0,0.0,2.0/
&MESH ID='MESH0202', IJK=20,20,20, XB=5.0,7.0,0.0,2.0,0.0,2.0/
&MESH ID='MESH03', IJK=20,20,20, XB=3.0,5.0,0.0,2.0,0.0,2.0/
&MESH ID='MESH0203', IJK=20,20,20, XB=1.0,3.0,2.0,4.0,0.0,2.0/
&MESH ID='MESH04', IJK=20,20,20, XB=-1.0,1.0,2.0,4.0,0.0,2.0/
&MESH ID='MESH020202', IJK=20,20,20, XB=5.0,7.0,2.0,4.0,0.0,2.0/
&MESH ID='MESH0302', IJK=20,20,20, XB=3.0,5.0,2.0,4.0,0.0,2.0/
&MESH ID='MESH0204', IJK=20,20,20, XB=1.0,3.0,4.0,6.0,0.0,2.0/
&MESH ID='MESH05', IJK=20,20,20, XB=-1.0,1.0,4.0,6.0,0.0,2.0/
&MESH ID='MESH020203', IJK=20,20,20, XB=5.0,7.0,4.0,6.0,0.0,2.0/
&MESH ID='MESH0303', IJK=20,20,20, XB=3.0,5.0,4.0,6.0,0.0,2.0/
&MESH ID='MESH0205', IJK=20,20,20, XB=1.0,3.0,6.0,8.0,0.0,2.0/
&MESH ID='MESH06', IJK=20,20,20, XB=-1.0,1.0,6.0,8.0,0.0,2.0/
&MESH ID='MESH020204', IJK=20,20,20, XB=5.0,7.0,6.0,8.0,0.0,2.0/
&MESH ID='MESH0304', IJK=20,20,20, XB=3.0,5.0,6.0,8.0,0.0,2.0/
&MESH ID='MESH0206', IJK=20,20,20, XB=1.0,3.0,0.0,2.0,2.0,4.0/
&MESH ID='MESH07', IJK=20,20,20, XB=-1.0,1.0,0.0,2.0,2.0,4.0/
&MESH ID='MESH020205', IJK=20,20,20, XB=5.0,7.0,0.0,2.0,2.0,4.0/
&MESH ID='MESH0305', IJK=20,20,20, XB=3.0,5.0,0.0,2.0,2.0,4.0/
&MESH ID='MESH020302', IJK=20,20,20, XB=1.0,3.0,2.0,4.0,2.0,4.0/
&MESH ID='MESH0402', IJK=20,20,20, XB=-1.0,1.0,2.0,4.0,2.0,4.0/
&MESH ID='MESH02020202', IJK=20,20,20, XB=5.0,7.0,2.0,4.0,2.0,4.0/
&MESH ID='MESH030202', IJK=20,20,20, XB=3.0,5.0,2.0,4.0,2.0,4.0/
&MESH ID='MESH020402', IJK=20,20,20, XB=1.0,3.0,4.0,6.0,2.0,4.0/
&MESH ID='MESH0502', IJK=20,20,20, XB=-1.0,1.0,4.0,6.0,2.0,4.0/
&MESH ID='MESH02020302', IJK=20,20,20, XB=5.0,7.0,4.0,6.0,2.0,4.0/
&MESH ID='MESH030302', IJK=20,20,20, XB=3.0,5.0,4.0,6.0,2.0,4.0/
&MESH ID='MESH020502', IJK=20,20,20, XB=1.0,3.0,6.0,8.0,2.0,4.0/
&MESH ID='MESH0602', IJK=20,20,20, XB=-1.0,1.0,6.0,8.0,2.0,4.0/
&MESH ID='MESH02020402', IJK=20,20,20, XB=5.0,7.0,6.0,8.0,2.0,4.0/
&MESH ID='MESH030402', IJK=20,20,20, XB=3.0,5.0,6.0,8.0,2.0,4.0/

&REAC ID='METHANE',
    FYI='Methane Properties',
    C=1.0,
    H=4.0,
```

```
    O=0.0,
    N=0.0/

&RAMP ID='4x8 CTRL_RAMP', T=966.75, F=-1.0/
&RAMP ID='4x8 CTRL_RAMP', T=967.25, F=1.0/
&RAMP ID='4x8 CTRL_RAMP', T=1558.75, F=1.0/
&RAMP ID='4x8 CTRL_RAMP', T=1559.25, F=-1.0/
&RAMP ID='4x8 CTRL_RAMP', T=2410.75, F=-1.0/
&RAMP ID='4x8 CTRL_RAMP', T=2411.25, F=1.0/
&RAMP ID='4x8 CTRL_RAMP', T=3398.75, F=1.0/
&RAMP ID='4x8 CTRL_RAMP', T=3399.25, F=-1.0/
&RAMP ID='4x8 CTRL_RAMP', T=3802.75, F=-1.0/
&RAMP ID='4x8 CTRL_RAMP', T=3803.25, F=1.0/
&RAMP ID='4x4 CTRL_RAMP', T=518.75, F=-1.0/
&RAMP ID='4x4 CTRL_RAMP', T=519.25, F=1.0/
&RAMP ID='4x4 CTRL_RAMP', T=1652.75, F=1.0/
&RAMP ID='4x4 CTRL_RAMP', T=1653.25, F=-1.0/
&RAMP ID='4x4 CTRL_RAMP', T=2012.75, F=-1.0/
&RAMP ID='4x4 CTRL_RAMP', T=2013.25, F=1.0/
&RAMP ID='4x4 CTRL_RAMP', T=3398.75, F=1.0/
&RAMP ID='4x4 CTRL_RAMP', T=3399.25, F=-1.0/
&RAMP ID='4x4 CTRL_RAMP', T=3585.75, F=-1.0/
&RAMP ID='4x4 CTRL_RAMP', T=3586.25, F=1.0/
&RAMP ID='4x8 CTRLReverse_RAMP', T=-0.25, F=-1.0/
&RAMP ID='4x8 CTRLReverse_RAMP', T=0.25, F=1.0/
&RAMP ID='4x8 CTRLReverse_RAMP', T=966.75, F=1.0/
&RAMP ID='4x8 CTRLReverse_RAMP', T=967.25, F=-1.0/
&RAMP ID='4x8 CTRLReverse_RAMP', T=1558.75, F=-1.0/
&RAMP ID='4x8 CTRLReverse_RAMP', T=1559.25, F=1.0/
&RAMP ID='4x8 CTRLReverse_RAMP', T=2410.75, F=1.0/
&RAMP ID='4x8 CTRLReverse_RAMP', T=2411.25, F=-1.0/
&RAMP ID='4x8 CTRLReverse_RAMP', T=3398.75, F=-1.0/
&RAMP ID='4x8 CTRLReverse_RAMP', T=3399.25, F=1.0/
&RAMP ID='4x8 CTRLReverse_RAMP', T=3802.75, F=1.0/
&RAMP ID='4x8 CTRLReverse_RAMP', T=3803.25, F=-1.0/
&DEVC ID='0_TC1_25mmBC', QUANTITY='THERMOCOUPLE', XYZ=3.15,1.9,2.35/
&DEVC ID='10_TC2_610mmBC', QUANTITY='THERMOCOUPLE', XYZ=3.15,6.19,1.8/
&DEVC ID='11_TC2_915mmBC', QUANTITY='THERMOCOUPLE', XYZ=3.15,6.19,1.5/
&DEVC ID='12_TC2_1220mmBC', QUANTITY='THERMOCOUPLE', XYZ=3.15,6.19,1.2/
&DEVC ID='13_TC2_1520mmBC', QUANTITY='THERMOCOUPLE', XYZ=3.15,6.19,0.9/
&DEVC ID='14_TC2_1830mmBC', QUANTITY='THERMOCOUPLE', XYZ=3.15,6.19,0.6/
&DEVC ID='15_TC2_2130mmBC', QUANTITY='THERMOCOUPLE', XYZ=3.15,6.19,0.3/
&DEVC ID='16_Door_TC1', QUANTITY='THERMOCOUPLE', XYZ=5.3,5.25,1.97/
&DEVC ID='17_Door_TC2', QUANTITY='THERMOCOUPLE', XYZ=5.3,5.25,1.8/
&DEVC ID='18_Door_TC3', QUANTITY='THERMOCOUPLE', XYZ=5.3,5.25,1.6/
&DEVC ID='19_Door_TC4', QUANTITY='THERMOCOUPLE', XYZ=5.3,5.25,1.4/
```

&DEVC ID='1_TC1_305mmBC', QUANTITY='THERMOCOUPLE', XYZ=3.15,1.91,2.08/
&DEVC ID='20_Door_TC5', QUANTITY='THERMOCOUPLE', XYZ=5.3,5.25,1.2/
&DEVC ID='21_Door_TC6', QUANTITY='THERMOCOUPLE', XYZ=5.3,5.25,1.0/
&DEVC ID='22_Door_TC7', QUANTITY='THERMOCOUPLE', XYZ=5.3,5.25,0.8/
&DEVC ID='23_Door_TC8', QUANTITY='THERMOCOUPLE', XYZ=5.3,5.25,0.6/
&DEVC ID='24_Door_TC9', QUANTITY='THERMOCOUPLE', XYZ=5.3,5.25,0.4/
&DEVC ID='25_Door_TC10', QUANTITY='THERMOCOUPLE', XYZ=5.3,5.25,0.2/
&DEVC ID='26_Door_BDP1', QUANTITY='U-VELOCITY', XYZ=5.3,5.25,1.97, ORIENTATION=1.0,0.0,0.0/
&DEVC ID='27_Door_BDP2', QUANTITY='U-VELOCITY', XYZ=5.3,5.25,1.8, ORIENTATION=1.0,0.0,0.0/
&DEVC ID='28_Door_BDP3', QUANTITY='U-VELOCITY', XYZ=5.3,5.25,1.6, ORIENTATION=1.0,0.0,0.0/
&DEVC ID='29_Door_BDP4', QUANTITY='U-VELOCITY', XYZ=5.3,5.25,1.4, ORIENTATION=1.0,0.0,0.0/
&DEVC ID='2_TC1_610mmBC', QUANTITY='THERMOCOUPLE', XYZ=3.15,1.91,1.78/
&DEVC ID='30_Door_BDP5', QUANTITY='U-VELOCITY', XYZ=5.3,5.25,1.2, ORIENTATION=1.0,0.0,0.0/
&DEVC ID='31_Door_BDP6', QUANTITY='U-VELOCITY', XYZ=5.3,5.25,1.0, ORIENTATION=1.0,0.0,0.0/
&DEVC ID='32_Door_BDP7', QUANTITY='U-VELOCITY', XYZ=5.3,5.25,0.8, ORIENTATION=1.0,0.0,0.0/
&DEVC ID='33_Door_BDP8', QUANTITY='U-VELOCITY', XYZ=5.3,5.25,0.6, ORIENTATION=1.0,0.0,0.0/
&DEVC ID='34_Door_BDP9', QUANTITY='U-VELOCITY', XYZ=5.3,5.25,0.4, ORIENTATION=1.0,0.0,0.0/
&DEVC ID='35_Door_BDP10', QUANTITY='U-VELOCITY', XYZ=5.3,5.25,0.2, ORIENTATION=1.0,0.0,0.0/
&DEVC ID='36_VENT_TC1', QUANTITY='THERMOCOUPLE', XYZ=2.7,4.65,2.73/
&DEVC ID='37_VENT_TC2', QUANTITY='THERMOCOUPLE', XYZ=3.15,4.65,2.73/
&DEVC ID='38_VENT_TC3', QUANTITY='THERMOCOUPLE', XYZ=3.15,4.2,2.73/
&DEVC ID='39_VENT_TC4', QUANTITY='THERMOCOUPLE', XYZ=2.7,3.45,2.73/
&DEVC ID='3_TC1_915mmBC', QUANTITY='THERMOCOUPLE', XYZ=3.15,1.91,1.48/
&DEVC ID='40_VENT_TC5', QUANTITY='THERMOCOUPLE', XYZ=3.15,3.45,2.73/
&DEVC ID='41_VENT_TC6', QUANTITY='THERMOCOUPLE', XYZ=3.15,3.9,2.73/
&DEVC ID='42_VENT_TC7', QUANTITY='THERMOCOUPLE', XYZ=3.15,5.1,2.73/
&DEVC ID='43_VENT_TC8', QUANTITY='THERMOCOUPLE', XYZ=3.15,3.0,2.73/
&DEVC ID='44_VENT_TC9', QUANTITY='THERMOCOUPLE', XYZ=3.6,4.65,2.73/
&DEVC ID='45_VENT_TC10', QUANTITY='THERMOCOUPLE', XYZ=3.6,3.45,2.73/
&DEVC ID='46_Vent_BDP1', QUANTITY='W-VELOCITY', XYZ=2.7,4.65,2.73, ORIENTATION=0.0,0.0,1.0/
&DEVC ID='47_Vent_BDP2', QUANTITY='W-VELOCITY', XYZ=3.15,4.65,2.73, ORIENTATION=0.0,0.0,1.0/
&DEVC ID='48_Vent_BDP3', QUANTITY='W-VELOCITY', XYZ=3.15,4.2,2.73, ORIENTATION=0.0,0.0,1.0/
&DEVC ID='49_Vent_BDP4', QUANTITY='W-VELOCITY', XYZ=2.7,3.45,2.73, ORIENTATION=0.0,0.0,1.0/
&DEVC ID='4_TC1_1220mmBC', QUANTITY='THERMOCOUPLE', XYZ=3.15,1.91,1.18/
&DEVC ID='50_Vent_BDP5', QUANTITY='W-VELOCITY', XYZ=3.15,3.45,2.73, ORIENTATION=0.0,0.0,1.0/
&DEVC ID='51_Vent_BDP6', QUANTITY='W-VELOCITY', XYZ=3.15,3.9,2.73, ORIENTATION=0.0,0.0,1.0/
&DEVC ID='52_Vent_BDP7', QUANTITY='W-VELOCITY', XYZ=3.15,5.1,2.73, ORIENTATION=0.0,0.0,1.0/
&DEVC ID='53_Vent_BDP8', QUANTITY='W-VELOCITY', XYZ=3.15,3.0,2.73, ORIENTATION=0.0,0.0,1.0/
&DEVC ID='54_Vent_BDP9', QUANTITY='W-VELOCITY', XYZ=3.6,4.65,2.73, ORIENTATION=0.0,0.0,1.0/
&DEVC ID='55_Vent_BDP10', QUANTITY='W-VELOCITY', XYZ=3.6,3.45,2.73, ORIENTATION=0.0,0.0,1.0/
&DEVC ID='56_HF_B3FTCEIL', QUANTITY='GAUGE HEAT FLUX', XYZ=3.15,1.6,0.93, IOR=3/
&DEVC ID='58_HF_BFLCEIL', QUANTITY='GAUGE HEAT FLUX', XYZ=3.15,2.05,0.17, IOR=3/
&DEVC ID='59_HF_DR3FTCEIL', QUANTITY='GAUGE HEAT FLUX', XYZ=3.15,6.49,0.95, IOR=3/
&DEVC ID='5_TC1_1520mmBC', QUANTITY='THERMOCOUPLE', XYZ=3.15,1.91,0.88/
&DEVC ID='61_HF_FLCEIL', QUANTITY='GAUGE HEAT FLUX', XYZ=3.15,6.04,0.17, IOR=3/
&DEVC ID='6_TC1_1830mmBC', QUANTITY='THERMOCOUPLE', XYZ=3.15,1.91,0.58/

```
&DEVC ID='7_TC1_2130mmBC', QUANTITY='THERMOCOUPLE', XYZ=3.15,1.91,0.28/
&DEVC ID='8_TC2_25mmBC', QUANTITY='THERMOCOUPLE', XYZ=3.15,6.19,2.37/
&DEVC ID='9_TC2_305mmBC', QUANTITY='THERMOCOUPLE', XYZ=3.15,6.19,2.1/
&DEVC ID='HRR', QUANTITY='HRR', XB=-1.0,7.0,0.0,8.0,0.0,4.0/
&DEVC ID='SMOKE LAYER HT DOORWAY', QUANTITY='LAYER HEIGHT', XB=5.3,5.3,5.25,5.25,0.0,2.0/
&DEVC ID='SMOKE LAYER HT FIRE Burner', QUANTITY='LAYER HEIGHT', XB=3.15,3.15,1.91,1.91,0.0,2.4/
&DEVC ID='SMOKE LAYER HT FIRE Door', QUANTITY='LAYER HEIGHT', XB=3.15,3.15,6.19,6.19,0.0,2.4/
&DEVC ID='SMOKE LAYER TEMP Burner', QUANTITY='UPPER TEMPERATURE', XB=3.15,3.15,1.91,1.91,0.0,2.4/
&DEVC ID='SMOKE LAYER TEMP Door', QUANTITY='UPPER TEMPERATURE', XB=3.15,3.15,6.19,6.19,0.0,2.4/
&DEVC ID='TIME', QUANTITY='TIME', XYZ=-1.0,0.0,0.0/
&CTRL ID='4x8 CTRL', FUNCTION_TYPE='CUSTOM', RAMP_ID='4x8 CTRL_RAMP', LATCH=.FALSE., INPUT_ID='TIME'/
&CTRL ID='4x4 CTRL', FUNCTION_TYPE='CUSTOM', RAMP_ID='4x4 CTRL_RAMP', LATCH=.FALSE., INPUT_ID='TIME'/
&CTRL ID='4x8 CTRLReverse', FUNCTION_TYPE='CUSTOM', RAMP_ID='4x8 CTRLReverse_RAMP', LATCH=.FALSE.,
INPUT_ID='TIME'/

&MATL ID='Drywall',
    SPECIFIC_HEAT=1.09,
    CONDUCTIVITY=0.16,
    DENSITY=676.0/
&MATL ID='CementBoard',
    SPECIFIC_HEAT=0.84,
    CONDUCTIVITY=0.183,
    DENSITY=923.0/

&SURF ID='Burner',
    COLOR='RED',
    HRRPUA=3788.0,
    RAMP_Q='Burner_RAMP_Q'/
&RAMP ID='Burner_RAMP_Q', T=0.0, F=0.462/
&RAMP ID='Burner_RAMP_Q', T=1324.0, F=0.462/
&RAMP ID='Burner_RAMP_Q', T=1325.0, F=0.215/
&RAMP ID='Burner_RAMP_Q', T=2909.0, F=0.215/
&RAMP ID='Burner_RAMP_Q', T=2910.0, F=1.0/
&SURF ID='Drywall',
    RGB=146,202,166,
    MATL_ID(1,1)='Drywall',
    MATL_ID(2,1)='Drywall',
    MATL_MASS_FRACTION(1,1)=1.0,
    MATL_MASS_FRACTION(2,1)=1.0,
    THICKNESS(1:2)=0.01,0.01/
&SURF ID='CementBoard',
    RGB=146,202,166,
    MATL_ID(1,1)='CementBoard',
    MATL_MASS_FRACTION(1,1)=1.0,
    THICKNESS(1)=0.016/
```

```
&OBST XB=1.02,1.782,1.02,1.782,0.0,0.54, RGB=255,0,51, SURF_ID='INERT'/ Burner
&OBST XB=0.9,5.4,0.9,1.0,0.0,2.4, RGB=255,255,204, SURF_ID='Drywall'/ Bottom Wall (Min X)
&OBST XB=5.3,5.4,0.9,7.2,0.0,2.4, RGB=255,255,204, SURF_ID='Drywall'/ Right Wall (Max Y)
&OBST XB=0.9,5.4,7.1,7.2,0.0,2.4, RGB=255,255,204, SURF_ID='Drywall'/ Top Wall (Max X)
&OBST XB=0.9,1.0,0.9,7.2,0.0,2.4, RGB=255,255,204, SURF_ID='Drywall'/ Left Wall (Min Y)
&OBST XB=0.9,5.4,0.9,7.2,2.4,2.5, RGB=255,255,204, SURF_ID='Drywall'/ Ceiling
&OBST XB=2.55,3.75,2.85,2.86,2.45,3.03, RGB=255,255,204, SURF_ID='Drywall'/ Bottom Wall (Min X)
&OBST XB=3.74,3.75,2.85,5.25,2.45,3.03, RGB=255,255,204, SURF_ID='Drywall'/ Right Wall (Max Y)
&OBST XB=2.55,3.75,5.24,5.25,2.45,3.03, RGB=255,255,204, SURF_ID='Drywall'/ Top Wall (Max X)
&OBST XB=2.55,2.56,2.85,5.25,2.45,3.03, RGB=255,255,204, SURF_ID='Drywall'/ Left Wall (Min Y)
&OBST XB=2.55,3.75,4.05,5.25,3.03,3.04, RGB=255,255,204, SURF_ID='Drywall'/ Left Vent Door
&OBST XB=2.55,3.75,2.85,2.86,3.03,3.13, RGB=255,255,204, SURF_ID='Drywall'/ Bottom Wall (Min X)
&OBST XB=3.74,3.75,2.85,4.05,3.03,3.13, RGB=255,255,204, SURF_ID='Drywall'/ Right Wall (Max Y)
&OBST XB=2.55,2.56,2.85,4.05,3.03,3.13, RGB=255,255,204, SURF_ID='Drywall'/ Left Wall (Min Y)
&OBST XB=2.55,3.75,4.04,4.05,3.03,3.13, RGB=255,255,204, SURF_ID='Drywall', CTRL_ID='4x8 CTRLReverse'/ Top
Wall (Max X)
&OBST XB=2.55,3.75,2.85,4.05,3.13,3.14, RGB=255,255,204, SURF_ID='Drywall'/ Right Vent Door
&OBST XB=1.0,2.2,1.0,1.02,0.0,2.4, RGB=255,255,204, SURF_ID='CementBoard'/ CementBoardX
&OBST XB=1.0,1.02,1.0,2.2,0.0,2.4, RGB=255,255,204, SURF_ID='CementBoard'/ CementBoardY
&OBST XB=-1.0,7.0,0.0,8.0,0.0,0.02, RGB=255,255,204, SURF_ID='CementBoard'/ Floor
&OBST XB=3.05,3.25,1.95,2.15,0.0,0.17, SURF_ID='INERT'/ HFBaseL1
&OBST XB=3.05,3.25,5.94,6.14,0.0,0.17, SURF_ID='INERT'/ HFBaseR1
&OBST XB=3.05,3.25,1.5,1.7,0.83,0.93, SURF_ID='INERT'/ HFBaseL1
&OBST XB=3.05,3.25,6.39,6.59,0.83,0.95, SURF_ID='INERT'/ HFBaseR1
&OBST XB=0.9,5.4,0.9,7.2,2.38,2.4, RGB=255,255,204, SURF_ID='CementBoard'/ Ceiling Cement
&OBST XB=2.2,5.3,1.0,1.02,0.6,2.4, RGB=255,255,204, SURF_ID='CementBoard'/ CementBoardX2
&OBST XB=1.0,1.02,2.2,3.7,0.6,2.4, RGB=255,255,204, SURF_ID='CementBoard'/ CementBoardY2
&OBST XB=5.28,5.3,1.0,2.2,1.4,2.4, RGB=255,255,204, SURF_ID='CementBoard'/ CementBoardY3

&HOLE XB=5.3,5.4,4.8,5.7,0.0,2.0/ Fire Room Door
&HOLE XB=2.55,3.75,2.85,5.25,2.35,2.5/ 4x8
&HOLE XB=2.55,3.75,4.05,5.25,3.03,3.04, CTRL_ID='4x8 CTRL'/ 4x4Right
&HOLE XB=2.55,3.75,2.85,4.05,3.13,3.14, CTRL_ID='4x4 CTRL'/ 4x4Left

&VENT SURF_ID='OPEN', XB=-1.0,-1.0,0.0,2.0,0.0,2.0, COLOR='INVISIBLE'/ Vent Min X for MESH
&VENT SURF_ID='OPEN', XB=1.0,1.0,0.0,2.0,0.0,2.0, COLOR='INVISIBLE'/ Vent Max X for MESH
&VENT SURF_ID='OPEN', XB=-1.0,1.0,0.0,0.0,0.0,2.0, COLOR='INVISIBLE'/ Vent Min Y for MESH
&VENT SURF_ID='OPEN', XB=-1.0,1.0,2.0,2.0,0.0,2.0, COLOR='INVISIBLE'/ Vent Max Y for MESH
&VENT SURF_ID='OPEN', XB=-1.0,1.0,0.0,2.0,2.0,2.0, COLOR='INVISIBLE'/ Vent Max Z for MESH
&VENT SURF_ID='OPEN', XB=3.0,3.0,0.0,2.0,0.0,2.0, COLOR='INVISIBLE'/ Vent Max X for MESH02
&VENT SURF_ID='OPEN', XB=1.0,3.0,0.0,0.0,0.0,2.0, COLOR='INVISIBLE'/ Vent Min Y for MESH02
&VENT SURF_ID='OPEN', XB=1.0,3.0,2.0,2.0,0.0,2.0, COLOR='INVISIBLE'/ Vent Max Y for MESH02
&VENT SURF_ID='OPEN', XB=1.0,3.0,0.0,2.0,2.0,2.0, COLOR='INVISIBLE'/ Vent Max Z for MESH02
&VENT SURF_ID='OPEN', XB=7.0,7.0,0.0,2.0,0.0,2.0, COLOR='INVISIBLE'/ Vent Max X for MESH0202
&VENT SURF_ID='OPEN', XB=5.0,7.0,0.0,0.0,0.0,2.0, COLOR='INVISIBLE'/ Vent Min Y for MESH0202
&VENT SURF_ID='OPEN', XB=5.0,7.0,2.0,2.0,0.0,2.0, COLOR='INVISIBLE'/ Vent Max Y for MESH0202
```

&VENT SURF_ID='OPEN', XB=5.0,7.0,0.0,2.0,2.0,2.0, COLOR='INVISIBLE'/ Vent Max Z for MESH0202
&VENT SURF_ID='OPEN', XB=5.0,5.0,0.0,2.0,0.0,2.0, COLOR='INVISIBLE'/ Vent Max X for MESH03
&VENT SURF_ID='OPEN', XB=3.0,5.0,0.0,0.0,0.0,2.0, COLOR='INVISIBLE'/ Vent Min Y for MESH03
&VENT SURF_ID='OPEN', XB=3.0,5.0,2.0,2.0,0.0,2.0, COLOR='INVISIBLE'/ Vent Max Y for MESH03
&VENT SURF_ID='OPEN', XB=3.0,5.0,0.0,2.0,2.0,2.0, COLOR='INVISIBLE'/ Vent Max Z for MESH03
&VENT SURF_ID='OPEN', XB=3.0,3.0,2.0,4.0,0.0,2.0, COLOR='INVISIBLE'/ Vent Max X for MESH0203
&VENT SURF_ID='OPEN', XB=1.0,3.0,4.0,4.0,0.0,2.0, COLOR='INVISIBLE'/ Vent Max Y for MESH0203
&VENT SURF_ID='OPEN', XB=1.0,3.0,2.0,4.0,2.0,2.0, COLOR='INVISIBLE'/ Vent Max Z for MESH0203
&VENT SURF_ID='OPEN', XB=-1.0,-1.0,2.0,4.0,0.0,2.0, COLOR='INVISIBLE'/ Vent Min X for MESH04
&VENT SURF_ID='OPEN', XB=1.0,1.0,2.0,4.0,0.0,2.0, COLOR='INVISIBLE'/ Vent Max X for MESH04
&VENT SURF_ID='OPEN', XB=-1.0,1.0,4.0,4.0,0.0,2.0, COLOR='INVISIBLE'/ Vent Max Y for MESH04
&VENT SURF_ID='OPEN', XB=-1.0,1.0,2.0,4.0,2.0,2.0, COLOR='INVISIBLE'/ Vent Max Z for MESH04
&VENT SURF_ID='OPEN', XB=7.0,7.0,2.0,4.0,0.0,2.0, COLOR='INVISIBLE'/ Vent Max X for MESH020202
&VENT SURF_ID='OPEN', XB=5.0,7.0,4.0,4.0,0.0,2.0, COLOR='INVISIBLE'/ Vent Max Y for MESH020202
&VENT SURF_ID='OPEN', XB=5.0,7.0,2.0,4.0,2.0,2.0, COLOR='INVISIBLE'/ Vent Max Z for MESH020202
&VENT SURF_ID='OPEN', XB=5.0,5.0,2.0,4.0,0.0,2.0, COLOR='INVISIBLE'/ Vent Max X for MESH0302
&VENT SURF_ID='OPEN', XB=3.0,5.0,4.0,4.0,0.0,2.0, COLOR='INVISIBLE'/ Vent Max Y for MESH0302
&VENT SURF_ID='OPEN', XB=3.0,5.0,2.0,4.0,2.0,2.0, COLOR='INVISIBLE'/ Vent Max Z for MESH0302
&VENT SURF_ID='OPEN', XB=3.0,3.0,4.0,6.0,0.0,2.0, COLOR='INVISIBLE'/ Vent Max X for MESH0204
&VENT SURF_ID='OPEN', XB=1.0,3.0,6.0,6.0,0.0,2.0, COLOR='INVISIBLE'/ Vent Max Y for MESH0204
&VENT SURF_ID='OPEN', XB=1.0,3.0,4.0,6.0,2.0,2.0, COLOR='INVISIBLE'/ Vent Max Z for MESH0204
&VENT SURF_ID='OPEN', XB=-1.0,-1.0,4.0,6.0,0.0,2.0, COLOR='INVISIBLE'/ Vent Min X for MESH05
&VENT SURF_ID='OPEN', XB=1.0,1.0,4.0,6.0,0.0,2.0, COLOR='INVISIBLE'/ Vent Max X for MESH05
&VENT SURF_ID='OPEN', XB=-1.0,1.0,6.0,6.0,0.0,2.0, COLOR='INVISIBLE'/ Vent Max Y for MESH05
&VENT SURF_ID='OPEN', XB=-1.0,1.0,4.0,6.0,2.0,2.0, COLOR='INVISIBLE'/ Vent Max Z for MESH05
&VENT SURF_ID='OPEN', XB=7.0,7.0,4.0,6.0,0.0,2.0, COLOR='INVISIBLE'/ Vent Max X for MESH020203
&VENT SURF_ID='OPEN', XB=5.0,7.0,6.0,6.0,0.0,2.0, COLOR='INVISIBLE'/ Vent Max Y for MESH020203
&VENT SURF_ID='OPEN', XB=5.0,7.0,4.0,6.0,2.0,2.0, COLOR='INVISIBLE'/ Vent Max Z for MESH020203
&VENT SURF_ID='OPEN', XB=5.0,5.0,4.0,6.0,0.0,2.0, COLOR='INVISIBLE'/ Vent Max X for MESH0303
&VENT SURF_ID='OPEN', XB=3.0,5.0,6.0,6.0,0.0,2.0, COLOR='INVISIBLE'/ Vent Max Y for MESH0303
&VENT SURF_ID='OPEN', XB=3.0,5.0,4.0,6.0,2.0,2.0, COLOR='INVISIBLE'/ Vent Max Z for MESH0303
&VENT SURF_ID='OPEN', XB=3.0,3.0,6.0,8.0,0.0,2.0, COLOR='INVISIBLE'/ Vent Max X for MESH0205
&VENT SURF_ID='OPEN', XB=1.0,3.0,8.0,8.0,0.0,2.0, COLOR='INVISIBLE'/ Vent Max Y for MESH0205
&VENT SURF_ID='OPEN', XB=1.0,3.0,6.0,8.0,2.0,2.0, COLOR='INVISIBLE'/ Vent Max Z for MESH0205
&VENT SURF_ID='OPEN', XB=-1.0,-1.0,6.0,8.0,0.0,2.0, COLOR='INVISIBLE'/ Vent Min X for MESH06
&VENT SURF_ID='OPEN', XB=1.0,1.0,6.0,8.0,0.0,2.0, COLOR='INVISIBLE'/ Vent Max X for MESH06
&VENT SURF_ID='OPEN', XB=-1.0,1.0,8.0,8.0,0.0,2.0, COLOR='INVISIBLE'/ Vent Max Y for MESH06
&VENT SURF_ID='OPEN', XB=-1.0,1.0,6.0,8.0,2.0,2.0, COLOR='INVISIBLE'/ Vent Max Z for MESH06
&VENT SURF_ID='OPEN', XB=7.0,7.0,6.0,8.0,0.0,2.0, COLOR='INVISIBLE'/ Vent Max X for MESH020204
&VENT SURF_ID='OPEN', XB=5.0,7.0,8.0,8.0,0.0,2.0, COLOR='INVISIBLE'/ Vent Max Y for MESH020204
&VENT SURF_ID='OPEN', XB=5.0,7.0,6.0,8.0,2.0,2.0, COLOR='INVISIBLE'/ Vent Max Z for MESH020204
&VENT SURF_ID='OPEN', XB=5.0,5.0,6.0,8.0,0.0,2.0, COLOR='INVISIBLE'/ Vent Max X for MESH0304
&VENT SURF_ID='OPEN', XB=3.0,5.0,8.0,8.0,0.0,2.0, COLOR='INVISIBLE'/ Vent Max Y for MESH0304
&VENT SURF_ID='OPEN', XB=3.0,5.0,6.0,8.0,2.0,2.0, COLOR='INVISIBLE'/ Vent Max Z for MESH0304
&VENT SURF_ID='OPEN', XB=3.0,3.0,0.0,2.0,2.0,4.0, COLOR='INVISIBLE'/ Vent Max X for MESH0206
&VENT SURF_ID='OPEN', XB=1.0,3.0,0.0,0.0,2.0,4.0, COLOR='INVISIBLE'/ Vent Min Y for MESH0206

&VENT SURF_ID='OPEN', XB=1.0,3.0,2.0,2.0,2.0,4.0, COLOR='INVISIBLE'/ Vent Max Y for MESH0206
&VENT SURF_ID='OPEN', XB=1.0,3.0,0.0,2.0,4.0,4.0, COLOR='INVISIBLE'/ Vent Max Z for MESH0206
&VENT SURF_ID='OPEN', XB=-1.0,-1.0,0.0,2.0,2.0,4.0, COLOR='INVISIBLE'/ Vent Min X for MESH07
&VENT SURF_ID='OPEN', XB=1.0,1.0,0.0,2.0,2.0,4.0, COLOR='INVISIBLE'/ Vent Max X for MESH07
&VENT SURF_ID='OPEN', XB=-1.0,1.0,0.0,0.0,2.0,4.0, COLOR='INVISIBLE'/ Vent Min Y for MESH07
&VENT SURF_ID='OPEN', XB=-1.0,1.0,2.0,2.0,2.0,4.0, COLOR='INVISIBLE'/ Vent Max Y for MESH07
&VENT SURF_ID='OPEN', XB=-1.0,1.0,0.0,2.0,4.0,4.0, COLOR='INVISIBLE'/ Vent Max Z for MESH07
&VENT SURF_ID='OPEN', XB=7.0,7.0,0.0,2.0,2.0,4.0, COLOR='INVISIBLE'/ Vent Max X for MESH020205
&VENT SURF_ID='OPEN', XB=5.0,7.0,0.0,0.0,2.0,4.0, COLOR='INVISIBLE'/ Vent Min Y for MESH020205
&VENT SURF_ID='OPEN', XB=5.0,7.0,2.0,2.0,2.0,4.0, COLOR='INVISIBLE'/ Vent Max Y for MESH020205
&VENT SURF_ID='OPEN', XB=5.0,7.0,0.0,2.0,4.0,4.0, COLOR='INVISIBLE'/ Vent Max Z for MESH020205
&VENT SURF_ID='OPEN', XB=5.0,5.0,0.0,2.0,2.0,4.0, COLOR='INVISIBLE'/ Vent Max X for MESH0305
&VENT SURF_ID='OPEN', XB=3.0,5.0,0.0,0.0,2.0,4.0, COLOR='INVISIBLE'/ Vent Min Y for MESH0305
&VENT SURF_ID='OPEN', XB=3.0,5.0,2.0,2.0,2.0,4.0, COLOR='INVISIBLE'/ Vent Max Y for MESH0305
&VENT SURF_ID='OPEN', XB=3.0,5.0,0.0,2.0,4.0,4.0, COLOR='INVISIBLE'/ Vent Max Z for MESH0305
&VENT SURF_ID='OPEN', XB=3.0,3.0,2.0,4.0,2.0,4.0, COLOR='INVISIBLE'/ Vent Max X for MESH020302
&VENT SURF_ID='OPEN', XB=1.0,3.0,4.0,4.0,2.0,4.0, COLOR='INVISIBLE'/ Vent Max Y for MESH020302
&VENT SURF_ID='OPEN', XB=1.0,3.0,2.0,4.0,4.0,4.0, COLOR='INVISIBLE'/ Vent Max Z for MESH020302
&VENT SURF_ID='OPEN', XB=-1.0,-1.0,2.0,4.0,2.0,4.0, COLOR='INVISIBLE'/ Vent Min X for MESH0402
&VENT SURF_ID='OPEN', XB=1.0,1.0,2.0,4.0,2.0,4.0, COLOR='INVISIBLE'/ Vent Max X for MESH0402
&VENT SURF_ID='OPEN', XB=-1.0,1.0,4.0,4.0,2.0,4.0, COLOR='INVISIBLE'/ Vent Max Y for MESH0402
&VENT SURF_ID='OPEN', XB=-1.0,1.0,2.0,4.0,4.0,4.0, COLOR='INVISIBLE'/ Vent Max Z for MESH0402
&VENT SURF_ID='OPEN', XB=7.0,7.0,2.0,4.0,2.0,4.0, COLOR='INVISIBLE'/ Vent Max X for MESH02020202
&VENT SURF_ID='OPEN', XB=5.0,7.0,4.0,4.0,2.0,4.0, COLOR='INVISIBLE'/ Vent Max Y for MESH02020202
&VENT SURF_ID='OPEN', XB=5.0,7.0,2.0,4.0,4.0,4.0, COLOR='INVISIBLE'/ Vent Max Z for MESH02020202
&VENT SURF_ID='OPEN', XB=5.0,5.0,2.0,4.0,2.0,4.0, COLOR='INVISIBLE'/ Vent Max X for MESH030202
&VENT SURF_ID='OPEN', XB=3.0,5.0,4.0,4.0,2.0,4.0, COLOR='INVISIBLE'/ Vent Max Y for MESH030202
&VENT SURF_ID='OPEN', XB=3.0,5.0,2.0,4.0,4.0,4.0, COLOR='INVISIBLE'/ Vent Max Z for MESH030202
&VENT SURF_ID='OPEN', XB=3.0,3.0,4.0,6.0,2.0,4.0, COLOR='INVISIBLE'/ Vent Max X for MESH020402
&VENT SURF_ID='OPEN', XB=1.0,3.0,6.0,6.0,2.0,4.0, COLOR='INVISIBLE'/ Vent Max Y for MESH020402
&VENT SURF_ID='OPEN', XB=1.0,3.0,4.0,6.0,4.0,4.0, COLOR='INVISIBLE'/ Vent Max Z for MESH020402
&VENT SURF_ID='OPEN', XB=-1.0,-1.0,4.0,6.0,2.0,4.0, COLOR='INVISIBLE'/ Vent Min X for MESH0502
&VENT SURF_ID='OPEN', XB=1.0,1.0,4.0,6.0,2.0,4.0, COLOR='INVISIBLE'/ Vent Max X for MESH0502
&VENT SURF_ID='OPEN', XB=-1.0,1.0,6.0,6.0,2.0,4.0, COLOR='INVISIBLE'/ Vent Max Y for MESH0502
&VENT SURF_ID='OPEN', XB=-1.0,1.0,4.0,6.0,4.0,4.0, COLOR='INVISIBLE'/ Vent Max Z for MESH0502
&VENT SURF_ID='OPEN', XB=7.0,7.0,4.0,6.0,2.0,4.0, COLOR='INVISIBLE'/ Vent Max X for MESH02020302
&VENT SURF_ID='OPEN', XB=5.0,7.0,6.0,6.0,2.0,4.0, COLOR='INVISIBLE'/ Vent Max Y for MESH02020302
&VENT SURF_ID='OPEN', XB=5.0,7.0,4.0,6.0,4.0,4.0, COLOR='INVISIBLE'/ Vent Max Z for MESH02020302
&VENT SURF_ID='OPEN', XB=5.0,5.0,4.0,6.0,2.0,4.0, COLOR='INVISIBLE'/ Vent Max X for MESH030302
&VENT SURF_ID='OPEN', XB=3.0,5.0,6.0,6.0,2.0,4.0, COLOR='INVISIBLE'/ Vent Max Y for MESH030302
&VENT SURF_ID='OPEN', XB=3.0,5.0,4.0,6.0,4.0,4.0, COLOR='INVISIBLE'/ Vent Max Z for MESH030302
&VENT SURF_ID='OPEN', XB=3.0,3.0,6.0,8.0,2.0,4.0, COLOR='INVISIBLE'/ Vent Max X for MESH020502
&VENT SURF_ID='OPEN', XB=1.0,3.0,8.0,8.0,2.0,4.0, COLOR='INVISIBLE'/ Vent Max Y for MESH020502
&VENT SURF_ID='OPEN', XB=1.0,3.0,6.0,8.0,4.0,4.0, COLOR='INVISIBLE'/ Vent Max Z for MESH020502
&VENT SURF_ID='OPEN', XB=-1.0,-1.0,6.0,8.0,2.0,4.0, COLOR='INVISIBLE'/ Vent Min X for MESH0602
&VENT SURF_ID='OPEN', XB=1.0,1.0,6.0,8.0,2.0,4.0, COLOR='INVISIBLE'/ Vent Max X for MESH0602

```
&VENT SURF_ID='OPEN', XB=-1.0,1.0,8.0,8.0,2.0,4.0, COLOR='INVISIBLE'/ Vent Max Y for MESH0602
&VENT SURF_ID='OPEN', XB=-1.0,1.0,6.0,8.0,4.0,4.0, COLOR='INVISIBLE'/ Vent Max Z for MESH0602
&VENT SURF_ID='OPEN', XB=7.0,7.0,6.0,8.0,2.0,4.0, COLOR='INVISIBLE'/ Vent Max X for MESH02020402
&VENT SURF_ID='OPEN', XB=5.0,7.0,8.0,8.0,2.0,4.0, COLOR='INVISIBLE'/ Vent Max Y for MESH02020402
&VENT SURF_ID='OPEN', XB=5.0,7.0,6.0,8.0,4.0,4.0, COLOR='INVISIBLE'/ Vent Max Z for MESH02020402
&VENT SURF_ID='OPEN', XB=5.0,5.0,6.0,8.0,2.0,4.0, COLOR='INVISIBLE'/ Vent Max X for MESH030402
&VENT SURF_ID='OPEN', XB=3.0,5.0,8.0,8.0,2.0,4.0, COLOR='INVISIBLE'/ Vent Max Y for MESH030402
&VENT SURF_ID='OPEN', XB=3.0,5.0,6.0,8.0,4.0,4.0, COLOR='INVISIBLE'/ Vent Max Z for MESH030402
&VENT SURF_ID='Burner', XB=1.02,1.782,1.02,1.782,0.54,0.54/ Vent

&SLCF QUANTITY='TEMPERATURE', PBY=5.25/
&SLCF QUANTITY='TEMPERATURE', PBX=3.15/
&SLCF QUANTITY='VELOCITY', VECTOR=.TRUE., PBY=5.25/
&SLCF QUANTITY='VELOCITY', VECTOR=.TRUE., PBX=3.15/
&SLCF QUANTITY='PRESSURE', PBX=3.15/
&SLCF QUANTITY='PRESSURE', PBY=5.25/
&SLCF QUANTITY='VELOCITY', VECTOR=.TRUE., PBZ=2.5/


&TAIL /
```

References

[1] S. Kerber and W.D.Walton, "Effect of Positive Pressure Ventilation on a Room Fire,"NISTIR 7213, Mar. 2005.

[2] S. Kerber and W.D.Walton, "Full-Scale Evaluation of Positive Pressure Ventilation In a Fire Fighter Training Building,"NISTIR 7342, July 2006.

[3] S. Kerber and D. Madrzykowski, "Evaluating Positive Pressure Ventilation In Large Structures: High-Rise Fire Experiments," NISTIR 7468, Nov. 2007.

[4] S. Kerber and D. Madrzykowski, "Evaluating Positive Pressure Ventilation In Large Structures: School Pressure and Fire Experiments," NIST Technical Note 1498, July 2008.

[5] S. Kerber and D. Madrzykowski, "Fire Fighting Tactics Under Wind Driven Fire Conditions: 7-Story Building Experiments," NIST Technical Note 1629, Apr. 2009.

[6] S. Kerber, "Impact of Ventilation on Fire Behavior in Legacy and Contemporary Residential Construction," Underwriters Laboratories, Inc., Dec. 2010.

[7] S. Kerber and T. Fabian, "Effectiveness of Fire Service Ventilation and Suppression Tactics," UL, 2011.

[8] A. Barowy and D. Madrzykowski, "The Thermal Behavior of Structural Fire-Fighting Protective Ensemble Samples Modified with Phase Change Material and Exposed in Full-Scale Room Fires," Gaithersburg, MD,NIST TN 1739, Mar. 2012.

[9] NIOSH F1999-21, "Two Fire Fighters Die and Two Are Injured in Townhouse Fire—District of Columbia," Morgantown, WV., Nov. 1999.

[10] D. Madrzykowski and R. L.Vettori, "Simulation of the Dynamics of the Fire at 3146 Cherry Road NE: Washington D.C., May 30, 1999,"NISTIR 6510, Apr. 2000.

[11] NIOSH F2002-34, "Career Lieutenant and Fire Fighter Die in a Flashover During a Live-Fire Training Evolution - Florida," Morgantown, WV., June 2003.

[12] D. Madrzykowski, "Fatal Training Fires: Fire Analysis for the Fire Service,", 11th Proceedings ed London, England: 2007.

[13] NIOSH F2007-18, "Nine Career Fire Fighters Die in Rapid Fire Progression at Commercial Furniture Showroom – South Carolina," Morgantown, WV.,Feb.2009.

[14] N.P.Bryner, Stephen P.Fuss, Bryan W.Klein, and Anthony D.Putorti, "Technical Study of the Sofa Super Store Fire - South Carolina, June 18, 2007," NIST-SP 1118 Volume I, Mar. 2011.

[15] NIOSH F2002-40, "Career Fire Fighter Dies After Roof Collapse Following Roof Ventilation - Iowa," Morgantown, WV, May 2003.

[16] S. Kerber, D. Madrzykowski, and D. Stroup, "Evaluating Positive Pressure Ventilation In Large Structures: High-Rise Pressure Experiments,"NISTIR 7412, Mar. 2007.

[17] D. Madrzykowski and S. Kerber, "Fire Fighting Tactics Under Wind Driven Conditions: Laboratory Experiments,"NIST Technical Note 1618, Jan. 2009.

[18] T.E.Waterman, "Fire Venting of Sprinklered Buildings," *Fire Journal*, vol. 78, no. 2, pp. 30-39, Mar. 1984.

[19] National Fire Protection Association, "NFPA 204 Standard on Smoke and Heat Venting,", 2012 Edition ed Quincy, MA: NFPA, 2012.

[20] M.R.Suchomel, "A Preliminary Study of Factors Influencing the Use of Vents with Ordinary-Degree Sprinklers," Underwriters' Laboratories Inc. for the National Board of Fire Underwriters, New York, NY,File NC449, Assignment 63K4340, July 1964.

[21] P.H.Thomas and P.L.Hinkley, "Design of Roof-venting Systems for Single-storey Buildings," HMSO, London,Fire Research Technical Paper No. 10, Oct. 1964.

[22] G. O. H. P.L.Hinkley, N.R.Marshall, and R.Harrison, "Sprinklers and Vents Interaction: Experiments at Ghent," *Fire Surveyor*, pp. 18-23, Oct. 1992.

[23] K. McGrattan, A. Hamins, and D. Stroup, "Sprinkler, Smoke & Heat Vent, Draft Curtain Interaction -- Large Scale Experiments and Model Development," NISTIR 6196-1, Sept. 1998.

[24] The International Fire Services Training Association, "Ventilation," in *Essentials of Fire Fighting,* 5th ed. Carl Goodson and Lynne Murnane, Eds. Stillwater: Fire Protection Publications Oklahoma State University, 2008, pp. 541-592.

[25] Personal Communication: S. Kerber, 2012.

[26] Underwriters Laboratories Inc., "Fire Test of Interior Finish Material," UL1715, 2011.

[27] L. G.Blevins, "Behavior of Bare and Aspirated Thermocouples in Components Fires,", HTD99 ed Albuquerque, New Mexico: 1999.

[28] Omega Engineering Inc., "The Temperature Handbook," Stamford, CT,Vol. MM, 2004.

[29] W.M.Pitts, A.V.Murthy, J.L.de Ris, J. Filtz, K. Nygård, D. Smith, and I. Wetterlund, "Round Robin Study of Total Heat Flux Gauge Calibration at Fire Laboratories," NIST Special Publication 1031, Oct.2004.

[30] Medtherm Corporation, "64 Series Heat Flux Transducers," Huntsville, AL,Medtherm Corporation Bulletin 118, Aug.2003.

[31] S. Kerber and D. Madrzykowski, "Evaluating Positive Pressure Ventilation In Large Structures: School Pressure and Fire Experiments," NIST TN 1498, July 2008.

[32] Setra Systems, "Very Low Pressure Transducer Data Sheet Rev. G," Boxborough, MA,Jan.2008.

[33] Ohaus Corporation, "Manual for SD Series Bench Scale," Pine Brook, NJ,2000.

[34] U.S.Nuclear Regulatory Commission and Electric Power Research Institute, "Verification & Validation of Selected Fire Models for Nuclear Power Plant Applications - Volume 2: Experimental Uncertainty," Rockville, MD,NUREG-1824, June 2007.

[35] National Fire Protection Association, "NFPA 1971 Standard on Protective Ensembles for Structural Fire Fighting and Proximity Fire Fighting,", 2012 Edition ed Quincy, MA: NFPA, 2012.

[36] R. Bryant, "A Comparison of Gas Velocity Measurement Techniques in the Doorway of a Full-Scale Enclosure Fire," *Fire Safety Journal*, vol. 44, no. 5, pp. 793-800, July2009.

[37] "Verification and Vaildation Cases," Gaithersburg, MD: National Institute of Standards and Technology, 2011.<http://fire.nist.gov/fds/verification_validation.html>

[38] K. McGrattan, S. Hostikka, J. Floyd, and R. McDermott, "Fire Dynamics Simulator (Version 5) Technical Reference Guide Volume 3: Validation," National Institute of Standards and Technology, Gaithersburg, MD, NIST Special Publication 1018-5, Oct. 2010.

[39] "Sheetrock Gypsum Panels: Regular and Firecode Cores," United States Gypsum Company, Chicago, IL,Submittal Sheet WB1473 rev. 1-07, 2007.

[40] "Solids - Specific Heats," The Engineering Toolbox, 2010. <http://www.engineeringtoolbox.com/>

[41] "DUROCK Cement Board," United States Gypsum Company, Chicago, IL,Submittal Sheet CB399 rev.11-11, 2011.

[42] K. McGrattan, R. McDermott, S. Hostikka, and J. Floyd, "Fire Dynamics Simulator (Version 5) User's Guide," National Institute of Standards and Technology, Gaithersburg, MD, NIST Special Publication 1019-5, Oct. 2007.